BOSE-EINSTEIN CONDENSATION
OF MICROCAVITY POLARITONS

THÈSE N^O 3906 (2007)

ÉCOLE POLYTECHNIQUE FÉDÉRALE DE LAUSANNE

POUR L'OBTENTION DU GRADE DE DOCTEUR ÈS SCIENCES

PAR

Davide SARCHI

Laurea in fisica nucleare e subnucleare, Università degli studi di Milano, Milan, Italie
et de nationalité italienne

EPFL

ÉCOLE POLYTECHNIQUE
FÉDÉRALE DE LAUSANNE

Suisse
2007

-

Abstract

This thesis presents a theoretical description of the phase transition, with formation of long-range spatial coherence, occurring in a gas of exciton-polaritons in a semiconductor microcavity structure. The results and predictions of the theories developed in this thesis suggest that this phase transition, recently observed in experiments, can be interpreted as the Bose-Einstein Condensation (BEC) of microcavity polaritons.

Our theoretical framework is conceived as a generalization to the microcavity polariton system of the standard theories describing the BEC of a weakly interacting Bose gas. These latter are reviewed in Chapter 2, where an introduction to the physics of polaritons is also given.

The polariton system is peculiar, basically due to three main features, i.e. the composite nature of polaritons, which are a linear superposition of photon and exciton states, their intrinsic 2-D nature, and the presence of two-body interactions, arising both from the mutual interaction between excitons and from the saturation of the exciton oscillator strength. Therefore it is not clear whether the observed phase transition can be properly described in terms of BEC of a trapped gas. To clarify this point, one has to describe self-consistently the linear exciton-photon coupling giving rise to polariton quasiparticles, and the exciton-nonlinearities. This is made in Chapter 3, where a bosonic theory is developed by generalizing the Hartree-Fock-Popov description of BEC to the case of two coupled Bose fields at thermal equilibrium. Hence, we derive the classical equations describing the condensate wave function and the Dyson-Beliaev equations for the field of collective excitations. In this way, for each value of the temperature and of the total polariton density, a self-consistent solution can be obtained, fixing the populations of the condensate and of the excited states. In particular, the theory allows to describe simultaneously the properties of the polariton, the exciton and the photon fields, this latter being directly investigated in the typical optical measurements. The predicted phase diagram, the energy shifts, the population energy distribution and the behavior of the resulting first order spatial correlation function agree with the recent experimental findings [Kasprzak 06, Balili 07]. These results thus support the idea that the observed experimental signatures are a clear evidence of polariton BEC.

However, from a quantitative pint of view, the measured coherence amount in the condensed regime is significantly lower than the predicted one. This discrepancy could be due to deviations from the weakly interacting Bose gas picture and/or to deviations from the thermal equilibrium regime. In particular, these latter are expected to be strong in current experiments, because polaritons have a short radiative lifetime, while the rate of the energy-relaxation mechanisms is very slow.

To investigate how the deviations from equilibrium could affect the condensate fraction and the formation of off-diagonal long-range correlations, in Chapter 4, we develop a kinetic theory of the polariton condensation, accounting for both the relaxation mechanisms and for the field dynamics of fluctuations. Within the Hartree-Fock-Bogoliubov limit, we derive a set of coupled equations of motion for the one-particle populations and for the two particle correlations describing quantum fluctuations. We account for the relaxation processes due both to the polariton-phonon coupling and to the exciton-exciton scattering. The actual spectrum of the system is evaluated within the Popov limit, during the relaxation kinetics. Within this model, we solve self-consistently the populations kinetics and the dynamics of the excitation field, for typical experimental conditions. In particular, we show that the role of quantum fluctuations is amplified by non-equilibrium, resulting in a significant condensate depletion. This behavior

could explain the partial suppression of off-diagonal long-range coherence reported in experiments [Kasprzak 06, Balili 07]. We complete the analysis, by studying how the deviations from equilibrium depend on the system parameters. Our results show that the polariton lifetime plays a crucial role. In particular, we expect that the increase of the polariton lifetime above 10 ps would lead to thermal-equilibrium polariton BEC in realistic samples.

In Chapter 5, devoted to the conclusions, we discuss which issues of BEC could be clarified, by achieving polariton BEC at thermal-equilibrium, and which extensions of the present work would be most promising in this respect.

Keywords: Microcavity polaritons; Exciton gas coherence; Semiconductor heterostructures; Bose-Einstein condensation; Hartree-Fock-Bogoliubov theory.

Version abrégée

Cette thèse donne une description théorique de la transition de phase, avec formation de cohérence spatiale à longue distance, qui a lieu dans un gaz de polaritons de microcavité, c'est à dire un gaz de quasiparticules produites par le couplage entre les exciton crées dans un ou plus puits quantiques à semiconducteur et le mode optique d'une microcavité. Les résultats et les prédictions des théories développées dans cette thèse suggèrent que cette transition de phase, observée récemment dans les expériences, peut être interprétée comme la Condensation de Bose-Einstein (BEC) des polaritons de microcavité.

Notre théorie est conçue comme une généralisation au système des polaritons de microcavité des théories standard qui décrivent la BEC d'un gaz de bosons faiblement interagissant. On introduit ces théories standard dans le Chapitre 2, où on donne aussi une introduction à la physique des polaritons.

Le système des polaritons est particulier, à cause de trois propriétés fondamentales, c'est à dire la nature composite des polaritons, qui sont une superposition linéaire des états de photon et d'exciton, leur nature intrinsèquement bidimensionnelle, et la présence de l'interactions à deux corps, produite par l'interaction mutuelle entre excitons and par la saturation de la force d'oscillateur de l'exciton. Donc il n'est pas clair si la transition de phase observée puisse être interprétée comme la BEC d'un gaz confiné. Pour clarifier ce point, on doit décrire de façon auto-consistante le couplage linéaire entre l'exciton et le photon et les non-linéarités excitoniques. Ce but est réalisé dans le Chapitre 3, où une théorie est développée en généralisant la théorie de Hartree-Fock-Popov au cas de deux champs de Bose couplés et à l'équilibre thermique. De là, on dérive les équations classiques qui décrivent la fonction d'onde du condensat et les équations de Dyson-Beliaev pour le champ des excitations collectives. En cette manière, pour chaque valeur de température et densité totale de polaritons, on détermine la solution auto-consistante qui fixe la populations du condensat et des états excités. En particulier, la théorie permet de décrire au même temps les propriétés des champs de polariton, d'exciton et de photon, ce dernier étant directement investigué dans les mesures optiques. Le diagramme de phase, les shifts d'énergie, la distribution énergétique de la population et le comportement de la fonction de corrélation spatiale ainsi obtenus sont en accord avec les évidences expérimentales récentes [Kasprzak 06, Balili 07]. Donc ces résultats supportent l'idée que les signatures expérimentales observées soient une évidence claire de la BEC d'un gaz de polaritons.

Cependant, d'un point du vue quantitatif, le dégrée de cohérence mesuré dans le régime condensé est significativement inférieur à notre prévision théorique. Cette différence peut être due à une déviation de la description de gaz faiblement interagissant et/ou aux déviations de l'équilibre thermique. En particulier, on peut prévoir que ces dernières soient larges dans les expérience actuelles, parce que les polaritons ont un temps de vie radiatif court, tandis que les mécanismes de relaxation énergétique sont très lents.

Pour étudier comment les déviations de l'équilibre peuvent affecter la fraction de condensat et la formation des corrélations non-diagonales à longue distance, dans le Chapitre 4, on développe une théorie cinétique de la condensation des polaritons, qui tient en compte soit des mécanismes de relaxation soit de la dynamique du champ de fluctuations. Dans la limite Hartree-Fock-Bogoliubov, on dérive un set d'équations cinétiques couplées pour les populations et pour les corrélations à deux particules qui représentent les fluctuations quantiques. On inclue les processus de relaxation due soit au couplage entre polaritons et phonons soit au collisions exciton-exciton. Pendant la cinétique de relaxation, le spectre actuel du système

est évalué dans la limite de Popov. Avec ce model, on résoudre de façon auto-consistante la cinétique des populations et la dynamique du champ d'excitation, en modélisant les conditions expérimentales typiques. En particulier, on trouve que le rôle des fluctuations quantiques est amplifié par le régime de non-équilibre, en résultant dans une déplétion significative du condensat. Ce comportement pourrait expliquer la suppression partielle de la corrélation à longue distance, observée dans les expériences [Kasprzak 06, Balili 07]. On complète notre analyse, étudiant comment les déviations de l'équilibre dépendent des paramètres. Nos résultats montrent que le temps de vie du polariton joue le rôle dominant. En particulier, on s'attend que, en augmentant le temps de vie au dessus de 10 ps, il serait possible d'obtenir la condensation à l'équilibre thermique.

Dans le Chapitre 5, consacré aux conclusions, on discute les issues qui pourraient être clarifiées en atteignant la BEC des polaritons à l'équilibre, et les extensions les plus intéressantes de ce travail.

Mots clef: Polaritons de microcavité; Cohérence d'un gaz d'excitons; Eterostructures à semiconducteur; Condensation de Bose-Einstein; Théorie Hartree-Fock-Bogoliubov.

Riassunto

Questa tesi fornisce una descrizione teorica della transizione di fase, con formazione di coerenza spaziale a lunga distanza, che ha luogo in un gas di polaritoni di microcavità, ovvero il gas di quasiparticelle create dall'accoppiamento tra gli eccitoni prodotti in uno o piu' pozzi quantici a semiconduttore e il modo ottico di una microcavità. I risultati e le predizioni delle teorie sviluppate in questa tesi suggeriscono che questa transizione di fase, osservata recentemente negli esperimenti, possa essere propriamente interpretata come la Condensazione di Bose-Einstein (BEC) dei polaritons di microcavità.

La nostra teoria è concepita come la generalizzazione ai polaritoni di microcavità delle teorie standard che descrivono la BEC di un gas di bosoni debolmente interagenti. Queste teorie sono introdotte nel Capitolo 2, dove si introducono anche i concetti fondamentali della fisica dei polaritoni.

I polaritoni costituiscono un sistema particolare, a causa di tre proprietà fondamentali, ovvero la loro natura composita, dal momento che un polaritone è la sovrapposizione lineare degli stati di fotone e di eccitone, la loro natura intrinsecamente bidimensionale, e la presenza dell'interazione a due corpi, originata sia dalla mutua interazione tra eccitoni sia dalla saturazione della forza d'oscillatore eccitonica. Non è quindi chiaro se la transizione di fase osservata possa essere interpretata come la BEC di un gas confinato. Per chiarire questo punto, si deve descrivere in modo autoconsistente l'accoppiamento lineare tra l'eccitone e il fotone e le nonlinearità eccitoniche. Questo è realizzato nel Capitolo 3, dove sviluppiamo una teoria che generalizza la teoria di Hartree-Fock-Popov al caso di due campi bosonici accoppiati e all'equilibrio termico. In particolare, deriviamo le equazioni di campo classico che descrivono la funzione d'onda del condensato e le equazioni di Dyson-Beliaev per il campo delle eccitazioni collettive. In questo modo, per ogni valore di temperatura e di densità totale di polaritoni, determiniamo la soluzione autoconsistente che fissa la popolazione del condensato e degli stati eccitati. La teoria permette di descrivere, allo stesso tempo, il campo di polaritone, di eccitone e di fotone, quest'ultimo essendo l'oggetto delle misure ottiche. Il diagramma di fase, le variazioni energetiche delle risonanze, la distribuzione in energia della popolazione e il comportamento della funzione di correlazione spaziale predetti da questa teoria, sono in accordo con le recenti misure sperimentali [Kasprzak 06, Balili 07]. Tutti questi risultati supportano l'idea che quanto osservato negli esperimenti sia una chiara evidenza della BEC dei polaritoni di microcavità.

Tuttavia, da un punto di vista quantitativo, il grado di coerenza misurato nel regime condensato è significativamente inferiore alla nostra previsione teorica. Questa discrepanza potrebbe essere imputabile sia a una deviazione dalla descrizione di gas debolmente interagente sia a deviazioni dal regime di equilibrio termico. Le deviazioni dall'equilibrio sono attese essere particolarmente importanti negli esperimenti correnti, perché i polaritoni hanno un tempo di vita radiativo corto mentre i processi di rilassamento sono molto lenti.

Per studiare come le deviazioni dall'equilibrio influenzino la frazione di condensato e la formazione di correlazioni a lunga distanza, nel Capitolo 4, sviluppiamo una teoria cinetica per la condensazione dei polaritoni, che tiene conto sia dei meccanismi di rilassamento sia della dinamica del campo delle fluttuazioni. Nel limite Hartree-Fock-Bogoliubov, deriviamo un set di equazioni accoppiate che descrivono l'evoluzione temporale delle popolazioni e delle correlazioni a due corpi che rappresentano le fluttuazioni quantistiche. Includiamo i processi di rilassamento dovuti sia all'accoppiamento tra polaritoni e fononi sia alle collisioni eccitone-eccitone. Durante la cinetica di rilassamento, lo spettro di eccitazione del sistema è valutato

nel limite di Popov. Con questo modello, risolviamo in modo auto-consistente la cinetica delle popolazioni e la dinamica del campo di eccitazione, modellizzando le tipiche condizioni sperimentali. In particolare, troviamo che il ruolo delle fluttuazioni quantistiche è amplificato dal regime di non-equilibrio, e risulta in una considerevole riduzione della frazione di condensato. Questo comportamento potrebbe spiegare la parziale soppressione della correlazione a lunga distanza incontrata negli esperimenti [Kasprzak 06, Balili 07]. Completiamo la nostra analisi, studiando come le deviazioni dall'equilibrio dipendano dai parametri. I risultati mostrano che il tempo di vita dei polaritoni gioca un ruolo dominante, e che, per un tempo di vita superiore a 10 ps, sarebbe possibile ottenere la BEC di polaritoni all'equilibrio termico

Nel Capitolo 5, dedicato alle conclusioni, discutiamo infine quali aspetti della fisica della BEC potrebbero essere efficacemente studiati se fosse possibile ottenere un condensato di polaritoni all'equilibrio. Discutiamo inoltre delle possibili e più promettenti estensioni di questo lavoro.

Parole chiave: Polaritoni di microcavità; Coerenza di un gas di eccitoni; Eterostrutture a semiconduttore; Condensazione di Bose-Einstein; Theoria Hartree-Fock-Bogoliubov.

Contents

Chapter 1

Introduction

Bose-Einstein condensation (BEC) is one of the most remarkable manifestations of quantum mechanics at the macroscopic scale [Pitaevskii 03]. In a Bose-Einstein condensate, many particles share the same quantum mechanical wave function, giving rise to the formation of off-diagonal long range order (ODLRO) [Penrose 56], i.e. the formation of spatial correlations extending over the whole system size. The experimental observation of BEC in diluted atomic gases in 1995 [Anderson 95, Davis 95, Bradley 95] renewed the interest on the fundamental aspects of the physics involved and stimulated the study of several linked applications. In particular, the idea to achieve the same phenomenon in semiconductor based systems was very appealing [Griffin 95]. This would help to answer several fundamental questions of the BEC physics. Indeed the main advantage of semiconductor systems is that measurements are made optically. This could allow the direct observation of several key properties of BEC, as the modification of the spectral function or the formation of spatial coherence. Another interesting property is the possibility of growing semiconductor structure of lower dimensionality, which are an ideal candidate to study the effects of the reduced dimensionality on quantum fluids. In addition, the critical temperature is expected to be much larger than in atom gases, due to the very small effective mass of the particles involved, thus possibly favoring the exploration of a large region of the phase diagram. Finally, achieving BEC in a solid-state device, with ease of control and integration, would represent a new promising way to the implementation of quantum information technology [Bouwmeester 00].

The most promising candidates for the observation of BEC in a semiconductor structure were excitons [Moskalenko 62, Blatt 62, Keldysh 68, Griffin 95, Moskalenko 00] and exciton-polaritons [Imamoglu 96, Moskalenko 00, Snoke 02b]. All the experimental attempts to obtain either a three-dimensional or a two-dimensional exciton quantum degenerate gas have given controversial results and the exciton BEC has not been observed up to now [Griffin 95, Fortin 93, Snoke 02a]. On the other hand, the signature of a quantum degenerate gas of microcavity polariton has been reported by several groups [Dang 98, Senellart 99, Deng 02, Deng 03, Richard 05b, Richard 05a, Kasprzak 06, Deng 06] in the previous years and the occurrence of ODLRO has been very recently observed [Kasprzak 06, Balili 07]. For this reason, microcavity polaritons has received an increasing attention in these years, from both the experimental and the theoretical point of view.

Due to the peculiarities of the polariton system, that we will discuss in the following subsection, many theoretical models have been introduced [Laussy 04, Keeling 04, Doan 05, Carusotto 05, Schwendimann 06, Marchetti 06, Szymanska 06, Wouters 07b]. We will briefly review them later on. In spite of the high relevance of all these theoretical frameworks, a basic question remains still unanswered. Are the experimental findings correctly interpreted in terms

of a quantum field theory of interacting bosons? The first main contribution of this thesis is to answer this question, by means of the bosonic theory developed in Chapter 3, which allows a clear interpretation of the phenomenon in terms of BEC and which results in a very good agreement with the experimental observations.

Another relevant open question of fundamental interest concerns the mechanism of the condensate growth, and how the non-equilibrium regime could affect the properties of the condensed system. This problem has been considered also in the context of atomic BEC and it is even more relevant for polaritons. Here, we study the problem by means of the kinetic model developed in Chapter 4, focusing on the interplay between the non-equilibrium regime and the formation of coherence in the polariton system. The description of this mechanism is the second main contribution of the present work.

1.1 Outlook of the present work

This thesis is organized in three parts: an introduction, reviewing the basic concepts and the existing literature about both microcavity polaritons and BEC, and two Chapters containing the original contribution of this work.

In Chapter 2, we introduce the basic features both of the microcavity polariton system and of the BEC physics. In particular, in Section 2.1 we review the theory of microcavity polaritons, focusing on three crucial points, i.e. the bosonic behavior, the mutual interactions and the finite lifetime. In Section 2.2 we review the main concepts related to BEC and the theoretical frameworks developed both for describing the condensed system at thermal equilibrium and for predicting the non-equilibrium condensate growth. In Section 2.3 we discuss the main experimental evidence of polariton BEC.

In Chapter 3 we develop a bosonic theory for polariton BEC at thermal equilibrium. We describe the main features of this theory, generalizing the Hartree-Fock-Popov approach to the case of two linearly coupled fields. In particular, we discuss the predictions of the theory for typical material parameters, showing that the experimental findings can be interpreted as evidence of polariton BEC.

In Chapter 4 we develop a kinetic model in order to describe the condensate growth, under typical experimental non-equilibrium conditions. We derive a set of kinetic equations for populations and two-body correlations, within a Number-conserving formalism. We compare the predictions of this model with recent experimental findings [Kasprzak 06, Balili 07]. The results suggest that deviations from equilibrium are responsible for the observed partial suppression of ODLRO, because of the enhancement of quantum fluctuations. In Section 4.3, we finally compare the results of the kinetic model and of the equilibrium theory. In particular, we study the dependence of the results of the kinetic model on the polariton lifetime, showing that the thermal equilibrium regime could be reached with a reasonable increase of the polariton lifetime, i.e. by slightly improving the quality of the microcavity mirrors.

Chapter 5 is devoted to the conclusions and the perspectives of the present work.

Chapter 2

Review on polaritons and Bose-Einstein Condensation

2.1 Microcavity polaritons

2.1.1 Excitons

In this subsection we give an overview of the physics of excitons in semiconductors. We report only the main results of the exciton theory, referring, for the details, to semiconductors textbooks [Bassani 75, Haug 90].

We start by considering a general crystal composed by an equal number N of positive ions and delocalized electrons. The full Hamiltonian of this problem, expressed in coordinate space, is

$$
\begin{aligned}
H_{cr} &= -\sum_\alpha \frac{\hbar^2 \nabla_\alpha^2}{2M_\alpha} - \sum_j \frac{\hbar^2 \nabla_j^2}{2m_0} + \\
&\quad + \frac{1}{2}\sum_{\alpha,\beta} \frac{Z_\alpha Z_\beta e^2}{|\mathbf{R}_\alpha - \mathbf{R}_\beta|} - \sum_{\alpha,j} \frac{Z_\alpha e^2}{|\mathbf{R}_\alpha - \mathbf{r}_j|} + \frac{1}{2}\sum_{j,l} \frac{e^2}{|\mathbf{r}_j - \mathbf{r}_l|},
\end{aligned}
\tag{2.1}
$$

where the ionic and the electronic kinetic terms are written in the first line, while in the second line we have the ion-ion, the ion-electron, and the electron-electron Coulomb interaction terms. Notice that here, for simplicity, we have neglected the spin interactions. Spin, and the spin-orbit interaction, play an important role in the determination of the semiconductor band structure and of the energy splitting between heavy and light hole bands. However, for our present purposes, it is sufficient to adopt the simplest possible assumption for the band structure. We will thus assume the system in a fully spin-polarized state, as produced by circularly-polarized optical excitation, and model it in terms of a scalar theory. The ground state of the Hamiltonian (2.1) is calculated within the Born-Oppenheimer approximation, i.e. by separating the motion of electrons and ions, because of the very different masses of the two species, and by assuming the electronic motion to adiabatically follow the ionic motion. Therefore the total ground state wave function is factored in a product of a ionic wave function and an electronic wave function, as

$$
\Psi\left(\{\mathbf{R}_\alpha\}, \{\mathbf{r}_j\}\right) = \Upsilon^{ion}(\{\mathbf{R}_\alpha\})\Phi^{el}(\{\mathbf{R}_\alpha\}, \{\mathbf{r}_j\}).
\tag{2.2}
$$

In this way, the electronic problem is solved by considering the ions as fixed in the equilibrium positions and neglecting the kinetic term of the ions. At the same time, the equilibrium positions of the ions are determined self-consistently by the requirement that the total energy

of the system be minimal. The electronic problem can be solved within the mean-field limit by means of the Hartree-Fock (HF) approach, i.e. by assuming the electronic many-body state to be a Slater determinant of single-particle wave functions

$$\Phi^{el}(\{\mathbf{r}_j\}) = \frac{1}{\sqrt{N!}} \, \text{Det} \, \{\psi_{n_1}(\mathbf{r}_1) \cdots \psi_{n_N}(\mathbf{r}_N)\} \, . \tag{2.3}$$

Here, each wave function $\psi_n(\mathbf{r})$ satisfies the Hartree-Fock equation

$$H_{HF}\psi_n(\mathbf{r}) = \left[-\frac{\hbar^2\nabla^2}{2m_0} - \sum_\alpha \frac{Z_\alpha e^2}{|\mathbf{R}_\alpha - \mathbf{r}|} + V_{dir} \right] \psi_n(\mathbf{r}) + V_{exch} = E_n\psi_n(\mathbf{r}), \tag{2.4}$$

where

$$V_{dir} = e^2 \sum_j \int d\mathbf{r}_1 \frac{|\psi_j(\mathbf{r}_1)|^2}{|\mathbf{r} - \mathbf{r}_1|} \tag{2.5}$$

is the direct local Coulomb potential, while

$$V_{exch} = -e^2 \sum_j \int d\mathbf{r}_1 \psi_j(\mathbf{r}) \frac{\psi_j^*(\mathbf{r}_1)\psi_n(\mathbf{r}_1)}{|\mathbf{r} - \mathbf{r}_1|} \tag{2.6}$$

is the non-local Fock term and the sum is taken over all the resulting HF single-particle states. Since the ions in the equilibrium positions form a lattice, Bloch's theorem holds. Then, it is useful to introduce the vectors $\mathbf{k}$ of the reciprocal lattice space, and the corresponding periodic Bloch functions

$$\psi_{n,\mathbf{k}}(\mathbf{r}) = \frac{1}{\sqrt{V}} u_{n,\mathbf{k}}(\mathbf{r}) e^{i\mathbf{k}\cdot\mathbf{r}} \, , \tag{2.7}$$

where V is the volume of the system. In the *band approximation* the wave functions $\psi_{n,\mathbf{k}}(\mathbf{r})$, are assumed to satisfy the Schroedinger equation

$$\left[-\frac{\hbar^2\nabla^2}{2m_0} + V(\mathbf{r}) \right] \psi_{n,\mathbf{k}}(\mathbf{r}) = E_{n,\mathbf{k}}\psi_{n,\mathbf{k}}(\mathbf{r}), \tag{2.8}$$

where $V(\mathbf{r})$ is an average, local and self-consistent, potential characterized by the lattice symmetries. The solution of Eq. (2.8) gives the band structure of the crystal.

Here we consider a two band model, i.e. we restrict ourselves to the case where the band index n represents the valence ($n = v$) or the conduction ($n = c$) band. The energy gap between the two bands is E_g. Therefore, for small vectors $\mathbf{k}$ the energy dispersion of the two bands can be simply written within the effective mass approximation as

$$E_{v,\mathbf{k}\to\mathbf{0}} \simeq -\frac{\hbar^2 k^2}{2m_h}$$

$$E_{c,\mathbf{k}\to\mathbf{0}} \simeq E_g + \frac{\hbar^2 k^2}{2m_e}, \tag{2.9}$$

where m_e is the effective mass of an electron lying in the conduction band, while m_h is the effective mass of an electron in the valence band. Since a single-particle excitation in the valence band is produced when an electron is removed, producing a positive charged *hole*, m_h corresponds to an effective mass for the hole states. Clearly, the ground state of the

system corresponds to the configuration where electrons occupy only the valence band and the electronic wave function (2.3) reduces to

$$\Phi^{el}(\{\mathbf{r}_j\}) = \frac{1}{\sqrt{N!}} \, \text{Det} \, \{\psi_{v,\mathbf{k}_1}(\mathbf{r}_1) \cdots \psi_{v,\mathbf{k}_N}(\mathbf{r}_N)\}. \tag{2.10}$$

We notice that, in the expression for the ground state, the electronic states are self-consistently evaluated by using the mean-field Coulomb potential generated by the correspondent electronic density. Therefore, the correct many-body excited state with wave vector $\mathbf{K}$ is not simply given by a general configuration where an electron is promoted to the conduction band, i.e.

$$\Phi^{el}_{\mathbf{k}_n,\mathbf{K}}(\{\mathbf{r}_j\}) = \frac{1}{\sqrt{N!}} \, \text{Det} \, \{\psi_{v,\mathbf{k}_1}(\mathbf{r}_1) \cdots \psi_{c,\mathbf{k}_n+\mathbf{K}} \cdots \psi_{v,\mathbf{k}_N}(\mathbf{r}_N)\}, \tag{2.11}$$

because this operation also modifies the electron density and so the mean-field Coulomb potential. Actually, if E_0 is the ground state energy, every configuration of this kind has an energy $E_{\mathbf{k}_n,\mathbf{K}} = E_0 + E_{c,\mathbf{k}_n+\mathbf{K}} - E_{v,\mathbf{k}_n} \geq E_0 + E_g$. On the other hand, a good ansatz for the many-body excited state is a general linear combination of all the excited configurations (2.11), i.e.

$$\Phi^{exc}_{\mathbf{K}} = \sum_{\mathbf{k}} A_{\mathbf{k},\mathbf{K}} \Phi^{el}_{\mathbf{k},\mathbf{K}}(\{\mathbf{r}_j\}) \tag{2.12}$$

where the normalization

$$\sum_{\mathbf{k}} |A_{\mathbf{k},\mathbf{K}}|^2 = 1 \tag{2.13}$$

is imposed. The combination $\Phi^{exc}_{\mathbf{K}}$ which minimizes the expectation value of the Hamiltonian (2.1) is the actual many-body excitation at wave vector $\mathbf{K}$ and it is called *exciton*. The minimization procedure, starting from the ansatz (2.12), accounts for the Coulomb correlation, namely for the corrections to the HF result represented by the single Slater determinant (2.11). The main effect of Coulomb correlation is that the difference between the exciton energy and the ground state energy is lower than the energy band gap E_g.

If we consider the case of weakly bound excitons (Wannier excitons), i.e. excitons whose wave function extends over a region much larger than the lattice characteristic length, we can safely assume

$$u_{v(c),\mathbf{k}}(\mathbf{r}) \simeq u_{v(c),\mathbf{0}}(\mathbf{r}) = u_{v(c)}(\mathbf{r}), \tag{2.14}$$

and that only the contributions for small wavevectors $\mathbf{k}$ are relevant. In this limit, we adopt the effective mass approximation Eq. (2.9) for the electron/hole energies. Consequently the exciton wave function takes the form

$$\Phi^{exc}_{\mathbf{K}} = \sum_{\mathbf{k}} A_{\mathbf{k},\mathbf{K}} \Phi^{el}_{\mathbf{k}-\frac{m_h}{M}\mathbf{K},\mathbf{K}}(\{\mathbf{r}_j\}), \tag{2.15}$$

with $M = m_e + m_h$. The expectation value

$$\langle \Phi^{exc}_{\mathbf{K}} | H_{cr} | \Phi^{exc}_{\mathbf{K}} \rangle = \langle \Phi^{exc}_{\mathbf{K}} | (H_{kin} + U) | \Phi^{exc}_{\mathbf{K}} \rangle, \tag{2.16}$$

where H_{kin} is the one-body kinetic term, and U is the two-body Coulomb interaction between electrons, can be written in terms of matrix elements between states containing one electron and one hole [Bassani 75]. In particular, each interaction matrix element between Slater determinants produces two contributions,

$$\langle \Phi^{el}_{\mathbf{k}_h,\mathbf{k}_h+\mathbf{k}_e} | U | \Phi^{el}_{\mathbf{k}'_h,\mathbf{k}'_h+\mathbf{k}'_e} \rangle = \delta_{\mathbf{k}_e-\mathbf{k}_h,\mathbf{k}'_e-\mathbf{k}'_h} \left(\langle \psi_{c,\mathbf{k}_e} \psi_{v,\mathbf{k}'_h} | U | \psi_{v,\mathbf{k}_h} \psi_{c,\mathbf{k}'_e} \rangle \right.$$
$$\left. - \langle \psi_{c,\mathbf{k}_e} \psi_{v,\mathbf{k}'_h} | U | \psi_{c,\mathbf{k}'_e} \psi_{v,\mathbf{k}_h} \rangle \right). \tag{2.17}$$

15

The first matrix element on the right hand side of (2.17) represents the electron-hole exchange interaction, which gives a small, repulsive contribution. On the other hand, the second matrix element represents the direct electron-hole interaction[1] and it is attractive. This term is responsible for exciton binding energy. By neglecting for the moment the electron-hole exchange interaction, whose implications will be discussed later on, from the minimization of the expectation value (2.16), with the normalization constraint Eq. (2.13), we finally obtain the equation

$$\left[E_0 - E_{\mathbf{K}}^{exc} + \frac{\hbar^2 k^2}{2\mu} + \frac{\hbar^2 K^2}{2M} \right] A_{\mathbf{k},\mathbf{K}} - \sum_{\mathbf{q}} A_{\mathbf{q},\mathbf{K}} \frac{e^2}{\epsilon_\infty |\mathbf{q} - \mathbf{k}|^2} = 0, \tag{2.18}$$

where $\mu^{-1} = m_e^{-1} + m_h^{-1}$, giving the exciton energy $E_{\mathbf{K}}^{exc}$, entering in (2.18) as the Lagrange multiplier. Notice that here we have included the dynamical dielectric constant ϵ_∞, accounting for the effect of screening due to the medium, neglected up to now. This effect corresponds to the vertex renormalization of the Coulomb interaction, which is overlooked in the Hartree-Fock limit [Bassani 75, Mahan 81]. We need to account for this effect in order to obtain a realistic exciton binding energy. We mention that the electron-hole exchange interaction, neglected in deriving Eq. (2.18), can be taken into account by means of perturbation theory. Its main implication is the energy splitting between the mode with longitudinal polarization and the two degenerate modes with transverse polarization, with respect to the exciton center of mass motion.[2] This result, the so called *LT splitting* has important consequences in the problem of the exciton-photon coupling [Andreani 94], which will be treated in following subsections. It is interesting to mention that the evaluation of the electron-hole exchange term does not require the inclusion of the screening dielectric constant, because the electron-hole exchange diagrams are already included in the definition of ϵ_∞ [Mahan 81].

Notice that, by Fourier transforming Eq. (2.18), we get for the Fourier transform of the exciton envelope function

$$F_{\mathbf{K}}(\mathbf{r}) = \frac{1}{\sqrt{V}} \sum_{\mathbf{k}} A_{\mathbf{k},\mathbf{K}} e^{i\mathbf{k}\cdot\mathbf{r}} , \tag{2.19}$$

the hydrogenic Schroedinger equation

$$\left[E_0 + \frac{\hbar^2 K^2}{2M} - \frac{\hbar^2 \nabla^2}{2\mu} \right] F_{\mathbf{K}}(\mathbf{r}) - F_{\mathbf{K}}(\mathbf{r}) \frac{e^2}{\epsilon_\infty |\mathbf{r}|} = E_{\mathbf{K}}^{exc} F_{\mathbf{K}}(\mathbf{r}) . \tag{2.20}$$

This feature suggests the interpretation of the exciton state as the bound state of an hydrogenic atom formed by an electron in the conduction band and an hole in the valence band. Following this analogy it is useful to define the exciton Bohr radius a_0 and the exciton binding energy $E_{\mathbf{K}}^b = E_0 + E_g - E_{\mathbf{K}}^{exc}$.

By adopting the second quantization formalism, the operator that transforms the ground state into state (2.15) is

$$\hat{b}_{\mathbf{K}}^\dagger = \sum_{k} A_{\mathbf{k},\mathbf{K}} \hat{e}_{\mathbf{k}+\frac{m_e}{M}\mathbf{K}}^\dagger \hat{h}_{-\mathbf{k}+\frac{m_h}{M}\mathbf{K}}^\dagger, \tag{2.21}$$

where $\hat{e}^\dagger$ and $\hat{h}^\dagger$ are the electron and the hole creators, respectively. From Eq. (2.21), using the canonical anti-commutation rules (CAR) for the electron and hole fields and the useful

---

[1]To avoid confusion, we stress the point that the electron-hole direct interaction originates from the *exchange* term of the matrix element between Slater determinants, while the electron-hole exchange interaction originates from the *direct* term of the matrix element between Slater determinants

[2]Notice that only the transverse polarized modes, which correspond to a total exciton spin equal to ± 1, are optical active. Therefore the coupling with the electromagnetic field only affects the transverse polarized exciton modes.

operator relation

$$\left[\hat{O}_1, \hat{O}_2\hat{O}_3\right] = \left\{\hat{O}_1, \hat{O}_2\right\}\hat{O}_3 - \hat{O}_2\left\{\hat{O}_1, \hat{O}_3\right\} \tag{2.22}$$

we derive the exact exciton commutation rule

$$\begin{aligned}
\left[\hat{b}_{\mathbf{K}}, \hat{b}_{\mathbf{Q}}^\dagger\right] &= \sum_{\mathbf{k}} A_{\mathbf{k},\mathbf{K}}^* A_{\mathbf{k}+\frac{m_e}{M}(\mathbf{K}-\mathbf{Q}),\mathbf{Q}}\delta_{-\frac{m_e}{M}\mathbf{K}+\mathbf{Q},\frac{m_h}{M}\mathbf{K}} \\
&\quad - \sum_{\mathbf{k}} A_{\mathbf{k},\mathbf{K}}^* A_{\mathbf{k}+\frac{m_e}{M}(\mathbf{K}-\mathbf{Q}),\mathbf{Q}}\hat{h}_{-\mathbf{k}+\frac{m_h}{M}\mathbf{K}}^\dagger \hat{h}_{-\mathbf{k}-\frac{m_e}{M}\mathbf{K}+\mathbf{Q}} \\
&\quad - \sum_{\mathbf{k}} A_{\mathbf{k},\mathbf{K}}^* A_{\mathbf{k}-\frac{m_h}{M}(\mathbf{K}-\mathbf{Q}),\mathbf{Q}}\hat{e}_{\mathbf{k}+\frac{m_e}{M}\mathbf{K}}^\dagger \hat{e}_{\mathbf{k}-\frac{m_h}{M}\mathbf{K}+\mathbf{Q}} \\
&= \delta_{\mathbf{K},\mathbf{Q}} + \hat{D}_{\mathbf{K},\mathbf{Q}} \tag{2.24}
\end{aligned}$$

where the first term has been obtained by using the normalization of the exciton wave function. As shown by Eq. (2.24) the exciton field obeys a quasi-Bose commutation rule. The deviation from the Bose commutator rule is expressed by the operator $\hat{D}_{\mathbf{K},\mathbf{Q}}$, acting on the electron-hole space. To estimate this deviation, we calculate the expectation value of Eq. (2.24) for $\mathbf{Q} = \mathbf{K}$,

$$\begin{aligned}
\left\langle\left[\hat{b}_{\mathbf{K}}, \hat{b}_{\mathbf{K}}^\dagger\right]\right\rangle &= 1 - \sum_{\mathbf{k}}|A_{\mathbf{k},\mathbf{K}}|^2\left[n_h(-\mathbf{k} + \frac{m_h}{M}\mathbf{K}) + n_e(\mathbf{k} + \frac{m_e}{M}\mathbf{K})\right] \\
&\sim 1 - \frac{N_h^{\mathbf{K}} + N_e^{\mathbf{K}}}{N_{\mathrm{conf}}(\mathbf{K})}, \tag{2.25}
\end{aligned}$$

where $n_{e(h)}$ is the electron (hole) population in the single state, while $N_{e(h)}^{\mathbf{K}}$ is the total electron (hole) population in the $N_{\mathrm{conf}}(\mathbf{K})$ electron-hole configurations contributing to the $\mathbf{K}$ exciton state. In the second line of (2.25), we have assumed for simplicity that each electron-hole configuration equally contributes to the exciton state (i.e. we assume a constant weight $|A_{\mathbf{k},\mathbf{K}}|^2 = 1/N_{\mathrm{conf}}(\mathbf{K})$). Eq. (2.25) shows that excitons behave as Bose quasi-particles if the number of electrons and holes per state is much smaller than 1. This result can be explained in an intuitive way: since many electron/hole states contribute to one exciton state, the population of the latter can be large although the population in each electron/hole state is much smaller than 1, thus in a regime where the effects of the Pauli principle are vanishingly small. The fact that excitons follow Bose statistics at moderate excitation densities has suggested, long time ago, the possibility to achieve BEC of an exciton gas [Moskalenko 62, Blatt 62, Keldysh 68].

In the next subsection we will see how the concept of semiconductor exciton can be translated to the two dimensional case.

2.1.2 Excitons in quantum wells

Due to the advances of the crystal growth, nowadays it is possible to realize low-dimensional semiconductor structures, where electrons and holes are confined in one or two dimensions [Bastard 89]. Therefore, it is interesting to understand if the exciton bound state is well defined also in reduced dimensions, and to explore how the exciton properties change due to the quantum confinement. For our purposes, here we address to the two-dimensional case, i.e. the case of quantum well excitons.

A semiconductor quantum well can be modeled as a small gap semiconductor sandwiched in a large gap semiconductor. In such a geometry, the translational symmetry is broken along the direction orthogonal to the semiconductor plane and the lowest energy excitations are

localized inside the small gap semiconductor. As a consequence, the total wave vector $\mathbf{k}$ is no more conserved in these structures, while the only conserved quantity is the in-plane component of the wave vector $\mathbf{k}_\parallel$.

Nevertheless, the problem can be treated in perfect analogy with the bulk case, the only difference lying in the form of the band wave functions, which in the present case are written as

$$\psi_{c(v),\mathbf{k}_\parallel}(\rho, z) = \frac{1}{\sqrt{S}} e^{-i\mathbf{k}_\parallel \cdot \rho} f_{c(v)}(z) u_{\mathbf{k}_\parallel}^{c(v)}(\rho), \tag{2.26}$$

where S represents the area of the quantum well, ρ is the in-plane real coordinate, $u_{\mathbf{k}_\parallel}^{c(v)}(\rho)$ are the Bloch functions in the plane and $f_{c(v)}(z)$ represent the envelope functions accounting for the confinement in the orthogonal direction. With the exception of the envelope functions in the z-direction, the expression (2.26) is just the 2-D version of Eq. (2.7).

The Slater determinants for the ground and excited states are defined as in the bulk case. Correspondingly, the ansatz for the excited state with a given $\mathbf{K}_\parallel$ is

$$\Phi_{\mathbf{K}_\parallel}^{exc} = \sum_{\mathbf{k}} A_{\mathbf{k}_\parallel, \mathbf{K}_\parallel} \Phi_{\mathbf{k}_\parallel - \frac{m_h}{M} \mathbf{K}_\parallel, \mathbf{K}_\parallel}^{el}(\{\rho_j\}). \tag{2.27}$$

Then, by using the approximation of weakly bound excitons, $u_{\mathbf{k}_\parallel}^{c(v)}(\rho) \simeq u_0^{c(v)}(\rho)$ and the effective mass approximation, we get, for the 2-D Fourier transform of the exciton envelope function

$$F_{\mathbf{K}_\parallel}(\rho) = \frac{1}{\sqrt{V}} \sum_{\mathbf{k}_\parallel} A_{\mathbf{k}_\parallel, \mathbf{K}_\parallel} e^{i\mathbf{k}_\parallel \cdot \rho}, \tag{2.28}$$

the Schroedinger equation

$$\left[E_0 + \frac{\hbar^2 K_\parallel^2}{2M} - \frac{\hbar^2 \nabla^2}{2\mu} \right] F_{\mathbf{K}_\parallel}(\rho) - \tilde{U}(\rho) F_{\mathbf{K}_\parallel}(\rho) = E_{\mathbf{K}}^{exc} F_{\mathbf{K}_\parallel}(\rho), \tag{2.29}$$

where

$$\tilde{U}(\rho = \rho_1 - \rho_2) = \int dz_1 dz_2 \frac{e^2}{\epsilon_\infty |\mathbf{r_1} - \mathbf{r_2}|} |f_v(z_1)|^2 |f_c(z_2)|^2 \tag{2.30}$$

is the electron-hole direct Coulomb interaction, weighted by the envelope functions $f_{c,v}(z)$. In the limit where the confinement length is much shorter than the exciton Bohr radius, we can replace $f_{c,v}(z)$ with delta-functions. In this case, we recover a purely two dimensional hydrogenic problem. We mention that this calculation predicts a binding energy of the lowest energy exciton state four times larger than the corresponding quantity in the 3-D case [Haug 90].

It is important to remark that, in real systems, structural disorder is present and it destroys the translational invariance. This effect is particularly important in quantum wells and it reflects on the physics of excitons [Zimmermann 95, Zimmermann 03]. Therefore, the most general expression of the exciton state in real systems is a linear superposition of several wave functions (2.27) having different wave vector.

In the next subsection we will see how the concept of semiconductor exciton has to be generalized by taking into account the presence of the external electromagnetic field.

2.1.3 Exciton Polaritons

In this subsection we will show that the normal excitation modes of a semiconductor structure are not simply the exciton states, but the polariton modes, i.e. states arising from the strong coupling between the excitons and the electromagnetic field.

First, we briefly discuss why the solution of Hamiltonian (2.1), derived in the previous subsections, does not describe completely the problem. To this purpose, we consider for a moment the effect of the spin, neglected up to now, and we focus on the exciton modes which are optically active in a bulk semiconductor (i.e. having total spin equal to 1). The different projections of the spin of the exciton modes correspond to longitudinal or transverse polarization with respect to the motion of the exciton center of mass. As we have mentioned before, these two polarizations are not degenerate in energy, because of the exchange electron-hole Coulomb interaction [Andreani 88]. On the other hand, we know that, for symmetry reasons, in cubic crystals, the true eigenstates of the system have to be threefold degenerate at $\mathbf{k} = \mathbf{0}$. This apparent contradiction is explained by the fact that the exciton states are not the eigenstates of the system for small wave vectors. Intuitively, this fact is not surprising because the creation of an exciton population induces a polarization in the medium. Therefore the full Hamiltonian of the system has to include a term describing the interaction between excitons and the electromagnetic field, which has been neglected up to now. The inclusion of this term is crucial because the transverse component of the electromagnetic field results to be *strongly coupled* with the transverse exciton states with wave vectors $k \leq n\omega/c$, where ω is the frequency of the field, n the refraction index and c the light velocity [Andreani 88].[3]

Such a coupling mechanism results in two new eigenstates of the system, called lower and upper polariton states [Hopfield 58, Agranovich 66, Quattropani 86, Andreani 94], each one twofold degenerate by polarization. It turns out that the upper polariton states are degenerate with the longitudinal exciton mode at $\mathbf{k} = 0$, thus permitting to recover the required symmetry property.

To derive the polariton states in a bulk semiconductor, the starting point is the minimal coupling expression of the radiation-matter interaction

$$H_i = -\frac{e}{mc} \sum_i \mathbf{A}(\mathbf{x}_i) \cdot \mathbf{p}_i + \frac{e^2}{mc^2} \sum_i \mathbf{A}^2(\mathbf{x}_i), \qquad (2.31)$$

where the sum is over all the electrons of the crystal, $\mathbf{A}$ is the electromagnetic vector potential while $\mathbf{p}_i$ is the momentum of the electron. To write in the second quantization formalism the Hamiltonian (2.31), we introduce the second quantization expression of the electromagnetic field

$$\mathbf{A}(\mathbf{x}) = \sum_{\mathbf{k}} \sqrt{\frac{2\pi\hbar c}{nV|\mathbf{k}|}} \hat{\epsilon}_{\mathbf{k}} e^{i\mathbf{k}\cdot\mathbf{x}} \hat{c}_{\mathbf{k}}^\dagger + h.c., \qquad (2.32)$$

where $\hat{c}_{\mathbf{k}}$ is the operator which destroys a photon with wave vector $\mathbf{k}$, $\hat{\epsilon}_{\mathbf{k}}$ is the polarization vector of the field and $\sqrt{\frac{2\pi\hbar c}{nV|\mathbf{k}|}}$ is the factor accounting for the proper density of states. The total exciton-photon Hamiltonian is finally obtained by calculating the matrix elements

$$\langle 0|\mathbf{A}(\mathbf{x}_i) \cdot \mathbf{v}_i|\Phi_{\mathbf{k}}^{exc}\rangle = \frac{1}{i\hbar} \langle 0|\mathbf{A}(\mathbf{x}_i) \cdot [\mathbf{x}_i, H_{exc}]|\Phi_{\mathbf{k}}^{exc}\rangle, \qquad (2.33)$$

between the electronic many-body ground-state and the exciton state $|\Phi_{\mathbf{k}}^{exc}\rangle$, and

$$\langle 0|\mathbf{A}^2(\mathbf{x}_i)|0\rangle = \frac{1}{i\hbar} \sum_{\mathbf{k}} \langle 0|[\mathbf{A}(\mathbf{x}_i)\mathbf{x}_i, \mathbf{A}(\mathbf{x}_i)\mathbf{v}_i|\Phi_{\mathbf{k}}^{exc}\rangle, \qquad (2.34)$$

---

[3]Here, *strongly coupled* means that the effect of coupling cannot be treated via a perturbation approach. We will see in the next subsection that, in the case of quantum well excitons coupled to the microcavity photon field, the strong coupling regime occurs only if the coupling strength is much larger than the linewidth of the cavity mode.

and reads [Quattropani 86]

$$\hat{H}_{XC} = \sum_{\mathbf{k}} E_{\mathbf{k}}^{exc}\hat{b}_{\mathbf{k}}^{\dagger}\hat{b}_{\mathbf{k}} + \sum_{\mathbf{k}} \hbar c|\mathbf{k}|\hat{c}_{\mathbf{k}}^{\dagger}\hat{c}_{\mathbf{k}} \qquad (2.35)$$
$$+i\sum_{\mathbf{k}} \Omega_{\mathbf{k}}(\hat{c}_{\mathbf{k}}^{\dagger} + \hat{c}_{-\mathbf{k}})(\hat{b}_{-\mathbf{k}} - \hat{b}_{\mathbf{k}}^{\dagger}) + \sum_{\mathbf{k}} S_{\mathbf{k}}(\hat{c}_{\mathbf{k}}^{\dagger} + \hat{c}_{-\mathbf{k}})(\hat{c}_{\mathbf{k}}^{\dagger} + \hat{c}_{-\mathbf{k}}),$$

where the quantity

$$\Omega_{\mathbf{k}} = E_{\mathbf{k}}^{exc}\sqrt{\frac{2\pi n}{c\hbar k}}F_{\mathbf{k}}(\mathbf{r} = 0)\hat{\epsilon}_{\mathbf{k}} \cdot \mu_{cv} \qquad (2.36)$$

represents the exciton-photon coupling strength, while $S_{\mathbf{k}} = \frac{|\Omega_{\mathbf{k}}|^2}{E_{\mathbf{k}}^{exc}}$. In Eq. (2.36), $F_{\mathbf{k}}(\mathbf{r})$ is the Fourier transform of the exciton envelope function, defined in Eq. (2.19) and

$$\mu_{cv} = \int_{V_0} \mathbf{r}u_c^*(\mathbf{r})e\mathbf{r}u_v(\mathbf{r}) \qquad (2.37)$$

is the dipole matrix element between the conduction and the valence band, evaluated inside each elementary cell V_0. The compact form of the matrix element (2.36) is a direct consequence of the band and envelope function approximations. We stress that this latter limit is valid when the Bohr radius of the exciton is much larger than the lattice parameter. Eq. (2.36) has a simple interpretation. While the scalar product $\hat{\epsilon}_{\mathbf{k}} \cdot \mu_{vc}$ describes the coupling between the electromagnetic field and the exciton dipole field inside each elementary cell, the amplitude $F_{\mathbf{k}}(\mathbf{r} = 0)$ weights the probability to have one electron and one hole at the same position.

Hamiltonian (2.36) essentially describes two coupled oscillators. It clearly conserves the wave vector and so each term of the sum can be diagonalized separately. In the 3-D case, each contribution is quadratic and it is diagonalized exactly via the so called Hopfield transformation of the operators [Hopfield 58, Quattropani 86]. The resulting eigenmodes are the lower and upper polariton states, shown in Fig. 2.1. At $\mathbf{k} = 0$, the upper polariton and the longitudinal exciton mode are degenerate, proving that the exciton-photon coupling is exactly equal to the LT splitting at $\mathbf{k} = 0$. For increasing wave vectors, the lower polariton mode tends to the unperturbed transverse exciton mode, while the upper polariton mode tend to the electromagnetic mode. These results are in perfect agreement with the experimental observation, shown in Fig. 2.2. In particular we stress that, due to momentum conservation, each polariton state is given by the superposition of *one exciton state and one photon state*. Since *only one* photon mode contributes to the polariton mode, the coupling with the electromagnetic field does not introduce any additional dissipation. Consequently polaritons are stationary modes propagating in the crystal. This fact suggests the interpretation of polaritons as hybrid exciton-photon quasi-particles.

It is useful to make some additional comments about the form of Hamiltonian (2.36). First of all, we notice that the term proportional to $\mathbf{A}^2$ is typically negligible because the matrix elements $S_{\mathbf{k}}$ are much smaller than $\Omega_{\mathbf{k}}$, since $\Omega_{\mathbf{k}} \sim 10$ meV, while $E_{\mathbf{k}}^{exc} \sim 1.5$ eV. Second, the Hamiltonian (2.36) contains anharmonic terms, which do not conserve the number of excitations. These terms are responsible for two phenomena, i.e. the intrinsic *squeezing* of the polariton states and the renormalization of the HF vacuum state. The *squeezing* is the possibility to reduce below the quantum limit the uncertainty on the phase or on the amplitude of a quantum field, whereas the fluctuations in the other observable become larger than this limit. Squeezing of bulk polaritons has been predicted [Schwendimann 93] but never detected experimentally. The renormalization of the vacuum state is due to the fact that the true
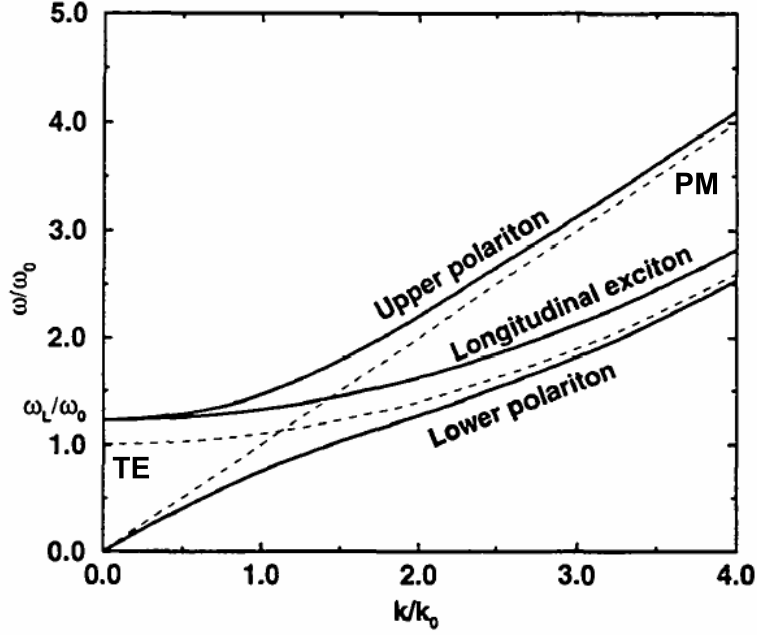
Figure 2.1: Calculated dispersion of the lower and upper polariton and of the longitudinal exciton mode (solid lines), compared with the dispersion of the transverse exciton mode (TE) and of the photon mode (PM). Here $k_0 = nE_0^{exc}/\hbar c$. From Ref. [Savona 97].
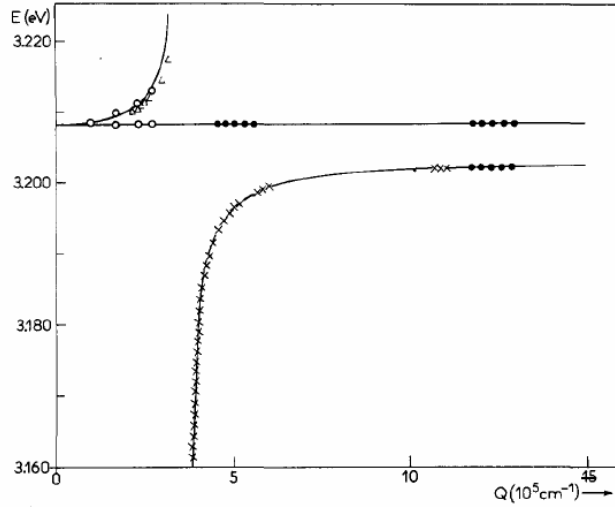
Figure 2.2: Experimental polariton dispersion for excitons in CuCl, obtained by two photon absorption (circles) and hyper-Raman scattering (dots and crosses) and reported in Ref. [Honerlage 85].

ground state of Hamiltonian (2.36) includes virtual processes where exciton-photon pairs are spontaneously created and reabsorbed.

In this subsection we have seen that the bulk polariton modes are the eigenmodes of a system of two coupled oscillators. In the next subsection we will see how the polariton physics can be recovered in two-dimensional artificial structures.

21

2.1.4 Microcavity Polaritons

In this subsection we discuss how the polariton physics is translated to the two-dimensional case. We will show that, due to the artificial confinement of both the exciton and the photon fields in two dimensions, microcavity polaritons can be considered as *2-D bulk polaritons*.

In the previous subsection, we have seen that the conservation of the total wave vector **k** imposes that each exciton mode be coupled only to one photon mode. On the other hand, in a quantum well the total wave vector in not conserved and, consequently, an exciton with in-plane wave vector $\mathbf{k}_\parallel$ can be created via the absorption (or recombine via the emission) of a photon with the same $\mathbf{k}_\parallel$ but many different values k_z of the orthogonal component of the wave vector. Thus, the discrete quantum well exciton modes are coupled to the continuum of photon modes. The resulting polariton mode is a resonance in a continuum. Since for a bare quantum well the density of photon modes at varying k_z is very broad, the exciton-photon coupling reduces to a small perturbation, only introducing the finite lifetime of the excitations, and the polariton modes result to be a small correction of the exciton modes [Andreani 94].

Clearly the reason for this behavior resides in the different dimensionality of the quantum well excitons, which are two-dimensional, and the electromagnetic field, which is three-dimensional. Therefore, to recover the bulk behavior in a 2-D situation, it is necessary to reduce the dimensionality of the electromagnetic field, i.e. to confine photons in a two-dimensional structure.

The simpler way to realize such a confinement is by means of a Fabry-Pérot resonator. The general idea is that in a ideal Fabry-Perot resonator, the light is perfectly reflected by two parallel mirrors and an electromagnetic mode with in-plane wave vector $\mathbf{k}_\parallel$ and frequency ω can exist inside the cavity only if the component k_z satisfies the condition

$$\sqrt{\frac{\omega^2}{c^2} n_{cav}^2 - |\mathbf{k}_\parallel|^2} \equiv k_z = N \frac{\pi}{L_c} \,, \tag{2.38}$$

where n_{cav} is the refraction index and L_c the width of the cavity. Due to the condition (2.38), only discrete values of k_z are admitted. In this situation, the one-to-one coupling between the exciton and the photon modes would be essentially restored, because only one discrete photon mode could possibly result enough close in energy to the exciton resonance. Nevertheless, this ideal condition can be only approached in real systems, but never achieved, because real mirrors are never perfectly reflecting. Consequently, for real systems, the component k_z of the confined electromagnetic field has to be always considered as a continuous variable, taking values accordingly to a distribution peaked around the cavity resonance.

The most efficient realization of the ideal mechanism of confinement is given by semiconductor based microcavities, whose scheme is sketched in Fig. 2.3. In a semiconductor microcavity the mirrors are constituted by stacks of semiconductor $\lambda/4$-layers with alternating refraction indices (interferential mirrors), called Distributed Bragg Reflectors (DBR). The number of these mirrors is usually different for the left and the right side of the cavity. Between the mirrors a dielectric material, called "spacer" layer is present. Finally, one or more semiconductor quantum wells can be embedded inside the microcavity. The crucial property of these structures is that the reflectivity R of DBR is very close to one within a large frequency region, called stop-band, resulting in finesse factors $F = \pi R/(1-R)^2$ up to 5000 [Stanley 94]. Consequently the cavity resonance can be very sharp. In addition, the microcavity can be designed in order to have the optical mode roughly in resonance with the quantum well exciton mode. The resulting resonances of these structures are microcavity polaritons, experimentally characterized for the first time in 1992 [Weisbuch 92]. The finite width of the cavity resonance
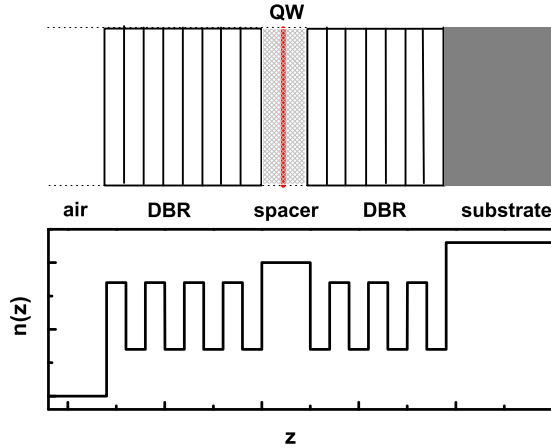
Figure 2.3: Schematic of a quantum well (vertical red solid line) embedded in a planar semiconductor microcavity. The spatial dielectric profile $n(z)$ in the z-direction is also shown. Notice that, as displayed in figure, real semiconductor microcavities usually have the substrate on one side and the air on the other side.

is directly related to the finite lifetime of the photon, the photon mode becoming stationary in the limit of a delta-peaked resonance. Correspondingly, the microcavity polariton has a finite radiative lifetime τ, because it has a finite probability to transform into a photon outside the cavity. The finite polariton lifetime is an intrinsic property in the 2-D case. On the other hand, in the 3-D case, the polariton lifetime is an extrinsic property depending either on the degree of impurity and on the finite size of the system.

Microcavity polaritons has been studied either within a semiclassical treatment [Chen 95, Savona 95] and by means of a quantum theory allowing for the diagonalization of the total Hamiltonian of the coupled exciton and radiation fields [Savona 96]. Since this latter is the more useful picture for our purposes, here we only sketch the quantum approach, reporting the main steps and results of the theory developed in Ref. [Savona 96] and discussing the crucial implication on the possible condensation of polaritons.

In order to write the exciton-photon Hamiltonian, we need to express the electromagnetic modes of the microcavity. By using the translational symmetry, the electric field with in-plane wave vector $\mathbf{k}_\parallel$ and frequency ω is written as

$$\mathbf{E_k}(\mathbf{r}, z) = \hat{\epsilon}_\mathbf{k} U_\mathbf{k}(z) e^{i\mathbf{k}_\parallel \cdot \mathbf{r}}, \tag{2.39}$$

where $\hat{\epsilon}_\mathbf{k}$ is the polarization vector. The function $U_\mathbf{k}$ satisfies the Maxwell's differential equation

$$\frac{d^2 U_\mathbf{k}(z)}{dz^2} + \left(\frac{\omega^2}{c^2} \varepsilon(z) - |\mathbf{k}_\parallel|^2 \right) U_\mathbf{k}(z) = 0, \tag{2.40}$$

where $\varepsilon(z)$ indicates the space-dependent dielectric constant. The equation (2.40) admits two degenerate orthogonal solutions $U_{j,\mathbf{k}_\parallel,k_z}$, $j = 1, 2$, for each of the two polarizations. Here and in what follows, we do not indicate the polarization dependence. The cavity electromagnetic modes enter in the microcavity polariton Hamiltonian which, in perfect analogy with the bulk

Hamiltonian Eq. (2.36), reads

$$
\begin{aligned}
\hat{H}_{XC} &= \hat{H}_X + \hat{H}_C + \hat{H}_{int} \\
&= \sum_{\mathbf{k}_\parallel} E^{exc}_{\mathbf{k}_\parallel} \hat{b}^\dagger_{\mathbf{k}_\parallel} \hat{b}_{\mathbf{k}_\parallel} + \sum_{j=1,2} \sum_{\mathbf{k}_\parallel} \int_0^\infty dk_z \hbar \frac{c}{n_{cav}} (|\mathbf{k}_\parallel|^2 + k_z^2)^{1/2} \hat{c}^\dagger_{j,\mathbf{k}_\parallel,k_z} \hat{c}_{j,\mathbf{k}_\parallel,k_z} \\
&\quad + i \sum_{j=1,2} \sum_{\mathbf{k}_\parallel} \int_0^\infty dk_z \Omega_{j,\mathbf{k}_\parallel,k_z} (\hat{c}^\dagger_{j,\mathbf{k}_\parallel,k_z} + \hat{c}_{j,-\mathbf{k}_\parallel,k_z})(\hat{b}_{-\mathbf{k}_\parallel} - \hat{b}^\dagger_{\mathbf{k}_\parallel}) \\
&\quad + \sum_{j,j'} \sum_{\mathbf{k}_\parallel} \int_0^\infty dk_z dk'_z S_{j,j',\mathbf{k}_\parallel,k_z,k'_z} (\hat{c}^\dagger_{j,\mathbf{k}_\parallel,k_z} + \hat{c}_{j,-\mathbf{k}_\parallel,k_z})(\hat{c}^\dagger_{j',-\mathbf{k}_\parallel,k'_z} + \hat{c}_{j',\mathbf{k}_\parallel,k'_z}), \quad (2.41)
\end{aligned}
$$

where

$$
S_{j,j',\mathbf{k}_\parallel,k_z,k'_z} = \frac{\Omega_{j,\mathbf{k}_\parallel,k_z} \Omega^*_{j',\mathbf{k}_\parallel,k'_z}}{E^{exc}_{\mathbf{k}_\parallel}} \tag{2.42}
$$

and

$$
\Omega_{j,\mathbf{k}_\parallel,k_z} = \frac{E^{exc}_{\mathbf{k}_\parallel}}{\hbar c} \sqrt{\frac{\hbar v}{|\mathbf{k}|}} F_{\mathbf{k}_\parallel}(0) \hat{\epsilon}_{\mathbf{k}} \cdot \mu_{cv} \int dz U_{j,\mathbf{k}_\parallel,k_z}(z) \rho(z), \tag{2.43}
$$

where μ_{cv} is the dipole matrix element between the valence and the conduction band in an elementary cell, defined as in the bulk case, $F_{\mathbf{k}_\parallel}(\mathbf{r})$ is the exciton envelope function in the plane of the quantum well and $\rho(z) = f_c(z)f_v(z)$ is the exciton envelope function in the growth direction [Andreani 94].

Notice that in Hamiltonian (2.41) we treat the sum over k_z in the integral limit, in order to highlight the presence of the continuum. As in the bulk case, the last term of Eq. (2.41), proportional to the square of the electromagnetic field, is very small if compared to the exciton-photon coupling term [Savona 94], $S_{j,j',\mathbf{k}_\parallel,k_z,k'_z} \sim \Omega_{j,\mathbf{k}_\parallel,k_z}/1000$, and it will be neglected in the following analysis. In addition, here we omit the polarization indices, thus restricting to the case of materials where the interaction doesn't introduce polarization mixing, as in the case of heavy-hole excitons in GaAs-based semiconductors. We finally stress the point that the exciton-photon interaction explicitly conserves the in-plane component of the wave vector $\mathbf{k}_\parallel$. Thus we can separately find the resonances for each value of $\mathbf{k}_\parallel$.

The resonances of Hamiltonian (2.41) can be obtained by means of the Green's function formalism. Indeed, the propagator of an exciton with wave vector $\mathbf{k}_\parallel$ obeys the Dyson equation

$$
G^{(ret)}_{\mathbf{k}_\parallel}(E) = \frac{1}{E - E^{exc}_{\mathbf{k}_\parallel} + i\hbar\gamma_x - \hbar\Sigma_{\mathbf{k}_\parallel}(E)}, \tag{2.44}
$$

where we have included an imaginary part $\hbar\gamma_x$, modeling the nonradiative exciton broadening due to all the possible dissipation mechanisms, and the self-energy is

$$
\hbar\Sigma_{\mathbf{k}_\parallel}(E) = \lim_{\eta \to 0} \sum_{j=1,2} \int_0^\infty dk_z |\Omega_{j,\mathbf{k}_\parallel,k_z}|^2 \frac{2\hbar v(|\mathbf{k}_\parallel|^2 + k_z^2)^{1/2}}{(E - i\eta)^2 - \hbar^2 v^2(|\mathbf{k}_\parallel|^2 + k_z^2)}. \tag{2.45}
$$

The two complex poles $E = E^{lp,up}_{\mathbf{k}_\parallel}$ of $G^{(ret)}_{\mathbf{k}_\parallel}(E)$ correspond to the lower and upper polariton modes.

The dispersion relation of the polariton modes can be written analytically, as a function of the reflectivity of the DBR [Savona 96]. This is possible because the Maxwell's equation (2.40), for DBR mirrors, defines a Sturm-Liouville problem, whose solutions have a form which

allows to express analytically the result of the integration over k_z. Nevertheless, we leave aside the exact solution, because we are more interested in deriving an approximated solution in a very compact form, useful for further applications.

Starting from the exact solution, it is possible to show that the self-energy $\hbar\Sigma_{\mathbf{k}_\parallel}(E)$ has a complex pole approximately at $E = \hbar\omega^c_{\mathbf{k}_\parallel} - i\gamma_c$, where

$$\hbar\omega^c_{\mathbf{k}_\parallel} = \hbar\frac{c}{n_{cav}}(|\mathbf{k}_\parallel|^2 + (k_z^{(0)})^2)^{1/2}\,, \tag{2.46}$$

with $k_z^{(0)} = \pi/L_c$, is the energy of the cavity photon mode and

$$\hbar\gamma_c = \hbar\frac{c}{n_{cav}(L_c + L_{DBR})}\frac{(1-\sqrt{R})^2}{2\sqrt{R}} \tag{2.47}$$

is the cavity mode linewidth, L_{DBR} being an effective length estimating the dephasing across the DBR mirror. Therefore, we can expand $\hbar\Sigma_{\mathbf{k}_\parallel}(E)$ in Laurent series around its complex pole. In this way, the dispersion relation for polariton modes is reduced into the compact form

$$(E - E^{exc}_{\mathbf{k}_\parallel} + i\gamma_x)(E - \hbar\omega^c_{\mathbf{k}_\parallel} + i\gamma_c) = \hbar^2\Omega_R^2\,, \tag{2.48}$$

where the quantity $\hbar\Omega_R$ thus defines an effective exciton-photon coupling strength. It is possible to show [Savona 97] that

$$\hbar\Omega_R \simeq \hbar\sqrt{\frac{c\Gamma_0}{n_{cav}(L_c + L_{DBR})}\frac{1+\sqrt{R}}{2\sqrt{R}}}\,, \tag{2.49}$$

where

$$\hbar\Gamma_0 = \frac{2\pi E_0^{exc}}{n_{cav}\hbar c}|F(0)|^2|\mu_{cv}\cdot\hat{\epsilon}_{\mathbf{k}}|^2 \tag{2.50}$$

is the exciton radiative linewidth at $\mathbf{k}_\parallel = 0$, for a bare quantum well [Andreani 94]. It turns out that usually the linewidths are much smaller than the effective coupling strength. Indeed typical values are $\hbar\gamma_x \sim 1 - 100\ \mu$eV and $\hbar\gamma_c \sim 0.1 - 1$ meV, while $\hbar\bar{\Omega} \sim 2 - 15$ meV. Therefore we can interpret Eq. (2.48) as the secular equation associated to the Hamiltonian of two coupled oscillators

$$\hat{H} = \sum_{\mathbf{k}} E^{exc}_{\mathbf{k}_\parallel}\hat{b}^\dagger_{\mathbf{k}}\hat{b}_{\mathbf{k}} + \hbar\omega^c_{\mathbf{k}_\parallel}\hat{c}^\dagger_{\mathbf{k}}\hat{c}_{\mathbf{k}} + \hbar\Omega_R\sum_{\mathbf{k}}(\hat{b}^\dagger_{\mathbf{k}}\hat{c}_{\mathbf{k}} + h.c.)\,, \tag{2.51}$$

thus recovering the same physics of bulk polaritons, with the exception that now polaritons have a finite radiative lifetime.

The two solutions of Eq. (2.48) are

$$E^{lp(up)}_{\mathbf{k}_\parallel} = \frac{1}{2}\left[E^{exc}_{\mathbf{k}_\parallel} + \hbar\omega^c_{\mathbf{k}_\parallel} - i(\gamma_x + \gamma_c)\right] \mp \sqrt{\hbar^2\Omega_R^2 + \frac{1}{4}\left[E^{exc}_{\mathbf{k}_\parallel} - \hbar\omega^c_{\mathbf{k}_\parallel} - i(\gamma_x - \gamma_c)\right]^2}\,, \tag{2.52}$$

In Fig. 2.4, we show the real (a) and the imaginary (b) parts of $E^{lp,up}_{\mathbf{k}}$ using the parameters, $\hbar\Omega_R = 4$ meV, $\hbar\gamma_c = 0.66$ meV, $\hbar\gamma_x = 6.6\ \mu$eV, and for zero exciton-photon detuning. The largest effect of coupling is at $\mathbf{k} = 0$, where the energy splitting between the lower and the upper polariton states is maximum. On the other hand, for large wave vectors, the lower polariton tends to the exciton mode while the upper polariton tends to the photon mode. At $\mathbf{k} = \mathbf{0}$, the lower and the upper polariton have the same linewidth (the equality is the consequence
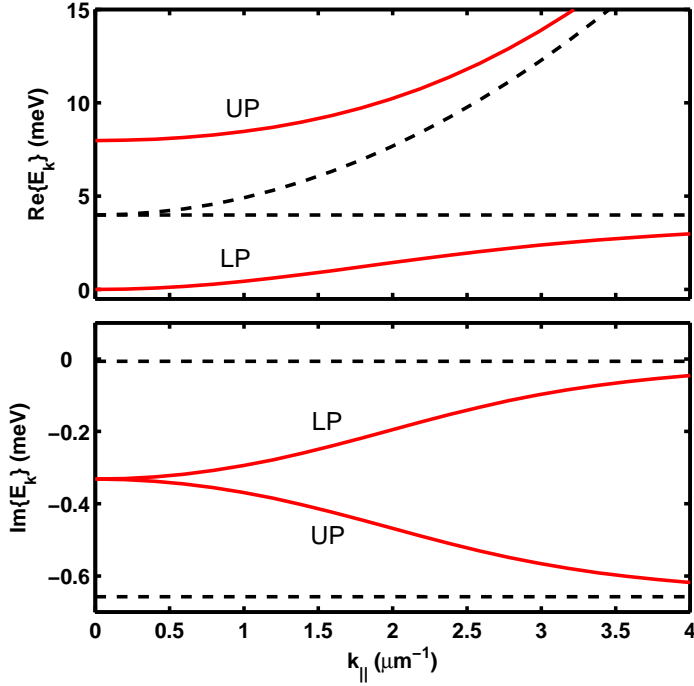
Figure 2.4: (a) Energy dispersion of lower (solid line) and upper (dash-dotted line) microcavity polaritons, compared with the dispersion of the exciton (dotted line) and the cavity photon (dashed line) fields. (b) Imaginary part of the energy of the two polariton, the exciton and the cavity photon modes.

of the zero detuning). For increasing wave vectors, the linewidth of the lower polariton tends to the exciton one, while the linewidth of the upper polariton tends to the cavity photon one. Since the imaginary part of the modes determines the lifetime of polaritons along the energy dispersion, we can conclude that the lowest energy polariton state has a lifetime shorter than the lower polariton excited states. This fact has important consequences in the problem of polariton condensation, because it will deplete the ground state population under steady-state non-resonant pumping, the so called relaxation bottleneck.

In this subsection we have seen that the concept of polariton can be extended to two-dimensional artificial structures confining both the exciton and the photon field, i.e. semiconductor quantum wells embedded in a microcavity. We have shown that the physics of 2-D polaritons is the physics of the damped coupled oscillators. However, up to now, we have overlooked an important aspect of the exciton and polariton problems, i.e. the presence of two-body interactions. In the next subsection, we will see how two-body interactions can be included in our description of the microcavity polariton system.

2.1.5 Effective two-body interaction

In this subsection, we will address to the problem of the exciton two-body interactions, focusing on the 2-D case. We will discuss how an effective interaction Hamiltonian for microcavity polaritons can be obtained.

We have shown via Eq. (2.25) that, for low and moderate density regimes, excitons follow

a quasi-Bose statistics. However, a picture in terms of ideal Bose quasi-particles would be extremely oversimplified for the exciton gas, for two crucial reasons. First, Coulomb interaction acts between the components of different excitons. This interaction is responsible for the exciton-exciton scattering and for the formation of the bound singlet state of two excitons, i.e. the biexciton [Hanamura 77]. Second, excitons are composite particles, as shown by Eq. (2.21), without a defined statistics. Indeed, the fermionic components of the exciton obey the Pauli exclusion principle. Therefore it is not clear if the deviation from the Bose statistics can be included as an effective interaction in a bosonic exciton Hamiltonian. Here we do not discuss in detail this very complicated problem. In fact, two difficulties are present. First, exciton has to be represented as a Bose particle in a consistent way. Second, the nature of composed particle has to be formally written as two-body interaction terms.

There exist works claiming for the formal impossibility of writing a bosonic exciton Hamiltonian, because it would be intrinsically not-Hermitian [Combescot 02]. Nevertheless, many different approaches [Stolz 81, Rochat 00, Okumura 01, Ben-Tabou de Leon 01, Zimmermann 07] have suggested that, at low and moderate densities, excitons can be correctly described by means of an effective bosonic Hamiltonian, provided that the *saturation* terms arising from Pauli exclusion are properly included. All these works agree on the final formal expression of the effective Hamiltonian, the only differences residing in the quantitative values of the matrix elements. Focusing on the 2-D case, the exciton field $\hat{b}_{\mathbf{k}}$ (to simplify the notation, here and in the following equations $\mathbf{k}$ represents the in-plane wave-vector) is considered as an exact Bose field, i.e.

$$[\hat{b}_{\mathbf{k}}, \hat{b}_{\mathbf{k}'}^{\dagger}] = \delta_{\mathbf{k},\mathbf{k}'} . \tag{2.53}$$

Correspondingly the effective interaction Hamiltonian, accounting either for the exciton-exciton scattering and for the coupling with an electromagnetic field, can be written in the general form

$$\hat{H}_{int} = \hat{H}_x + \hat{H}_s, \tag{2.54}$$

where

$$\hat{H}_x = \frac{1}{2A} \sum_{\mathbf{k}\mathbf{k}'\mathbf{q}} v_x(\mathbf{k}, \mathbf{k}', \mathbf{q}) \hat{b}_{\mathbf{k}+\mathbf{q}}^{\dagger} \hat{b}_{\mathbf{k}'-\mathbf{q}}^{\dagger} \hat{b}_{\mathbf{k}'} \hat{b}_{\mathbf{k}} \tag{2.55}$$

is the 2-body exciton term arising from the Coulomb interaction and the Pauli exclusion and

$$\hat{H}_s = \frac{1}{A} \sum_{\mathbf{k}\mathbf{k}'\mathbf{q}} v_s(\mathbf{k}, \mathbf{k}', \mathbf{q}) (\hat{c}_{\mathbf{k}+\mathbf{q}}^{\dagger} \hat{b}_{\mathbf{k}'-\mathbf{q}}^{\dagger} \hat{b}_{\mathbf{k}'} \hat{b}_{\mathbf{k}} + h.c.) \tag{2.56}$$

is the term arising from the coupling with the electromagnetic field. Here A is the system size. We notice that the contribution $\hat{H}_s$ is entirely due to the fermionic saturation. Furthermore the Pauli exclusion also enters in the determination of the contribution $\hat{H}_x$. Both terms are made by a direct and an exchange part [Rochat 00]. In Hamiltonian (2.54) we have omitted the spin. For the full expression accounting for the spin degree of freedom we refer to Ref. [Ben-Tabou de Leon 01, Zimmermann 07].

The term $\hat{H}_x$ describe the Coulomb scattering of two excitons. Having omitted the spin, here we limit to treat the repulsive interaction in the triplet channel, while we are neglecting the spin-flip processes [Zimmermann 07] and the scattering in the singlet channel, which is responsible for the biexciton bound state. Nevertheless we expect that these two latter effects are of minor importance in the diluted regime that we are considering.

The term $\hat{H}_s$ is a mixed term, describing two excitons scattering in one photon and one exciton. This term can be interpreted as the first order correction to the linear exciton-photon

coupling entering in Eq. (2.51). As a matter of fact, if we take the mean field limit

$$\hat{b}_{\mathbf{k}}^{\dagger}\hat{b}_{\mathbf{k}'} \sim \delta_{\mathbf{k},\mathbf{k}'} n_{\mathbf{k}}^{x}, \qquad (2.57)$$

$\hat{H}_s$ becomes

$$\hat{H}_s \sim n_x \sum_{\mathbf{k}} (\hat{c}_{\mathbf{k}}^{\dagger}\hat{b}_{\mathbf{k}} + h.c.), \qquad (2.58)$$

where $n_x = \sum_{\mathbf{k}} n_{\mathbf{k}}^{x}$ is the total exciton density. Therefore we notice that (2.58) represents a correction, scaling with the exciton density, for the linear coupling term. We will see later on that the matrix elements v_s are negative, thus resulting in a net decrease of the effective exciton-photon coupling, for increasing exciton density.

Though the formal expression (2.54) is almost universally accepted in literature, the quantitative value of the scattering matrix elements, $v_x(\mathbf{k}, \mathbf{k}', \mathbf{q})$ and $v_s(\mathbf{k}, \mathbf{k}', \mathbf{q})$, and their momentum dependence, are strongly model dependent. The Hartree-Fock approximation [Hanamura 77, Stolz 81, Zimmermann 88, Ciuti 98] of the Coulomb exciton-exciton scattering problem is known to be very poor. In particular, since screening effects are neglected, the effect of the exciton density is overestimated. Moreover, in the HF limit, the normalization of the exciton wave function is not consistent with the composite nature of excitons [Okumura 01]. A formal tool which allows in principle the derivation of an effective bosonic Hamiltonian at all orders is the Usui transformation [Hanamura 77], resulting in the direct correspondence between the space of fermion pairs (electrons and holes) and the bosonic space of excitons [Rochat 00]. Nevertheless, the Hamiltonian resulting from such a bozonization scheme is usually truncated, by means of a perturbation approach, thus recovering again the HF limit [Rochat 00]. Several approaches beyond the HF approximation have been recently developed. In Ref. [Ben-Tabou de Leon 01] the Hamiltonian is obtained within a systematic expansion in small exciton density. In Ref. [Okumura 01] the Heitler-London (HL) approach is applied to the exciton case, in order to account for a consistent normalization of the exciton wave function. Finally, in Ref. [Zimmermann 07] the HF and HL approaches are extended, including the van der Waals effect.

We mention that, in experiments, it is very difficult to evaluate the correct value of the exciton-exciton scattering matrix element, because only indirect evidence is obtained. For example, one can measure the density dependence of the excitonic blue-shift. For this reason, and since for our present purposes we are only interested in a rough quantitative estimation of the scattering matrix elements, we adopt here the HF result obtained in Ref. [Rochat 00]. Within this approximation, in the zero-momentum limit, the matrix elements tend to the values

$$v_x(0,0,0) = v_x = 6E_b a_0^2, \qquad (2.59)$$

$$v_s(0,0,0) = v_s = -\frac{\hbar\Omega_R}{n_{sat}}, \qquad (2.60)$$

where E_b is the exciton binding energy, a_0 is the exciton Bohr radius, $\hbar\Omega_R$ represents the linear contribution to the coupling strength between the exciton and the photon oscillators, and $n_{sat} = 7/(16\pi a_0^2)$ represents the density at which the total coupling oscillator strength vanishes (see Eq. (2.58)).

Effective interaction for microcavity polaritons

The total exciton-photon Hamiltonian describing the microcavity polariton system can now be obtained by combining Eq. (2.51) and Eq. (2.54). Since in many realistic situations only

the lower polariton branch is significantly populated, it is very useful to derive an effective Hamiltonian restricted to the lower polariton field. This can be obtained straightforwardly, by first diagonalizing the linear Hamiltonian Eq. (2.51) and then by writing the non-linear terms in the polariton basis, by means of the Hopfield transformation Eq. (2.66). By collecting the terms describing scattering processes inside the lower polariton branch, we obtain the effective two-body interaction term

$$\hat{H}_{int}^{lp} = \frac{1}{2} \sum_{\mathbf{k}\mathbf{k'}\mathbf{q}} v_{\mathbf{k}\mathbf{k'}}^{(\mathbf{q})} \hat{p}_{\mathbf{k}+\mathbf{q}}^{\dagger} \hat{p}_{\mathbf{k'}-\mathbf{q}}^{\dagger} \hat{p}_{\mathbf{k'}} \hat{p}_{\mathbf{k}}, \qquad (2.61)$$

where

$$
\begin{aligned}
v_{\mathbf{k}\mathbf{k'}}^{(\mathbf{q})} = {} & \frac{v_x}{A} X_{\mathbf{k}+\mathbf{q}} X_{\mathbf{k'}-\mathbf{q}} X_{\mathbf{k}} X_{\mathbf{k'}} + \\
& + \frac{2|v_s|}{A} X_{\mathbf{k'}-\mathbf{q}} (|C_{\mathbf{k}+\mathbf{q}}| X_{\mathbf{k}} + X_{\mathbf{k}+\mathbf{q}} |C_{\mathbf{k}}|) X_{\mathbf{k'}},
\end{aligned} \qquad (2.62)
$$

is the polariton-polariton scattering matrix element. Here the two contributions arising from the exciton Hamiltonian, written in the limit of contact interactions, are properly weighted by the Hopfield coefficients giving the exciton/photon amount in the lower polariton state, i.e.

$$\hat{p}_{\mathbf{k}} = X_{\mathbf{k}} \hat{b}_{\mathbf{k}} + C_{\mathbf{k}} \hat{c}_{\mathbf{k}} . \qquad (2.63)$$

We notice that both contributions are positive and so the interaction inside the lower polariton branch is repulsive. On the other hand, we mention that the interaction between the lower and the upper polariton branches can also be attractive, if the saturation contribution is larger than the Coulomb contribution [Ciuti 04].

We stress the point that the derivation just performed is strictly valid only at zero exciton density, because the energy and the structure of the polariton states are affected by interactions and so they depend on the density. Therefore, the use of the polariton basis obtained via the diagonalization of the linear Hamiltonian is generally not self-consistent. We will see in Chapter 3 how the interacting polariton problem can be solved in a self-consistent way.

It is worth mentioning that polariton-polariton interaction can produce parametric phenomena, clearly observed in experiments. A brief review of the main experimental signatures of the polariton optical parametric oscillator will be given later on. Now we give a simple theoretical picture of the physics behind the parametric mechanisms. A parametric process is possible when an optical excitation (the laser pump) acting resonantly on the polariton system, produces the macroscopic occupation of a single quantum state. As we will see in the next section, when this condition is accomplished, the system manifests coherence and a classical field can be safely adopted to model the coherent part of the Bose field. Within this approximation the resonantly pumped polariton mode can be expressed by $\hat{p}_{\mathbf{k_p}} = P$, where P is a classical amplitude. Thus the Hamiltonian restricted to the non-pumped states becomes

$$\hat{H}_{mf}^{lp} = \sum_{\mathbf{k}} \left(E_{\mathbf{k}}^{lp} + 2v|P|^2 \right) \hat{p}_{\mathbf{k}}^{\dagger} \hat{p}_{\mathbf{k}} + \frac{v}{2} \left(P^2 \sum_{\mathbf{k}\mathbf{k'}\mathbf{q}} \hat{p}_{\mathbf{k_p}+\mathbf{q}}^{\dagger} \hat{p}_{\mathbf{k_p}-\mathbf{q}}^{\dagger} + h.c. \right), \qquad (2.64)$$

where we assume a constant interaction matrix element v and we neglect the interaction terms linear in P, consistently to our assumptions. In Eq. (2.64), we see that the macroscopic occupation of the pumped mode, results either in a shift of the energy levels, and in processes where two polaritons in the pumped mode scatter in the two states $\mathbf{k_p} - \mathbf{q}$ and $\mathbf{k_p} + \mathbf{q}$. Due

to the peculiar dispersion of the lower polariton (see Fig. 2.4), a set of $\mathbf{k}$ values fulfill energy and momentum conservation in the parametric scattering. In particular, the value of $\mathbf{k_p}$ can be chosen in such a way that the resonant processes have $k = 0$ as final state. Then, for P larger than a threshold value P_{th}, a macroscopic population arises also in the $\mathbf{k} = 0$ state, as a result of the stimulated scattering originated by the bosonic nature of polaritons. Starting from this point, the system behaves as a parametric oscillator between the pump state, the *signal* state at $\mathbf{k} = 0$ and the *idler* state at $2\mathbf{k_p}$. The polariton parametric oscillator shows that the physics of the polariton system is that of an interacting Bose gas out of equilibrium.

In this subsection we have seen how an effective interaction Hamiltonian can be written for microcavity polaritons. This result completes our introduction of the problem. In the next subsection, we will summarize the results obtained in this section, extracting the simplest theoretical framework to describe microcavity polaritons.

2.1.6 Minimal theoretical approach to microcavity polaritons

Making use of the results reviewed in the previous subsections, we have now a very efficient tool to describe the physics of microcavity polaritons and we can focus on the crucial properties of this system.

The exciton and the photon field are treated as Bose fields. The exciton-photon coupling in a microcavity structure is described by the 2-D Hamiltonian of two coupled oscillators

$$\hat{H}_0 = \sum_{\mathbf{k}} \epsilon_{\mathbf{k}}^x \hat{b}_{\mathbf{k}}^\dagger \hat{b}_{\mathbf{k}} + \epsilon_{\mathbf{k}}^c \hat{c}_{\mathbf{k}}^\dagger \hat{c}_{\mathbf{k}} + \hbar\Omega_R \sum_{\mathbf{k}} (\hat{b}_{\mathbf{k}}^\dagger \hat{c}_{\mathbf{k}} + h.c.) \,, \tag{2.65}$$

where $\epsilon_{\mathbf{k}}^{x(c)} = \hbar\omega_{\mathbf{k}}^{x(c)}$ gives the unperturbed exciton (cavity photon) energy, $\mathbf{k}$ labeling the in-plane wave vector of the state, while $\hbar\Omega_R$ represents the effective coupling strength between the two oscillators. The two distinct normal modes of Hamiltonian (2.65), $E_{\mathbf{k}}^{(i)}$ $i = lp, up$, are the lower and the upper polaritons, defined via the Hopfield transformation

$$\hat{p}_{\mathbf{k}}^{(i)} = X_{\mathbf{k}}^{(i)} \hat{b}_{\mathbf{k}} + C_{\mathbf{k}}^{(i)} \hat{c}_{\mathbf{k}} \,, \tag{2.66}$$

where $\hat{p}_{\mathbf{k}}^{(lp,up)}$ thus define a Bose operator destroying a lower or an upper polariton, respectively.

The mutual Coulomb interaction between excitons, and the fermionic nature of the components of the exciton, are accounted for via an effective two-body interaction for the exciton-photon system. Within this contribution, the total exciton-photon Hamiltonian reads

$$\hat{H} = \hat{H}_{lin} + \hat{H}_x + \hat{H}_s \,, \tag{2.67}$$

where

$$\hat{H}_x = \frac{v_x}{2A} \sum_{\mathbf{k}\mathbf{k'}\mathbf{q}} \hat{b}_{\mathbf{k}+\mathbf{q}}^\dagger \hat{b}_{\mathbf{k'}-\mathbf{q}}^\dagger \hat{b}_{\mathbf{k'}} \hat{b}_{\mathbf{k}} \tag{2.68}$$

is the exciton-exciton interaction term while

$$\hat{H}_s = -\frac{\hbar\Omega_R}{n_{sat}A} \sum_{\mathbf{k}\mathbf{k'}\mathbf{q}} \hat{c}_{\mathbf{k}+\mathbf{q}}^\dagger \hat{b}_{\mathbf{k'}-\mathbf{q}}^\dagger \hat{b}_{\mathbf{k'}} \hat{b}_{\mathbf{k}} + h.c. \tag{2.69}$$

represents a saturation term for the exciton-photon coupling.

Hamiltonian (2.67) can be written in the non-interacting polariton basis defined by Eq. (2.66) and restricted to the lower polariton branch to give

$$\hat{H}^{lp} = \sum_{\mathbf{k}} E_{\mathbf{k}} \hat{p}_{\mathbf{k}}^\dagger \hat{p}_{\mathbf{k}} + \frac{1}{2} \sum_{\mathbf{k}\mathbf{k'}\mathbf{q}} v_{\mathbf{k}\mathbf{k'}}^{(\mathbf{q})} \hat{p}_{\mathbf{k}+\mathbf{q}}^\dagger \hat{p}_{\mathbf{k'}-\mathbf{q}}^\dagger \hat{p}_{\mathbf{k'}} \hat{p}_{\mathbf{k}} \,, \tag{2.70}$$

i.e. an effective two-body Hamiltonian for the lower polariton.

Microcavity polaritons have an intrinsically finite lifetime, related to the quality factor of the microcavity. This means that a polariton population in the state $\mathbf{k}$ decays after a finite time τ_k. This decay can be accounted for in the rate equations for the polariton populations

$$\dot{n}_{\mathbf{k}}^{(lp)}(t) = -\frac{i}{\hbar}\langle[\hat{p}_{\mathbf{k}}^{\dagger}(t)\hat{p}_{\mathbf{k}}(t), \hat{H}^{lp}]\rangle - \gamma_{\mathbf{k}}n_{\mathbf{k}}^{(lp)}(t)\,, \qquad (2.71)$$

where the decay rate $\gamma_{\mathbf{k}} = \tau_{\mathbf{k}}^{-1}$ can be safely related to the photonic Hopfield coefficient and the cavity photon lifetime, $\gamma_{\mathbf{k}} = |C_{\mathbf{k}}|^2\gamma_c$.

The problem of the polariton finite lifetime deserves some additional comments. In Fig. 2.4(b) we see that polaritons in the lowest energy state, i.e. lower polaritons at $\mathbf{k} = \mathbf{0}$, have a lifetime much shorter than the lower polariton in the excited states. Therefore, when a polariton population is created[4] somewhere along the polariton dispersion, two different regimes are possible. If the relaxation mechanisms and/or the coupling with an external bath are fast enough, taking place on a time scale much shorter than the lifetime of the lowest state, the occupation of the different states reaches the equilibrium distribution (i.e. the Bose distribution) before polaritons decay. In the opposite case, if all the mechanisms bringing the system towards equilibrium are not fast enough, the polariton decay will occur while the system still lies in a non-thermal configuration. We observe that, also in the case of complete polariton thermalization, the system is never in an equilibrium regime, because of the population decay. Nevertheless, the population distribution can be made stationary, in a steady-state regime, i.e. when a continuous pumping balances the polariton decay. Within this regime, and if complete polariton thermalization is possible, the system can reach a stationary quasi-equilibrium distribution.

It is well known that all the relaxation mechanisms are very poorly effective within the low-energy region of the polariton dispersion and that, for the actual microcavity samples, the radiative lifetime is too close to the typical relaxation time scale to allow a complete thermalization, although recent improvement in this direction have been recently reported [Deng 06]. In particular, the coupling between polaritons and the bath of acoustical phonons is very inefficient, giving rise to a sort of bottleneck in the relaxation process [Tassone 97]. At the same time, the typical dispersion curve of the lower polariton is responsible for an abrupt decrease of the density of states at small wave vectors, resulting in the suppression of the polariton collisions inside this energy region [Doan 05]. While the first property contrasts the thermalization at the sample temperature, the second property hinders the evolution towards an internal equilibrium.

We anticipate that all these features are crucial for the technical realization of polariton BEC. Nevertheless, before discussing the possibility of polariton BEC, and the properties of a polariton condensate, it is instructive to remind the fundamental concepts related to the BEC physics. This will be the argument of the next section.

---

[4]From a practical point of view, the polariton system is connected with the environment via photon absorption and emission. A polariton population can be created only by optically pumping the system. If the pump is in resonance with the polariton energy dispersion, polaritons are directly created in this region of the dispersion. If the pump is strongly non-resonant with the polariton modes, it creates an initial particle-hole excitation at high energy, which rapidly relaxes along the lower polariton dispersion at large wave-vector, via the emission of optical phonons. [Tassone 97]

2.2 Bose-Einstein condensation

In this section we review the history of BEC, focusing on the properties of the weakly interacting Bose gases in three and two dimensions. Since several reviews devoted to this problem have been written [Griffin 95, Dalfovo 99, Leggett 01, Zagrebnov 01, Pitaevskii 03], here we sketch the basic facts which are relevant for the problem of polariton BEC and refer to these reviews for a more complete account of the experimental and theoretical facts behind BEC.

2.2.1 Basic concepts related to the BEC physics

It was in 1924 that S. N. Bose introduced a new statistics to describe the energy distribution of the quanta of light [Bose 24]. In the same year, A. Einstein suggested that a novel phase transition could occur for a gas of *identical bosons*, i.e. particles obeying the Bose statistics [Einstein 24, Einstein 25]. This phase transition consists of the macroscopic occupation of a single microscopic state by an ensemble of these particles. To give an intuitive picture of this phenomenon, in analogy with a classical phase transition, Einstein interprets the formation of a macroscopic population as the *condensation* of a part of the gas. This picture has the important advantage of immediately suggesting that the condensate and the non-condensate population manifest very different behaviors.

Ideal Bose gas

Accordingly to the Bose statistics, a gas of N free noninteracting Bose particles in thermal equilibrium at temperature T is distributed in the wave vector space as

$$N_{\mathbf{k}} = n_B(\epsilon_{\mathbf{k}}) = \frac{1}{e^{\beta(\epsilon_{\mathbf{k}} - \mu)} - 1}, \tag{2.72}$$

where $\epsilon_{\mathbf{k}} = \hbar^2 k^2/(2m)$ is the energy-momentum dispersion of free particles, and $\beta = (k_B T)^{-1}$. The total number of particles

$$\sum_{\mathbf{k}} N_{\mathbf{k}} = N, \tag{2.73}$$

determines the chemical potential μ in (2.72). We see that μ is always smaller than the lowest energy eigenvalue ϵ_0, so as to guarantee that the occupation be finite. Moreover, if μ approaches the value ϵ_0, the occupation of the lowest level N_0 becomes increasingly large. On the other hand, the total occupation in the excited states depends on the density of states, which in turn depends on the dimensionality of the system. For an isotropic system, in the limit of very large size $V = L^d$, we can treat the wave vector as a continuous variable, obtaining

$$\tilde{N} = \sum_{\mathbf{k} \neq 0} N_{\mathbf{k}} \quad \rightarrow \quad \left(\frac{L}{2\pi}\right)^d \Omega_d \int{}' dk k^{d-1} n_B(\epsilon(k))$$

$$= \left(\frac{L}{2\pi}\right)^d \frac{\Omega_d}{2} \left(\frac{2m}{\hbar^2}\right)^{\frac{d}{2}} \int{}' dE E^{(\frac{d}{2}-1)} n_B(E), \tag{2.74}$$

where $\Omega_1 = 1$, $\Omega_d = 2^{(d-1)}\pi$ for $d > 1$, and the prime indicates that the value $k = 0$ is excluded from the integration. If $d = 3$, the density $\tilde{n} = \tilde{N}/V$ remains finite, at finite temperature, also for $\mu = \epsilon_0$. This means that, in the three-dimensional case, the density in the excited states cannot exceed a finite saturation value $n_c/V = \tilde{n}(T, \mu = \epsilon_0)$. This is no more valid for $d = 1, 2$, because, in that case, the density in the excited states $\tilde{n}$ increases indefinitely for $\mu \to \epsilon_0$.

Therefore, for a three dimensional system and for a fixed temperature T, two situations are possible. If the total density n is smaller than n_c, the normalization condition (2.73) is satisfied for $\mu < \epsilon_0$, also in the thermodynamic limit $N, V \to \infty$ with $N/V = $ constant. Consequently the occupation of the lowest energy state N_0 is of order of one and $N_0/V \to 0$ for $V \to \infty$. If on the other hand n is larger than n_c, the exceeding density occupies the lowest energy state in order to fulfill the normalization condition (2.73), and $\mu \to \epsilon_0$, in the thermodynamic limit. In this latter case, the population in the lowest state is an extensive quantity proportional to the system volume and the density N_0/V remains finite also in the thermodynamic limit. Consequently, the ratio N_0/N has a finite value, independent on V, which is called the condensate fraction. It is important to point out that, for a finite volume V and a finite number of particles N, the chemical potential is strictly smaller than ϵ_0 even when the system is condensed. It is only in the thermodynamic limit that $\mu = \epsilon_0$.

We notice that $n_c = n_c(T) \sim T^{3/2}$ depends on temperature. Therefore, for a fixed density n, there exist a critical temperature T_c, such as, if $T < T_c$ then $n > n_c(T)$ and BEC occurs. For an ideal Bose gas, the critical temperature is given by

$$ k_B T_c = \frac{2\pi \hbar^2}{m} \left(\frac{n}{2.612} \right)^{2/3} . \tag{2.75} $$

The idea of critical temperature is generally more useful than the one of critical density, because it can be extended to treat interacting systems. Indeed we will see that the description in terms of weakly interacting gases only apply to very diluted systems, i.e. for densities $na^3 \ll 1$, where a describes the scattering length. Therefore, the concept of critical density can be translated to weakly interacting systems only if, at a given temperature, $n_c a^3 \ll 1$. Furthermore, particles with repulsive interaction probably cannot condense at very high density, due to the too strong repulsion. Nevertheless, the idea of critical density is very useful to treat the problem of polariton BEC, and, for this reason, we have introduced the BEC problem in this way.

By inspection of Eq. (2.74), we see that, for uniform one-dimensional and two-dimensional systems, the transition discussed above is not possible, because the density in the excited states is not limited for T finite. However, in presence of trapping, the density of states is modified with respect to what assumed in Eq. (2.74). In this case, the macroscopic occupation of a single state might be restored also in system with reduced dimensionality [Bagnato 91, Ketterle 96, Lauwers 03]. We will return to this point later on.

Off-Diagonal Long Range Order

For a system of finite size, the above considerations seem to suggest that BEC is just characterized by the quantitative criterion that n_0 be significantly larger than $n_{\mathbf{k} \neq 0}$. This naturally leads to the question whether BEC makes any sense for a finite size system. Now we will see that there is actually a more stringent criterion for BEC, which can be easily extended to non uniform, and eventually interacting systems. To this purpose, we consider a system, whose Hamiltonian admits a set of single-particle eigenstates $|j\rangle$, defined by the energies E_j and wave functions $\phi_j(\mathbf{r})$. We introduce the field operator

$$ \hat{\psi}(\mathbf{r}) = \phi_0(\mathbf{r})\hat{a}_0 + \sum_{j \neq 0} \phi_j(\mathbf{r})\hat{a}_j , \tag{2.76} $$

where $\hat{a}_j$ is the operator which destroys a particle in the state $|j\rangle$ and it obeys Bose commutation rules. The field operator describes the quantum field of the many-body Bose system. Now we

evaluate the one-body density matrix

$$
\begin{aligned}
n(\mathbf{r}, \mathbf{r}') &= \langle \hat{\psi}^\dagger(\mathbf{r}) \hat{\psi}(\mathbf{r}') \rangle = N_0 \phi_0^*(\mathbf{r}) \phi_0(\mathbf{r}') + \sum_{j \neq 0} N_j \phi_j^*(\mathbf{r}) \phi_j(\mathbf{r}') \\
&= n_0(\mathbf{r}, \mathbf{r}') + \tilde{n}(\mathbf{r}, \mathbf{r}')
\end{aligned}
\tag{2.77}
$$

where we have used the orthonormality of the wave functions, and the average $\langle \cdots \rangle$ is taken over the equilibrium state of the system. This quantity describes the correlation between the particle quantum field at two different positions in space. The first contribution in Eq. (2.77) corresponds to the condensate occupation. Obviously this contribution remains finite over distances $s = |\mathbf{r} - \mathbf{r}'|$, comparable to the extension of the condensate wave function. On the other hand, the contribution of the sum tends to zero at large distance, because the contributions of the different states, thermally occupied, cancel out. This is evident, if we consider again the uniform system, i.e. $\phi_j(\mathbf{r}) = L^{-3/2} e^{i \mathbf{k_j} \cdot \mathbf{r}}$, and $\mathbf{k_j} = (2\pi/L) j$, in the thermodynamic limit. In that case, above T_c, n_0 is vanishing and it is easy to show that the one-body density matrix decays with the distance s according to an exponential law, with a characteristic length given by the thermal De Broglie wavelength

$$
\lambda_T = \sqrt{2\pi\hbar^2/(m k_B T)} \,.
\tag{2.78}
$$

This means that for a normal gas, spatial correlations survive only on the scale λ_T, whereas at larger distance the system is uncorrelated as expected for a classical gas. On the other hand, below T_c, the one-body density matrix $n(\mathbf{r}, \mathbf{r}')$ tends to the finite value n_0, in the limit $s \to \infty$. Since the one-body density matrix is equal to the Fourier transform of the momentum distribution $n(\mathbf{k})$ of the particle density, this property is related to the fact that the $\mathbf{k}$-distribution below T_c becomes

$$
N(\mathbf{k}) = N_0 \delta(\mathbf{k}) + \frac{V}{(2\pi)^3} \frac{1}{e^{\beta E(\mathbf{k})} - 1} \,,
\tag{2.79}
$$

i.e. manifests a delta-peak at $\mathbf{k} = 0$. This result allows to state the Penrose-Onsager criterion for BEC [Penrose 56, Pitaevskii 03], stating that a Bose-condensed system is characterized by a finite long-range one-body correlation. This feature, called *Off-Diagonal Long Range Order* or ODLRO, is the true peculiar property of BEC, at the origin of spectacular effects like the matter-wave interference and amplification [Pitaevskii 03]. Since Eq. (2.77) can be written for any system, after having defined a proper single-particle spectrum, the Penrose-Onsager criterion can be extended to confined and interacting systems. However an important restriction exists for confined systems. Indeed, in order to adopt the occurrence of ODLRO as the signature of BEC in a finite size system, we need that the thermal De Broglie wavelength λ_T be much smaller than both the size of the system and the *extension of the condensate wave function*. In addition, it has been recently proven that BEC could occur without formation of ODLRO, in systems where disorder results in a very small localization length [Lenoble 04].

In this subsection we have discussed a general criterion for the definition of BEC, which can be applied to both the ideal and the real interacting gas. In the next subsection we will see that interactions are responsible for important features manifested by a Bose condensate and we will show how they can be accounted for.

The weakly interacting Bose gas

In this subsection we will see that the ideal gas picture is inadequate to describe the crucial properties of BEC and we will discuss the standard approach developed to treat the interactions

in a Bose condensed system. Here, we specialize the analysis to the three dimensional system with repulsive interaction.

We have seen in subsection 2.2.1 that the condensation of a uniform free Bose gas is a pure statistical result, not modifying the parabolic free-particle spectrum of the system. This fact results in the instability of the condensate against local density fluctuations. Indeed any external perturbation, producing a local inhomogeneity, would induce single-particle excitations, thus depleting the condensate and reducing the coherence (see Eq. (2.77)). Such a property is directly related to the incompressibility of the free gas and it is no more valid for real, interacting, systems. Indeed, interactions are responsible for a finite compressibility, resulting in a restoring force against inhomogeneities [Nozières 89, Pitaevskii 03]. Therefore the inclusion of interactions is necessary to correctly describe the properties of the Bose condensed system.

A microscopic approach to the problem of interacting Bose system has been developed only in the case of weak interaction or in the case of very diluted gas. Within these two limits, the treatment can be safely restricted to only include two-particles scattering processes. In particular, the interaction between condensed and non-condensed particles can be accounted for by means of a perturbation scheme [Nozières 89, Pitaevskii 03]. In addition, since in the diluted regime only the long range part of the interaction potential is relevant, the results can be obtained in function of the two-body T-matrix (which, for small momenta, tends to a constant term proportional to the s-wave scattering amplitude), without any dependence on the peculiar form of the interaction potential [Nozières 89, Pitaevskii 03]. This procedure is valid in three dimensions. On the other hand, in two dimensions, the two-body energy dependent T-matrix does not tend to a constant, in the small momenta limit, and it vanishes at zero energies [Morgan 02]. Therefore, in the 2-D case, a self-consistent energy renormalization of the single-particle states is required [Lee 02] to apply an analogous procedure.

We consider the general system described by the two-body Hamiltonian

$$\hat{H} = -\int d\mathbf{r}\hat{\psi}^\dagger(\mathbf{r})\frac{\hbar^2\nabla^2}{2m}\hat{\psi}(\mathbf{r}) + \frac{1}{2}\int d\mathbf{r}d\mathbf{r}'v(\mathbf{r}-\mathbf{r}')\hat{\psi}^\dagger(\mathbf{r})\hat{\psi}^\dagger(\mathbf{r}')\hat{\psi}(\mathbf{r}')\hat{\psi}(\mathbf{r})\,, \qquad (2.80)$$

expressed in terms of the field operator (2.76) and where $v(\mathbf{r}-\mathbf{r}')$ is the microscopic two-body potential. The exact time evolution of the field operator is thus given by the Heisenberg equation

$$i\hbar\frac{\partial}{\partial t}\hat{\psi}(\mathbf{r}) = [\hat{\psi}(\mathbf{r}),\hat{H}] = -\frac{\hbar^2\nabla^2}{2m}\hat{\psi}(\mathbf{r}) + \int d\mathbf{r}'v(\mathbf{r}-\mathbf{r}')\hat{\psi}^\dagger(\mathbf{r}')\hat{\psi}(\mathbf{r}')\hat{\psi}(\mathbf{r})\,. \qquad (2.81)$$

We anticipate that, for a fully Bose condensed system ($N_0 \simeq N$), this exact operator equation tends to a classical limit [Pitaevskii 03]. Indeed, since BEC occurs with the formation of a coherent field, (see Eq. (2.77)), and a coherent field can be approximated by means of a classical field, the field operator can be written as

$$\hat{\psi}(\mathbf{r}) = \psi_0(\mathbf{r}) + \delta\hat{\psi}(\mathbf{r})\,, \qquad (2.82)$$

i.e. as the sum of an extensive classical part $\psi_0(\mathbf{r}) = N^{1/2}\phi_0(\mathbf{r})$, playing the role of the order parameter for the Bose-Einstein phase transition, and an incoherent part represented by the quantum operator $\delta\hat{\psi}(\mathbf{r})$. Thus, within the assumption (2.82), and by neglecting the incoherent contribution, we obtain the Gross-Pitaevskii equation [Pitaevskii 03]

$$i\hbar\frac{\partial}{\partial t}\phi_0(\mathbf{r}) = -\frac{\hbar^2\nabla^2}{2m}\phi_0(\mathbf{r}) + gN|\phi_0(\mathbf{r})|^2\phi_0(\mathbf{r})\,. \qquad (2.83)$$

Here, we have introduced the effective contact interaction strength $g = 4\pi\hbar^2 a/m$, related to the s-wave scattering length a of the true interaction potential.[5] The quantity g is the first order term of the expansion of the energy-dependent two-body T-matrix in the low-momenta limit [Morgan 02]. Eq. (2.83) describes the dynamical evolution of the condensate field. Although the determination of the solutions of (2.83) is not trivial, some properties of the condensate field can be easily extracted. The stationary solution of this equation is found by substituting the evolution $\phi_0(\mathbf{r}, t) = e^{-i\mu t/\hbar}\phi_0(\mathbf{r}, 0)$, defining the condensate energy μ. In particular, if the condensate field is uniform,

$$\mu = \int d\mathbf{r}' v(\mathbf{r} - \mathbf{r}')N|\phi_0(\mathbf{r}')|^2 = gN|\phi_0(\mathbf{r})|^2 \,. \tag{2.84}$$

Consistently with our assumption that all the N particles are in the condensate, the energy of the system is $U = \mu N$ and thus μ is nothing else than the chemical potential, $\mu = \frac{\partial U}{\partial N}$. We stress the important point that, while for the ideal gas the chemical potential is determined by the constraint over the number of particles Eq. (2.73), for the condensed interacting system it is fixed by the interaction energy. Another important result can be immediately derived from the Gross-Pitaevskii equation (2.83). In fact, also in a non uniform geometry like a finite box with Dirichelet boundary conditions $\phi_0(\mathbf{r})|_B = 0$, the lowest energy solution of Eq. (2.83) turns out to be quasi-uniform everywhere apart for an interval of length

$$\xi = \frac{\hbar}{(2mgN)^{1/2}} \,, \tag{2.85}$$

close to the boundaries. The quantity ξ is called *healing length* and it represents the maximal length over which a local inhomogeneity can be admitted by interactions [Nozières 89, Pitaevskii 03]. Obviously, this quantity tends to infinity for the ideal system. This result shows that interaction forces the condensate field towards uniformity.

We now return to the assumption (2.82). It reposes on the fact that the population of the condensate microscopic state is much larger than one: $N_0 \gg 1$. If this is the case, the order of application of the two Bose operators $\hat{a}_0$ and $\hat{a}_0^\dagger$ over the many-body state of the system $|\Phi(N)\rangle$ is of minor importance because

$$\hat{a}_0^\dagger\hat{a}_0|\Phi(N)\rangle = \sqrt{N_0(N_0 - 1)}|\Phi(N)\rangle \simeq \sqrt{N_0(N_0 + 1)}|\Phi(N)\rangle = \hat{a}_0\hat{a}_0^\dagger|\Phi(N)\rangle \,. \tag{2.86}$$

This means that the commutator $[\hat{a}_0, \hat{a}_0^\dagger] = 1$ can be neglected with respect to terms proportional to the condensate population. In other words, the condensate operator,

$$\hat{a}_0 \to N^{1/2} \,, \tag{2.87}$$

is treated as a complex number and, correspondingly, the condensate field as a classical field. This ansatz was introduced by Bogoliubov [Bogoliubov 47], in order to allow the perturbation treatment of the interaction and describe the behavior of the non-condensed particles, whose role has been neglected up to now. To this purpose, Bogoliubov introduced another ansatz for the model Hamiltonian. Actually, since the kinetic energy of the condensate state $\mathbf{k} = 0$ is zero, any interaction term would result too large to be treated as a perturbation of the ground-state

---

[5]We stress the point that the Gross-Pitaevskii equation, i.e. the substitution of the quantum field operator by its classical limit, is only valid if expressed in terms of the contact interaction g. Indeed, the effect of the short range contribution of a realistic potential v would not be correctly described in the present classical limit. On the other hand, the condition of diluteness of the gas allows to characterize the interaction potential only via the resulting s-wave scattering length [Pitaevskii 03].

energy of the non-interacting system. The solution proposed by Bogoliubov was a truncation of the full Hamiltonian (2.80). The idea is that the effect of the mutual interaction inside the condensate (which gives the larger contribution of the interaction energy) can be included in the energy of the ground state, as $U_{gs}^0 = gN_0^2/2V$, while the interaction of condensed particles with particles out of the condensate can be treated as a perturbation. In terms of the excited single particle operators, and by using the relation (2.87), the Bogoliubov Hamiltonian for a uniform system then reads

$$\hat{H} = \frac{g}{2V}N^2 + \frac{g^2}{2}n^2 \sum_{\mathbf{k}\neq 0} \frac{m}{p^2} + \sum_{\mathbf{k}\neq 0} \left\{ \frac{\hbar^2 k^2}{2m} \hat{a}_{\mathbf{k}}^\dagger \hat{a}_{\mathbf{k}} + \frac{gN}{2} \left[2\hat{a}_{\mathbf{k}}^\dagger \hat{a}_{\mathbf{k}} + \left(\hat{a}_{\mathbf{k}}^\dagger \hat{a}_{-\mathbf{k}}^\dagger + h.c. \right) \right] \right\}, \qquad (2.88)$$

where the relation $\hat{a}_0^\dagger \hat{a}_0^\dagger \hat{a}_0 \hat{a}_0 \simeq N^2 - N \sum_{\mathbf{k}} \hat{a}_{\mathbf{k}}^\dagger \hat{a}_{\mathbf{k}}$ has been used, while the second term arises from the expression of the scattering length in the second order Born approximation [Pitaevskii 03]. Since the Hamiltonian (2.88) is quadratic, it is diagonalized via the linear transformation

$$\hat{a}_{\mathbf{k}} = u_{\mathbf{k}} \hat{\alpha}_{\mathbf{k}} + v_{-\mathbf{k}} \hat{\alpha}_{-\mathbf{k}}^\dagger, \qquad (2.89)$$

where $\alpha_{\mathbf{k}}$ are Bose operators and, consequently, $|u_{\mathbf{k}}|^2 - |v_{\mathbf{k}}|^2 = 1$. In terms of the operator $\hat{\alpha}_{\mathbf{k}}$ the Hamiltonian (2.88) takes the diagonal form

$$\hat{H} = U_0 + \sum_{\mathbf{k}\neq 0} E_{\mathbf{k}} \hat{\alpha}_{\mathbf{k}}^\dagger \hat{\alpha}_{\mathbf{k}}, \qquad (2.90)$$

where

$$U_0 = \frac{g}{2V}N^2 + \frac{g^2}{2}n^2 \sum_{\mathbf{k}\neq 0} \frac{m}{p^2} + \frac{1}{2} \sum_{\mathbf{k}\neq 0} \left(E_{\mathbf{k}} - gn - \frac{\hbar^2 k^2}{2m} \right), \qquad (2.91)$$

is the energy of the ground state, corrected by the inclusion of the interaction with the non-condensed particles, $U_0 = U_{gs}^0 + U_{gs}^1$, while

$$E_{\mathbf{k}} = \left[\frac{gn}{m} \hbar^2 k^2 + \left(\frac{\hbar^2 k^2}{2m} \right)^2 \right]^{1/2} \qquad (2.92)$$

is the excitation spectrum of the interacting system. The diagonalization fixes the amplitudes of the Bogoliubov transformation (2.89)

$$u_{\mathbf{k}}, v_{-\mathbf{k}} = \left[\frac{\hbar^2 k^2/2m + gn}{2E_{\mathbf{k}}} \pm \frac{1}{2} \right]^{1/2}. \qquad (2.93)$$

This result shows that the Bose weakly interacting system can be described in terms of free quasi-particles, described by the operators $\hat{\alpha}_{\mathbf{k}}$. Correspondingly, the ground state of the system coincides with the vacuum of quasi-particles. The Bogoliubov spectrum (2.92) is shown in Fig. 2.5. We notice that for small wave vectors, $k < \xi^{-1}$ where ξ is the healing length defined in Eq. (2.85), the excitation spectrum of the system is linear, instead of parabolic as in the ideal case. In other words, the long wavelength excitations are phonon modes, $E_{\mathbf{k}\to 0} = ck$, where $c = \hbar\sqrt{gn/m}$ is the corresponding sound velocity. The linear energy-momentum dispersion of the excitation spectrum is at the basis of the superfluid behavior of a Bose fluid, as pointed out by Landau [Landau 41] and then demonstrated by Bogoliubov within the present microscopic approach. Indeed, if a Bose condensate moves with a velocity $v_s < c$ inside a pipeline, all the accessible excited states $E_{\mathbf{k}}$ have an energy larger than the energy that the condensate and the
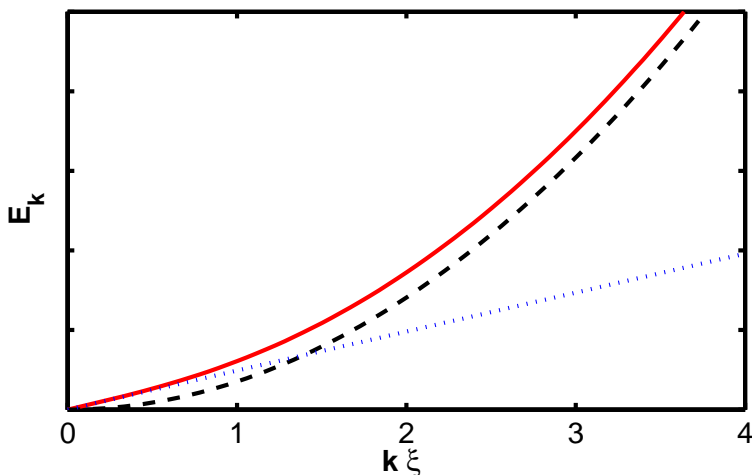
Figure 2.5: Energy dispersion of the Bogoliubov quasi-particle excitations (solid red line) compared with the single-particle dispersion (dashed black line). The dotted blue line highlights the linear behavior at low wave vectors, $k < \xi^{-1}$, where $E_{\mathbf{k}} = ck$, with $c = \hbar\sqrt{gn/m}$.

walls could possibly exchange. Consequently particles cannot be promoted to excited states and the energy dissipation in the flow of the Bose gas is prevented [Bogoliubov 47, Nozières 89, Pitaevskii 03].

The Bogolubov transformation (2.89) shows that a particle out of the condensate can be produced either by creating a quasi-particle (with probability $|u_{\mathbf{k}}|^2$), or by destroying a quasi-particle (with probability $|v_{\mathbf{k}}|^2$). This fact has a deep physical meaning which will become more clear when we will consider the particle propagator, in the next subsection. However, two consequences of this feature are already clear. First, the particle populations differs from the quasi-particle ones. Indeed, since quasi-particles are the true excitations of the system, their occupation follows, per definition, the Bose distribution at the given temperature, i.e.

$$\bar{N}_{\mathbf{k}} \equiv \langle \hat{\alpha}_{\mathbf{k}}^{\dagger} \hat{\alpha}_{\mathbf{k}} \rangle = n_B(E_{\mathbf{k}}). \tag{2.94}$$

On the other hand, the particle occupation does not follow a Bose distribution as in the ideal case but it is given by

$$N_{\mathbf{k}} = \langle \hat{a}_{\mathbf{k}}^{\dagger} \hat{a}_{\mathbf{k}} \rangle = \left(|u_{\mathbf{k}}|^2 + |v_{\mathbf{k}}|^2 \right) \bar{N}_{\mathbf{k}} + |v_{\mathbf{k}}|^2, \tag{2.95}$$

where we have used the relations $|v_{\mathbf{k}}|^2 = |v_{-\mathbf{k}}|^2$ and $\bar{N}_{\mathbf{k}} = \bar{N}_{-\mathbf{k}}$, valid for an isotropic system. In particular we notice that the particle population in the excited states is finite also at zero temperature and equal to $|v_{\mathbf{k}}|^2$. This quantity represents the amount of quantum fluctuations, depleting the condensate also at zero temperature via the relation [Pitaevskii 03]

$$
\begin{aligned}
N_0 &= N - \sum_{\mathbf{k} \neq 0} N_{\mathbf{k}} \\
&\rightarrow N \left(1 - \frac{8}{3\pi}\sqrt{na^3} \right) (T = 0).
\end{aligned}
\tag{2.96}
$$

Second, since the ground state of the system corresponds to the vacuum of quasi-particles, then it doesn't corresponds to the vacuum of excited particles. This means that particles in the excited states *partially* contribute to the ground-state configuration of the system. The amount

of this *partial* anomalous contribution is again determined by the amplitudes $v_{\mathbf{k}}$, which for this reason are usually called the *anomalous components*, the *normal components* $u_{\mathbf{k}}$ representing on the other hand the normal behavior of the excitations. Like the phonon-like spectrum, also the anomalous components are relevant only for long wavelength excitations, as displayed in Fig. 2.6.
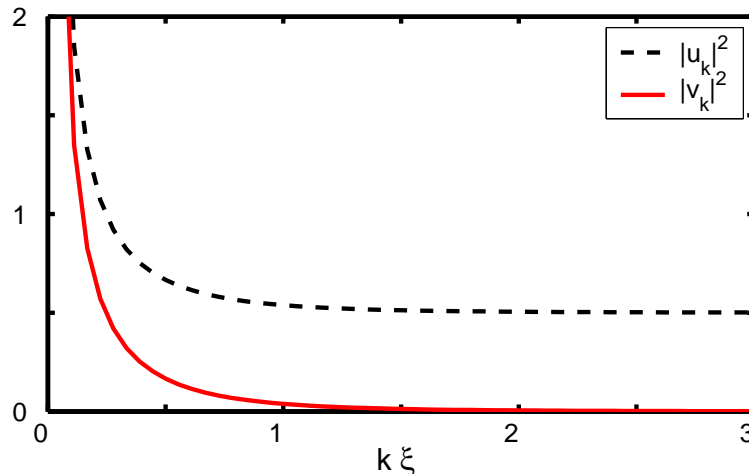

Figure 2.6: Bogoliubov components $|v_{\mathbf{k}}|^2$, $|u_{\mathbf{k}}|^2$, as a function of the rescaled wave vector $k\xi$. The anomalous component becomes negligible for $k > \xi^{-1}$.

It is interesting to notice that the contribution of the excited particles to the one-body density matrix, $\tilde{n}(s)$, manifests a different distance dependence, according to whether the fluctuations have a quantum or a thermal origin. To highlight this behavior, we display in Fig. 2.7 the quantity $\tilde{n}(s)/\tilde{n}(0)$ for the weakly interacting gas at $T = 0$ and for an ideal gas at finite temperature $T < T_c$. We see that, for the thermal fluctuations regime, the characteristic length is the De Broglie length λ_B and the resulting $\tilde{n}^{(1)}(s) \sim s^{-1}$ at large distance, while, for the quantum fluctuations regime, the characteristic length is the healing length ξ and $\tilde{n}^{(1)}(s) \sim s^{-2}$.

To conclude this brief review of the Bogolubov approach, we just mention that, within the Bogoliubov approach, the total energy of the excited non-condensed particles is a well defined quantity. On the other hand, the kinetic and the interaction contributions to the total energy are not well defined in the Bogoliubov limit, due to the behavior of the populations $N_{\mathbf{k}}$ at large momenta, i.e. $N_{\mathbf{k}} \sim k^{-4}$.

Symmetry breaking

We point out that the Bogoliubov ansatz implies that the expectation value

$$\langle \hat{\psi}(\mathbf{r}) \rangle = \psi_0(\mathbf{r}), \tag{2.97}$$

has a well defined phase in the complex plane. The Hamiltonian of the system, however, does not depend on the phase of the order parameter. This broken gauge symmetry is analogous to that emerging from the semiclassical theory of a laser [Mandel 95, DeGiorgio 70, Scully 99, Kocharovsky 00]. A contradiction then arises, as the Heisenberg uncertainty principle states that the expectation values of the phase and of the number of particles cannot be simultaneously determined. The point is that the number of particles in the excited states is no more
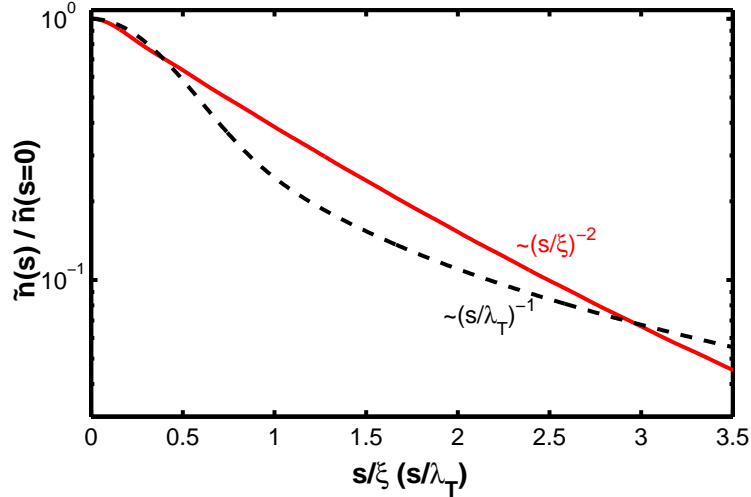
Figure 2.7: Contribution $\tilde{n}(s)$ of the non-condensed particles to the one-body density matrix $n(s) = n_0 + \tilde{n}(s)$, for an interacting gas at $T = 0$ (red solid line) and for the ideal gas at finite temperature (black dashed line). The two functions are renormalized to their value at $s = 0$. The distance is rescaled to the healing length ξ for the interacting case and to the De Broglie wavelength λ_T for the ideal case.

conserved by the Bogoliubov Hamiltonian, as clearly shown by the last two terms of Eq. (2.88). Since the condensate acts as a classical reservoir of particles, excited particles can be created or destroyed by the coupling with this reservoir. In this respect, Eq. (2.96), fixing the number of particles in the condensate and in the excited states, has to be interpreted as a relation between expectation values.

Density and phase fluctuations of the condensate are at the origin of the phenomenon of phase spreading [Lewenstein 96, Svidzinsky 06, Sinatra 07]. We will return to this problem in subsection 2.2.3.

Reduced dimensionality

For the purpose of the present work it is essential to extend our discussion to systems of reduced dimensionality, in particular 2D systems. In one or two dimensions, for the ideal gas, the critical density $N_c(T)$ diverges for any finite temperature. This amounts to the fact that BEC only occurs at $T = 0$ [Pitaevskii 03]. A more general result holds for interacting particles where, according to the Hohenberg-Mermin-Wagner theorem [Hohenberg 67], the thermal fluctuations of the phase of the order parameter destroy the condensate at any finite temperature. As a result, in two dimensions, the one-body density matrix does not approach a constant value at large distance, but vanishes according to a power law [Pitaevskii 03]. This behaviour is still significantly different from that of a normal gas and can be shown to still exhibit the phenomenon of superfluidity below a finite superfluid critical temperature $\tilde{T}_c$ [Popov 72]. This superfluid-normal transition is however not allowed, as another critical phenomenon occurs at temperatures lower than $\tilde{T}_c$ in a 2D system. In two dimensions, a compressible fluid can form free vortices by spending a finite energy. This is not possible in three dimensions where a vortex-line costs a macroscopic energy proportional to its length. Unbound pairs of vortices in two dimensions, however, can only be spontaneously created above a critical temperature T_{BKT} which characterizes the so called Berezinskii-Kosterlitz-Thouless

transition [Kosterlitz 73]. Above T_{BKT} the presence of free vortices results in a nonvanishing friction and the superfluid behaviour disappears. For a two dimensional system the relation $T_{BKT} < \tilde{T}_c$ is always fulfilled and the KBT mechanism is the one determining the transition from a superfluid to a normal phase [Pitaevskii 03].

Spatial confinement

Spatial confinement cannot be neglected when studying the properties of BEC of real diluted atomic gases, as these systems are experimentally prepared in spatial magnetic trap used to increase the gas density. Therefore all the experimental evidence is relative to confined systems. The theory of uniform weakly interacting Bose gases, reviewed above, gives only a qualitative understanding of the physics of these systems. Nevertheless, the nonuniform Bose gas is theoretically described in terms of a quantum-field theory under the same assumptions as in the spatially uniform case but including the effect of a confining potential. To the lowest order in the density of noncondensed particles, this theory reduces to the Gross-Pitaevskii equation (2.83), with an additional term describing the confining potential. This theory successfully describes the spatial and time evolution of the condensate wave function. The main features of BEC, such as a collective excitation spectrum and superfluidity, are also found in the case of confined Bose systems, and confirmed experimentally [Steinhauer 02]. Spatial confinement has also important consequences on the thermodynamics of BEC, modifying the critical temperature and the condensate fraction.

In reduced dimensionality, confinement has a more dramatic effect on the basic properties of BEC and its role is still poorly understood. An ideal trapped one or two-dimensional Bose gas, with a finite number of particles, differently from its spatially uniform counterpart, is expected to undergo BEC at finite temperature [Ketterle 96]. The Hohenberg-Mermin-Wagner theorem in fact applies only to uniform systems. Physically, a confined system has a dramatically reduced density of states and therefore the effects of phase fluctuations, responsible for the absence of BEC, are quenched at low enough temperature. In presence of interactions the physics of BEC in two dimensions is not well understood. From the theoretical point of view, it has been rigorously proven that BEC can occur in an interacting two-dimensional system, provided a finite gap in the one-particle spectrum exists [Lauwers 03]. On the other hand, the experimental observation of the crossover between the BEC regime and the regime dominated by the spontaneous formation of vortices typical of the KBT transition was recently reported [Hadzibabic 06].

In this subsection, we have seen that the fundamental concepts related to the physics of BEC can be discussed on the basis of the standard Bogoliubov approach. However, in order to get a deeper understanding of the BEC features and to give a more realistic description of the phenomenon, theories going beyond the Bogoliubov limit have been developed. In the next subsection we will briefly discuss these theories, showing how some tricky aspects of the Bogoliubov results have a very clear physical meaning.

2.2.2 Equilibrium theory beyond the Bogoliubov approach

In the previous subsection we have briefly discussed the physics of BEC in different geometries. We have also reviewed in some details the Bogoliubov description of the weakly interacting Bose gas in three dimensions. In this subsection we aim to show how the Bogoliubov description can be obtained as a particular limit of a more general quantum field theory approach. To this purpose, we will follow the analysis contained in Ref. [Griffin 96]. The description obtained in this way will allow a better understanding of the BEC properties.

Dyson-Beliaev formalism

We remind that the one-particle propagator is defined by the Green function

$$G(1,2) \equiv G(\mathbf{r}_1, t_1, \mathbf{r}_2, t_2) = \langle \hat{\psi}(\mathbf{r}_1, t_1) \hat{\psi}^\dagger(\mathbf{r}_2, t_2) \rangle \,, \tag{2.98}$$

where the symbol $\langle ... \rangle$ represents the simultaneous operations of time-ordering and averaging [Fetter 71].[6] The free propagator, i.e the one-particle propagator in absence of interactions, is $G_0(1,2)$. Thus, in a general way, the one-particle propagator $G(1,2)$ obeys a Dyson equation

$$G(1,2) = G_0(1,2) + G_0(1,3)\Sigma(3,4)G(4,2) \,, \tag{2.99}$$

where we integrate over the intermediate time-spatial coordinate $\mathbf{r}_{3,4}, t_{3,4}$ and where Σ represents the one-particle self-energy, resulting from interaction. The explicit expression of Σ in terms of the one-particle propagator and of the interaction strength depends on the approximation considered.

In particular, for the interacting Bose gas, below the critical temperature, it is very hard to write a consistent expression for the self-energy Σ, essentially because the usual perturbation approaches fail. As already explained, this is due to the macroscopic occupation of the ground state.

The most suited way to solve this problem is to adopt the separation (2.82) of the field operator in a symmetry breaking classical term describing the condensate plus a quantum operator describing the fluctuation field, i.e. the presence of particles out of the condensate. Within this approximation, the standard quantum field theory scheme is then restricted to only treat excited particles. Accordingly to this separation, which automatically imposes the non-conservation of the number of the excited particles, we need to define the new set of propagators of the excited particles

$$\tilde{G}_{\alpha,\beta}(1,2) = \begin{pmatrix} \tilde{G}_{11} & \tilde{G}_{12} \\ \tilde{G}_{21} & \tilde{G}_{22} \end{pmatrix} \,, \tag{2.100}$$

where

$$\tilde{G}_{11}(1,2) = \langle \delta\hat{\psi}(\mathbf{r}_1, t_1) \delta\hat{\psi}^\dagger(\mathbf{r}_2, t_2) \rangle \tag{2.101}$$

and $\tilde{G}_{22}(1,2) = \tilde{G}_{11}(2,1)$ are the *normal* one-particle propagators, while

$$\tilde{G}_{12}(1,2) = \langle \delta\hat{\psi}(\mathbf{r}_1, t_1) \delta\hat{\psi}(\mathbf{r}_2, t_2) \rangle \tag{2.102}$$

and $\tilde{G}_{21}(1,2) = [\tilde{G}_{12}(1,2)]^*$ are the *anomalous* propagators describing a pair of excited particles scattering in or out of the condensate, respectively. The Green's function matrix $\tilde{G}$ obeys a matrix Dyson equation, the so called Dyson-Beliaev equation [Shi 98]

$$\tilde{G}_{\alpha,\beta}(1,2) = G_0(1,2)\delta_{\alpha,\beta} + G_0(1,3)\tilde{\Sigma}_{\alpha,\gamma}(3,4)\tilde{G}_{\gamma,\beta}(4,2) \,, \tag{2.103}$$

where $\tilde{\Sigma}_{\alpha,\beta}$ is a 2-by-2 self-energy matrix. The diagrams corresponding to Eq. (2.103) are shown in Fig.2.8. As before, the explicit expression of $\tilde{\Sigma}$, depends on which approximation

---

[6]In this subsection, for simplicity, we prefer to leave unspecified if the propagator is taken for real times, or for imaginary times. Indeed, the following analysis can be specified to be applied to both the cases with minor changes. Real time Green functions describe real propagation and they are used to describe the response of the system. For imaginary time Green functions, the average symbol represents the finite temperature average, in the Matsubara formalism. In this case the propagator gives the thermodynamical and the spectral properties of the system.
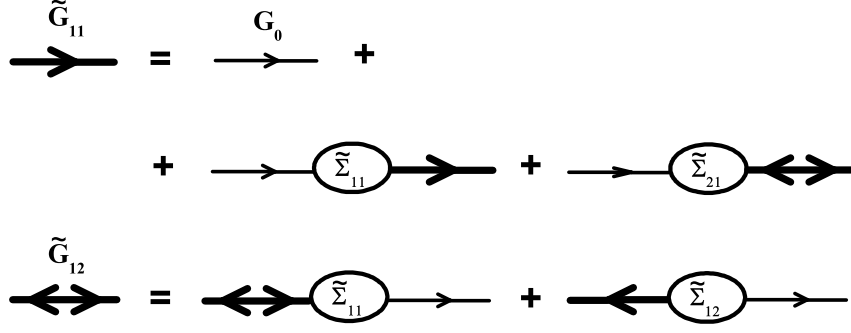
Figure 2.8: Diagrams corresponding to the Dyson-Beliaev equation for excited particles. Thick lines represents self-consistent one-particle propagators, while the thin lines are the free propagators.

has been considered. It is useful to consider the uniform case. In this limit Eq. (2.103) can be expressed in the energy-momentum space as

$$\tilde{G}_{\alpha,\beta}(\mathbf{k}, E) = G_0(\mathbf{k}, E)\delta_{\alpha,\beta} + G_0(\mathbf{k}, E)\tilde{\Sigma}_{\alpha,\gamma}(\mathbf{k}, E)\tilde{G}_{\gamma,\beta}(\mathbf{k}, E) \,. \tag{2.104}$$

For a given $\mathbf{k}$, the four propagators $\tilde{G}_{\alpha,\beta}(\mathbf{k}, E)$ share the same poles, which correspond to the energies $E_{\mathbf{k}}$ of the excitations with respect to the condensate.

Eq. (2.103) is coupled to a time independent equation satisfied by the condensate complex field $\psi_0(1) = \psi_0(\mathbf{r}_1, t_1) = e^{-i\mu t/\hbar}\psi_0(\mathbf{r}_1, 0)$, i.e.

$$\mu\Psi_\alpha(1) = \left[-\frac{\hbar^2\nabla^2}{2m} + V_{ext}(\mathbf{r}_1)\right]\Psi_\alpha(1) + \Sigma^0_{\alpha,\beta}(1, 2)\Psi_\beta(2) \,, \tag{2.105}$$

where $\Psi(1) = (\psi_0(1) \quad \psi_0^*(1))^T$, while the 2 by 2 matrix Σ^0 represents the self-energy of condensed particles. Eq. (2.105) determines the energy of the condensate μ, which plays the role of chemical potential, and which enters in the definition of the unperturbed Green's function G_0

$$\left[i\hbar\frac{\partial}{\partial t_1} + \frac{\hbar^2\nabla_1^2}{2m} - V_{ext}(\mathbf{r}_1) + \mu\right] G_0(1, 2) = \delta(\mathbf{r}_1 - \mathbf{r}_2)\delta(t_1 - t_2) \,. \tag{2.106}$$

Therefore, in order to obtain a consistent one-particle excitation spectrum, the condensate problem (2.105) and the excitation problem (2.103) have to be solved within the same approximation. Quite surprisingly, using the *same approximation* does not correspond to adopting the *same form* for the self energies Σ^0 and $\tilde{\Sigma}$.

Before discussing which general requirements must be satisfied by the self-energies, it is interesting to consider the Bogoliubov limit for the uniform gas already discussed before. Within such a limit, the solution of Eq. (2.104) is

$$\tilde{G}_{11}(\mathbf{k}, E) = \frac{E + \epsilon_{\mathbf{k}} + gn_0}{E^2 - \epsilon_{\mathbf{k}}(\epsilon_{\mathbf{k}} + 2gn_0)}$$

$$\tilde{G}_{12}(\mathbf{k}, E) = \frac{-gn_0}{E^2 - \epsilon_{\mathbf{k}}(\epsilon_{\mathbf{k}} + 2gn_0)} \,, \tag{2.107}$$

where $\epsilon_{\mathbf{k}} = \hbar^2 k^2/2m$ is the energy of a free particles, and $\mu = gn_0$. Therefore, the normal and anomalous one-particle propagators have two poles, at $E = \pm E_{\mathbf{k}} = \pm(\epsilon_{\mathbf{k}}^2 + 2\epsilon gn_0)^{1/2}$, where

$E_{\mathbf{k}}$ coincides with the Bogoliubov quasiparticle energy derived in Eq. (2.92). Furthermore, the spectral function [Fetter 71]

$$A(\mathbf{k}, E) = 2\text{Im}\tilde{G}_{11}(\mathbf{k}, E) = u_{\mathbf{k}}^2 \delta(E - E_{\mathbf{k}}) - v_{\mathbf{k}}^2 \delta(E + E_{\mathbf{k}}) \,, \tag{2.108}$$

where the amplitudes $u_{\mathbf{k}}$, $v_{\mathbf{k}}$ are the same as in Eq. (2.93). This simple result allows to clarify an important point of the BEC physics. In fact, the creation of a non-condensed particle in a Bose condensed system involves a coherent weighted combination of creating an excitation and destroying an excitation. This is due to the many-body nature of the ground state, whose energy is minimized by the presence of non-condensed particles, also at zero temperature (see Eq. (2.96).

The Hugenholtz-Pines theorem and the different approximations beyond Bogoliubov

The exact solution of the coupled problem (2.105)-(2.103) would verify two properties. First, the two-particle propagators, derived from the single-particle ones, would fulfill conservation laws, as the continuity equation. Second, it would result in a *gapless* one-particle spectrum at zero wave vector, i.e. $E_{\mathbf{k}\to 0} = 0$. Indeed this latter property has been proven to rigorously hold for the interacting Bose gas at equilibrium [Hugenholtz 59, Hohenberg 65, Griffin 96] and represents the so-called Hugenholtz-Pines theorem, which is a consequence of the Ward identities [Boyanovsky 02].

It is possible to show that a theory verifies the conservation laws if it is possible to obtain the self-energies Σ^0 and $\tilde{\Sigma}$ by deriving a functional $W[\Psi, \tilde{G}]$ [Griffin 96]

$$\begin{aligned}
\tilde{\Sigma}_{\alpha,\beta}(1, 2) &= \frac{\delta W}{\delta \tilde{G}_{\alpha,\beta}(1, 2)} \\
\Sigma^0_{\alpha,\beta}(1, 2)\Psi_\beta(2) &= \frac{i}{2}\frac{\delta W}{\delta \Psi_\alpha(1)} \,,
\end{aligned} \tag{2.109}$$

where repeated indices are summed. On the other hand, a theory verifies the Hugenholtz-Pines theorem if the self-energies for excited particles, expressed in the energy-momentum space, verify the relation

$$\tilde{\Sigma}_{11}(\mathbf{k} = 0, E = 0) - \tilde{\Sigma}_{12}(\mathbf{k} = 0, E = 0) = \mu \,, \tag{2.110}$$

or, equivalently [Griffin 96], if

$$\tilde{\Sigma}_{\alpha,\beta}(1, 2) = \frac{\delta\left[\Sigma^0_{\alpha,\gamma}(1, 3)\Psi_\gamma(3)\right]}{\delta \Psi_\beta(2)} \,. \tag{2.111}$$

We see that this latter is an additional condition different from (2.109). Consequently, a theory can be conservative but not verify the Hugenholtz-Pines theorem or viceversa. Unfortunately, it is very hard to get approximated theories satisfying simultaneously these two properties [Hohenberg 65, Griffin 96]. This is essentially due to the absence of a well-established renormalized perturbation theory for Bose systems [Hohenberg 65].

Manifestly, the Bogoliubov theory is not conservative, due to the intrinsic asymmetry of the condensate and non-condensate self-energies. However it is gapless, as shown by Eq. (2.92). A self-consistent way to extend the Bogoliubov result by including the effect of excited particles is to apply the self-consistent Wick decomposition procedure to the many-body terms appearing

44

in the equation of motion of the field operator. The mean field limit of such a procedure is the so called Hartree-Fock-Bogoliubov (HFB) approximation, which essentially corresponds to adopt factorizations like

$$\delta\hat{\psi}^\dagger(1)\delta\hat{\psi}(2)\delta\hat{\psi}(3) \simeq \langle\delta\hat{\psi}^\dagger(1)\delta\hat{\psi}(2)\rangle\delta\hat{\psi}(3) + \langle\delta\hat{\psi}^\dagger(1)\delta\hat{\psi}(3)\rangle\delta\hat{\psi}(2) + \langle\delta\hat{\psi}(2)\delta\hat{\psi}(3)\rangle\delta\hat{\psi}^\dagger(1), \quad (2.112)$$

for the products involving the fluctuation field. For a uniform system, the self-energies in the HFB approximation result

$$\tilde{\Sigma}(1,2) = \delta(1-2)g \begin{pmatrix} 2n(\mathbf{r}_1) & m(\mathbf{r}_1) \\ m^*(\mathbf{r}_1) & 2n(\mathbf{r}_1) \end{pmatrix}, \quad (2.113)$$

and

$$\Sigma^0(1,2) = \delta(1-2)g \begin{pmatrix} n(\mathbf{r}_1) + \tilde{n}(\mathbf{r}_1) & \tilde{m}(\mathbf{r}_1) \\ \tilde{m}^*(\mathbf{r}_1) & n(\mathbf{r}_1) + \tilde{n}(\mathbf{r}_1) \end{pmatrix}, \quad (2.114)$$

where

$$\begin{aligned} n(\mathbf{r}) &= |\psi_0(\mathbf{r})|^2 + \tilde{n}(\mathbf{r}) = |\psi_0(\mathbf{r})|^2 + \tilde{G}_{11}(\mathbf{r},t,\mathbf{r},t^+) \\ m(\mathbf{r}) &= \psi_0^2(\mathbf{r}) + \tilde{m}(\mathbf{r}) = \psi_0^2(\mathbf{r}) + \tilde{G}_{12}(\mathbf{r},t,\mathbf{r},t). \end{aligned} \quad (2.115)$$

It is easy to see that the HFB approximation is conservative but it does not verify the
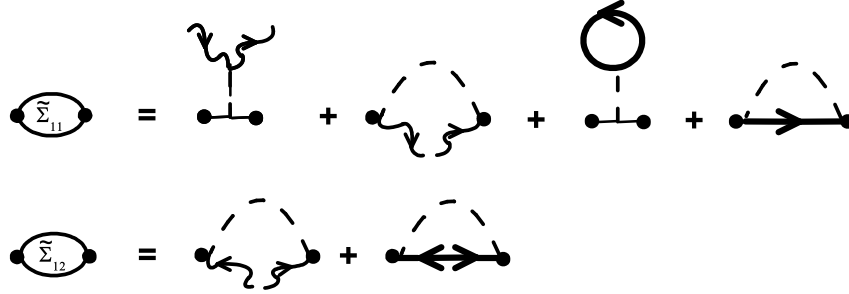

Figure 2.9: Diagrams corresponding to the HFB self-energy $\tilde{\Sigma}$. Thick lines represents self-consistent one-particle propagators, while the wavy lines represent the condensate and the dashed lines the interaction. In $\tilde{\Sigma}_{11}$ we recognize the direct and the exchange term of interaction. The second term in $\tilde{\Sigma}_{12}$ is neglected in the HFP limit.

Hugenholtz-Pines theorem, thus the one-particle spectrum manifests a gap for $\mathbf{k} \to 0$.[7] Actually, to obtain a gapless theory via the Wick's procedure, it is necessary to retain also second order contributions in the interaction, i.e. to adopt the so-called Beliaev approximation [Shi 98]. This suggests that the pathology of the HFB approximation arises from an inconsistent treatment of the order of perturbation. Indeed, the anomalous contribution $g\tilde{m}$, which appears as a first order contribution in the bare perturbation scheme, is in reality of second order because, at the first order, the non-diagonal propagators $\tilde{G}_{12}$ are vanishing. This

---

[7]Nevertheless, the HFB approximation, and in general all the conservative approximations, results in a gapless density fluctuation spectrum, given by the poles of the two-particle propagators. In particular, the HFB density fluctuation spectrum coincides with the result of the Beliaev second order theory. However, a consistent theory, like the Beliaev theory, predicts the same spectrum for the one-particle and the two-particle excitations, as a general result of the spontaneous symmetry breaking [Hohenberg 65].

results in an over counting of this contribution in the HFB approach. The second order terms present in the Beliaev theory are then required to cancel out this over counting.

Though the second order Beliaev theory solves the problems of consistency, it is of hard applicability in realistic cases and at finite temperature [Shi 98]. For this reason several *corrections* of the HFB approximations have been suggested, in order to establish a mean field approach, satisfying the Hugenholtz-Pines theorem and extending at finite temperatures the basic Bogoliubov treatment. The most natural way to obtain this result is to perform the so called Hartree-Fock-Popov (HFP) limit of the HFB approach, consisting in totally neglecting the *dangerous* $\tilde{m}$ terms in the self-energies [Griffin 96]. This approximation is demonstrated to be a good approximation for temperatures not too close to the critical temperature T_c, both above and below T_c. In particular, the spectrum of excitations is in good agreement with the experimental one for $T \leq 0.5 T_c$ [Dodd 98, Liu 04]. Clearly, although not conservative, the HFP approximation has the important advantage of resulting in a physical gapless one-particle spectrum accounting for the presence of non-condensed particles. In this respect, HFP is an improvement of the Bogoliubov theory, and maintains a clear interpretation in terms of interaction diagrams.

Other attempts have been made to derive *by hand* a mean field theory both conservative *and* gapless. We just mention two possible way to realize this idea. The first consists in choosing a proper form for the functional $W[\tilde{G}, \Psi_0]$, which guarantee the fulfillment of relations (2.109) and (2.110) [Kita 06]. This corresponds to partially, but not completely as in HFP, cancel out the effects of the anomalous contribution. However, within this kind of approach, the form of the self-energies is not unique. Furthermore, and more problematic, the BEC transition results as a first order one and the chemical potential is not minimized in the condensed regime [Andersen 04]. The second approach consists in introducing a different chemical potential for the condensed and the non-condensed particles (the spectral gap can be seen as a consequence of assuming the same chemical potential for the two phases) [Yukalov 06]. The condensate chemical potential is then fixed by the requirement that the number of particles in the condensate be fixed. This is an interesting approach pointing out the problem of the conservation of the number of particles. However the assumption of two distinct chemical potentials has not a clear physical meaning for a system at equilibrium. Furthermore, imposing a fixed number of particles in the condensate, seems to be in contradiction with the phase coherence of the condensate.

Finally we just mention a crucial problem arising in the description of BEC around the critical temperature. Indeed, since BEC is a second order phase transition, the real interaction is expected to vanish at the critical temperature, where correlations are expected to become infinite. Clearly, in order to capture this feature, it is necessary to develop a theory accounting for the temperature dependence of the scattering length. Essentially for this purpose, an improved version of the Popov approximation has been realized, treating the interaction in the T-matrix description [Shi 98]. This corresponds to substitute the two-body interaction g, which is temperature independent, with a many-body renormalized interaction, which depends on the energy of the scattering particles and on the temperature. Within the approaches of this kind, it is in principle possible to analyze the properties of the system close to the transition temperature, and to predict the dependence of the critical temperature on the density of the system. However, there is not a general full agreement between the different theories developed up to now.

In this subsection we have briefly discussed the properties and the open problems related to the theoretical description of the condensation of an interacting Bose gas at thermal equilibrium. In the next subsection, we will see that a Bose condensate can be realized in a true

equilibrium regime only in few cases, while usually BEC is obtained in metastable regimes with a finite lifetime. In these conditions, the dynamics of condensation, and in particular the rate of growth of the condensate, become crucial in determining if thermalization and eventually BEC can occur during the metastable regime. In the next subsection, we will briefly discuss non-equilibrium issues, which are of great interest also for the polariton system.

2.2.3 Condensate growth and non-equilibrium

In the previous subsections we have analyzed the features of an interacting Bose gas, in terms of theories assuming thermal equilibrium. Nevertheless, in real systems, thermal equilibrium limit is possible only if the condensate formation is sufficiently rapid. In this subsection we will focus on this point, discussing the problem of condensate growth and evolution. In particular we will give a brief review of the main theoretical approaches used to study this subject. Furthermore, we will discuss the most relevant features related to the deviation from equilibrium.

It is important to remind that, for a Bose gas, condensation is expected to occur well below the temperature of solidification. For these systems, the thermal equilibrium thus coincides with the solid phase. In current experiments on trapped Bose gases, the solidification is prevented only because the gas is very diluted, and isolated from any material wall via magnetic trapping. Indeed in these conditions three-body collisions and consequently molecular recombination are strongly inhibited. Therefore, BEC of a trapped gas can only occur in a metastable regime, whose lifetime is of the order of seconds, depending on the efficiency of molecular recombination [Pitaevskii 03]. The possibility of reaching thermal equilibration and eventually BEC in this period of time, depends on the relaxation rate, which in turn depends on the efficiency of two-body collisions.

Many theoretical efforts have been made to describe the dynamics of condensate formation [Kagan 92, Stoof 92, Griffin 95, Jaksch 97, Gardiner 97b, Gardiner 98, Schmitt 01, Mieck 02, Pitaevskii 03]. A generally accepted result for a weakly interacting Bose gas in three dimensions is that BEC is achieved in more than one step, involving different timescales [Kagan 92, Stoof 92, Griffin 95, Gardiner 98]. In the pioneering works about this subject, two different and in some respect opposite, growth mechanisms were been proposed. Kagan et al. [Kagan 92] suggested the initial formation of a *quasi-condensate*, characterized by the suppression of density fluctuations, but manifesting strong phase fluctuations and thus no phase coherence. This would be the result of the initial global increase of the population in an *ensemble* of low-energy states. Only in a second time, the population is expected to concentrate in a *single* condensate state, thus resulting in the formation of long-range phase coherence. On the other hand, Stoof [Stoof 92] suggested the idea of the *nucleation* of the condensate already in the initial stage stage of condensation. In this picture, a seed of coherent field, stable against phase fluctuations, is formed before the suppression of density fluctuations. Only in the second stage, the condensate population grows according to kinetic equations and density fluctuations are suppressed. In fact, the picture of Kagan et al. [Kagan 92] seems to be supported by experiments [Ritter 07] and by the quantitative predictions of the quantum kinetic theory developed by Gardiner et al. [Gardiner 97b, Gardiner 98]. The main idea of this latter approach is that of separating the spectrum into two energy regions. The high energy region represents the levels occupied by the thermal vapor of incoherent atoms. These energy levels are assumed to be thermally populated and not affected by the possible presence of the condensate. On the other hand, in the low-energy region, the states can be strongly affected by the presence of the condensate and form the so-called *condensate band*. The growth of the population within the *condensate band* is determined by means of a kinetic theory, in terms of quantum Boltzmann

equations modified by including the energy shifts induced by interaction. In particular, within this theory, the equation describing the time dependence of the number N_0 of atoms in the condensate results to be

$$N_0 = 2W^+(N_0)[(1 - e^{(\mu^0(N_0)-\mu)/k_B T})N_0 + 1]\,, \qquad (2.116)$$

where $\mu^0(N_0)$ is the chemical potential of the condensate, determined in the spirit of the Gross-Pitaevskii equation, μ is the chemical potential of the thermal vapor, $\mu^0(N_0) \leq \mu$, and W^+ is an analytically known rate factor [Gardiner 98]. The growth dynamics predicted by Eq. 2.116 can be separated in three stages. In the first one, starting from $N_0 = 0$, the condensate initially grows at a finite rate. At the same time, the population in the other low-energy states also increases, remaining comparable to N_0. The scattering rate which enters in this stage, in the s-wave approximation, is

$$W \simeq 4ma^2/(\pi\hbar^3)\,, \qquad (2.117)$$

where a is the characteristic scattering length of the interacting system. Since the scattering rate is proportional to the mass and to the scattering length, the formation is thus inhibited for very light particles or for very weak interactions. After this kinetic process has taken place, we can argue that the system is still characterized by short-range correlation and large phase fluctuations because the condensate density is vanishing. When N_0 becomes larger than one, the condensate growth becomes exponential, thus resulting in the relaxation of the phase fluctuations and in the formation of a genuine condensate, according to the Penrose-Onsager criterion (see Eq. (2.77)). Finally, for longer times, N_0 reaches its asymptotic equilibrium value, correspondingly to the fact that the condensate chemical potential approaches that of the thermal cloud.

We just mention that the subjects related to the condensate dynamics can also be treated by means of non-equilibrium field theories starting from the formalism resumed in the previous subsection. These theories essentially apply the Kadanoff-Baym [Imamović-Tomasović 99, Nikuni 99, Walser 00], or the Keldish [Stoof 92, Boyanovsky 02] techniques to the Beliaev theory of condensation, resulting in coupled kinetic equations for the condensate and the non-condensate fields. However, these approaches seem to be more appropriate to treat situations where the system is not too far from local equilibrium [Imamović-Tomasović 99].

Furthermore, the quantum kinetic theory developed by Gardiner *et al.* [Gardiner 97b, Gardiner 98], has the interesting property of adopting a Number-conserving approach, i.e. an approach which guarantees that the total number of particles is conserved [Gardiner 97a, Castin 98]. We point out that this property is lost when the condensate field is treated as a pure classical field as in the Bogoliubov ansatz Eq. (2.97) and the $U(1)$ symmetry is broken. Indeed, in this latter case, the number of condensed particles is no longer defined (the condensate represents a classical reservoir). Therefore the number of non-condensed particles is not conserved by the Bogoliubov two-body Hamiltonian, imposing the adoption of the *grand-canonical* statistical ensemble. We remind that already Bogoliubov introduced an alternative approach, preserving the $U(1)$ symmetry of the Hamiltonian and thus not requiring the adoption of the grand-canonical ensemble [Bogoliubov 48, Zagrebnov 01]. Clearly the number-conserving approach is equivalent to the symmetry-breaking one, in determining the thermodynamic properties of the system at equilibrium, like the quasi-particle excitation spectrum [Castin 98]. Nevertheless, it is more suitable for a quantum kinetic treatment of the condensate growth, because it allows a clear distinction between particles and quasi-particles, which can be created or destroyed without a modification of the number of particles [Gardiner 97a]. Furthermore Number-conserving approaches allow a very clear description of other non-equilibrium dynam-

ical features of BEC. We focus in particular on the problems of phase spreading [Castin 98] and condensate instabilities [Castin 97].

The Bogoliubov theory corresponds to linearize the fluctuations around the mean value of the field operator (where the mean value represents the classical condensate field). As shown by Lewenstein and You [Lewenstein 96], this linearization procedure is valid only for times shorter than a characteristic time τ_c. Indeed, the amplitude of quantum fluctuations diverges in time and it is comparable to the amplitude of the condensate field already for $t \sim \tau_c$. This behavior can be interpreted as the quantum phase spreading of the condensate phase.[8] Indeed, the symmetry breaking approach defines the condensate state as a coherent state. However, a coherent state cannot be stationary, because the number of particles is not well-defined. We stress the point that this is in principle true also for an ideal, non-interacting, system [Svidzinsky 06]. At zero temperature, the effect of phase spreading is expected to be maximum, because the fluctuation of the number of condensed particles N_0 is minimum. At finite temperature, the effect is expected to be reduced, because the fluctuations of N_0 are increased [Lewenstein 96]. The role of interactions in determining the phase spreading can be understood simply by considering the Gross-Pitaevskii equation (2.83). If we assume that the phase of the classical field ϕ_0 is fixed at every time, and its evolution is given by (we omit the spatial dependence for simplicity)

$$\phi_0(t) = e^{-i\mu t/\hbar} \phi_0(t=0) \,, \tag{2.118}$$

then we cannot define a fixed number of particles $N = N(t)$ entering in the GPE and consequently the value of μ. In other words, we can only define a probability distribution for the values taken by μ and thus for the subsequent evolution of the phase. Number-conserving theories allow for a more proper interpretation of this phenomenon [Castin 98, Sinatra 07]. In fact, in the Number-conserving approaches the mean value of the field operator is always considered as vanishing, and the quantity defining the time coherence of the condensed system is the time correlation $g_t(\mathbf{r}, \mathbf{r}', t) = G(\mathbf{r}, t, \mathbf{r}', 0)$. If the number of particles in the condensate is fixed, this quantity remains finite for $t \to \infty$, its amplitude being proportional to the condensate population. If, on the other hand, we admit a poissonian distribution of the number of particles in the condensate, centered at $\bar{N}$, the dependence on time turns out to be [Castin 98]

$$g_t(\mathbf{r}, \mathbf{r}', t) \simeq \bar{N} e^{i\mu t/\hbar} e^{-t^2/2\tau_c^2} \phi_0^*(\mathbf{r}) \phi_0(\mathbf{r}') \,, \tag{2.119}$$

for $t(d\mu/dN) \ll 1$. Here, ϕ_0 is the condensate wave function, whose dependence on N_0 has been neglected, μ has been linearized around the mean value $\bar{N}$ and

$$\tau_c = \frac{\hbar}{\sqrt{\bar{\bar{N}}} (d\mu/dN)|_{\bar{N}}} \,. \tag{2.120}$$

This relation shows that the time coherence is expected to be lost for times larger than the *collapse* time τ_c. Since for typical experiments on trapped gases the value of τ_c is much longer than the period of observation, the effect of phase spreading does not affect current measurements [Hall 98, Shin 04]. On the other hand, for BEC confined in a 3-D optical lattice (where in each potential well a coherent superposition of states with different number of condensed particles can be prepared), this phenomenon is clearly visible, strongly affecting the time dependence of the phase correlation [Greiner 02].

---

[8]We just mention that the phase spreading of BEC can also depend on the coupling with the environment [Graham 98].

Another interesting application of the Number-conserving approaches is in determining the dynamical response of a real condensed system under a time-dependent excitation [Castin 97]. In particular, within symmetry breaking theories, it is difficult to distinguish the condensate instabilities with a physical meaning, from the mathematical instabilities due to the introduction of a classical field. For this reason, Number-conserving theories are expected to better predict under which perturbations the condensate will be robust or, conversely, it will be unstable and rapidly depleted. We remind that in the Number-conserving theory the fluctuation operator is defined by [Castin 98]

$$\hat{\Lambda}(\mathbf{r}, t) = \frac{1}{\sqrt{N}} \hat{a}_0^\dagger \delta\hat{\psi}(\mathbf{r}, t), \tag{2.121}$$

where N is the total number of particles, $\hat{a}_0$ is the condensate Bose operator and $\delta\hat{\psi}$ describes the non-condensate field (orthogonal to the condensate wave function ϕ_0). To determine the stability of the condensate we need to know the time evolution of the density of non condensed particles, which can be written using Eq. (2.121) as

$$\delta\rho(\mathbf{r}, t) = \langle \delta\hat{\psi}^\dagger(\mathbf{r}, t)\delta\hat{\psi}(\mathbf{r}, t) \rangle = \langle \hat{\Lambda}^\dagger(\mathbf{r}, t)\hat{\Lambda}(\mathbf{r}, t) \rangle, \tag{2.122}$$

having assumed $N_0/N \simeq 1$. To this purpose, the fluctuation field is expressed in terms of Bose quasi-particle operators $\hat{\alpha}$ via a Bogoliubov transformation

$$\hat{\Lambda}(\mathbf{r}, t) = \sum_j u_j(\mathbf{r}, t)\hat{\alpha}_j + v_j^*(\mathbf{r}, t)\hat{\alpha}_j^\dagger, \tag{2.123}$$

where the quasi-particle states $|j\rangle$ are orthogonal. It is interesting to remark that, in the atomic BEC case, it is usually possible to assume that quasi-particles follow a Bose distribution also in presence of a time-dependent perturbation. This kind of approximation, corresponding to consider an instantaneous thermal rearrangement, allows to directly relate the time evolution of $\delta\rho(\mathbf{r}, t)$ to the time evolution of the modal functions u_j, v_j

$$\delta\rho(\mathbf{r}, t) = \sum_j (|u_j(\mathbf{r}, t)|^2 + |v_j(\mathbf{r}, t)|^2)n_B(E_j) + |v_j(\mathbf{r}, t)|^2. \tag{2.124}$$

We anticipate that this kind of approximation is not possible, in the case of microcavity polaritons, due to their very long thermalization rate. For these reason, we will be adopt a different, and in some respect opposite, approximation to study the polariton condensate depletion in Chapter 4.

In this section we have reviewed the main concepts related to BEC and we have briefly discussed the theories developed for the description of this phenomenon in the general case and in the special case of trapped gases. We can now address the problem of BEC of microcavity polaritons. In the next section, we will review the main experimental evidence, suggesting the occurrence of this phase transition and we will discuss for which reasons polariton BEC is so appealing from a theoretical point of view.

2.3 Experimental evidence of polaritons BEC

The idea of BEC of excitons in solids was formulated about 40 years ago in the works by Moskalenko [Moskalenko 62], Blatt [Blatt 62], and Keldysh and Kozlov [Keldysh 68]. Excitonic BEC was investigated in several systems including bulk semiconductors [Griffin 95, Snoke 90, Snoke 91, Fortin 93] (exciton molecules have also been considered for BEC [Peyghambarian 83, Hasuo 93]), quantum wells [Lozovik 76, Zhu 95, Snoke 02a, Butov 02] and on more exotic systems such as Hall bilayers [Eisenstein 04]. Excitons have basically two properties favoring the possible occurrence of BEC. First, excitons have a very light effective mass, of the order of the free electron mass. Provided thermal equilibrium can be obtained, according to (2.75) this effective mass implies a very high critical temperature for BEC, i.e. $T_c \simeq 2$ K at typical experimental densities $n \simeq 10^{17}$ cm^{-3} (for bulk excitons in Cu$_2$O crystals). Second, due to the charge neutrality, the mutual repulsive interaction in the exciton gas is expected to be much weaker than in the case of liquid systems like superfluid ^{4}He [Ivanov 98]. Nevertheless, excitons have a finite lifetime, ranging from a few picoseconds to microseconds, the longer lifetimes being reached by orthoexciton in Cu$_2$O. As we have discussed in the previous subsection, BEC requires a finite time for the long range correlations to build up, as observed in the atomic case [Ritter 07]. In particular, the rate of formation of a quasi-condensate is proportional to the mass and to the scattering length, as shown in Eq. (2.117). Therefore the light mass, allowing a high critical temperature, has the disadvantage of resulting in a very long condensation time. If this time is comparable or longer than the actual exciton lifetime, BEC cannot be achieved. Exciton equilibrium BEC is therefore only expected in systems where excitons have a very long lifetime, such as ortho- or para-excitons in Cu$_2$O [Snoke 90, Snoke 91, Fortin 93] or indirect excitons in coupled quantum wells [Snoke 02a, Butov 02].

We have seen in subsection 2.1.3 that, especially for bulk semiconductors, excitons cannot be described without taking into account the strong coupling to the electromagnetic field, which result in the polariton modes. In this respect, several authors have proposed the possible occurrence of BEC of bulk polaritons [Hanamura 77, Comte 82, Griffin 95]. To discuss this possibility, it is useful to consider the bulk polariton dispersion E_k displayed in Fig. 2.1. The energy-momentum dispersion of the lowest polariton branch deviates from a quasi-particle behavior at low momentum, where the coupled modes show an anticrossing in the dispersion curves. In this region of energy and momentum the polariton is almost totally photon-like and the linear dispersion of photons holds. Consequently the group velocity of polaritons approaches the light speed and the rate of polariton escape through recombination at the system boundaries increases. A bottleneck effect thus arises at $k \simeq k_0$, as the rate of polariton relaxation through acoustic phonon emission becomes slower than the radiative recombination rate. In steady-state, a polariton population builds up around the bottleneck momentum region $k \simeq k_0$, where photoluminescence is experimentally observed [Andreani 94]. It has been argued by several authors [Keldysh 68, Hanamura 77] that the population buildup at the bottleneck might give rise to BEC. At present, however, no experimental evidence of bulk polariton BEC exists. At the same time, theoretical models of polariton dynamics and interactions seem to suggest that the condensate depletion would occur in a too short time, thus preventing the formation of coherence [Beloussov 96].

The situation is very different for microcavity polaritons, essentially for two reasons, as suggested by the analysis carried out in subsection 2.1.4. First, the exciton amount of the lowest energy polariton states (i.e. the amplitude of the Hopfield coefficients X_k) is non vanishing even for $k \to 0$ and it can be tuned by tuning the frequency of the cavity mode. Second, the photon lifetime can be increased by increasing the quality of the mirrors. This

two features make it possible to significantly reduce the relaxation bottleneck, thus allowing the relaxation of the system up to the lowest energy polariton state. Starting from these ideas, it was in 1996 that Imamoglu *et al.* [Imamoglu 96] first suggested that microcavity polaritons might undergo BEC. In particular, this work was addressed to a possible realization of an exciton laser, operating without population inversion. Indeed, while the realization of a laser of photon-like polaritons requires to reach the usual population inversion regime, in the opposite limit of exciton-like polaritons, the build up of the population in a single polariton mode, with coherent single-mode emission, could be possible without population inversion. The intermediate case was called the *exciton-polariton laser*. Although a rigorous definition of this transition has never been given, it is considered the non-equilibrium BEC of polaritons. The analysis made in subsection 2.1.4 also suggests that microcavity polaritons have other advantages with respect to excitons as possible candidates for BEC. Indeed, the polariton quasi-particle (quadratic) dispersion is consistent with an effective mass, close to $k = 0$, of the order of 10^{-5} times the free electron mass, i.e. much smaller than the effective mass of excitons. Furthermore, the polariton mutual interaction is expected to be weaker than for bare excitons, due to the photonic amount.

Before entering the discussion of the experimental findings, let us comment on the fact that occurrence of polariton BEC is claimed exclusively when the system is nonresonantly excited at high-energy. As we know, BEC is a process where a macroscopic quantum state exhibiting long-range correlation spontaneously forms out of a (thermal) uncorrelated gas of particles. In semiconductors, high-energy excitation of electron-hole pairs is followed by energy relaxation through interaction with a thermal bath of phonons. The initial correlation induced by the excitation laser is thus lost after interaction with the bath, and it can be reasonably assumed that if a correlation is present after population buildup in the lowest energy levels, this is due to the BEC mechanism. In particular, BEC requires the gas thermalization. In this respect, it is important to point out that thermalization can be achieved in two ways, i.e. by the coupling with a bath, and/or by two-body collisions. This latter mechanism is the most efficient for polaritons, because the phase space available for final state in the process of absorption or emission of phonons is very small in the low-energy region of the energy dispersion. As a consequence, the observed polariton effective temperature (extracted by the occupation energy distribution) is typically larger than the sample temperature [Deng 03, Kasprzak 06, Balili 07].

The resonant laser excitation of low energy levels can also be used to form and study coherence properties of the polariton gas, which in this case can be considered as an example of highly non-equilibrium Bose-Einstein condensate. We will discuss this situation in subsection 2.3.1.

Just after the work by Imamoglu et al., it was generally accepted within the polariton community that the required condition to observe polariton BEC would be the achievement of bosonic final-state stimulation and the consequent population build up at $k = 0$. In reality, as we have seen in section 2.2.3, the population buildup is only the first step towards BEC, the only clear signature of the occurred phase transition being the formation of long-range correlations. Nevertheless, pioneering experiments have been addressed only to observe final state stimulation and lowest energy occupation while only very recently the formation of coherence has been experimentally investigated. For this reason, the existing experimental literature can be classified in two categories:

- experiments reporting the transition to a strongly degenerate population distribution;

- experiments reporting the formation of coherence.

Before discussing these experiments, we point out that all the experimental observations on the polariton system are made optically. Indeed, the radiative decay of one polariton results in the emission of one photon from the microcavity. Therefore, measuring the frequency and the angle of emission of the outcoming photons directly gives the information about the polariton energy and momentum, respectively. Furthermore, the spatial coherence of the emitted light, which can be measured using an interference setup, is directly related to the coherence of the decayed polaritons.

A clear evidence of final state stimulation has been reported by nonresonantly exciting the system with a continuous pump both in the electron-hole continuum [Dang 98, Senellart 99, Boeuf 00], and along the upper polariton branch [Bleuse 98]. In particular, in these experiments, a nonlinear increase of the lower polariton emission as a function of pump intensity is observed, above a threshold in the excitation intensity. This demonstrated that, in the steady state regime, and above a density threshold, the relaxation mechanism becomes efficient enough to provide a macroscopic occupation in the lowest energy state.

More recently, a first attempt to prove appearance of coherence was made by Deng *et al.* [Deng 02, Deng 03]. This work, additionally to the nonlinear behavior shown in the previous works, also reports on the simultaneous measurement of the polariton dispersion, the momentum and real-space profiles of the emission, and the second order time correlation of the emitted field. The momentum and the spatial distribution of polaritons indicate a polariton buildup at the lowest energy level and remind of the results obtained in the case of diluted atom BEC [Anderson 95, Davis 95, Bradley 95]. When, however, the expected superfluid velocity is estimated from the polariton-polariton interaction constant, consistent with the observed blue-shift (see Eq. (3) of Ref. [Deng 03]), it turns out that the linear Bogoliubov dispersion expected above BEC threshold would strongly deviate from the perfectly quadratic dispersion which is actually measured up to a pump intensity 7.6 times its threshold value. This suggests that polaritons recombine before the long-range order required for BEC is actually formed, and a description in terms of a single-particle picture still holds. Moreover, results show that above threshold the second-order time correlation at zero time delay slowly decreases from a value of 1.8 slightly above threshold to 1.5 for a pump intensity 17 times larger than threshold. On the other hand, in the case of BEC of a weakly interacting Bose gas, one might expect, around the transition threshold, the rapid change of the second order time correlation from the value of 2, expected for a thermal population, to a value slightly larger than 1, indicating the formation of a coherent state, i.e. a behavior quite similar to that of a laser transition [Mandel 95, Laussy 04].[9] For these reasons, the observations reported in these two papers are not a clear signature of polariton BEC.

A first evidence of formation of coherence has been reported by Richard *et al.* [Richard 05b], in a CdTe semiconductor based microcavity. In this case, however, the system does not relax to the lowest energy state. Furthermore, the coherent emission originates from states with an energy larger than the energy of the lowest-energy state and with a finite momentum. Probably, the large amount of disorder of CdTe based microcavity and the use of a very small excitation laser spot affect this result, inhibiting the relaxation towards the true energy minimum and resulting in the formation of a quasicondensate at higher energy. The subsequent work by Richard *et al.* [Richard 05a] seems to confirm this behavior. Indeed, by using a larger excitation spot, and thus producing an initial population more homogeneous in space, the system relaxes in the lowest energy state. Interestingly, the emission is peaked at $k = 0$ in the Fourier space while, in the real space, it is fragmented in several spots. In this case

---

[9]In the BEC of a trapped weakly interacting gas, the reaching of a value exactly equal to 1 would be prevented both by the presence of interactions and by the confinement.

however the coherence of the emitted light is not measured. Only very recently, again for
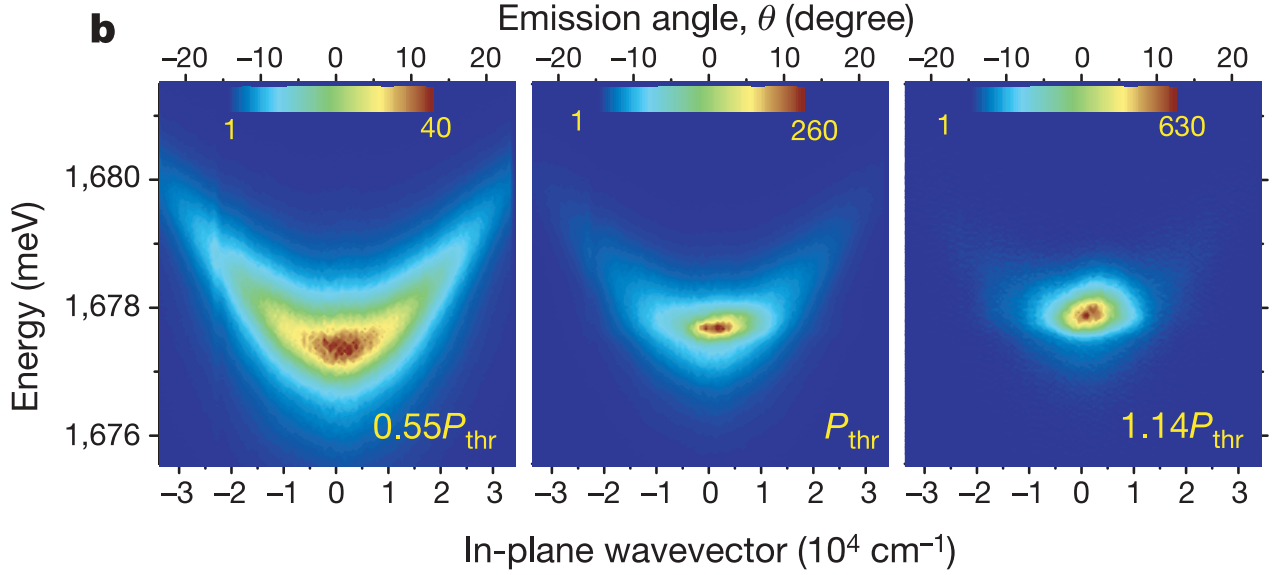

Figure 2.10: Emission intensity in function of the wave-vector (i.e. the emission angle) and the energy, for 3 values of excitation intensity. From the paper by Kasprzak *et al.* [Kasprzak 06].

a CdTe microcavity, the work by Kasprzak *et al.* [Kasprzak 06] has given the first evidence for quantum degeneracy and formation of long-range correlations, in a steady state regime, above a density threshold. In this experiment, polaritons simultaneously manifest an highly degenerate energy distribution, and off-diagonal long range order over distances well exceeding both the thermal length and the estimated healing length. As we will see in Chapter 4, all the experimental findings are consistent with the occurrence of steady-state BEC in a weakly interacting gas, where the effect of fluctuations on the condensate is enhanced by the non-equilibrium regime. In particular, in Fig. 2.10 we report the measured emission intensity, as a function of the light wave-vector and energy, for increasing excitation intensities. This quantity is directly related to the photon population and thus it is given by the product of the photon spectral function $\mathrm{Im}\{(g_{11}^{cc})^{ret}(\mathbf{k}, E)\}$ (see Chapter 3) times the Bose distribution function. From this measurement it is then possible to directly access the photon and the polariton spectral function (see Chapter 3 for the relation between the two quantities).

Clearly, for a system manifesting a large amount of disorder, it is difficult to measure and to give a quantitative account of the properties of the condensed system, like the spectral features. However, just after this first clear signature of BEC, another experimental work by Balili *et al.* [Balili 07] confirmed the same behavior for GaAs semiconductor based microcavity, i.e. a system having a small amount of disorder and more promising in view of a full characterization of the features of polariton BEC. In particular, GaAs based microcavities are very promising for approaching true equilibrium condensation [Deng 06] and for realizing confined structures, by trapping the photon field and thus polaritons in small, homogeneous regions [Daif 06, Kaitouni 06, Bajoni 07].

Before concluding this short overview, let us briefly point out why polariton condensation is so appealing from a theoretical point of view. First, since all the measurements are made optically, the polariton gas would be an ideal system to study the evolution of the spectral function across the transition, in particular to directly observe the appearance of the negative

Bogoliubov poles. Second, for the same reasons, the correlation properties and the role played by density and phase fluctuations could be explored in a very straightforward way. Third, since the system is 2D, it would be an excellent candidate to analyze crossover between BEC and Kosterlitz-Thouless transition, provided that BEC could be realized in homogeneous mesas of various size [Kaitouni 06].

We have discussed the main experimental signatures of polariton BEC, considering experiments where the excitation is produced nonresonantly, i.e. a kind of excitation for which it is difficult to obtain an efficient relaxation of polaritons in the lowest excited-state. However, in polariton systems, polariton formation can be made more efficient by means of resonant excitation. The drawback of resonant excitation, however, is that any correlation observed in the lowest polariton levels might be a residual of the coherent excitation, thus making the interpretation in terms of BEC more ambiguous. Nevertheless the properties manifested by the system are very interesting because, in such a regime, the coherence of the polariton gas is obtained for much lower densities and in strongly nonequilibrium conditions. This phenomenon is called Optical Parametric Oscillator (OPO) and it will be the subject of the next section.

2.3.1 Optical Parametric Oscillator

Resonant excitation gives rise to parametric polariton processes, which are strongly resonant on the energy-momentum curve and display a nonlinear threshold in the polariton emission [Stevenson 00, Houdré 00, Ciuti 01]. Parametric scattering is a driven wave-mixing process and therefore does not directly relate to BEC in the thermodynamic sense.[10] We should point out, however, that the special case of parametric photoluminescence bears a strong analogy with BEC. In a parametric process, two identical polaritons created by the pump resonantly scatter to a pair of *signal* and *idler* polaritons, conserving the total energy and momentum. In the case of parametric amplification, the process is stimulated by an external laser beam which resonantly probes the signal polariton, and is fully described in terms of wave-mixing of classical fields. In parametric photoluminescence, on the contrary, the process is driven by vacuum-field fluctuations of the signal and idler polaritons, and the polariton is a quantum fluctuating field with zero classical amplitude [Ciuti 01]. Recently Savona *et al.* described how the signal polaritons involved in the parametric photoluminescence might undergo a symmetry-breaking transition, driven by the quantum correlations, with the formation of an order parameter – the polariton classical field amplitude – similar to BEC [Savona 05]. An analysis of this quantum state in terms of the self-consistent mean-field theory [Carusotto 04, Carusotto 05] shows that a collective behavior spontaneously arises above the parametric emission threshold, with the polariton dispersion changing from the single-particle behavior to a Bogoliubov-like energy spectrum. In particular, Carusotto and Ciuti derived in the mean field approximation the analogous of the Gross-Pitaevskii equation [Pitaevskii 03] in the case of polaritons, aiming at a generalized description of the parametric photoluminescence [Carusotto 04]. For a weakly interacting Bose system, this equation is the first approximation describing the dynamics of the condensate at zero temperature. For polaritons, the generalized Gross-Pitaevskii model should describe the polariton condensate in the limit where quantum as well as thermal fluctuations are negligible. With the inclusion of fluctuations, Carusotto and Ciuti investigate the spontaneous formation of coherence above the parametric emission threshold [Carusotto 05], a phenomenon

---

[10]It is worth to mention that the polariton OPO is basically different from the standard OPO. In particular, Wouters and Carusotto have shown that the behavior of polariton OPO is much richer than the one of standard OPOs based on passive $\chi^{(2)}$ material [Wouters 07a]. This is due to the $\chi^{(3)}$ nature of the collisional polariton nonlinearity, and thus to the interplay of optical bistability and optical parametric oscillation.

that was previously predicted by a simplified three-mode approach [Savona 05].

Chapter 3

Theory of polariton Bose-Einstein condensation

In this Chapter, we formulate a theory of polariton BEC based on the extension of the standard formalism developed for the equilibrium weakly interacting Bose gas. This theory will provide a very clear and useful description of the polariton phase transition. Clearly, the assumption that a full equilibrium can be reached during the lifetime of the metastable polariton regime is not verified by present experimental conditions. However, giving an equilibrium description of the phenomenon is crucial for two reasons. First, in order to assess for polariton BEC (which differs from a laser, non-equilibrium, mechanism) it is necessary that the features manifested by the system be interpreted as the result of a thermodynamic phase transition, i.e. a mechanism taking place also when the equilibrium conditions are reached. Second, our theoretical predictions (see section 4.3) and the recent experimental evidences [Deng 06] suggest that in future experiments a full polariton thermalization will be possible.

Furthermore, we have seen in section 2.2 that all the main features predicted for the equilibrium BEC are manifested also by trapped atomic condensates, i.e. systems which cannot be considered *exactly* at equilibrium. Therefore an equilibrium theory of polariton BEC is expected to be very helpful for the interpretation of present and future experimental evidence, in particular highlighting the main differences between standard BEC and the BEC of the polariton quasi-particles.

Before explaining the derivation of the theory and discussing the main results, let us give a brief review of the previous theory adopted to describe the polariton problem.

3.1   Overview of the theoretical approaches

In this section, we briefly discuss how the problem of polariton BEC has been theoretically treated in literature.

We have seen in section 2.3 that many experimental works have reported the evidence of polariton quantum degeneracy [Deng 02, Deng 03, Deng 06] with formation of ODLRO [Kasprzak 06, Balili 07].

Bose-Einstein condensation (BEC) is the most appealing way of interpreting these findings. However, the two-dimensional nature of the system, the presence of disorder, the hybrid exciton-photon composition of polaritons, and the composite nature of excitons, certainly call for models that account for all the peculiar aspects of the polariton gas. Along this line, recent theoretical works have been successful in describing many specific aspects of the system. Quite

surprisingly, the existing theoretical descriptions prefer to adopt *ad hoc* models, while a field theory in terms of BEC have never been developed to describe the polariton gas.

In particular, the polariton population buildup has been described by several authors in terms of a simple Boltzmann equation including scattering via phonon absorption or emission as well as mutual polariton scattering [Senellart 99, Tassone 99, Huang 00, Porras 02, Erland 01, Cao 04, Shelykh 04, Doan 05]. These results, while predicting a population buildup arising from final-state stimulation, cannot account for the actual collective behaviour of a condensate, namely the collective Bogoliubov spectrum and the long-range correlations. More recently, some authors have focused on the analogy between the polariton nonequilibrium BEC and laser, proposing a simple polariton laser model based on the quantum theory of laser [Rubo 03, Laussy 04]. This approach however, does not account for the important role played by two-body interactions, in determining on one hand the spectral properties and the amount of fluctuations and on the other hand in allowing the condensation growth. Other works [Keeling 04, Marchetti 06, Szymanska 06] have treated the polariton Bose gas in the framework developed to describe BCS transition in the Fermi-Bose mixtures [Ohashi 02]. In this picture, the transition occurs as a direct consequence of the saturation of the Fermi field and thus can only hardly be interpreted as a genuine BEC. For the same reason, a population of polaritons is not well-defined in this formalism and it is thus unclear whether the thermodynamic properties are correctly modeled. Moreover they assume strongly localized excitons, thus overestimating the deviations from the Bose statistics.

All the existing theoretical works thus leave a basic question still unanswered. Are the main experimental findings correctly interpreted in terms of a quantum field theory of interacting Bose particles? Obviously, to derive such a theory it is necessary to account self-consistently for the linear coupling between two Bose fields – photons and excitons – and for the Coulomb and Pauli non-linearities arising from the composite nature of excitons.

In the next section, we will see how this problem can be solved, by generalizing the standard Bogoliubov approach to the case of two linearly coupled Bose fields.

3.2 Theory of two coupled Bose fields

The physics of the polariton system is basically that of two linearly coupled oscillators, the exciton and the cavity photon fields, as discussed in subsection 2.1.6. Considering the limit of low density, the exciton field can be treated as a Bose field, subject to two kinds of interactions, the mutual exciton-exciton interaction and the effective exciton-photon interaction, originating from the saturation of the exciton oscillator strength. Therefore, to describe polariton BEC we need a theory which extend to the case of two coupled interacting Bose fields the formalism adopted in describing the BEC of a single Bose field, resumed in section 2.2.

It is useful to make some preliminary comments on the main consequences that the exciton-photon coupling has on the manifestation of BEC in this system. First, since we are considering two coupled Bose fields, the occurrence of BEC implies the formation of a condensed phase for each of the two coupled fields. In other words, the polariton condensate can be seen as the constructive superposition between the exciton condensate and the photon condensate. Second, the normal modes of the system are polariton modes. Therefore, the only population which has a thermodynamical meaning is the polariton population. This implies that the total polariton population is well defined, if we can assume that the system is at equilibrium, while the exciton and the photon populations are not individually defined. Furthermore, given a temperature T, the equilibrium regime imposes that the polariton excitations are thermally occupied, following the Bose distribution $n_B(E, T)$. On the other hand, the occupation of the

uncoupled exciton and photon modes does not follow a defined statistical distribution. We stress that, since polaritons simply arise as a consequence of the linear coupling between the exciton and photon fields and thus they do not depend on the occurrence of condensation, their quasi-particle nature and the subsequent statistical properties must hold both below and above the condensation threshold.

In what follows, we will develop a theory that fulfills these requirements. This will be made by generalizing the Hartree-Fock-Popov (HFP) [Griffin 96, Shi 98] description of BEC to the case of two coupled Bose fields. The Coulomb interaction and the Pauli exclusion principle will be treated by means of the effective bosonic Hamiltonian discussed in subsection 2.1.5 [Rochat 00, Ben-Tabou de Leon 01, Okumura 01], valid well below the exciton Mott density. We will derive coupled equations for the condensate wave function and the field of collective excitations. We will study the solutions for material parameters relative to recently studied samples [Kasprzak 06, Balili 07]. In particular we will discuss the collective excitation spectrum, the density-dependent energy shifts, the onset of off-diagonal long-range correlations and the phase diagram, by comparing the results to the experimental findings.

3.2.1 Coupling between two Bose fields

We express the exciton and photon field operators in the Heisenberg representation via the notation

$$\hat{\Psi}_x(\mathbf{r}, t) = \frac{1}{\sqrt{A}} \sum_{\mathbf{k}} e^{i\mathbf{k}\cdot\mathbf{r}} \hat{b}_{\mathbf{k}}(t) \,, \tag{3.1}$$

and

$$\hat{\Psi}_c(\mathbf{r}, t) = \frac{1}{\sqrt{A}} \sum_{\mathbf{k}} e^{i\mathbf{k}\cdot\mathbf{r}} \hat{c}_{\mathbf{k}}(t) \,, \tag{3.2}$$

where A is system area, while $\hat{b}_{\mathbf{k}}$ and $\hat{c}_{\mathbf{k}}$ are Bose operators destroying a particle in the state $\mathbf{k}$ and obey the commutation rules

$$[\hat{b}_{\mathbf{k}}, \hat{b}_{\mathbf{k}'}^{\dagger}] = [\hat{c}_{\mathbf{k}}, \hat{c}_{\mathbf{k}'}^{\dagger}] = \delta_{\mathbf{k},\mathbf{k}'}$$
$$[\hat{b}_{\mathbf{k}}, \hat{b}_{\mathbf{k}'}] = [\hat{c}_{\mathbf{k}}, \hat{c}_{\mathbf{k}'}] = 0$$
$$[\hat{b}_{\mathbf{k}}, \hat{c}_{\mathbf{k}'}^{\dagger}] = 0 \,. \tag{3.3}$$

Notice that in this work we assume scalar exciton and photon fields. However, the theory can be generalized to include their vector nature, accounting for light polarization and exciton spin.[1]

The bosonic exciton-photon Hamiltonian, including the exciton non-linearities (see subsection 2.1.5), reads

$$\hat{H} = \hat{H}_0 + \hat{H}_R + \hat{H}_x + \hat{H}_s, \tag{3.4}$$

where, in the wave-vector basis,

$$\hat{H}_0 = \sum_{\mathbf{k}} \left(\epsilon_{\mathbf{k}}^x \hat{b}_{\mathbf{k}}^{\dagger} \hat{b}_{\mathbf{k}} + \epsilon_{\mathbf{k}}^c \hat{c}_{\mathbf{k}}^{\dagger} \hat{c}_{\mathbf{k}} \right) \tag{3.5}$$

is the noninteracting exciton and photon term, while

$$\hat{H}_R = \hbar\Omega_R \sum_{\mathbf{k}} (b_{\mathbf{k}}^{\dagger} \hat{c}_{\mathbf{k}} + h.c.) \tag{3.6}$$

---

[1]Shelykh *et al.* [Shelykh 06] have recently studied the effects of polarization and spin at $T = 0$, within the Gross-Pitaevskii limit restricted to the lower polariton field

describes the linear exciton-photon coupling. The term

$$\hat{H}_x = \frac{1}{2A} \sum_{\mathbf{k},\mathbf{k}',\mathbf{q}} v_x(\mathbf{k},\mathbf{k}',\mathbf{q}) \hat{b}^\dagger_{\mathbf{k}+\mathbf{q}} \hat{b}^\dagger_{\mathbf{k}'-\mathbf{q}} \hat{b}_{\mathbf{k}'} \hat{b}_{\mathbf{k}} \tag{3.7}$$

is the effective exciton-exciton scattering Hamiltonian, modeling both Coulomb interaction and the non-linearity due to the Pauli exclusion principle for the electrons and holes that form the exciton. The remaining term

$$\hat{H}_s = \frac{1}{A} \sum_{\mathbf{k},\mathbf{k}',\mathbf{q}} v_s(\mathbf{k},\mathbf{k}',\mathbf{q}) (\hat{c}^\dagger_{\mathbf{k}+\mathbf{q}} \hat{b}^\dagger_{\mathbf{k}'-\mathbf{q}} \hat{b}_{\mathbf{k}'} \hat{b}_{\mathbf{k}} + h.c.) \tag{3.8}$$

models the effect of Pauli exclusion on the exciton oscillator strength [Rochat 00, Okumura 01], that is reduced for increasing exciton density [Schmitt-Rink 85].

In this work, we account for the full momentum dependence of $v_x(\mathbf{k},\mathbf{k}',\mathbf{q})$ and $v_s(\mathbf{k},\mathbf{k}',\mathbf{q})$ [Rochat 00, Okumura 01]. In particular, we point out that these potentials vanish at large momentum, thus preventing the ultraviolet divergence typical of a contact potential [Pitaevskii 03], without introducing an arbitrary cutoff. However, in the present two-dimensional case an additional problem arises. Indeed many-body correlations are known to affect significantly the two-body scattering amplitude, eventually leading to a vanishing T-matrix at small collision energy and in the thermodynamic limit [Lee 02]. In the HF approximation, it is then customary to replace the microscopic value of the interaction potential $v(\mathbf{k},\mathbf{k}',\mathbf{q})$ by the many-body T-matrix $T(\mathbf{k},\mathbf{k}',\mathbf{q},E)$ obtained by a self-consistent summation of ladder diagrams. Here, we have generalized this approach and computed the many-body T-matrices $T_x(\mathbf{k},\mathbf{k}',\mathbf{q},E)$ and $T_s(\mathbf{k},\mathbf{k}',\mathbf{q},E)$. We find that, for typical values of the parameters, and taking into account both the real and the imaginary part of the many body T-matrix, the correction to v_x and v_s is only of a few percent. We report the expression of the polariton T-matrices and the quantitative estimation of their value in the Appendix A.

For clarity of notation, in the following equations we omit the momentum dependence (the momentum dependent equations are reported in Appendix B). In particular, we use the limit introduced in subsection 2.1.5, i.e. $v_x(\mathbf{k},\mathbf{k}',\mathbf{q}) \to v_x = 6E_b a_0^2$ and $v_s(\mathbf{k},\mathbf{k}',\mathbf{q}) \to \hbar\Omega_R/n_s$, where n_s is the saturation density of the exciton oscillator strength [Rochat 00].

Two-body interactions and self-energies

Hamiltonian (3.4) contains three interaction terms. We can represent these interactions by means of the diagrams in Fig. 3.1. The linear coupling induce the spontaneous scattering of one exciton into one photon and the opposite. The exciton-exciton scattering is a standard 2-body interaction term, while the saturation of the exciton oscillator strength results in peculiar 2-body scattering processes where two excitons scatter into one exciton and one photon. Therefore we need to introduce four different thermal one-particle propagators

$$
\begin{aligned}
G_{xx}(\mathbf{r},\tau;\mathbf{r}',\tau') &= \mathrm{Tr}\left[e^{\beta(\Omega-\hat{H}+\mu\hat{N})} T_\tau \hat{\Psi}_x(\mathbf{r},\tau)\hat{\Psi}^\dagger_x(\mathbf{r}',\tau') \right] = \langle \hat{\Psi}_x(\mathbf{r},\tau)\hat{\Psi}^\dagger_x(\mathbf{r}',\tau') \rangle_{\tau,\beta}, \\
G_{cc}(\mathbf{r},\tau;\mathbf{r}',\tau') &= \mathrm{Tr}\left[e^{\beta(\Omega-\hat{H}+\mu\hat{N})} T_\tau \hat{\Psi}_c(\mathbf{r},\tau)\hat{\Psi}^\dagger_c(\mathbf{r}',\tau') \right] = \langle \hat{\Psi}_c(\mathbf{r},\tau)\hat{\Psi}^\dagger_c(\mathbf{r}',\tau') \rangle_{\tau,\beta}, \\
G_{xc}(\mathbf{r},\tau;\mathbf{r}',\tau') &= \mathrm{Tr}\left[e^{\beta(\Omega-\hat{H}+\mu\hat{N})} T_\tau \hat{\Psi}_x(\mathbf{r},\tau)\hat{\Psi}^\dagger_c(\mathbf{r}',\tau') \right] = \langle \hat{\Psi}_x(\mathbf{r},\tau)\hat{\Psi}^\dagger_c(\mathbf{r}',\tau') \rangle_{\tau,\beta}, \\
G_{cx}(\mathbf{r},\tau;\mathbf{r}',\tau') &= \mathrm{Tr}\left[e^{\beta(\Omega-\hat{H}+\mu\hat{N})} T_\tau \hat{\Psi}_c(\mathbf{r},\tau)\hat{\Psi}^\dagger_x(\mathbf{r}',\tau') \right] = \langle \hat{\Psi}_c(\mathbf{r},\tau)\hat{\Psi}^\dagger_x(\mathbf{r}',\tau') \rangle_{\tau,\beta}, \quad (3.9)
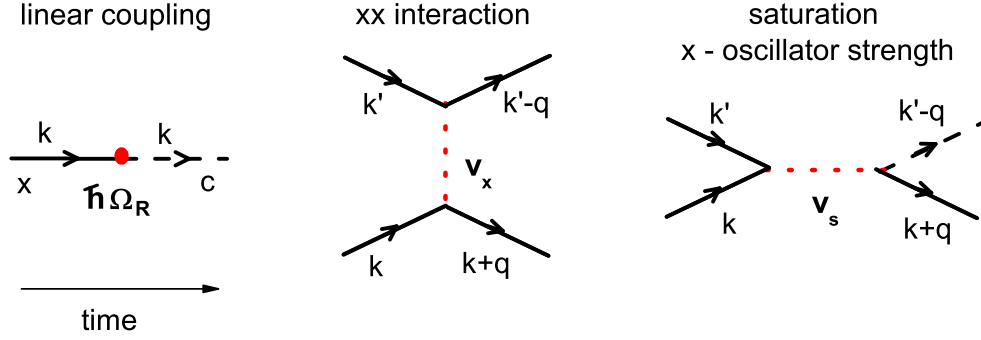\end{aligned}
$$

Figure 3.1: Diagrams representing the linear coupling and the two-body interactions. The linear coupling and the saturation two-body term result in the scattering of one exciton into one photon. These interaction terms enter in the one-particle self-energy.

where $\beta = 1/k_B T$, Ω is the thermodynamic potential

$$e^{-\beta\Omega} = \mathrm{Tr}\left[e^{-\beta(\hat{H} - \mu\hat{N})}\right], \tag{3.10}$$

and $\langle ... \rangle_{\tau,\beta}$ is the compact notation that we adopt to represent the thermal average of the imaginary-time ordered product. Here G_{xx} and G_{cc} are the usual one-exciton and one-photon imaginary-time propagators while G_{xc} and G_{cx} are mixed propagators accounting for the spontaneous scattering between the two species of particles. Notice that the thermal average is taken within the grand-canonical ensemble. The chemical potential μ represents the chemical potential of polaritons and it will be explicitly defined later on. Therefore, the same chemical potential enters in the equations for the two fields[2], as a consequence of the equilibrium hypothesis.

The one-particle self-energy depends on both the linear coupling and the two-body interactions. Accordingly with this picture, the Dyson equation for the one-particle propagators can be represented by the diagrams displayed in Fig. 3.2. Notice that in the equations for the mixed propagators G_{xc} and G_{cx} an unperturbed term does not appear, because the exciton and photon operators commute. Here, we are considering the Green's functions of the total field operator, thus the diagrams of Fig. 3.2 refer to the non-condensed regime. Analogously to the theory for a single Bose field, when condensation occurs, the field operator has to be separated in the condensate part and in the part describing excitations, in order to develop a standard perturbation scheme. In the condensate regime, the Dyson equations in Fig. 3.2 will be replaced by the Gross-Pitaevskii equations for the condensate and in the Beliaev equations for the excitation field, as we will see explicitly below.

Bogoliubov ansatz

To describe the condensed system, we extend the Bogoliubov ansatz to both the exciton and the photon Bose fields, i.e. we write each field as

$$\hat{\Psi}_{x(c)}(\mathbf{r}, t) = \Phi_{x(c)}(\mathbf{r}, t) + \tilde{\psi}_{x(c)}(\mathbf{r}, t), \tag{3.11}$$

---

[2]Uncoupled photons have not a defined chemical potential. The appearance of a well defined chemical potential is due to the fact that the normal modes of the system are light-matter quasiparticles.
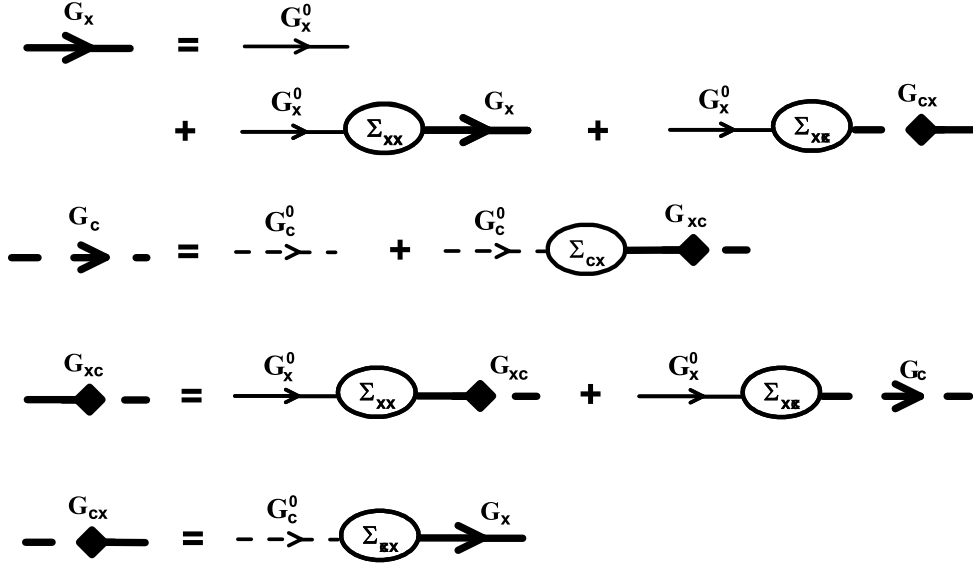
Figure 3.2: Dyson equations for the one-particle propagators G. $G^0_{x(c)}$ is the unperturbed exciton (photon) propagator.

i.e. as the sum of a classical symmetry-breaking term $\Phi_{x(c)}(\mathbf{r}, t)$ for the condensate wave function, and of a quantum fluctuation field $\tilde{\psi}_{x(c)}(\mathbf{r}, t)$, having zero thermal average, i.e.

$$\langle \hat{\Psi}_{x(c)}(\mathbf{r}, t) \rangle_\beta = \Phi_{x(c)}(\mathbf{r}, t) \,. \tag{3.12}$$

By taking the thermal expectation values of the Heisenberg equations of motion of $\hat{\Psi}_{x(c)}(\mathbf{r}, t)$, we obtain two coupled classical equations for the two condensate wave functions. In these equations, the self-energy terms represented in Fig. 3.2 reduce to a density functional, whose explicit expression depends on the approximation adopted.

At the same time, as in the one-field theory (see subsection 2.2.2), the Bogoliubov ansatz imposes to introduce anomalous propagators for the excited particles, describing processes where a pair of particles is scattered to or from the condensate reservoir [Shi 98]. We write the resulting 16 thermal propagators in the matrix form (in the energy-momentum Fourier space, assuming a uniform system)

$$G(\mathbf{k}, i\omega_n) = \begin{pmatrix} g^{xx}(\mathbf{k}, i\omega_n) & g^{xc}(\mathbf{k}, i\omega_n) \\ g^{cx}(\mathbf{k}, i\omega_n) & g^{cc}(\mathbf{k}, i\omega_n) \end{pmatrix}, \tag{3.13}$$

where the elements of each 2 by 2 matrix block are ($j, l = 1, 2$; $\chi, \xi = x, c$)

$$g^{\chi\xi}_{jl}(\mathbf{k}, i\omega_n) = -\int_0^\beta d\tau e^{i\omega_n \tau} \langle \hat{O}^j_\chi(\mathbf{k}, \tau) \hat{O}^l_\xi(\mathbf{k}, 0)^\dagger \rangle_{\tau, \beta}, \tag{3.14}$$

and $\hbar\omega_n = 2\pi n/\beta$, $n = 0, \pm 1, \ldots$ are the Matsubara energies for bosons. Here we have introduced the useful compact notation

$$\hat{O}^1_\xi(\mathbf{k}) = \hat{O}_\xi(\mathbf{k}),$$
$$\hat{O}^2_\xi(\mathbf{k}) = \hat{O}^\dagger_\xi(-\mathbf{k}),$$
$$\hat{O}_x = \hat{b}, \hat{O}_c = \hat{c}, \tag{3.15}$$

to represent the exciton and the photon fields.

Within the Bogoliubov ansatz, also the generalized one-particle density

$$n_{\chi\xi} = n_{\chi\xi}^0 + \tilde{n}_{\chi\xi}\,, \tag{3.16}$$

with $\chi, \xi = x, c$, is separated in the contribution of the condensate $n_{\chi\xi}^0 = \Phi_\chi^* \Phi_\xi$ and in the contribution of the excited particles

$$\tilde{n}_{\chi\xi} = \sum_{\mathbf{k}\neq\mathbf{0}} n_{\chi\xi}(\mathbf{k}) = \sum_{\mathbf{k}\neq\mathbf{0}} \langle \hat{O}_\chi^2(\mathbf{k}) \hat{O}_\xi^1(\mathbf{k}) \rangle\,. \tag{3.17}$$

This latter quantity represents the excited-state density matrix, expressed in the exciton-photon basis, and it is directly related to the corresponding normal propagator via the well known relation [Shi 98]

$$\tilde{n}_{\chi\xi}(\mathbf{k}) = -\frac{1}{\beta} \lim_{\eta\to 0} \sum_{\omega_n} e^{i\omega_n \eta} g_{11}^{\chi\xi}(\mathbf{k}, i\omega_n) = -\int \frac{d\omega}{\pi} \mathrm{Im}\{(g_{11}^{\chi\xi})^{ret}(\mathbf{k}, \omega)\} n_B(\omega)\,, \tag{3.18}$$

where the retarded Green's function is the analytical continuation to the real axis of the imaginary-frequency Green's function [Shi 98]

$$(g_{11}^{\chi\xi})^{ret}(\mathbf{k}, \omega) = g_{11}^{\chi\xi}(\mathbf{k}, i\omega_n \to \omega + i0^+)\,. \tag{3.19}$$

The propagator matrix $G(\mathbf{k}, i\omega_n)$ obeys the Dyson-Beliaev equation

$$G(\mathbf{k}, i\omega_n) = G^0(\mathbf{k}, i\omega_n)\left[\mathbf{1} + \Sigma(\mathbf{k}, i\omega_n) G(\mathbf{k}, i\omega_n)\right]\,, \tag{3.20}$$

where G^0 is the matrix of the unperturbed propagators, which is diagonal (because the exciton and the photon field commute) and reads

$$G^0(\mathbf{k}, i\omega_n) = \mathbf{1} \cdot \left[\begin{array}{cccc} g_0^x(\mathbf{k}, i\omega_n) & g_0^x(-\mathbf{k}, -i\omega_n) & g_0^c(\mathbf{k}, i\omega_n) & g_0^c(-\mathbf{k}, -i\omega_n) \end{array}\right]^{\mathbf{T}}\,, \tag{3.21}$$

with

$$g_0^\xi(\mathbf{k}, i\omega_n) = \frac{1}{i\omega_n - \epsilon_{\mathbf{k}}^{(\xi)} + \mu}\,. \tag{3.22}$$

The general form of the 4×4 self-energy matrix is

$$\Sigma(\mathbf{k}, i\omega_n) = \left(\begin{array}{cc} \Sigma^{xx}(\mathbf{k}, i\omega_n) & \Sigma^{xc}(\mathbf{k}, i\omega_n) \\ \Sigma^{cx}(\mathbf{k}, i\omega_n) & \Sigma^{cc}(\mathbf{k}, i\omega_n) \end{array}\right)\,, \tag{3.23}$$

here written in a (2×2)-block form. The explicit expression of the self-energy also depends on the approximation used. In a consistent theory, the self energy (3.23) and the density functional entering in the equation for the condensate wave functions are written within the same level of approximation. To guarantee that the excitation spectrum be gapless, the self-energy must fulfill the Hugenholtz-Pines condition extended to the present two-field case. The most simple approximation accounting for thermal populations and giving a gapless spectrum is, also in this case, the Popov approximation.

3.2.2 Popov approximation

We have seen in subsection 2.2.2 that the mean field theories for bosons which fulfill all the conservation laws result in a nonphysical one-particle spectrum with an energy gap. Indeed, only the second order Beliaev theory satisfies simultaneously these two physical requirements. Since our present purpose is to describe the one-particle properties of the polariton BEC, we prefer to adopt the simplest gapless theory valid at finite temperature, i.e. the Hartree-Fock-Popov approximation [Griffin 96, Shi 98]. Furthermore, this approximation seems to be the most suited for a possible extension to nonuniform systems and to treat deviations from equilibrium. As explained in subsection 2.2.2, the Popov limit corresponds to totally omitting the contribution of the anomalous correlations in the self-energies, i.e. to neglecting the terms

$$\tilde{m}_{\chi\xi}(\mathbf{k}) = \lim_{\eta \to 0} \sum_{\omega_n} e^{i\omega_n \eta} g_{12}^{\chi\xi}(\mathbf{k}, i\omega_n) \,. \tag{3.24}$$

Generalized Gross-Pitaevskii equation

Within the Popov approximation, for a uniform system, the two coupled equations for the condensate amplitudes are

$$i\hbar\dot{\Phi}_x = \left[\epsilon_0^x - 2\frac{\hbar\Omega_R}{n_s}Re\left\{n_{xc} + \tilde{n}_{xc}\right\} + v_x\left(n_{xx} + \tilde{n}_{xx}\right)\right]\Phi_x + \hbar\Omega_R\left(1 - \frac{n_{xx}}{n_s}\right)\Phi_C$$

$$i\hbar\dot{\Phi}_c = \epsilon_0^c\Phi_c + \hbar\Omega_R\left(1 - \frac{n_{xx} + \tilde{n}_{xx}}{n_s}\right)\Phi_x. \tag{3.25}$$

We look for the condensate eigenstates. This means that we assume that both the condensate fields evolve with the same characteristic frequency $E/\hbar$, i.e.

$$\Phi_{x(c)}(t) = e^{-i\frac{E}{\hbar}t}\Phi_{x(c)}(0) \,, \tag{3.26}$$

By replacing this evolution into (3.25), we obtain a generalized set of two coupled time-independent Gross-Pitaevskii equations, which can be formally written in the matrix form

$$E\begin{pmatrix} X_0 \\ C_0 \end{pmatrix} = \begin{pmatrix} \epsilon_0^x + v_x\left(n_{xx} + \tilde{n}_{xx}\right) - 2\frac{\hbar\Omega_R}{n_s}Re\left\{n_{xc} + \tilde{n}_{xc}\right\} & \hbar\Omega_R\left(1 - \frac{n_{xx}}{n_s}\right) \\ \hbar\Omega_R\left(1 - \frac{n_{xx} + \tilde{n}_{xx}}{n_s}\right) & \epsilon_0^c \end{pmatrix} \begin{pmatrix} X_0 \\ C_0 \end{pmatrix}, \tag{3.27}$$

where we have defined the normalized Hopfield coefficients of the condensate state

$$\Phi_x = X_0\Phi$$
$$\Phi_c = C_0\Phi$$
$$|X_0|^2 + |C_0|^2 = 1 \,, \tag{3.28}$$

and $n_0 = |\Phi|^2$ is the actual density of the polariton condensate. The two solutions $E = E^{lp,(up)}$ of (3.27) give the lower and upper polariton condensate modes

$$\Phi_{lp(up)} = X_0^{lp(up)*}\Phi_x + C_0^{lp(up)*}\Phi_c \,. \tag{3.29}$$

The lower energy solution E_0^{lp} represents the actual condensate state, because it corresponds to the minimal energy of the polariton gas. In the present U(1) symmetry-breaking approach, it also represents the chemical potential of the polariton system, i.e. $E_0^{lp} = \mu$, thus entering in the grand-canonical thermal averages.

Equations for the excited states

Within the HFP theory, the self-energy elements in Eq. (3.23) are independent of frequency and read

$$\Sigma_{11}^{xx} = \Sigma_{22}^{xx} = 2 \left[v_x n_{xx} - \frac{\hbar\Omega_R}{n_s} (n_{cx} + n_{xc}) \right],$$

$$\Sigma_{12}^{xx} = (\Sigma_{21}^{xx})^* = v_x \Phi_x^2 - 2\frac{\hbar\Omega_R}{n_s} \Phi_x \Phi_c,$$

$$\Sigma_{11}^{xc} = \Sigma_{22}^{xc} = \hbar\Omega_R \left(1 - 2\frac{n_{xx}}{n_s} \right),$$

$$\Sigma_{12}^{xc} = (\Sigma_{21}^{xc})^* = -\frac{\hbar\Omega_R}{n_s} \Phi_x^2,$$

$$\Sigma_{jl}^{cx} = \Sigma_{jl}^{xc},$$

$$\Sigma_{jl}^{cc} = 0 \,. \tag{3.30}$$

The solutions of Eq. (3.20) can be written analytically in terms of the self-energy elements and the unperturbed propagators. For example we obtain

$$g_{11}^{xx}(\mathbf{k}, i\omega_n) = \frac{g_0^x(\mathbf{k}, i\omega_n) \left[1 - g_0^x(-\mathbf{k}, -i\omega_n) N_D^*(\mathbf{k}, i\omega_n) \right]}{|1 - g_0^x(\mathbf{k}, i\omega_n) N_D(\mathbf{k}, i\omega_n)|^2 - |g_0^x(\mathbf{k}, i\omega_n) N_B(\mathbf{k}, i\omega_n)|^2} \,, \tag{3.31}$$

where

$$
\begin{aligned}
N_D(\mathbf{k}, i\omega_n) &= \Sigma_{11}^{xx} + g_0^c(\mathbf{k}, i\omega_n)|\Sigma_{11}^{xc}|^2 + g_0^c(-\mathbf{k}, -i\omega_n)|\Sigma_{12}^{xc}|^2 \\
N_B(\mathbf{k}, i\omega_n) &= \Sigma_{12}^{xx} + \left[g_0^c(\mathbf{k}, i\omega_n) + g_0^c(-\mathbf{k}, -i\omega_n) \right] \Sigma_{11}^{xc}\Sigma_{12}^{xc},
\end{aligned}
\tag{3.32}
$$

and

$$g_{21}^{xx}(\mathbf{k}, i\omega_n) = \frac{g_0^x(-\mathbf{k}, -i\omega_n) N_B^*(\mathbf{k}, i\omega_n)}{\left[1 - g_0^x(-\mathbf{k}, -i\omega_n) N_D^*(\mathbf{k}, i\omega_n) \right]} g_{11}^{xx}(\mathbf{k}, i\omega_n) \,. \tag{3.33}$$

For each value of $\mathbf{k}$, the analytic continuation of each Green's function $g_{jl}^{\chi\xi}(\mathbf{k}, z)$ shares the same four simple poles at $z = \pm E_{\mathbf{k}}^{lp(up)}$, i.e.

$$
\begin{aligned}
g_{11}^{xx}(\mathbf{k}, z) &= \frac{|X_u^{lp}(\mathbf{k})|^2}{z - E^{lp}(\mathbf{k})} + \frac{|X_v^{lp}(\mathbf{k})|^2}{z + E^{lp}(\mathbf{k})^*} + \frac{|X_u^{up}(\mathbf{k})|^2}{z - E^{up}(\mathbf{k})} + \frac{|X_v^{up}(\mathbf{k})|^2}{z + E^{up}(\mathbf{k})^*} \\
g_{12}^{xx}(\mathbf{k}, z) &= \frac{X_u^{lp}(\mathbf{k})^* X_v^{lp}(\mathbf{k})}{z - E^{lp}(\mathbf{k})} + \frac{X_v^{lp}(\mathbf{k})^* X_u^{lp}(\mathbf{k})}{z + E^{lp}(\mathbf{k})^*} + \frac{X_u^{up}(\mathbf{k})^* X_v^{up}(\mathbf{k})}{z - E^{up}(\mathbf{k})} + \frac{X_v^{up}(\mathbf{k})^* X_u^{up}(\mathbf{k})}{z + E^{up}(\mathbf{k})^*} \\
g_{11}^{cc}(\mathbf{k}, z) &= \frac{|C_u^{lp}(\mathbf{k})|^2}{z - E^{lp}(\mathbf{k})} + \frac{|C_v^{lp}(\mathbf{k})|^2}{z + E^{lp}(\mathbf{k})^*} + \frac{|C_u^{up}(\mathbf{k})|^2}{z - E^{up}(\mathbf{k})} + \frac{|C_v^{up}(\mathbf{k})|^2}{z + E^{up}(\mathbf{k})^*} \\
g_{11}^{xc}(\mathbf{k}, z) &= \frac{X_u^{lp}(\mathbf{k})^* C_u^{lp}(\mathbf{k})}{z - E^{lp}(\mathbf{k})} + \frac{X_v^{lp}(\mathbf{k})^* C_v^{lp}(\mathbf{k})}{z + E^{lp}(\mathbf{k})^*} + \frac{X_u^{up}(\mathbf{k})^* C_u^{up}(\mathbf{k})}{z - E^{up}(\mathbf{k})} + \frac{X_v^{up}(\mathbf{k})^* C_v^{up}(\mathbf{k})}{z + E^{up}(\mathbf{k})^*} \,,
\end{aligned}
$$

and so on.[3] The poles of the propagators represent the positive and negative Bogoliubov-Beliaev eigen-energies of the lower- and upper-polariton modes. The residual in each pole depends on the corresponding generalized Hopfield coefficients.

---

[3]Here we write the general expression with the complex conjugates of the energies $E^{lp(up)}(\mathbf{k})$. Within such a notation, the formulas can be in principle extended to include a phenomenological imaginary part to the energies, in order to account for the finite radiative lifetime of polaritons.

We point out that the polariton excitation modes for a given $\mathbf{k}$ can be also obtained by directly diagonalizing the problem

$$E(\mathbf{k})\begin{pmatrix} X_u \\ X_v \\ C_u \\ C_v \end{pmatrix} = \begin{pmatrix} \epsilon_{\mathbf{k}}^x - \mu + \Sigma_{11}^{xx} & \Sigma_{12}^{xx} & \Sigma_{11}^{xc} & \Sigma_{12}^{xc} \\ -\Sigma_{21}^{xx} & -(\epsilon_{\mathbf{k}}^x - \mu + \Sigma_{22}^{xx})^* & -\Sigma_{21}^{xc} & -\Sigma_{22}^{xc} \\ \Sigma_{11}^{cx} & \Sigma_{12}^{cx} & \epsilon_{\mathbf{k}}^c - \mu & 0 \\ -\Sigma_{21}^{xc} & -\Sigma_{11}^{cx} & 0 & -(\epsilon_{\mathbf{k}}^c - \mu)^* \end{pmatrix}\begin{pmatrix} X_u \\ X_v \\ C_u \\ C_v \end{pmatrix}.$$

(3.34)

The components of the 4 eigenvectors $\mathbf{h}_i(\mathbf{k}) \equiv (X_u, X_v, C_u, C_v)_j(\mathbf{k})$ $(j = 1, ..., 4)$ are again the generalized Hopfield coefficients corresponding to the normal (X_u, C_u) and anomalous (X_v, C_v) components of the polariton field, in analogy with the one-field HFP theory. They obey the normalization relation

$$|X_u^j|^2 - |X_v^j|^2 + |C_u^j|^2 - |C_v^j|^2 = 1,$$

(3.35)

a condition which guarantees that the operator destroying the lower (upper) polariton excitation with wave vector $\mathbf{k}$,

$$\hat{\pi}_{\mathbf{k}}^{lp(up)} = X_u^{lp(up)}(\mathbf{k})\hat{b}_{\mathbf{k}} + X_v^{lp(up)}(\mathbf{k})\hat{b}_{-\mathbf{k}}^\dagger + C_u^{lp(up)}(\mathbf{k})\hat{c}_{\mathbf{k}} + C_v^{lp(up)}(\mathbf{k})\hat{c}_{-\mathbf{k}}^\dagger$$
$$\equiv u^{lp(up)}(\mathbf{k})\hat{p}_{\mathbf{k}} + v^{lp(up)}(-\mathbf{k})^*\hat{p}_{-\mathbf{k}}^\dagger,$$

(3.36)

obey Bose commutation rules. Here we have defined the lower (upper) polariton one-particle operators $\hat{p}_{\mathbf{k}}^{lp(up)}$ and the normal and anomalous polariton coefficients

$$u^{lp(up)}(\mathbf{k}) = \left[[X_u^{lp(up)}(\mathbf{k}) + C_u^{lp(up)}(\mathbf{k})]^{1/2}\right],$$
$$v^{lp(up)}(\mathbf{k}) = \left[X_v^{lp(up)}(\mathbf{k}) + C_v^{lp(up)}(\mathbf{k})\right]^{1/2},$$
$$|u^{lp(up)}(\mathbf{k})|^2 - |v^{lp(up)}(\mathbf{k})|^2 = 1.$$

(3.37)

The excitation states, i.e. the normal modes, are thermally populated via the Bose distribution

$$\bar{N}_{\mathbf{k}}^j \equiv \langle \hat{\pi}_{\mathbf{k}}^{j\dagger} \hat{\pi}_{\mathbf{k}}^j \rangle = \frac{1}{e^{\beta E_{\mathbf{k}}^j} - 1},$$

(3.38)

while the lower- and upper-polariton one-particle densities are given by

$$\tilde{n}_{\mathbf{k}}^j \equiv \frac{1}{A}\left[\left(|u^j(\mathbf{k})|^2 + |v^j(\mathbf{k})|^2\right)\bar{N}_{\mathbf{k}}^j + |v^j(\mathbf{k})|^2\right].$$

(3.39)

Therefore, for a fixed total polariton one-particle density n_p, the density of the polariton condensate is given by

$$n_0 \equiv |\Phi|^2 = n_p - \sum_{\mathbf{k} \neq 0}[\tilde{n}_{\mathbf{k}}^{lp} + \tilde{n}_{\mathbf{k}}^{up}].$$

(3.40)

Notice that this equation is analogous to Eq. (2.96) for a single Bose gas. From n_0, the exciton and the photon condensed densities are finally obtained via Eq.(3.28).

Hence, for a given polariton density n_p and temperature T, a self-consistent solution can be obtained by solving iteratively Eqs. (3.20), (3.27), (3.18), and (3.40), until convergence of the chemical potential μ and the density matrix $n_{\chi\xi}(\mathbf{k})$ is reached. From this self-consistent solution, we obtain the exciton and photon components of the condensate fraction as well as the spectrum of collective excitations and the one-particle populations. We point out that the self-consistent solution must be independent on the initial condition used in Eq. (3.20) and

(3.27). An advantageous[4] initial condition is provided by the ideal gas solution, i.e. the solution obtained by neglecting the two-body interactions, and considering the resulting polariton states occupied accordingly to the Bose distribution.

Single-particle states

Since the microcavity polariton system is intrinsically two-dimensional, an analysis in terms of BEC is possible only for finite size geometries, because, in the thermodynamic limit, thermal fluctuations would prevent the occurrence of BEC. In literature the problem of BEC in confined systems is usually addressed by introducing a trap potential (commonly the harmonic potential) [Bagnato 91, Ketterle 96]. However, for microcavity polaritons, the confinement is physically due to both the intrinsic disorder [Langbein 02, Richard 05a] and to the finite size of the exciting laser spot [Deng 03, Richard 05b] and thus realistic conditions would be only approximated by using a regular trap potential. Furthermore, for GaAs based microcavity, the finite size region where polaritons are created results to be homogeneous enough to practically preserve the wave-vector as a good quantum number [Langbein 02]. In this respect, the simplest way to model the effect of confinement is by adopting exciton and photon modes in a finite box of fixed area A with periodic boundary conditions. For equilibrium BEC, the energy spacings between the lowest-lying states determine the effect of fluctuations. We will show in Appendix C that the density of states at low-energy, resulting from a typical disordered potential, is well modeled by a finite box with area $A \simeq 10^2 - 10^3 \ \mu\text{m}^2$. While for equilibrium BEC, within this realistic range of size the results are weakly affected by the actual value of A (see Fig. 3.11 for example), in presence of important deviations from equilibrium, the actual value of A has a strong influence on the occurrence of BEC, as we will see in Chapter 4.

3.3   Predictions of the theory

In this section, we present the main results of the present equilibrium theory, by adopting realistic parameters describing the CdTe semiconductor based microcavity studied by Kasprzak *et al.* [Kasprzak 06]. As we will see in subsection 3.3.4, the main predictions of the theory weakly depend on system parameters and thus also apply to the case of GaAs based microcavities studied by Deng *et al.* [Deng 02, Deng 03, Deng 06] and by Balili *et al.* [Balili 07].

In particular, for the numerical calculations (with the exception of subsection 3.3.4), we assume the linear coupling strength $\hbar\Omega_R = 13$ meV, the photon-exciton detuning $\delta = \epsilon_0^c - \epsilon_0^x = 5$ meV and exciton parameters of a CdTe quantum well. We study the results as a function of the system area A, ranging from 100 μm^2 to 1 cm^2. For the interaction potentials $v_x(\mathbf{k}, \mathbf{k}', \mathbf{q})$ and $v_s(\mathbf{k}, \mathbf{k}', \mathbf{q})$, we use momentum-dependent values following Ref [Rochat 00]. Where not differently specified, we assume a temperature $T = 20$ K, consistent with the estimated effective temperature [Kasprzak 06]

3.3.1   Excitation spectrum

We start our analysis from the spectral features manifested by the polariton condensate. In Fig. 3.3 we show the energy-momentum dispersion of the collective excitations, $\pm E_{\mathbf{k}}^{lp}$ and $\pm E_{\mathbf{k}}^{up}$, as obtained for two different values of the total polariton density n_p above the condensation

---

[4]With the term *advantageous* we refer to the efficiency of the iteration procedure in reaching the self-consistent solution.

threshold. The curves correspond to the positive- and negative-weight resonances for the lower- and the upper-polariton.

Close to zero momentum the dispersion of the lower polariton branch, above threshold, becomes linear, giving rise to phonon-like Bogolubov modes, as in the standard single-field Bogolubov theory [Pitaevskii 03].[5] This feature is highlighted in the inset, where the small momentum region is magnified. We further notice that, for the largest value of n_p, the polariton splitting decreases, due to both the exciton saturation, decreasing the effective exciton-photon coupling Σ_{11}^{xc}, and to the change in the exciton-photon detuning produced by the exciton blueshift, given by Σ_{11}^{xx}. For the largest value of density, $n_p = 400\ \mu\mathrm{m}^{-2}$, in Fig. 3.4 we display
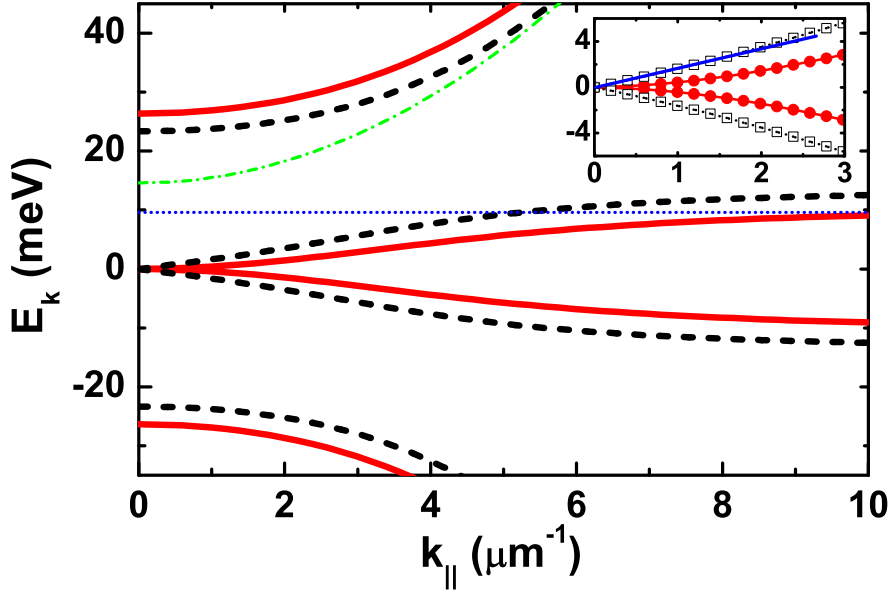

Figure 3.3: The dispersion of the normal modes of the system for polariton density $n_p = 15\ \mu\mathrm{m}^{-2}$ (solid) and $n_p = 400\ \mu\mathrm{m}^{-2}$ (dashed). The uncoupled photon (dash-dotted) and exciton (dotted) modes are also shown. Inset: detail of the low-energy region, showing the onset of the linear Bogolubov dispersion (the blue line is a guide to the eye).

the generalized Hopfield coefficients for the positive-weight lower polariton resonance. In panel (a) of this figure, we plot the coefficients on a linear scale. At small momentum, the lower polariton modes have about the same amount of photonic and excitonic character, while for wave vectors larger than $5\ \mu\mathrm{m}^{-1}$ they becomes exciton-like, as expected. The anomalous exciton and photon components are comparable at small momentum, while they become vanishingly small for $k > 2\ \mu\mathrm{m}^{-1}$. For the given density, we can thus estimate a generalized healing length for the polariton gas close to $\xi \sim 0.5\ \mu\mathrm{m}$. We can thus argue that our assumption of a uniform condensate wave function is justified by the fact that this value of ξ is much smaller than the assumed system size $A^{1/2} = 10\ \mu\mathrm{m}$. In panel (b) of Fig. 3.4, we show the same quantities, but on a double logarithmic scale. We can appreciate how the excitonic anomalous component X_v

---

[5]Recent theoretical works have suggested that deviations from equilibrium would result in a modification of the expected gapless Bogoliubov spectrum, giving rise to the appearance of a diffusive mode of excitation [Boyanovsky 02, Szymanska 06, Wouters 07b]. By means of the present equilibrium theory we obtain a phonon-like behavior at low momenta. It is interesting to mention that, within the Bogoliubov limit of our theory, we can model non-equilibrium simply by imposing a different chemical potential for the condensed and the non-condensed particles. In that case, we obtain an energy gap or a diffusive mode close to zero momentum. Results are shown in Appendix D.
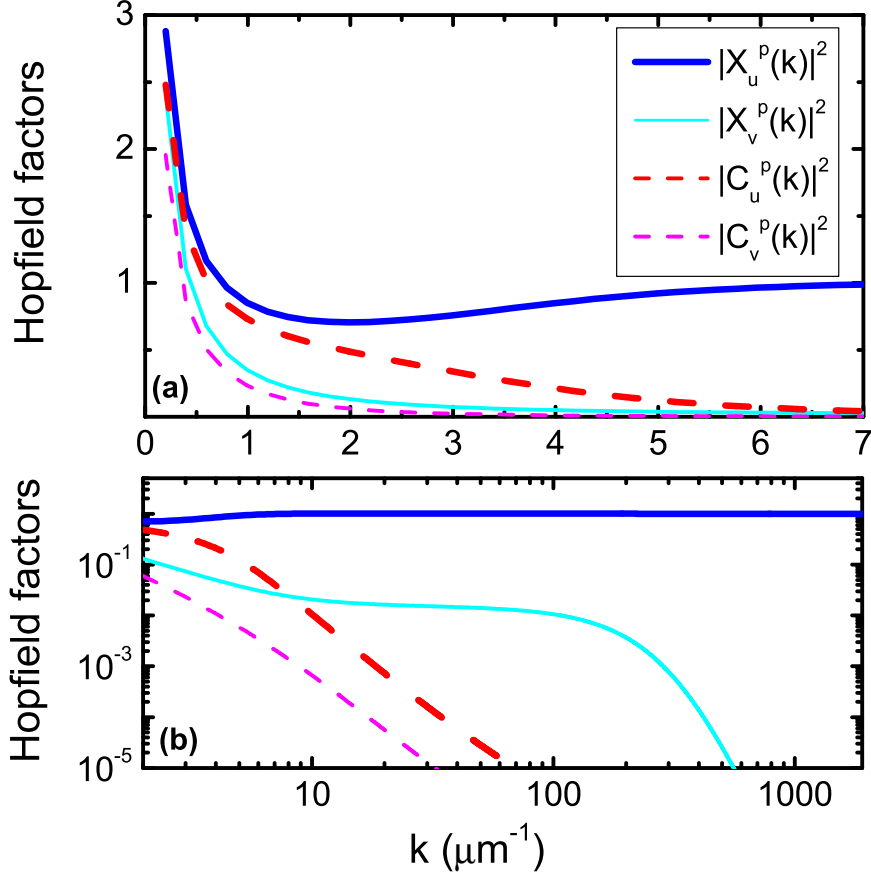
Figure 3.4: Hopfield coefficients for the lower positive polariton branch, for polariton density $n_p = 400\mu\mathrm{m}^{-2}$. The exciton and photon anomalous components are non vanishingly small only for wave vectors smaller than $\xi^{-1} = 1 - 2\mu\mathrm{m}^{-1}$. The value ξ can be interpreted as the generalized healing length of the polariton system at the given density.

remains larger than 10^{-2}, and about constant, up to wave-vectors larger than $100~\mu\mathrm{m}^{-1}$. This behavior is due to the characteristic energy *plateau* of the exciton-like part of the dispersion of the lower polariton, and to the slow momentum dependence of the two-body interaction matrix elements. This result highlights the crucial role played by the very small effective mass of polaritons at $k = 0$, which strongly reduces the amplitude of quantum fluctuations with respect to case of the exciton gas. In Fig. 3.5 we also display the resulting spectral function of the normal one-particle photon propagator $A(\mathbf{k}, E) = -2\mathrm{Im}\{(g_{11}^{cc})^{ret}(\mathbf{k}, E)\}$, for $n_p = 100~\mu\mathrm{m}^{-2}$. We see that for the negative-energy polariton resonances $E < 0$, the photon spectral function is negative, as expected. This should give rise to light amplification (gain) which however was never observed to our knowledge.

We now return to the modification of the energy splitting between the lower and the upper polariton branch. This feature was accurately characterized in recent experiments (see e.g. the supplementary online material of Kasprzak *et al.* [Kasprzak 06]). The interplay between exciton saturation and interactions in determining the energy shifts has no counterpart in the BEC of a single Bose gas, where interactions simply determine the value of the chemical potential. Here, the two effects produce an *independent* energy shift of the two polaritons. To characterize this trend, we plot in Fig. 3.6 (a) the energy shifts of the two polariton
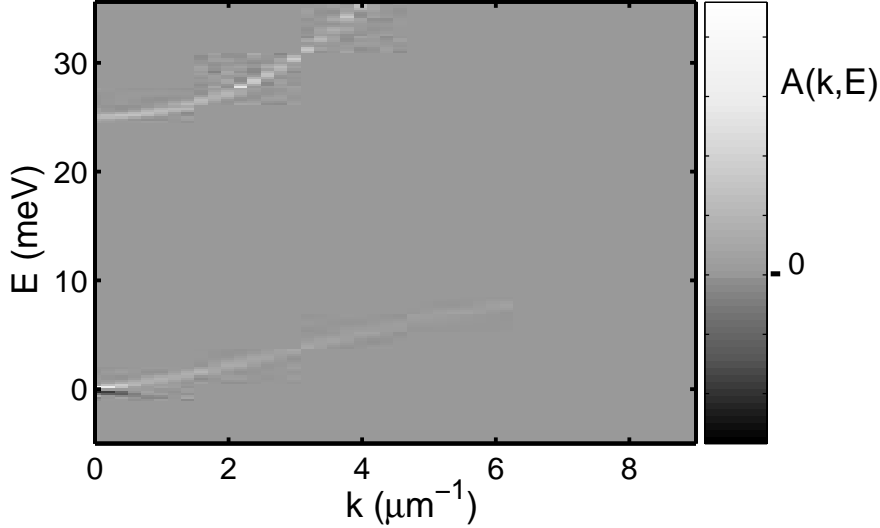
Figure 3.5: Spectral function of the normal one-particle photon propagator $A(\mathbf{k}, E) = -2\text{Im}\{(g_{11}^{cc})^{ret}(\mathbf{k}, E)\}$, for $n_p = 100 \ \mu\text{m}^{-2}$.

modes at $k = 0$, as a function of the density. Exciton saturation and interactions result in a global blue-shift of the lower polariton and a red-shift of the upper polariton. The shifts are linear as a function of the density, but their slope varies close to threshold by a factor two, as highlighted in the inset, because the contribution of the condensed populations n_{xx}^0, n_{xc}^0 is one half the contribution of the thermal populations $\tilde{n}_{xx}$, $\tilde{n}_{xc}$, as shown in Eq. (3.25).[6] This trend and the magnitude of the shifts reproduce fairly well the experimental observations (see online supplementary material in Ref. [Kasprzak 06]). To explain the origin of the opposite shifts of the two polaritons, we plot in Fig. 3.6 (b) the density dependence of the exciton energy $E_0^x \equiv \epsilon_0^x + \Sigma_{11}^{xx}$ and of the exciton-photon coupling Σ_{11}^{xc}. The two quantities vary by a comparable amount. This suggests that, within the adopted model for the exciton saturation and interaction potentials v_s and v_x, the two effects contribute equally to the deviations from the picture of non-interacting Bose gas. The reduction of the polariton splitting, according to our theory, is very small up to the largest polariton density estimated from the experiments. This supports the idea that polaritons – as hybrid exciton-photon quasiparticles – are stable up to densities above the BEC threshold.

3.3.2 Thermodynamical properties

We now turn to study the thermodynamical properties of the system. We stress the point that only the polariton population is well defined from a thermodynamical point of view, because the density matrix is diagonal only in the polariton basis. On the other hand, in experiments, only the photon population (which is related to the photon normal propagator g_{11}^{cc} via Eq. (3.18))

---

[6]The predicted change in the slope is only qualitative. In real situations, two effects can affect this result. First, in current experiments the rate of the relaxation mechanisms (basically due to final state stimulation) and thus the occupation of the polariton states, increases exponentially around the threshold (as we will see in Chapter 4). This clearly results in an analogous non-linear increase of the blue-shift close to threshold. Second, here we are neglecting the exciton spin and the polarization of the photon field. The inclusion of these degrees of freedom would modify the factor 2, arising from the exchange term. In any case, above threshold the progressive accumulation of particles in a macroscopically populated state, is expected to reduce the slope of the blue-shift increase.
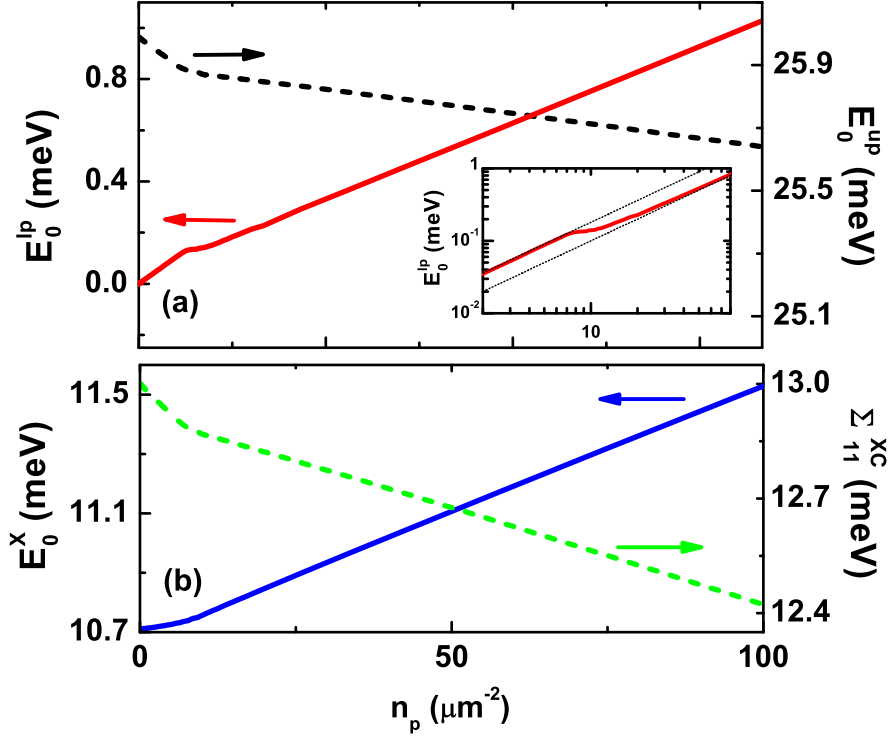
Figure 3.6: (a) Lower (solid) and upper (dashed) polariton energies at $k = 0$ vs polariton density n_p. Inset: Double logarithmic plot of the lower polariton energy. The thin dotted lines highlight the two different slopes below and above threshold. (b) Bare exciton energy E_0^x (solid) and effective exciton-photon coupling Σ_{11}^{xc} (dashed). All quantities were computed for $T = 20$ K.

is directly measured. For this reason, it is important to have a theory predicting both these populations. In Fig. 3.7, we show the one-particle populations of polaritons $\tilde{n}_{\mathbf{k}}$, excitons $\tilde{n}_{\mathbf{k}}^{xx}$ and photons $\tilde{n}_{\mathbf{k}}^{cc}$, as a function of the wave-vector $\mathbf{k}$, below and above the BEC density threshold. The trend of the three populations is very similar, except at large momentum, where the populations of excitons and polaritons obviously coincide. In particular, for wave vectors $k \in (10 - 100)\mu m^{-1}$, the polariton population is weakly k-dependent, related to the weak k-dependence of the energy dispersion of polariton in the exciton-like region. On the other hand, at small wave vectors, the photon population is close to the polariton population, both below and above the density threshold. In particular, thermal long-wavelength fluctuations of the photon occupation are important also above threshold. We just mention that the momentum distribution of the photon population is experimentally measured via the detection of the angle distribution of the emitted light. To characterize the phase transition, it is more useful to study the energy distribution of the populations, because this is directly determined by the Bose distribution. Fig. 3.8 shows the total polariton population $n_{lp}(E) + n_{up}(E)$ for three values of the total density n_p, below, above and far above the density threshold. Below threshold, polaritons are distributed according to a Maxwell-Boltzmann curve. Above threshold, the distribution becomes strongly degenerate, with a macroscopic occupation of the lowest-energy state, and a saturation of the population at high-energy. For large densities, due to two-body interactions, the energy distribution of the one-particle population differs from the ideal Bose function (while the Bogoliubov quasi-particles are distributed accordingly to the BE function). We have seen in subsection 2.2 that this discrepancy is due to quantum fluctuations (see
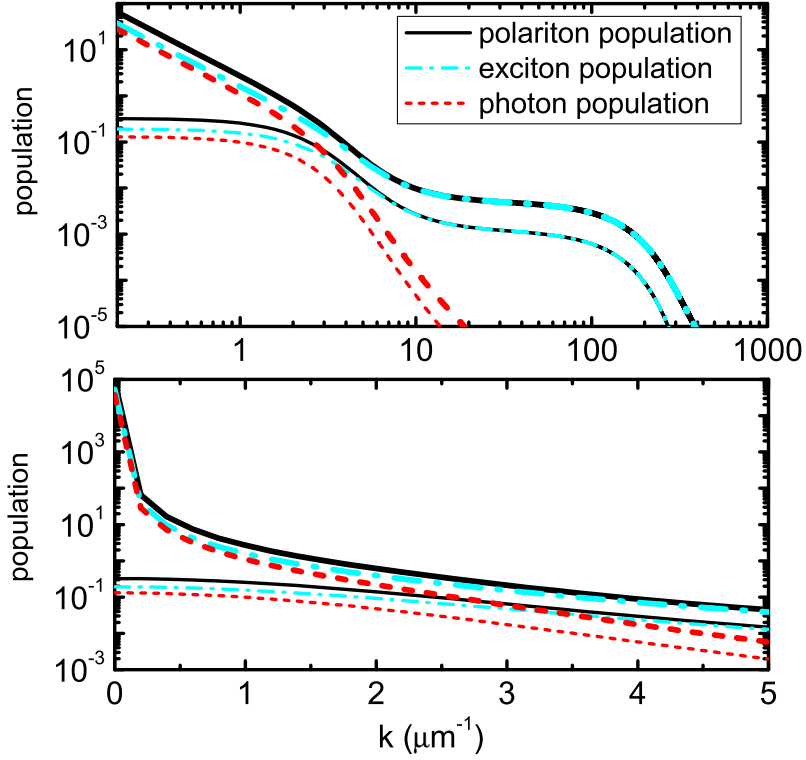
Figure 3.7: Populations of the lower polariton **k**-states below ($n_p = 3$ μm^{-2}) and above ($n_p = 100$ μm^{-2}) the density threshold. The photon and the exciton populations are also shown for comparison. Upper panel: double logarithmic scale. Lower panel: semi logarithmic scale.

Eq.(2.95)), whose amplitude in the present case is determined by the amplitude of the exciton and photon anomalous Hopfield coefficients, as shown by Eq. (3.37) and Eq. (3.39).

The appearance of a quantum degenerate distribution manifests itself also in the correlation properties. In particular, according to the Penrose-Onsager criterion [Pitaevskii 03], the main feature of BEC of an interacting gas would be the occurrence of ODLRO (see subsection 2.2.1). However, this is a good criterion only if the thermal decay of the one-body spatial correlation function $g^{(1)}(\mathbf{r})$ takes place over much smaller distance than the localization length. Differently, the thermal de Broglie wavelength λ_T would approach the system size and the concept of ODLRO would be ill-defined. For polaritons this is not obvious in principle. In Fig. 3.9 we display the simulated one-body spatial correlation function, for increasing density, both for the polariton field

$$g_p^{(1)}(\mathbf{r}) = \frac{\langle \hat{\Psi}^\dagger(\mathbf{r})\hat{\Psi}(0)\rangle}{[n_p(\mathbf{r})n_p(0)]^{1/2}} \, , \tag{3.41}$$

and for the photon field

$$g_{cc}^{(1)}(\mathbf{r}) = \frac{\langle \hat{\Psi}_c^\dagger(\mathbf{r})\hat{\Psi}_c(0)\rangle}{[n_c(\mathbf{r})n_c(0)]^{1/2}} = \frac{(g_{11}^{cc})^<(0,\mathbf{r})}{[(g_{11}^{cc})^<(\mathbf{r},\mathbf{r})(g_{11}^{cc})^<(0,0)]^{1/2}} \, , \tag{3.42}$$
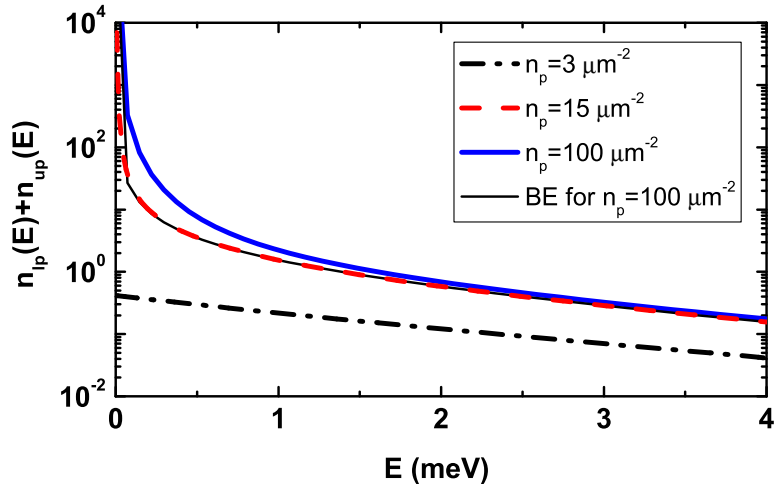
Figure 3.8: Polariton population vs. energy for $n_p = 3 \ \mu m^{-2}$, $n_p = 15 \ \mu m^{-2}$ and $n_p = 100 \mu m^{-2}$. For the larger density, we also display the ideal BE distribution.

where $(g_{11}^{cc})^<(0, \mathbf{r}) = g_{11}^{cc}(0, t; \mathbf{r}, t^+)$. The photon correlation function $g_{cc}^{(1)}(\mathbf{r})$ is the quantity measured in an optical experiment, via the observation of an interference pattern [Kasprzak 06, Balili 07]. Fig. 3.9 shows however that the photon correlation is a good mirror of the polariton correlation function $g^{(1)}$, although we predict that the actual polariton coherence is systematically lower than the measured photon coherence. Fig. 3.9 predicts the clear observation of ODLRO for the polariton system. Below threshold, spatial correlations extend only over the thermal wavelength $\lambda_T \simeq 1 \ \mu m$ which is well below the typical localization length. This value is in agreement with what measured in experiments [Kasprzak 06]. On the other hand, just above the density threshold, spatial correlations extend over the whole system size. At twice the density threshold, the amount of photon correlation is expected to exceed 80%. Also this result is in qualitative agreement with the experiment by Kasprzak *et al.* [Kasprzak 06], although in the experiment the correlation pattern is shaped by interface disorder and the maximal distance over which the correlation can be measured is lower than 10 μm. However, the measured amount of photon correlation is never larger than 40%, as compared to 80% of our prediction. We will see in Chapter 4, by means of a kinetic model [Sarchi 06, Sarchi 07a], that this discrepancy is the main result of deviations from thermodynamical equilibrium, with enhanced quantum fluctuations that deplete the condensate in favor of excitations. Furthermore, we will see that these deviations should become negligible for polariton lifetimes above 10 ps [Sarchi 07b]. In fact, the amount of spatial correlation is directly related to the condensate fraction. The predicted condensate fraction at equilibrium is shown in Fig. 3.10, where we report the density dependence of the three quantities

$$f_p = \frac{|\Psi|^2}{n_p} ,$$

$$f_c = \frac{|\Psi_c|^2}{n_{cc}} ,$$

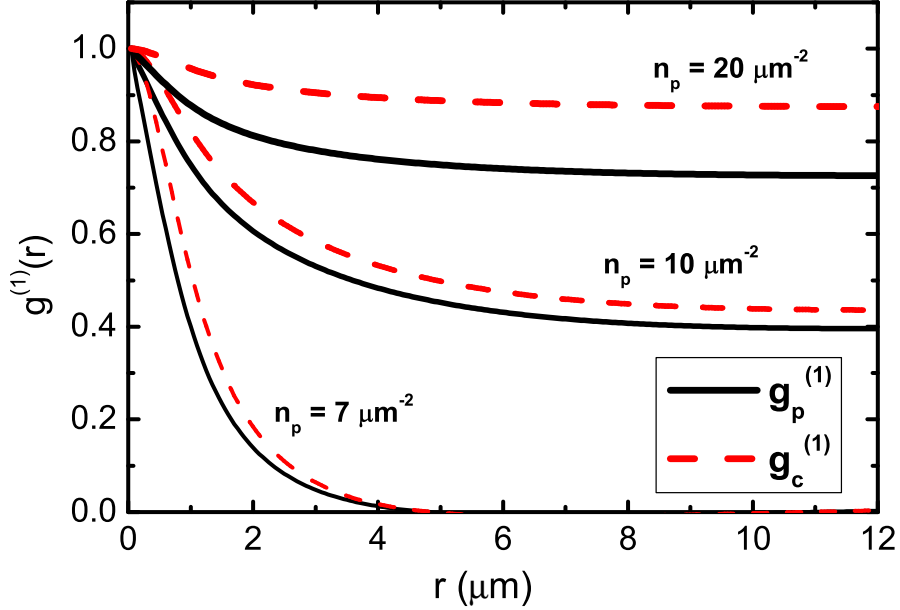$$f_x = \frac{|\Psi_x|^2}{n_{xx}} . \tag{3.43}$$

73

Figure 3.9: One-body spatial correlation function $g^{(1)}(\mathbf{r})$ for both the polariton and the photon fields.

Clearly, due to the large excitonic amount of the lower polariton modes, the increase of the photon condensate fraction is faster than the increase of the polariton condensate fraction (the only quantity which is physically meaningful), and it reaches about the 80% already at twice the density threshold. However, all the quantities increase with density and also the exciton condensate fraction is expected to become very large for the present system parameters. This feature confirms the formation of a condensate of matter degrees of freedom, thus suggesting the possible manifestation of superfluidity [Nozières 89].

3.3.3 Phase diagram

For current experiments, the temperature of the system is not a real tunable parameter, because, to achieve BEC, it is necessary to optically excite the system above an intensity threshold, thus heating up the sample. In addition, due to the weak coupling to the phonon thermal bath, it is very difficult for polaritons to reach equilibrium at the temperature of the crystal lattice (only one evidence has been recently reported [Deng 06]). For this reasons, we can only refer to an effective temperature for the polariton system. Furthermore, it is presently impossible to reach very low effective temperatures, i.e. temperatures lower than $T = 10$ K. However, a future improvement of the quality of the microcavity mirrors is expected to allow achieving polariton BEC close to thermal equilibrium and at very low temperatures (see section 4.3) [Sarchi 07b]. Therefore, a systematic study of the BEC phase diagram is of some interest. In Fig. 3.11(a), we report the density-temperature phase diagram, as computed for $A = 100$ $\mu\mathrm{m}^2$. The phase boundary in the calculations has been set by the occurrence of a finite fraction of polariton condensate larger than 1%. In the plot, a few values of the quantity $|X_0|^2$ along the
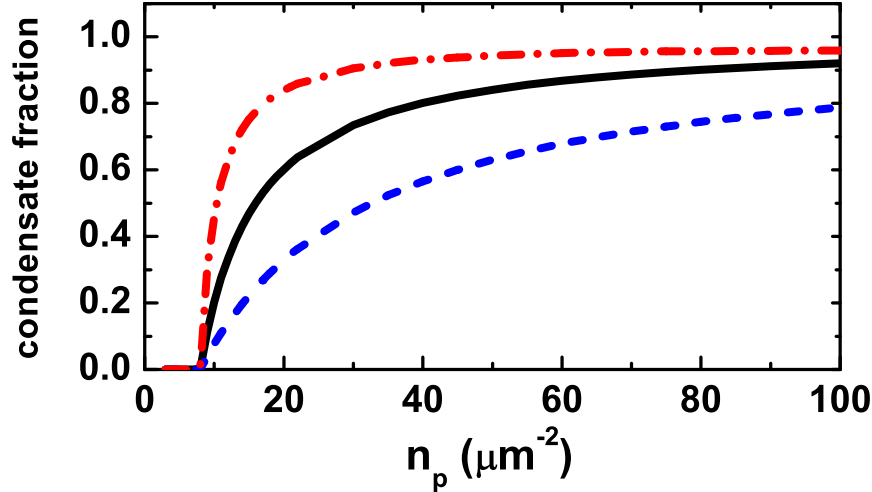
Figure 3.10: Polariton condensate fraction (solid line) computed at $T = 20$ K, as function of the polariton density. We display also the photonic (dash-dot line) and the excitonic (dashed line) condensate fractions, whose definition is given and discussed in the text.

phase boundary are indicated. This quantity represents the exciton amount in the polariton condensate. It decreases for increasing density, due to the exciton saturation and the change in detuning. For very large densities this quantity eventually vanishes, corresponding to the crossover to a photon-laser regime. However, for the studied CdTe sample, the variation of the exciton amount in the condensate field remains very small up to densities far above the experimentally estimated polariton density.

Fig. 3.11(b) shows a detail of the low-T region of the phase diagram, computed for different system areas A. In the same plot, we also display the boundary for the normal-superfluid transition, i.e. the transition to a quasicondensate, as obtained from an extension of the Landau formula [Pitaevskii 03] to the present two-field case (see Appendix E). In a homogeneous two-dimensional system, in the limit of infinite size, a true condensate cannot exist due to the divergence of low-energy thermal fluctuations. The transition to a superfluid state is instead expected, giving rise to the Berezinski-Kosterlitz-Thouless crossover with spontaneous unbinding of vortices. The divergence of the condensate fluctuations has however a logarithmic dependence on the system size. Fig. 3.11(b) shows this behaviour as a slow increase of the critical density for increasing A. Quantitatively, the critical density varies by no more than a decade, for A increasing from 100 μm^2 to 1 cm^2, and is comparable to the value predicted for the superfluid transition. This variation is even smaller, at the polariton temperature $T = 20$ K reported in experiments [Kasprzak 06]. As anticipated, the predicted dependence on the system size could be experimentally verified only in samples with improved interface quality and manifesting thermalization at a lower polariton temperature [Sarchi 07b].

The thin lines in Fig. 3.11 (b) are the result of the Bogoliubov approximation, obtained by neglecting the contribution of the excited particles in the self-energy. This approximation overestimates the group velocity of the excitations, thus underestimating dramatically the critical density at low temperature. This comparison shows that the adoption of the Popov approximation is required to give realistic predictions at low temperature.
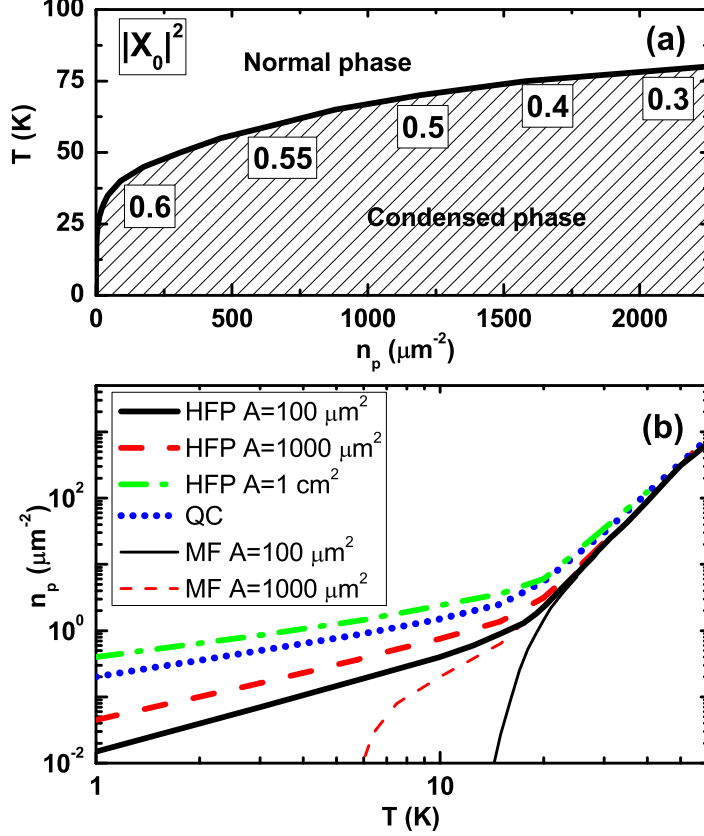
Figure 3.11: (a). Phase diagram of the polariton condensation, computed for the parameters of Ref. [Kasprzak 06], and $A = 100\ \mu m^2$. The exciton fraction in the condensate $|X_0|^2$, along the phase boundary, is indicated in boxes. (b) Detail of the low-T region. HFP denotes the result of the present theory at varying A. MF is the mean-field result. QC denotes the quasi-condensate transition, corresponding to the onset of a superfluid density.

3.3.4 Dependence on system parameters

All the predictions reported up to now are relative to a very specific set of parameters. We now apply our analysis to other samples, like the GaAs based microcavities [Deng 03, Deng 06, Balili 07], where quantitative differences are expected. In particular, we argue that the crucial parameters of the theory are the ratios

$$R_T = \frac{\hbar\Omega_R(1 - n_{xx}/n_s)}{k_B T}, \tag{3.44}$$

and

$$R_{int}\frac{\hbar\Omega_R(1 - n_{xx}/n_s)}{E_{int}}, \tag{3.45}$$

where the quantity $\hbar\Omega_R(1 - n_{xx}/n_s)$ gives an estimate of the effective exciton-photon coupling, $k_b T$ is the thermal energy while

$$E_{int} = v_x n_{xx} - 2\hbar\Omega_R\mathrm{Re}\{n_{xc}\}/n_s \tag{3.46}$$

gives an estimate of the interaction energy. The first quantity determines the actual effect of thermal fluctuations, which eventually deplete the condensate in favor of excited states in the exciton-like region of the lower polariton dispersion. The second quantity fixes the amplitude of
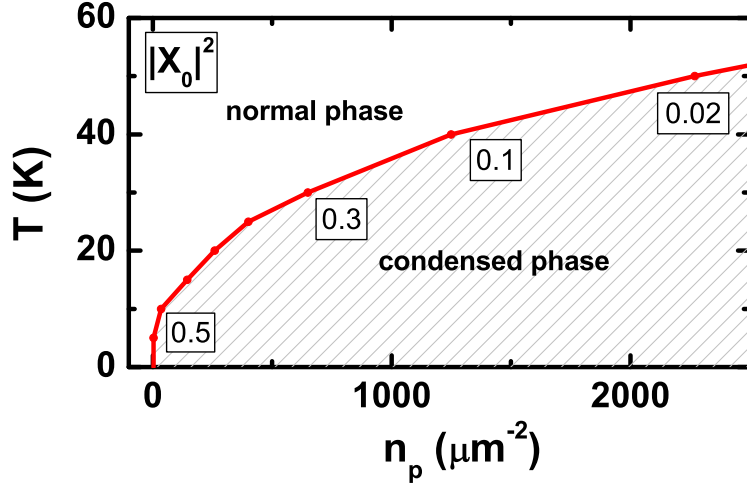
Figure 3.12: BEC phase diagram for GaAs parameters. The excitonic amount in the condensate is also shown for some values of the density threshold.

quantum fluctuations at a given density and the subsequent condensate depletion. Notice that a small ratio R_T and/or R_{int} can be the result of the reduction of the effective exciton-photon coupling, due to exciton saturation. This latter effect would strongly reduce the excitonic amount of the condensate already at moderate densities, and the photon-laser transition would eventually occurs in place of BEC.

To highlight this feature, we display in Fig. 3.12 the phase diagram obtained for system parameters of a sample constituted by a single quantum well embedded in a GaAs microcavity, with a linear exciton-photon coupling $\hbar\Omega_R = 2$ meV and zero exciton-photon detuning.[7] We see that in this case the exciton amount in the condensate decreases faster for increasing density. However, up to polariton densities close to 10^3 μm^{-2}, the exciton amount in the condensate remains finite and larger than 30%, implying that the phase transition can be interpreted as polariton BEC. This result suggests that, if the polariton system can be prepared very close to the equilibrium regime, polariton BEC could occur at sufficiently low densities, where the weakly Bose gas description still holds. We further analyze the dependence on the exciton-photon linear coupling, by plotting in Fig. 3.13 a different phase diagram, where the density threshold curves are now displayed as a function of $2\hbar\Omega_R$, i.e. the vacuum-field energy splitting between the lower and the upper polariton modes. Since the increase of $\hbar\Omega_R$ results in the suppression of both thermal and quantum fluctuations, the equilibrium density threshold is expected to decrease. We predict the same behavior for CdTe and GaAs samples, and very small quantitative differences. We just anticipate that increasing the energy splitting between lower and upper polaritons has also a negative counterpart. Indeed, we will see in Chapter 4 that the deviations from equilibrium are larger for increasing $\hbar\Omega_R$, basically because it is necessary to produce a very large incoherent population in the exciton like part of the lower polariton dispersion before the relaxation mechanisms become effective.

---

[7]We can consider this case as a limiting case for realistic samples, because GaAs manifests an exciton-photon linear coupling smaller than CdTe. In addition, the linear exciton-photon coupling scales as $\sqrt{N_Q}$, where N_Q is the number of embedded quantum wells, and in typical samples the microcavity contains several quantum wells.
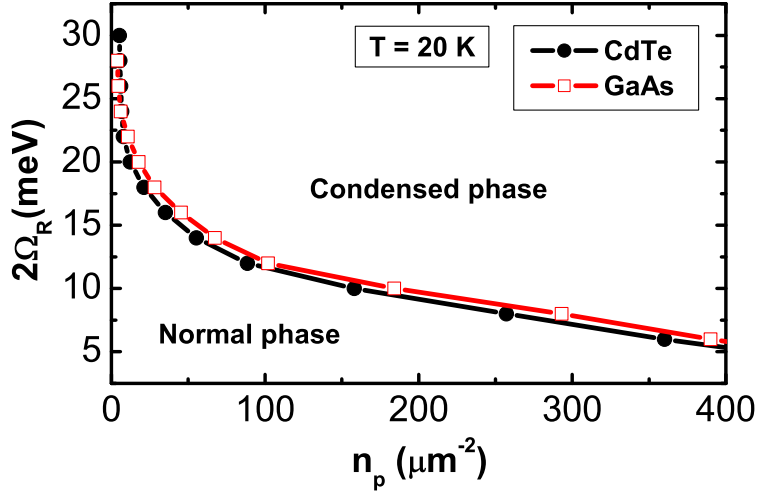
Figure 3.13: BEC threshold line on a $\hbar\Omega_R - n_p$ phase diagram for the parameters relative to CdTe and GaAs.

3.4 Conclusions and outlook

In conclusion, we have generalized the Hartree-Fock-Popov theory to the case of two coupled Bose fields at thermal equilibrium. The theory allows modeling the BEC of polaritons in semiconductor microcavities in very close analogy with the BEC of a weakly interacting gas [Pitaevskii 03]. In particular we are able to treat simultaneously both the linear exciton-photon coupling and the effect of interactions. In this way, the polariton modes are density dependent, i.e. they are not simply obtained by the diagonalization of the non-interacting limit of the exciton-photon problem. Within this description we are able to predict the modification of the spectral functions for increasing density. An important property of this theory is that the exciton and the photon propagators share the same poles, which correspond to the positive and the negative lower and upper polariton branches.

Our treatment allows to describe simultaneously the properties of the polariton, the photon and the exciton fields. This is particularly important because, while the physical field is the polariton field, all the typical optical measurements catch the properties of the photon field. Thanks to the inclusion of the excited non-condensed population, the present Popov theory can be applied at finite temperature.

In particular the predicted critical density is in good agreement with the very recent experimental estimate [Kasprzak 06]. Our analysis thus supports the interpretation of the recent experimental findings in terms of a transition to a quantum degenerate fluid. In particular, we show that the observed occurrence of photon spatial correlations is, also from a quantitative point of view, closely related to the spatial correlation of the polariton field.

Open questions remain, basically related to the role of disorder and localization. In particular, the effect of dimensionality and fluctuations and the possible crossover between BEC and BKT transitions need further analysis.

The present theory can be generalized to non homogeneous systems, and then applied to study condensation in new artificial polariton traps, like the polariton mesas [Daif 06, Kaitouni 06] or pillars [Bajoni 07]. The formalism developed in this chapter can also be extended in order to include non-equilibrium features by means of the Kadanoff-Baym (or Keldish) treatment.

Chapter 4

Polariton condensation in the non-equilibrium regime

As discussed in section 2.3, the polariton gas is realized and evolves within an intrinsic non-equilibrium regime. Qualitatively, this is also the case of trapped atomic gases, where BEC is made possible only because the cooling mechanisms are efficient enough to relax the system into thermal equilibrium within the lifetime of the metastable gas. However, in the polariton case, the relaxation mechanisms are so poorly effective that it is not clear if the equilibrium regime can be approached in realistic experimental conditions.

To answer this question, we develop in this Chapter a non-equilibrium approach, describing the condensate formation and growth, in order to investigate the possible occurrence of polariton BEC, and to clarify if, under typical experimental conditions, the transition takes place close to or far from the equilibrium regime. The present non-equilibrium model will also predict possible deviations from the equilibrium behavior described by the theory developed in Chapter 3.

4.1   Kinetic model: theory

In this section we develop a kinetic model for the description of the polariton system within the condensed regime. To this purpose, we derive kinetic equations in terms of the density matrix formalism. Since we address the specific problem of polariton relaxation and condensation, we will adopt approximations specific for the polariton system, in order to include the coherent field dynamics, driven by the presence of a condensate, and the incoherent relaxation mechanisms.

In particular, we develop a kinetic theory for polaritons in the lower polariton branch, subject to mutual interaction, in which the field dynamics of collective excitations is treated self-consistently along with the condensation kinetics. We start from a number-conserving Bogolubov approach [Gardiner 97a, Castin 98] that describes the collective modes of a Bose gas properly accounting for the number of particles in the condensate. This is required in order to develop kinetic equations for the description of condensate formation. We then derive a hierarchy of density matrix equations, including polariton-phonon scattering via deformation-potential interaction [Tassone 97] and exciton-exciton scattering in the exciton-like part of the lower-polariton branch [Tassone 99]. This latter mechanism follows the model recently developed by Porras *et al.* [Porras 02]. The hierarchy is truncated to include coupled equations for the populations in the lower polariton branch and for the two-particle correlations between the condensate and the excitations. For the truncation, we assume that higher-order correlations

evolve much faster than the relaxation dynamics. The kinetic equations obtained in this way are solved numerically, assuming a steady-state pump at high energy within the exciton-like part of the polariton branch. The solution is carried out by accounting self-consistently for the density-dependent Bogolubov spectrum of the collective excitations of the polariton gas. We will show how this model predicts an enhancement of quantum fluctuations that result in a significant condensate depletion under typical excitation conditions. In particular, we will discuss the role of quantum confinement in a system of finite size and show how ODLRO manifests itself in typical experimental conditions. Our results will provide a clear explanation of the partial suppression of ODLRO that characterizes the experimental findings [Kasprzak 06, Balili 07].

4.1.1 Lower-Polariton Hamiltonian

We restrict to consider polaritons in the lower branch of the dispersion. Obviously, this restriction implies the approximation of structureless polaritons. In other words, we are assuming that the Rabi splitting and the Hopfield factors do not change within the range of densities considered. The results of Chapter 3 (in particular the results shown in Fig. 3.11(a)) suggest that this assumption is quantitatively justified for typical systems. However, since in the non-equilibrium regime the condensation density is larger than the equilibrium prediction, we have also checked its validity by evaluating, for each considered excitation intensity, the resulting density-renormalized lower/upper- polariton Rabi splitting

$$\hbar\tilde{\Omega}_R = \hbar\Omega_R \left(1 - \frac{n_x}{n_s}\right) , \tag{4.1}$$

where n_x is the resulting total exciton density.

The lower-polariton field $\hat{p}_\mathbf{k}$ describes a Bose quasi-particle in two dimensions. The polariton operator thus obeys the Bose commutation rules

$$[\hat{p}_\mathbf{k}, \hat{p}_{\mathbf{k}'}^\dagger] = \delta_{\mathbf{k}\mathbf{k}'} . \tag{4.2}$$

The corresponding lower polariton effective Hamiltonian, in presence of two-body interaction (see subsection 2.1.6) and polariton-phonon scattering [Tassone 97] is

$$\hat{H} = \hat{H}_0 + \hat{H}_{int}^{lp} + \hat{H}_{ph} , \tag{4.3}$$

where, in the momentum representation,

$$\hat{H}_0 = \sum_\mathbf{k} \hbar\omega_\mathbf{k} \hat{p}_\mathbf{k}^\dagger \hat{p}_\mathbf{k} + \sum_\mathbf{q} \hbar\omega_\mathbf{q} \hat{D}_\mathbf{q}^\dagger \hat{D}_\mathbf{q} \tag{4.4}$$

is the free Hamiltonian for polaritons and acoustic phonons ($\hat{D}_\mathbf{k}$ represents the Bose operator destroying a phonon with wave-vector $\mathbf{k}$),

$$\hat{H}_{int}^{lp} = \frac{1}{2} \sum_{\mathbf{k}\mathbf{k}'\mathbf{q}} v_{\mathbf{k}\mathbf{k}'}^{(\mathbf{q})} \hat{p}_{\mathbf{k}+\mathbf{q}}^\dagger \hat{p}_{\mathbf{k}'-\mathbf{q}}^\dagger \hat{p}_{\mathbf{k}'} \hat{p}_\mathbf{k} , \tag{4.5}$$

is the effective two-body interaction for lower polaritons, and

$$\hat{H}_{ph} = \sum_{\mathbf{k}\mathbf{k}'\mathbf{q}} g_{\mathbf{k}\mathbf{k}'}^{(\mathbf{q})} \left(\hat{D}_\mathbf{q}^\dagger + \hat{D}_{-\mathbf{q}}\right) \left(\hat{p}_\mathbf{k}^\dagger \hat{p}_{\mathbf{k}'} + \hat{p}_{\mathbf{k}'}^\dagger \hat{p}_\mathbf{k}\right) \tag{4.6}$$

is the Hamiltonian describing the coupling between polaritons and the bath of acoustic phonons. This Hamiltonian describes processes where one phonon is absorbed or emitted while one polariton scatters between two energy states.

We have seen in subsection 2.1.6 that the quantity $v_{\mathbf{kk'}}^{(\mathbf{q})}$ arises from the exciton-exciton interaction between excitons v_x and from the oscillator strength saturation due to Pauli exclusion v_s [Rochat 00, Ben-Tabou de Leon 01, Okumura 01], as

$$v_{\mathbf{kk'}}^{(\mathbf{q})} = \frac{v_x}{A} X_{\mathbf{k+q}} X_{\mathbf{k'-q}} X_{\mathbf{k}} X_{\mathbf{k'}} + \frac{2|v_s|}{A} X_{\mathbf{k'-q}}(|C_{\mathbf{k+q}}|X_{\mathbf{k}} + X_{\mathbf{k+q}}|C_{\mathbf{k}}|) X_{\mathbf{k'}} \,. \tag{4.7}$$

Here the $X_{\mathbf{k}}, C_{\mathbf{k}}$ are the Hopfield coefficients representing the excitonic and the photonic weights respectively, in the lower polariton field, i.e.

$$\hat{p}_{\mathbf{k}} = X_{\mathbf{k}} \hat{b}_{\mathbf{k}} + C_{\mathbf{k}} \hat{c}_{\mathbf{k}} \,, \tag{4.8}$$

where, as before, $\hat{b}_{\mathbf{k}}$ and $\hat{c}_{\mathbf{k}}$ represent the exciton and the photon destruction Bose operators respectively. Notice that, in the present approximation, we neglect the density dependence of the Hopfield coefficients (in Chapter 3 we have seen that they weakly depend on density for typical experimental conditions) and consequently their time dependence during the time evolution. In Eq. (4.7) we have written the interaction matrix elements in the small-momentum limit Eqs. (2.59,2.60) [Rochat 00, Porras 02, Doan 05]. Indeed the full momentum dependence is neglected in the present approach, because we are restricting to the lower polariton branch and, in the numerical calculations, we will include the states with large momentum only in an effective way.

The polariton-phonon matrix element $g_{\mathbf{kk'}}^{(\mathbf{q})}$ is derived from the deformation potential interaction with acoustic phonons, [Tassone 97, Doan 05] which is expected to dominate at low temperature, but could also include other electron-phonon coupling mechanisms. In terms of the electron and hole deformation potentials we have

$$g_{\mathbf{kk'}}^{(\mathbf{q})} = i\sqrt{\frac{\hbar|\mathbf{q}|}{2\rho A L_z u}} X_{\mathbf{k}} X_{\mathbf{k'}} \left[a_e I_e^{||}(|\mathbf{q}_{||}|) I_e^{\perp}(q_z) - a_h I_h^{||}(|\mathbf{q}_{||}|) I_h^{\perp}(q_z) \right] \,, \tag{4.9}$$

where $|\mathbf{q}_{||}| = |\mathbf{k} - \mathbf{k'}|$ because of the in-plane momentum conservation. Here, ρ and u are the density and the longitudinal sound velocity in the semiconductor, respectively, L_z is the quantum well width and $a_{e(h)}$ are the electron (hole) deformation potentials. The terms $I_{e(h)}^{||}(|\mathbf{q}_{||}|)$ and $I_{e(h)}^{\perp}(q_z)$ are the superposition integrals of the exciton envelope function with the phonon wave function (plane wave) in the in-plane and z-directions, respectively, and read

$$I_{e(h)}^{||}(|\mathbf{q}_{||}|) = [1 + (a_0|\mathbf{q}_{||}|m_{e(h)}/2(m_e + m_h))^2]^{-3/2}$$

$$I_{e(h)}^{\perp}(q_z) = \int dz |f_{e(h)}(z)|^2 e^{iq_z z}, \tag{4.10}$$

where $m_{e(h)}$ is the electron (hole) mass while $f_{e(h)}(z)$ are the electron/hole envelope functions along the growth direction, according to the exciton envelope function picture (see Eq. (2.29)) [Tassone 97].

4.1.2 Number-conserving approach

We have discussed in subsection 2.2.3 the advantages of the Number-conserving approaches in describing the non-equilibrium features of BEC, and in particular the condensate growth.

This kind of approach is useful also in the polariton case. Indeed, Hamiltonian (4.3) conserves the number of particles because of the $\chi^{(3)}$ nonlinearity.[1] Therefore the chemical potential is well defined for polaritons, also in presence of the non-equilibrium input/output regime, due to the external pump and to the finite escape probability through the mirrors. We remind that the situation is different for a laser, where photons have not a well defined chemical potential because of the $\chi^{(2)}$ nonlinearity (i.e. one photon can scatter into two photons)[Mandel 95]. As discussed in subsection 2.2.3, the description of the condensate as a classical field would result in an unphysical kinetic equation for the condensate, in which the spontaneous in-scattering term vanishes.[2] Moreover, at any fixed time the number of particles is well defined in the real system and the scattering of a particle between the condensate and the excited state conserves the total number of particles. In particular, the energy eigenvalues of the excited states depend self-consistently on the actual number of condensed and non-condensed particles [Gardiner 97a, Gardiner 98]. When including relaxation mechanisms, this dependence also affects the energy relaxation rates. Here, we adopt the formalism developed by Castin and Dum [Castin 98] and, in an equivalent way, by Gardiner [Gardiner 97a] and we will derive kinetic equations by following the Hartree-Fock-Bogoliubov scheme. We remind however that already Bogoliubov introduced a Number-conserving version of his theory, predicting the same thermodynamical properties of the U(1) symmetry breaking approach [Zagrebnov 01].

In the number-conserving approach, the polariton Bose field is expressed as

$$\hat{p}_{\mathbf{k}} = P_{\mathbf{k}}\hat{a} + \tilde{p}_{\mathbf{k}}\,, \tag{4.11}$$

i.e. the sum of a condensate part $P_{\mathbf{k}}\hat{a}$ and a one-particle excitation operator $\tilde{p}_{\mathbf{k}}$. The condensate part is the product of the condensate wave function (in the wave vector space) $P_{\mathbf{k}}$ times the Bose operator $\hat{a}$, destroying one particle in the condensate. Obviously $\hat{a}$ obeys

$$[\hat{a}, \hat{a}^{\dagger}] = 1\,. \tag{4.12}$$

Considering the normalization relation

$$\sum_{\mathbf{k}} |P_{\mathbf{k}}|^2 = 1\,, \tag{4.13}$$

the condensate population is simply given by the average $N_c = \langle \hat{a}^{\dagger}\hat{a} \rangle$. The one-particle excitation field $\tilde{p}_{\mathbf{k}}$ is orthogonal to the wave function of the condensate, i.e.

$$\sum_{\mathbf{k}} P_{\mathbf{k}}^{*}\tilde{p}_{\mathbf{k}} = 0 \tag{4.14}$$

and, since

$$\left[\tilde{p}_{\mathbf{k}}, \hat{a}^{\dagger}\right] = 0\,, \tag{4.15}$$

it obeys the modified Bose commutation rule

$$[\tilde{p}_{\mathbf{k}}, \tilde{p}_{\mathbf{k}'}^{\dagger}] = \delta_{\mathbf{k}\mathbf{k}'} - P_{\mathbf{k}}P_{\mathbf{k}'}^{*}\,, \tag{4.16}$$

---

[1]We point out that, in real systems, a $\chi^{(2)}$ nonlinearity is also present, but, for typical samples like GaAs based microcavities, it is very small due to symmetry reasons and thus it is safely neglected in the system Hamiltonian (4.3).

[2]One way to overcome this problem within a symmetry-breaking approach consists in writing a separate semi-classical Boltzmann equation for the condensate density and introducing a stimulation term scaling as the inverse of the area, as was done by Doan *et al.* [Doan 05].

where the deviation from the exact Bose commutation rule depends on the wave function of the condensate.[3] By using these definitions, and by assuming that there is not first order coherence between the condensate and the one-particle excitations, i.e. $\langle \hat{a}^\dagger \tilde{p}_{\mathbf{k}} \rangle = 0$, the total population at momentum $\mathbf{k}$ is

$$N_{\mathbf{k}} = \langle \hat{p}_{\mathbf{k}}^\dagger \hat{p}_{\mathbf{k}} \rangle = |P_{\mathbf{k}}|^2 N_c + \tilde{N}_{\mathbf{k}} \,, \tag{4.17}$$

where

$$\tilde{N}_{\mathbf{k}} = \langle \tilde{p}_{\mathbf{k}}^\dagger \tilde{p}_{\mathbf{k}} \rangle \tag{4.18}$$

is the population of non-condensed particles.

Within the number conserving approach, the fluctuation field is defined by the operator [Castin 98]

$$\hat{\Lambda}_{\mathbf{k}}^\dagger \equiv \frac{1}{\sqrt{N}} \hat{a} \tilde{p}_{\mathbf{k}}^\dagger \tag{4.19}$$

that promotes a particle from the condensate to the excited states. In Eq. (4.19) $N = \sum_{\mathbf{k}} N_{\mathbf{k}}$ is the total number of particles. This quantity is conserved in each process where a particle scatters between the condensate and the excited states.[4] Within the definition (4.19), the fluctuation field has obviously a vanishing expectation value

$$\langle \hat{\Lambda}_{\mathbf{k}}^\dagger \rangle = \frac{1}{\sqrt{N}} \langle \hat{a} \tilde{p}_{\mathbf{k}}^\dagger \rangle = 0 \,, \tag{4.20}$$

while its amplitude scales as the square root of the one-particle population $\tilde{N}_{\mathbf{k}}$, because

$$\sqrt{\langle \hat{\Lambda}_{\mathbf{k}}^\dagger \hat{\Lambda}_{\mathbf{k}} \rangle} \sim \sqrt{\frac{N_c \tilde{N}_{\mathbf{k}}}{N}} = f_c^{1/2} \sqrt{\tilde{N}_{\mathbf{k}}} \,, \tag{4.21}$$

and the condensate fraction $f_c = N_c/N$ is of the order of 1 for a condensed system. The fluctuation composite operator obeys quasi-Bose commutation rules

$$\left[\hat{\Lambda}_{\mathbf{k}}, \hat{\Lambda}_{\mathbf{q}} \right] = 0 \tag{4.22}$$

and

$$\begin{aligned}
\left[\hat{\Lambda}_{\mathbf{k}}, \hat{\Lambda}_{\mathbf{q}}^\dagger \right] &= \frac{1}{N} \left[\left(\delta_{\mathbf{k}\mathbf{q}} - P_{\mathbf{k}} P_{\mathbf{q}}^* \right) \hat{a}^\dagger \hat{a} - \tilde{p}_{\mathbf{q}}^\dagger \tilde{p}_{\mathbf{k}} \right] \\
&\simeq \delta_{\mathbf{k}\mathbf{q}} \frac{N_c}{N} - \frac{\tilde{N}_{\mathbf{q}\mathbf{k}} + P_{\mathbf{q}}^* P_{\mathbf{k}} N_c}{N} \,,
\end{aligned} \tag{4.23}$$

where in the second line we have approximated the product of operators with one-particle densities and $\tilde{N}_{\mathbf{q}\mathbf{k}} \equiv \langle \tilde{p}_{\mathbf{q}}^\dagger \tilde{p}_{\mathbf{k}} \rangle$. It is useful to define the formal Bogoliubov transformation,

$$\hat{\Lambda}_{\mathbf{k}} = \sum_j U_{j,\mathbf{k}} \hat{\alpha}_j + V_{j,\mathbf{k}}^* \hat{\alpha}_j^\dagger \,, \tag{4.24}$$

---

[3]This relation is particularly important when the formalism is applied to describe the time evolution of the condensate wave function in space. However, in what follows, we assume a constant uniform condensate wave function, i.e. $P_{\mathbf{k}} \sim \delta_{\mathbf{k}0}$, and the one-particle field obeys the exact Bose commutation rule.

[4]Recently, Gardiner and Morgan have suggested a different definition of the fluctuation field in the Number conserving approach [Gardiner 07]. Indeed they replace the total number of particles with the number of condensed particles at a given time. This has been done to avoid the assumption $N_c(t) \sim N$ in the derivation of the dynamical equations. However, for the polariton case, as we will see later on, basically due to the fact that the relaxation rates are slow with respect to the frequencies of the fluctuations $\hat{\Lambda}$, it is more convenient to scale the fluctuations with the total number of polaritons in the coherent energy region at a given time (we will define the coherent region later on).

which allow to express the fluctuation with wave-vector $\mathbf{k}$ in terms of the exact Bose operators $\hat{\alpha}_j$ representing the collective excitations of the system with energy E_j ($\bar{j}$ is the time reversal of the state j) [Pitaevskii 03, Castin 98]. The modal functions $U_{j,\mathbf{k}}$ and $V^*_{\bar{j},\mathbf{k}}$ obey the conditions

$$U_{j,\mathbf{k}}V^*_{j,\mathbf{q}} = U_{\bar{j},\mathbf{q}}V^*_{\bar{j},\mathbf{k}}, \tag{4.25}$$

imposed by the commutation rule (4.22), and

$$U^*_{j,\mathbf{q}}U_{j,\mathbf{k}} - V_{\bar{j},\mathbf{q}}V^*_{\bar{j},-\mathbf{k}} = \delta_{\mathbf{k}\mathbf{q}}\frac{N_c}{N} - \frac{\tilde{N}_{\mathbf{q}\mathbf{k}} + P^*_{\mathbf{q}}P_{\mathbf{k}}N_c}{N}, \tag{4.26}$$

imposed by the commutation rule (4.23). The explicit expression of the modal functions $U_{j,\mathbf{k}}$ and $V^*_{\bar{j},\mathbf{k}}$, within the Hartree-Fock-Popov limit, is given below, in Eq. (4.45).

In particular, for a uniform system,

$$P_{\mathbf{k}} = e^{i\phi}\delta_{\mathbf{k}0},$$
$$\tilde{N}_{\mathbf{q}\mathbf{k}} \equiv \langle \tilde{p}^\dagger_{\mathbf{q}}\tilde{p}_{\mathbf{k}}\rangle = \delta_{\mathbf{k}\mathbf{q}}\tilde{N}_{\mathbf{k}}, \tag{4.27}$$

the commutation rule (4.23) reduces to

$$\left[\hat{\Lambda}_{\mathbf{k}}, \hat{\Lambda}^\dagger_{\mathbf{q}}\right] \simeq \delta_{\mathbf{k}\mathbf{q}}\frac{N_c - \tilde{N}_k}{N} \equiv \delta_{\mathbf{k}\mathbf{q}}\xi_{\mathbf{k}}. \tag{4.28}$$

In the uniform case, the collective excitations have a well-defined wave-vector, and the Bogoliubov transformation is simply

$$\hat{\Lambda}_{\mathbf{k}} = U_{\mathbf{k}}\hat{\alpha}_{\mathbf{k}} + V^*_{-\mathbf{k}}\hat{\alpha}^\dagger_{-\mathbf{k}}, \tag{4.29}$$

where now the normalization of the modal functions $U_{\mathbf{k}}$ and $V^*_{-\mathbf{k}}$ reduces to

$$|U_{\mathbf{k}}|^2 - |V_{\mathbf{k}}|^2 = \xi_{\mathbf{k}}. \tag{4.30}$$

Using Eqs (4.29) and (4.19), we obtain a direct relation between the population in the collective modes

$$\bar{N}_{\mathbf{k}} = \langle \hat{\alpha}^\dagger_{\mathbf{k}}\hat{\alpha}_{\mathbf{k}}\rangle, \tag{4.31}$$

and the one-particle population

$$\langle \tilde{p}^\dagger_{\mathbf{k}}\tilde{p}_{\mathbf{k}}\rangle = \frac{N}{1 + N_c}\left[\left(\xi_{\mathbf{k}} + 2|V_{\mathbf{k}}|^2\right)\bar{N}_{\mathbf{k}} + |V_{\mathbf{k}}|^2\right]. \tag{4.32}$$

We point out that, while at thermal equilibrium the populations $\bar{N}_{\mathbf{k}}$ are fixed by the Bose distribution, in the non-equilibrium regime the populations evolve in time, during an initial transient, eventually reaching steady state if the pump intensity is constant over time. Therefore, in a non-equilibrium regime, it is difficult to apply relation (4.32), where the populations and the modal functions are in principle time dependent. For this reason, in our approach we will introduce two different time scales (an approximation justified by the physics of polaritons) and we will use Eq.(4.32) only to evaluate the actual occupation in the collective modes during the relaxation and, consequently, evaluate the two-body correlations.

4.1.3 Two-body interaction

The two-body interaction $\hat{H}_{int}^{lp}$ in Eq. (4.3) has two main effects. First, it introduces the collision processes which contribute to the thermalization of the gas. Second, it modifies the spectrum of the system, in particular when condensation occurs. Indeed, we have seen in section 2.2 that, already in the mean-field limit, for a condensed system, the spectrum is strongly modified with respect to the single-particle one, and the actual eigenmodes of the system are collective excitations with a phonon-like dispersion at low-momenta. In addition, and due to the spectrum modifications, in the condensed system two-body interaction also triggers the coherent scattering processes responsible for quantum fluctuations [Leggett 01].

Initially we totally disregard the effect of the incoherent collisions [Gardiner 98] driving the relaxation dynamics, and we treat the mutual interaction term by means of an Hartree-Fock-Bogoliubov approach. We will see later on how to address the problem of the incoherent collisions.

Hartree-Fock-Bogoliubov approximation

Within the Hartree-Fock-Bogoliubov (HFB) approximation, Hamiltonian $\hat{H}_{int}^{lp}$ is written in the truncated form

$$\hat{H}_{HFB} = \frac{1}{2}\sum_{\mathbf{kk'}} v_{\mathbf{kk'}}^{(\mathbf{0})}\hat{p}_{\mathbf{k}}^{\dagger}\hat{p}_{\mathbf{k'}}^{\dagger}\hat{p}_{\mathbf{k'}}\hat{p}_{\mathbf{k}} + \frac{1}{2}\sum_{\mathbf{k}\neq\pm\mathbf{k'}} v_{\mathbf{kk'}}^{(\mathbf{k-k'})}\hat{p}_{\mathbf{k}}^{\dagger}\hat{p}_{\mathbf{k'}}^{\dagger}\hat{p}_{\mathbf{k}}\hat{p}_{\mathbf{k'}} + \frac{1}{2}\sum_{\mathbf{k}\neq\mathbf{k'}} v_{\mathbf{kk'}}^{(\mathbf{k-k'})}\hat{p}_{\mathbf{k}}^{\dagger}\hat{p}_{-\mathbf{k}}^{\dagger}\hat{p}_{\mathbf{k'}}\hat{p}_{-\mathbf{k'}}\,, \quad (4.33)$$

where the first and the second terms correspond to the direct and the exchange terms of the HF approximation (and are equal in the limit where the matrix interaction does not depend on the exchanged wave vector), while the third term arises from the presence of anomalous correlations [Schmitt 01]. By separating the operator $\hat{p}$ in the condensate and non-condensate contributions accordingly with the Number-conserving expression Eq. (4.11), and specializing to a uniform system, Hamiltonian (4.33) reads

$$\begin{aligned}
\hat{H}_{HFB} &= \frac{1}{2}v_{\mathbf{00}}^{(\mathbf{0})}\hat{a}^{\dagger}\hat{a}^{\dagger}\hat{a}\hat{a} + \sum_{\mathbf{k}}{}' (v_{\mathbf{k0}}^{(\mathbf{0})}+v_{\mathbf{k0}}^{(\mathbf{k})})\tilde{p}_{\mathbf{k}}^{\dagger}\tilde{p}_{\mathbf{k}}\hat{a}^{\dagger}\hat{a} + \frac{1}{2}\sum_{\mathbf{k}}{}' v_{\mathbf{k0}}^{(\mathbf{k})}\left(\tilde{p}_{\mathbf{k}}^{\dagger}\tilde{p}_{-\mathbf{k'}}^{\dagger}\hat{a}\hat{a} + h.c.\right) \\
&+ \frac{1}{2}\sum_{\mathbf{kk'}}{}' v_{\mathbf{kk'}}^{(\mathbf{0})}\tilde{p}_{\mathbf{k}}^{\dagger}\tilde{p}_{\mathbf{k'}}^{\dagger}\tilde{p}_{\mathbf{k'}}\tilde{p}_{\mathbf{k}} + \frac{1}{2}\sum_{\mathbf{k}\neq\pm\mathbf{k'}}{}' v_{\mathbf{kk'}}^{(\mathbf{k-k'})}\tilde{p}_{\mathbf{k}}^{\dagger}\tilde{p}_{\mathbf{k'}}^{\dagger}\tilde{p}_{\mathbf{k}}\tilde{p}_{\mathbf{k'}} + \frac{1}{2}\sum_{\mathbf{k}\neq\mathbf{k'}}{}' v_{\mathbf{kk'}}^{(\mathbf{k-k'})}\tilde{p}_{\mathbf{k}}^{\dagger}\tilde{p}_{-\mathbf{k}}^{\dagger}\tilde{p}_{\mathbf{k'}}\tilde{p}_{-\mathbf{k'}}\,,
\end{aligned} \quad (4.34)$$

where the prime means that $\mathbf{k}=0$ is excluded from the sum. Clearly this Hamiltonian results in the self-energy diagrams displayed in Fig. 2.9.

From the Heisenberg equation of motion

$$i\hbar\dot{\hat{a}} = \left[\hat{a}, \hat{H}_{HFB}\right]$$

$$i\hbar\dot{\tilde{p}}_{\mathbf{k}} = \left[\tilde{p}_{\mathbf{k}}, \hat{H}_{HFB}\right] \quad (4.35)$$

we derive the kinetic equations for the populations in the condensate and in the one-particle excited states

$$\dot{N}_c = \frac{2}{\hbar}\text{Im}\left\{\sum_{\mathbf{k}} v_{\mathbf{k0}}^{(\mathbf{k})}\tilde{m}_{\mathbf{k}}\right\}\,, \quad (4.36)$$

$$\dot{\tilde{N}}_{\mathbf{k}} = -\frac{2}{\hbar}v_{\mathbf{k0}}^{(\mathbf{k})}\text{Im}\{\tilde{m}_{\mathbf{k}}\}\,, \quad (4.37)$$

where we have defined the scattering amplitude

$$\tilde{m}_k \equiv \langle \hat{a}^\dagger \hat{a}^\dagger \tilde{p}_{\mathbf{k}} \tilde{p}_{-\mathbf{k}} \rangle = N \langle \hat{\Lambda}_{\mathbf{k}} \hat{\Lambda}_{-\mathbf{k}} \rangle \,. \tag{4.38}$$

This quantity describes the scattering of two particles between the condensate and the excited states and it represents the main effect of quantum fluctuations. These processes do not conserve energy and could not be described in terms of Boltzmann equations for the populations of the single-particle states. They are made possible only because, in a condensed system, the actual eigenstates are collective modes and differ from the single-particle states. As a consequence, the quantities $\langle \hat{\Lambda}_{\mathbf{k}} \hat{\Lambda}_{-\mathbf{k}} \rangle$ are finite. Clearly, their amplitude decreases for increasing wave vector $\mathbf{k}$, because only the phonon-like long wavelength collective excitations differ significantly from the corresponding single-particle excitations, as suggested by the discussion in section 2.2 and explicitly shown later on. In particular, we will verify this trend in Fig. 4.5, where we will show that the amplitudes $\tilde{m}_k$ vanish at large $\mathbf{k}$. We point out the fact that, at thermal equilibrium, the amplitudes $\tilde{m}_{\mathbf{k}}$ would be given by the value

$$\tilde{m}_{\mathbf{k}} = N U_{\mathbf{k}} V_{-\mathbf{k}} \left(2\bar{N}_{\mathbf{k}} + 1 \right) \,, \tag{4.39}$$

where we have used the definitions (4.29) and (4.31) and the modal functions can be chosen as real. Therefore, at thermal equilibrium, $\tilde{m}_{\mathbf{k}}$ is a real quantity and, from Eqs. (4.36) and (4.37), the system is in a steady state as expected. In this case, the quantity in Eq. (4.39) represents the fluctuations of the number operator $\hat{N}_c$ around its mean value. On the other hand, in the non-equilibrium regime, the amplitudes $\tilde{m}_{\mathbf{k}}$ are not given by Eq. (4.39), because the actual expectation values N_c, $N_{\mathbf{k}}$ can be far from the equilibrium solution. Therefore we need an additional kinetic equation to establish the actual values of the amplitudes $\tilde{m}_{\mathbf{k}}$. Again from the Heisenberg equations we obtain (see Appendix F for the derivation)

$$
\begin{aligned}
\dot{\tilde{m}}_{\mathbf{k}} &= -2 \left[i\omega_{\mathbf{k}} + \frac{i}{\hbar} v_{\mathbf{k0}}^{(0)} (N_c - \tilde{N}_{\mathbf{k}} - 5/2) \right] \tilde{m}_{\mathbf{k}} \\
&\quad - \frac{i}{\hbar} \left[\sum_{\mathbf{q}} v_{\mathbf{qq}}^{(\mathbf{k}-\mathbf{q})} \tilde{m}_{\mathbf{q}} + 2 v_{\mathbf{kk}}^{(\mathbf{k})} N_c (N_c - 1) \right] (1 + 2\tilde{N}_{\mathbf{k}}) \\
&\quad + 2 \frac{i}{\hbar} (1 + 2N_c) \sum_{\mathbf{q}} v_{\mathbf{qq}}^{(\mathbf{q})} \langle \tilde{p}_{\mathbf{q}}^\dagger \tilde{p}_{-\mathbf{q}}^\dagger \tilde{p}_{\mathbf{k}} \tilde{p}_{-\mathbf{k}} \rangle \,.
\end{aligned} \tag{4.40}
$$

In deriving Eq. (4.40) we have adopted the following two simplifications. First, the higher order three-body correlations, arising as the next level of the correlation hierarchy, have been factored into products of one- and two-body correlations. Second, we have assumed the identity

$$\langle \hat{a}^\dagger \hat{a}^\dagger \hat{a} \hat{a} \rangle = N_c (N_c - 1) \tag{4.41}$$

to hold, as expected for a macroscopic condensate occupation, $N_c \gg 1$. In the resulting equation, the two-body correlation function *between* one-particle excitations,

$$\tilde{C}_{\mathbf{k},\mathbf{q}} = \langle \tilde{p}_{\mathbf{q}}^\dagger \tilde{p}_{-\mathbf{q}}^\dagger \tilde{p}_{\mathbf{k}} \tilde{p}_{-\mathbf{k}} \rangle \tag{4.42}$$

is written in an implicit way. This quantity is strongly affected by the presence of collective excitations and thus it cannot be simply factored into products of one-particle densities. We can estimate the effect of the modified spectrum, by expressing $\tilde{C}_{\mathbf{k}\mathbf{q}}$ in terms of the modal functions U_k and V_{-k}^*, obtained by diagonalizing the Bogoliubov problem in the Popov limit

at each time step in the kinetics. To this purpose, we write the dynamical equation of the fluctuation field in the mean-field limit (i.e. by performing the same factorizations in terms of the particle densities, used to derive Eq. 4.40)

$$\dot{\hat{\Lambda}}_{\mathbf{k}} = (\omega_{\mathbf{k}} + v_{\mathbf{k0}}^{(0)}\xi_{\mathbf{k}})\hat{\Lambda}_{\mathbf{k}} + v_{\mathbf{kk}}^{(\mathbf{k})}\xi_{\mathbf{k}}\hat{\Lambda}_{\mathbf{k}}^{\dagger} . \tag{4.43}$$

From there, we derive the eigenvalues

$$E_{\mathbf{k}} = [(\omega_{\mathbf{k}} + v_{\mathbf{k0}}^{(0)}\xi_{\mathbf{k}})^2 - (v_{\mathbf{kk}}^{(\mathbf{k})}\xi_{\mathbf{k}})^2]^{1/2} \tag{4.44}$$

and the modal functions

$$|V_{\mathbf{k}}|^2 = \xi_{\mathbf{k}} \frac{\left[E_{\mathbf{k}} - (\omega_{\mathbf{k}} + v_{\mathbf{k0}}^{(0)}\xi_{\mathbf{k}})\right]^2}{(v_{\mathbf{kk}}^{(\mathbf{k})}\xi_{\mathbf{k}})_{\mathbf{k}}^2 - \left[E_{\mathbf{k}} - (\omega_{\mathbf{k}} + v_{\mathbf{k0}}^{(0)}\xi_{\mathbf{k}})\right]^2} \tag{4.45}$$

In this limit, we can replace in (4.40) $\tilde{C}_{\mathbf{k},\mathbf{q}} \simeq \tilde{C}_{\mathbf{k},\mathbf{q}}^{Popov}$, with

$$
\begin{aligned}
\tilde{C}_{\mathbf{k},\mathbf{q}}^{Popov} = & \frac{N^2}{(N_c + 1)(N_c + 2)} \left\{ U_{\mathbf{k}}V_{\mathbf{k}}^* U_{\mathbf{q}}^* V_{\mathbf{q}}(1 + 2\bar{N}_{\mathbf{k}})(1 + 2\bar{N}_{\mathbf{q}}) \right. \\
& \left. + \delta_{\mathbf{kq}}\left[2\chi_{\mathbf{k}}\bar{N}_{\mathbf{k}}\left(\chi_{\mathbf{k}}\bar{N}_{\mathbf{k}} + 2\left|V_{\mathbf{k}}\right|^2\right) + 2\left|V_{\mathbf{k}}\right|^4\right] \right\} ,
\end{aligned}
\tag{4.46}
$$

where $\chi_{\mathbf{k}} = \xi_{\mathbf{k}} + 2\left|V_{\mathbf{k}}\right|^2$ and $\bar{N}_{\mathbf{k}}$ can be expressed in terms of the one-particle population via Eq. (4.32). This finally brings to a closed set of kinetic equations for the amplitudes $\tilde{m}_{\mathbf{k}}$, and the populations N_c, $\bar{N}_{\mathbf{k}}$.

We have derived the kinetic equations within the HFB limit, but, at the same time, we have computed the time-dependent spectrum of collective excitations, within the Popov limit. This might seem contradictory. However, this procedure is motivated by the purpose of fulfilling two physical requirements, by means of a consistent mean-field approach. Indeed, while the kinetic equations are derived accordingly to a conservative theory like the HFB approximation, the spectrum is determined within a gapless approximation, thus without introducing any artificial energy gap between the condensate and the excitations (in this way the actual energy gap only depends on the system size and it correctly goes to zero for $A \rightarrow \infty$). These two properties would be simultaneously fulfilled only within the second order Beliaev theory, whose application in a non-equilibrium regime is however problematic and requires several approximations [Imamović-Tomasović 99]. From a quantitative point of view, we remind that, at thermal equilibrium, the Popov collective spectra result to be in good agreement with the measured excitation spectra of a weakly interacting Bose gas, when the temperature is not too close to the critical temperature, i.e. $T \leq 0.5 T_c$. This condition corresponds to a density considerably above the critical density [Dodd 98, Liu 04]. Therefore, within the present model, we expect to correctly account for the effect of collective excitations above the condensation threshold, i.e. when ODLRO becomes detectable. At the same time we notice that, close to threshold, the polariton relaxation dynamics and the coherent scattering processes are expected to be only marginally affected by the presence of collective excitations, because the populations in the condensate and in the low-lying excited states are small, as argued by Porras *et al.* [Porras 02].

We have already highlighted the importance of spatial confinement in the physics of microcavity polaritons. In a kinetic treatment, it is however difficult to introduce a realistic confinement potential and thus to account for a nonuniform, time-dependent density profile. Therefore we assume a finite-size homogeneous system of square shape and area A with periodic boundary conditions, resulting in spatially a uniform condensate wave function, i.e.

$P_{\mathbf{k}} = e^{i\phi}\delta_{\mathbf{k},\mathbf{0}}$. In a realistic condensate, this assumption is valid everywhere, except within a distance from the boundary equal to the healing length $\xi = \hbar/\sqrt{Mvn}$ [Pitaevskii 03]. For polaritons, we find $\xi \approx 1~\mu$m for the estimated non-equilibrium density threshold (in agreement with the equilibrium estimate reported in Chapter 3). As discussed in Chapter 3 such a confinement can model both finite size polariton traps [Daif 06] and the situation close to a local minimum of the disorder potential in extended systems [Richard 05b, Langbein 02]. In particular, the finite size results in a discrete energy spectrum, with an energy gap between ground and first excited state $\Delta = \hbar^2(2\pi)^2/(M_{pol}A)$ [Doan 05].

Collision terms

Clearly, within the HFB limit, the incoherent collision terms are totally neglected. Indeed, the collision self-energy terms should appear only beyond the mean-field limit. However, they can be simply treated by means of semiclassical Boltzmann equations [Tassone 99]. Unfortunately, such a procedure would be inconsistent with the mean field approach just developed. The typical dispersion of the lower polariton will allow to solve this problem, by suggesting a net separation between a coherent low-energy region where incoherent collisions can be neglected and an incoherent high-energy region where the semiclassical approach can be adopted. We will discuss this separation later on. Here, we simply report the relaxation rates, as obtained
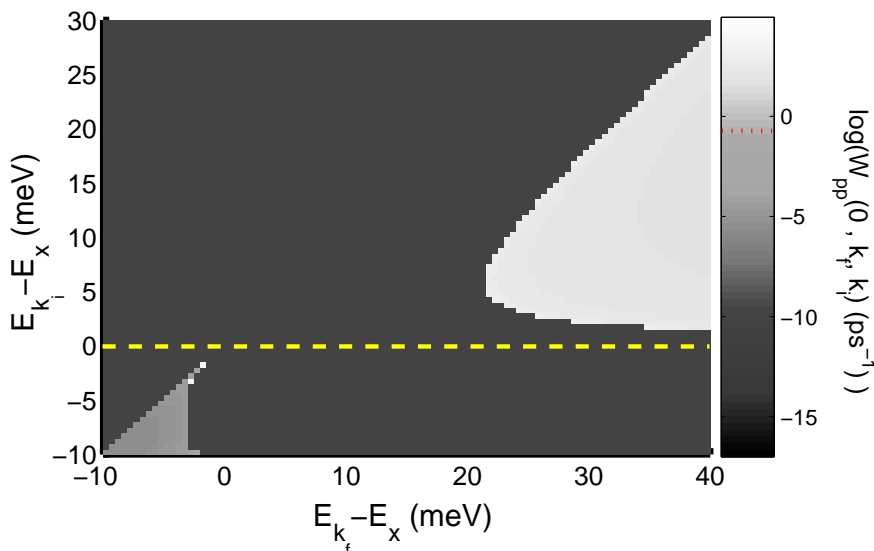

Figure 4.1: Polariton-polariton in-scattering rates for the lowest energy state $W_{pp}(k = 0, k_f, k_i)$ as a function of the energy of the initial and the final states. The energies are evaluated with respect to the bare exciton resonance. The rates are displayed on a logarithmic grey-scale. The dashed line indicates the position of the bare exciton resonance. The dotted line in the color bar indicates the value of the typical polariton radiative time. Parameters model the CdTe microcavity studied by Kasprzak et al. [Kasprzak 06].

according to the semiclassical Boltzmann equations and having neglected the mean-field effect of the interaction. The resulting in-scattering rates for the lowest energy state $\mathbf{k} = 0$ are displayed in Fig. 4.1. These results suggest that the main contribution to the relaxation dynamics arises from processes where three of the four states involved in the scattering lie in the energy region above the bare exciton resonance. Moreover, the scattering rates relative

to scattering processes inside the energy region below the bare exciton resonance, are much smaller than the typical range of the radiative decay rate $\tau^{-1} \simeq 0.1 - 1 \text{ ps}^{-1}$. Therefore, we can safely approximate the relaxation dynamics by only retaining the contributions arising from processes where two exciton-like polaritons scatter into another exciton-like polariton and into one polariton at low energy, as made by Porras *et al.* [Porras 02].

Within the developed procedure, the effect of two-body interactions is treated separately for the two energy regions, above and below the bare exciton resonance. At low energy, we account for the mutual interaction within the HFB limit and we describe the coherent effect induced by the presence of the condensate. At high energy, we neglect the effect of the condensate (i.e. we only account for the density dependent energy blue-shift) while we account for the collision processes within the semiclassical Boltzmann equations. The treatment of this contribution follows the model introduced by Porras *et al.* [Porras 02] and it will be explained in the next subsection.

4.1.4 Kinetic equations

In this subsection we derive the closed set of dynamical equations accounting for the one-particle self-energies within the HFB limit and for the relaxation mechanisms.

To this purpose we have introduced two key-assumptions. First, as explained in previous subsection, we separate the single-particle energy spectrum into a lower energy coherent part and an incoherent part at higher energies. This is depicted in Fig. 4.2 (a) for the typical energy-momentum dispersion of the lower polariton branch. This is possible because, as discussed in subsection 4.1.3, and more generally in section 2.2, the lower energy part of the spectrum is expected to be strongly modified by the presence of collective excitations, whereas in the higher energy part the actual excitations basically correspond to blue-shifted single-particle states. Correspondingly, it is mostly in the coherent region that quantum fluctuations will affect the condensate kinetics. In fact, only the lowest energy states, modified by interactions, can contribute to the scattering processes $\tilde{m}_{\mathbf{k}}$ triggering quantum fluctuations. It is therefore customary in the BEC literature [Gardiner 98] to restrict the quantum kinetic treatment to the coherent region, describing the dynamics within the incoherent region in terms of a simple Boltzmann population kinetics. Such a separation, for the lower polariton branch, naturally coincides with that between the strong-coupling region and the exciton-like part of the dispersion, as illustrated in Fig. 4.2(a). In addition, in the polariton case, as shown in the previous subsection, the incoherent two-body collisions can be neglected within the low-energy region.

The second approximation is made possible by the remark that, given the macroscopic occupation of the condensate above threshold, the field dynamics of collective excitations takes place much faster than energy relaxation mechanisms, made slow by the steep polariton energy-momentum dispersion that reduces the space of final states available for scattering processes (see Fig. 4.1).

The kinetics is thus described in terms of a density-matrix hierarchy whose time-evolution is obtained from the Heisenberg equations of motion.

Relaxation rates: Exciton-exciton scattering

The two-body interaction terms within the incoherent region are treated consistently with the Boltzmann picture, as was done by Porras *et al.* [Porras 02]. In particular, we assume that, in the incoherent region, the population of the exciton-like polaritons is thermally distributed
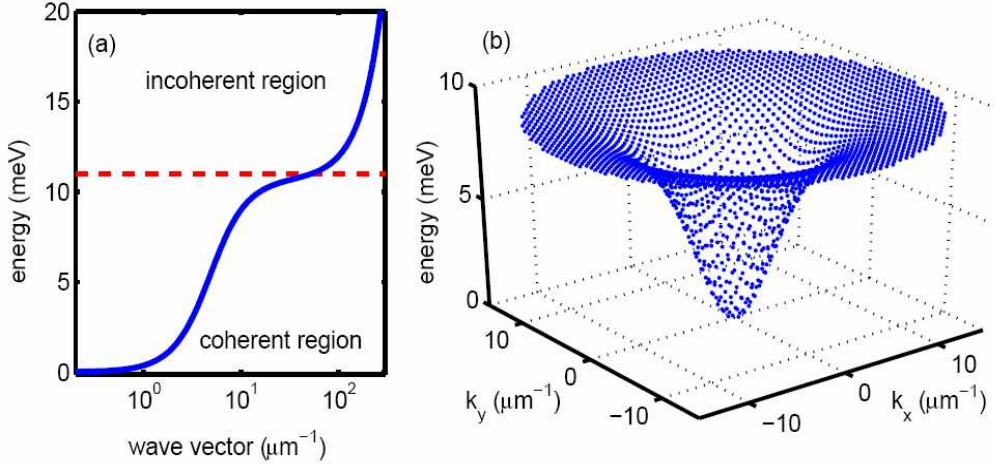
Figure 4.2: (a) Energy-momentum lower-polariton dispersion. Notice the logarithmic horizontal scale. (b) Energy-momentum plot of the discrete lower-polariton states in the coherent region, as used in the simulations for $A = 100 \ \mu m^2$.

with an effective temperature defined by

$$k_B T_x \equiv e_x / n_x \,, \tag{4.47}$$

where k_B is the Boltzmann constant, n_x is the total particle density inside the incoherent region, and e_x is the total energy density in the incoherent region (as shown below, these two quantities are determined self-consistently during relaxation, via Boltzmann equations). Within this picture, the processes of two particles in the incoherent region scattering into one particle in the incoherent region and one in the coherent region, result in an effective energy relaxation mechanism towards the bottom of the polariton branch.

The expressions derived are formally identical to what obtained in Ref. [Porras 02] (for exciton-exciton scattering), with an important difference: in the present case, the actual HFB Popov spectrum E_k replaces the non-interacting single-particle spectrum, because we make the approximation

$$\tilde{p}_{\mathbf{k}} \simeq f_c^{1/2} \hat{\Lambda}_{\mathbf{k}} = f_c^{1/2} \left(U_{\mathbf{k}} \hat{\alpha}_{\mathbf{k}} + V_{-\mathbf{k}}^* \hat{\alpha}_{-\mathbf{k}}^\dagger \right) \simeq f_c^{1/2} U_{\mathbf{k}} \hat{\alpha}_{\mathbf{k}} \,, \tag{4.48}$$

and we assume that at the given time the HFB Hamiltonian is diagonalized by the collective excitation modes, i.e.

$$\hat{H}_{HFB} = U_0 + \sum_{\mathbf{k}} E_{\mathbf{k}} \hat{\alpha}_{\mathbf{k}}^\dagger \hat{\alpha}_{\mathbf{k}} \,, \tag{4.49}$$

Therefore, the resulting expressions for the relaxation terms are [Porras 02]

$$\dot{N}_k \mid_{XX} = W_{x \to k}^{XX} n_x^2 (1 + N_k) - W_{k \to x}^{XX} n_x N_k, \tag{4.50}$$

and

$$\dot{n}_x \mid_{XX} = -\frac{1}{A} \sum_{k \in U_{coh}} \left[W_{x \to k}^{XX} n_x^2 (1 + N_k) - W_{k \to x}^{XX} n_x N_k \right] \,, \tag{4.51}$$

where

$$\eta A \equiv [(m_e + m_h) k_B T_x] A / 2\pi \hbar^2 \tag{4.52}$$

90

is the number of states in the incoherent region, and U_{coh} denotes the coherent region. Here, $N_{\mathbf{k}} = \tilde{N}_{\mathbf{k}}$ for $\mathbf{k} \neq 0$ and $N_0 = N_c$. Note that we use the fact that $n_x/\eta \ll 1$ and that $|\mathbf{k}| \ll k_x$, where k_x is the absolute value of the wave vector averaged in the incoherent region i.e.

$$k_x = \int_x d\epsilon N_x e^{\epsilon/K_B T_x} \frac{\sqrt{2m_x \epsilon}}{\hbar} \; . \tag{4.53}$$

The rates appearing in the equations are given by

$$W_{x \to k}^{XX} = \frac{2\pi}{\hbar k_B T_x} \left| v_{k_x,k_x}^{(k_x)} \right|^2 A^2 e^{(E_k - E_{k_x})/k_B T_x}; \tag{4.54}$$

and

$$W_{k \to x}^{XX} = \frac{(m_e + m_h)}{\hbar^3} \left| v_{k_x,k_x}^{(k_x)} \right|^2 A^2 e^{2(E_k - E_{k_x})/k_B T_x}. \tag{4.55}$$

In all these expressions, consistently with our assumption, the spectrum in the incoherent region is the single-particle spectrum, only accounting for the overall density-induced blue shift of the polariton branch $E_{BS} = vN$. Besides the set of equations (4.50,4.51), the model is completed by the introduction of an equation describing the evolution of the energy density in the incoherent region e_x. Following the procedure of Ref. [Porras 02], this equation reads

$$\dot{e}_x = -\sum_{k \in U_{coh}} \frac{E_k}{A} \left[W_{x \to k}^{XX} n_x^2 \left(1 + \tilde{N}_k \right) - W_{k \to x}^{XX} n_x N_k \right]$$
$$- \gamma_x (k_B T_x) n_x + (k_B T_L) f - w^{ph}. \tag{4.56}$$

Here, the first term represents the heating of the incoherent population, produced by the exciton-exciton scattering process and imposed by energy conservation; the second term is the cooling due to the exciton radiative recombination; the third term is originated by the assumption that the incoherent population is created at the lattice temperature T_L; the fourth term represents the cooling induced by exciton-phonon coupling and it is evaluated as in Eq. (21) of Ref. [Porras 02].

Relaxation rates: Polariton-Phonon coupling

The polariton-phonon scattering is treated within a shifted-pole Markov approximation, resulting in standard Boltzmann contributions [Tassone 97]. Notice that in this case, we evaluate the relaxation terms along all the lower polariton dispersion, i.e. both in the incoherent and in the coherent regions. Using again the approximated relations (4.48,4.49), the expressions of the relaxation rates are [Doan 05]

$$\dot{N}_k \mid_{ph} = A \left[W_{x \to k}^{ph} n_x (1 + N_k) - W_{k \to x}^{ph} N_k (\eta + \frac{N_{k'}}{A}) \right] +$$
$$+ \sum_{k' \in U_{coh}} \left[W_{k' \to k}^{ph} N_{k'} (1 + N_k) + \right.$$
$$\left. - W_{k \to k'}^{ph} N_k (1 + N_{k'}) \right], \tag{4.57}$$

and

$$\dot{n}_x \mid_{ph} = \sum_{k \in U_{coh}} \left[W_{k \to x}^{ph} N_k (\eta + n_x) - W_{x \to k}^{ph} n_x (1 + N_k) \right] \tag{4.58}$$

$$W_{k \to k'}^{ph} = \frac{2L_z}{\hbar} \left| g_{k,k'}^{\bar{q}} \right|^2 \frac{|E_k - E_{k'}|}{(\hbar u)^2 q_z} \left[n_{kk'}^{ph} + \theta \left(E_k - E_{k'} \right) \right],$$

$$|\bar{q}| = \sqrt{|k - k'|^2 + \bar{q}_z^2} = |E_k - E_{k'}|/\hbar u, \tag{4.59}$$

The population of phonons at the energy $E = E_k - E_{k'}$ is thermally distributed at the lattice temperature, i.e.

$$n_{kk'}^{ph} = \frac{1}{e^{(E_k - E_{k'})/k_B T_L} - 1}. \tag{4.60}$$

In principle, phonon-assisted correlations also enter the kinetic equations for the amplitudes $\tilde{m}_\mathbf{k}$, resulting in a complicated expression which cannot be solved analytically because two-body interaction couples different values of the wave vector. However, since in the present case the amplitudes $\tilde{m}_k$ evolve with characteristic frequencies much larger than the relaxation rates, we can safely neglect the phonon contribution in the kinetic equations for $\tilde{m}_\mathbf{k}$.

Kinetic equations

Collecting Eqs.(4.36,4.37,4.40,4.46,4.50,4.51,4.57) we finally obtain the kinetic equations:

$$\dot{N}_c = -\gamma_0 N_c + \dot{N}_c \big|_{ph} + \dot{N}_c \big|_{XX} + \frac{2}{\hbar} \sum_k v_{k,-k}^{(k)} \text{Im}\{\tilde{m}_k\}$$

$$\dot{\tilde{N}}_k = -\gamma_k \tilde{N}_k + \dot{\tilde{N}}_k \big|_{ph} + \dot{\tilde{N}}_k \big|_{XX} - \frac{2}{\hbar} v_{k,-k}^{(k)} \text{Im}\{\tilde{m}_k\}$$

$$\dot{\tilde{m}}_k = -2 \left[\gamma_0 + i\omega_k + \frac{i}{\hbar} v_{k,0}^{(0)} (N_c - \tilde{N}_k - 5/2) \right] \tilde{m}_k$$

$$- \frac{i}{\hbar} \left[\sum_q v_{q,-q}^{(k-q)} \tilde{m}_q + 2v_{k,-k}^{(k)} N_c (N_c - 1) \right] (1 + 2\tilde{N}_k)$$

$$+ 2\frac{i}{\hbar} (1 + 2N_c) \sum_q v_{q,-q}^{(q)} \tilde{C}_{\mathbf{k},\mathbf{q}}$$

$$\dot{n}_x = -\gamma_x n_x + \dot{n}_x \big|_{ph} + \dot{n}_x \big|_{XX} + f. \tag{4.61}$$

Here we have added the phenomenological polariton radiative lifetime $\gamma_k = \gamma_c |C_k|^2$, $|C_k|^2$ being the photon fraction in the polariton state and γ_c being the cavity photon lifetime, and the exciton lifetime γ_x. The quantity f denotes the pump intensity producing a population in the incoherent region.

This finally brings to a closed set of kinetic equations for the amplitudes $\tilde{m}_k$, the populations N_c, $\tilde{N}_k$, and the total density n_x in the incoherent region. In the next section, we will discuss the numerical solutions of these equations for parameters modeling typical experimental conditions.

4.2 Predictions of the kinetic theory

In this section we discuss the numerical solution of the set of kinetic equations (4.61), computed in the time domain.

Before discussing the condensation kinetics, however, we point out that Eqs. (4.61) reproduce the equilibrium results in the limit where the lifetimes are infinite $(\gamma_\mathbf{k}, \gamma_x \to 0)$ and the continuous source is substituted by a pulsed source or by an initial condition. The results for the equilibrium limit are shown in Fig. 4.3. In particular, the asymptotic occupation of the
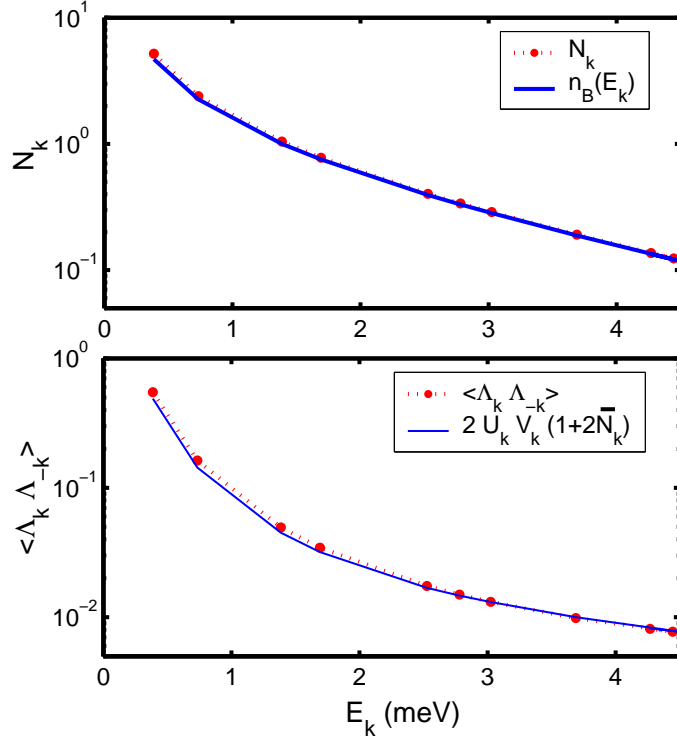
Figure 4.3: Stationary solutions of Eqs.(4.61), for infinite radiative times and lattice temperature $T_L = 20K$, obtained by imposing an initial condition. (a) Stationary populations of collective excitations $\bar{N}_{\mathbf{k}}$ displayed as a function of the energy $E_{\mathbf{k}}$, compared with the Bose distribution at the given temperature. (b) Asymptotic value of the time-dependent coherent scattering amplitudes $N^{-1}\tilde{m}_{\mathbf{k}} = \langle \hat{\Lambda}_{\mathbf{k}}\hat{\Lambda}_{-\mathbf{k}}\rangle$, compared with the equilibrium prediction Eq. (4.39), computed by using the Popov spectrum corresponding to the populations shown in panel (a).

collective excitations tends to the thermal Bose distribution, while the amplitudes $\tilde{m}_{\mathbf{k}}$ simply reduce to the equilibrium limit Eq. (4.39). Therefore, our kinetic model reduces to the Popov approximation, in the case of equilibrium. Consequently, any predicted deviation from the Popov result is a consequence of deviations from thermal equilibrium.

We now discuss the main predictions for the non-equilibrium regime. To this purpose, we assume a steady state pump and parameters modeling the CdTe microcavity studied by Kasprzak *et al.* [Kasprzak 06]. In particular, we consider a Rabi splitting $2\hbar\Omega_R = 26$ meV and cavity photon-exciton detuning $\delta = 5$ meV, at the lattice temperature $T = 10$ K. The quantization area is assumed everywhere $A = 100 \ \mu m^2$, unless specified, consistent with the estimates of the polariton localization length, [Richard 05b] and gives rise to the discrete set of polariton states plotted in Fig. 4.2(b). For this system we obtain from Eqs. (2.59,2.60) $v_x = 3.3 \times 10^{-5}$ meV, $v_s = -0.5 \times 10^{-5}$ meV and the resulting polariton-polariton interaction matrix element is $v_{0,0}^{(0)} = 6 \times 10^{-5}$ meV.

Time evolution

The solutions always display steady-state long-time values after an initial transient, as shown in Fig. 4.4. In panel (a), we display the time evolution of the populations of the condensate and of the first excited state. Correspondingly, in panel (b), we display the time evolution of the amplitude of the scattering processes between the condensate and the first excited state.
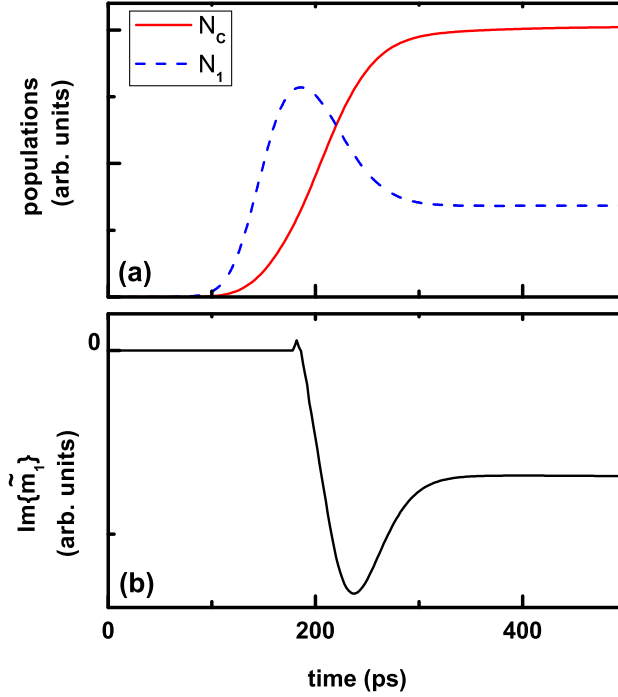
Figure 4.4: Time dependent results for the populations of the condensate state N_c and of the first excited state N_1 and for the imaginary part of the coherent scattering amplitude $\tilde{m}_1$, for a given value of the excitation pump f above condensation threshold. After an initial transient, all the quantities reach a stationary value.

We notice that, during the early stages of the condensate growth, the scattering processes favor condensation, through the positive values taken by $\mathrm{Im}\{\tilde{m}_k\}$. Immediately afterwards, when a large condensate population is reached, the quantity $\mathrm{Im}\{\tilde{m}_k\}$ changes sign and coherent scattering terms start depleting the condensate. In Fig. 4.4, it is also clear that the relaxation dynamics takes place over a time of the order of hundreds of ps. On the other hand, for the same parameters, the typical period of the collective excitations, is of the order of ps, thus confirming that the field dynamics occurs over a time scale much shorter than the time scale of the population dynamics. In particular, the predicted fast field dynamics is expected to assure that the spectrum of the system be close to the estimated quasi-stationary Popov spectrum, thus confirming our *a priori* assumption.

Population distribution

We now discuss the steady state solutions, as a function of the pump intensity. In Fig. 4.5 (a), we plot the steady-state populations per state, for varying pump intensity. A pump threshold is found at about $f = 12$ ps^{-1} μm^{-2}, corresponding to a polariton density in the coherent region $n = N/A \simeq 10$ μm^{-2} and a total exciton density (including the incoherent density n_x and using the renormalized exciton-photon coupling in Eq.(4.1)) $n_{exc} \simeq 100\mu$m^{-2}. We point out that the system studied in Ref. [Kasprzak 06] is composed by 16 quantum wells. Since the polariton modes are expected to extend quite homogenously over all the quantum wells, in experimental literature the exciton density per quantum well is usually estimated by simply dividing the total exciton density for the number of quantum wells [Deng 03, Richard 05b]. In the present case, following this prescription, the obtained exciton density per quantum well is
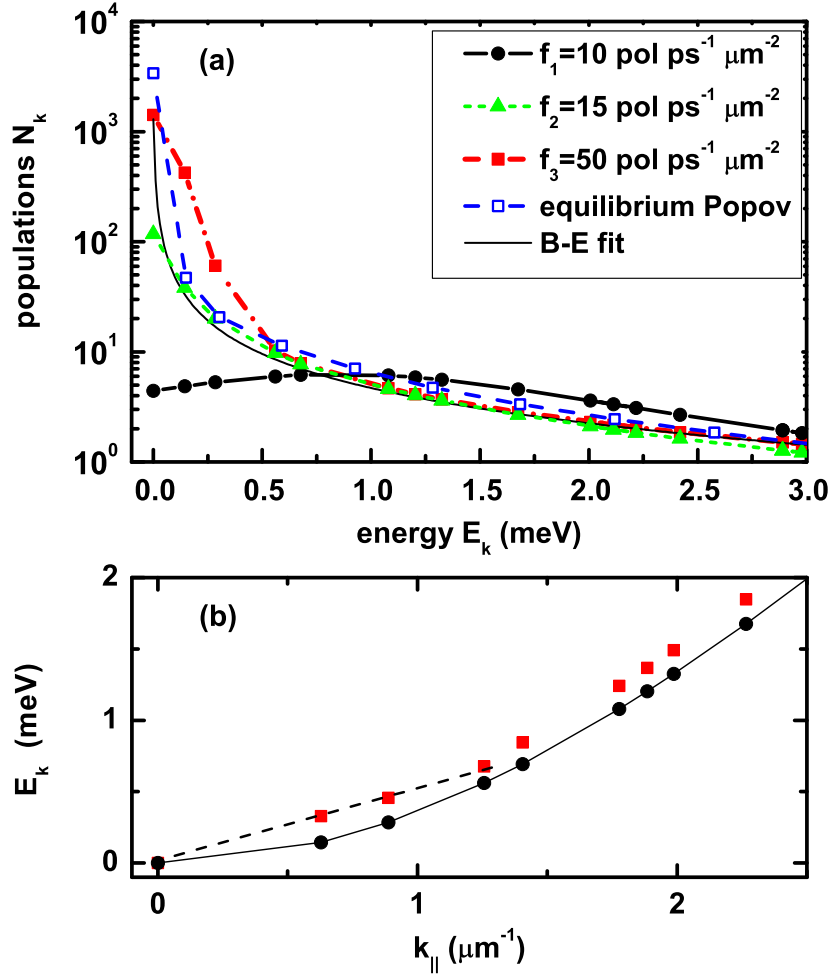
Figure 4.5: (a) Steady state populations for increasing pump intensity f. Open squares: equilibrium HFB Popov solution for (n,T) corresponding to the steady-state solution for $f = f_3$. Thin line: B-E distribution fitted to the high-energy tail and to the condensate population for $f = f_3$. (b) Energy dispersion below and above threshold (same legend as above). The dashed line is a guide to the eye to highlight the linear part of the dispersion.

two orders of magnitude lower than the CdTe saturation density $n_{sat} \simeq 5 \times 10^3 \mu\text{m}^{-2}$. This fact confirms that our treatment of the polariton field in terms of a weakly interacting Bose field is well justified. Below threshold, the relaxation bottleneck results in an energy distribution very far from a thermal distribution, with a maximal occupation in excited states. In this regime, the population in the lowest energy state is a vanishingly small fraction of the total population and consequently the system is expected to be incoherent. Above threshold the condensate population becomes macroscopic. Its growth for increasing f is however suppressed by the corresponding increase of the population of low energy excitations, i.e. excitations below $E = 0.5$ meV (on the other hand, the one-particle population in the higher energy states is predicted to saturate above threshold, consistently with the picture of BEC of a weakly interacting gas). Consequently, the population distribution cannot be fitted by a Bose-Einstein function at low-energy. The discrepancy is partly due to the presence of the collective phonon-like spectrum – characterizing an interacting Bose gas at thermal equilibrium – and partly to amplified quantum fluctuations. In order to distinguish the two contributions, we compare the

kinetic result to a distribution computed for an equilibrium interacting Bose gas in the HFB Popov limit [Griffin 96], accounting for spatial confinement. For this equilibrium distribution, we assume the same density as obtained from the kinetic model for the given pump f, while the temperature is extrapolated from the slope of the high-energy tail of the same kinetic model distribution. In Fig. 4.5 (a), the result for $f = 50$ ps^{-1} μm^{-2}, is compared to the equilibrium HFB Popov distribution with $n = 100$ μm^{-2} and $T = 20$ K. As expected, the equilibrium result already deviates from the ideal distribution, due to the modified spectrum of the interacting system. However, equilibrium and kinetic results differ significantly in the low-energy region. In particular, the kinetic model predicts a larger condensate depletion. The difference is due to the dominant role played by quantum fluctuations (see also Fig. (4.10) below), whose amplitude deviates from the equilibrium prediction and has to be evaluated by means of a proper kinetic treatment like the present one. We point out that these results are
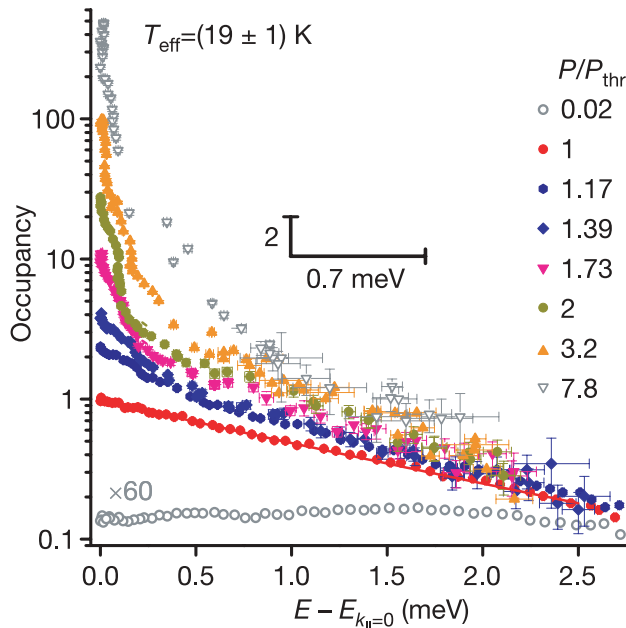

Figure 4.6: Measured energy distribution of populations, for increasing excitation intensity. From Kasprzak *et al.* [Kasprzak 06].

in good agreement with energy distribution data measured in the experiment by Kasprzak *et al.* [Kasprzak 06], which are shown for a direct comparison in Fig. 4.6. In particular, the predicted polariton density threshold is close to the experimental estimate. Moreover, above the threshold, a clear increase of the population at low energy is also reported. We point out that the energy broadening in this experiment is too large to extract from this behavior an estimate of the condensate depletion predicted by our model. However, we will see later on that small deviations from the thermal occupation result in a significant change for the one-particle spatial correlation function at long distance, which is also measured in the same experiment.

Also in the kinetic model, the energy dispersion, evaluated within the Popov approximation Eq. (4.44), is modified by the presence of the condensate because of the two-body interaction, displaying the linear spectrum of collective excitations at low momenta, [Steinhauer 02] as shown in Fig. 4.5 (b). Here, the dashed line highlights the linear part of the spectrum. Recent works have proposed that, in the non-equilibrium regime, the spectrum of collective excitations

could show a diffusive behavior at low momenta in place of the equilibrium phonon-like behavior [Boyanovsky 02, Szymanska 06, Wouters 07b]. Clearly, with the present non-equilibrium model, we cannot predict if this typical behavior would possibly arise, because we are assuming a priori that the finite polariton lifetime only affects the kinetics of populations and correlations, while it does not enter in the determination of the spectrum Eq. (4.44).[5]. However, our approximation, also adopted in other non-equilibrium approaches [Imamović-Tomasović 99], is expected to be realistic for densities sufficiently above the density threshold, where the contribution of the mutual interaction in determining the rate of the field dynamics (this contribution is responsible for the linear behavior at small momenta) is quantitatively larger than the typical polariton decay rate. This idea seems to be confirmed for the polariton system, by the non-equilibrium Gross-Pitaevskii approach recently developed by Wouters and Carusotto [Wouters 07b]. In particular, as can be estimated from equations (8)-(10) of Ref. [Wouters 07b], the excitation spectrum should tend to the equilibrium one (a part for values of momentum well below the experimental resolution), for lifetimes $\tau > 3$ ps.

Spatial correlation function

We now turn to discuss how the deviations from the thermal occupation affect the one-body spatial correlation

$$g^{(1)}(\mathbf{r}, \mathbf{r}') = n(\mathbf{r}, \mathbf{r}')/\sqrt{n(\mathbf{r})n(\mathbf{r}')} \tag{4.62}$$

As seen in subsection 2.2.1, the one-body density matrix $n(\mathbf{r}, \mathbf{r}')$ is the direct expression of ODLRO that characterizes BEC [Penrose 56, Ritter 07]. The function $g^{(1)}$ depends on the distance $|\mathbf{r} - \mathbf{r}'|$ for a uniform system and can be computed in terms of the Fourier transform of the population N_k. The density in the denominator renormalizes the shape of the condensate wave function, hence we expect the averaged quantity $g^{(1)}(\mathbf{r}) \equiv 1/A \int d\mathbf{R} g^{(1)}(\mathbf{R}, \mathbf{R} + \mathbf{r})$ to be scarcely affected by the assumption of a uniform condensate. In Fig. 4.7, we plot $g^{(1)}(\mathbf{r})$ below and above the condensation threshold. Below BEC density threshold, spatial correlations vanish for distances larger than $1 - 2\mu$m, as predicted by both the present kinetic model and by the equilibrium Popov approximation. On the other hand, above the density threshold, the correlation length increases and $g^{(1)}(r)$ remains finite over the whole system size. However, for all values of the pump, the value of $g^{(1)}(r)$ predicted by the kinetic model remains smaller than 0.5 at large distance, whereas the value predicted by the equilibrium HFB Popov is significantly larger, due to a larger condensate fraction, as seen in Chapter 3. This effect is due to the larger amount of population in the low energy excited states with respect to the equilibrium prediction. Therefore the non-equilibrium, enhanced quantum fluctuations turn out to strongly affect the formation of ODLRO. The quantity $g^{(1)}(r)$ can be optically accessed in an experiment. Indeed, the light emitted by a spatial region of the sample is originated by the radiative recombination of polaritons in this region. Therefore the interference pattern formed by the light emitted by different positions on the sample corresponds to the interference pattern formed by the polariton field evaluated in different positions. For such an experiment, we therefore predict the increase of the spatial correlation length (i.e. the largest distance for which interference is visible) as a signature of BEC, also when deviations from the thermal

---

[5]Here we express the coupling with the environment in a phenomenological way, i.e. by the introduction of a finite lifetime for the populations and the non-diagonal correlations $\tilde{m}$. A more correct description of the decay in terms of the coupling with a bath has been recently adopted by Szymanska *et al.* [Szymanska 06] within the Keldish non-equilibrium formalism. In this case however the Coulomb two-body interaction (responsible for the phonon-like behavior) is neglected and so it is not clear if the predicted diffusive behavior is robust against the presence of a realistic two-body interaction.
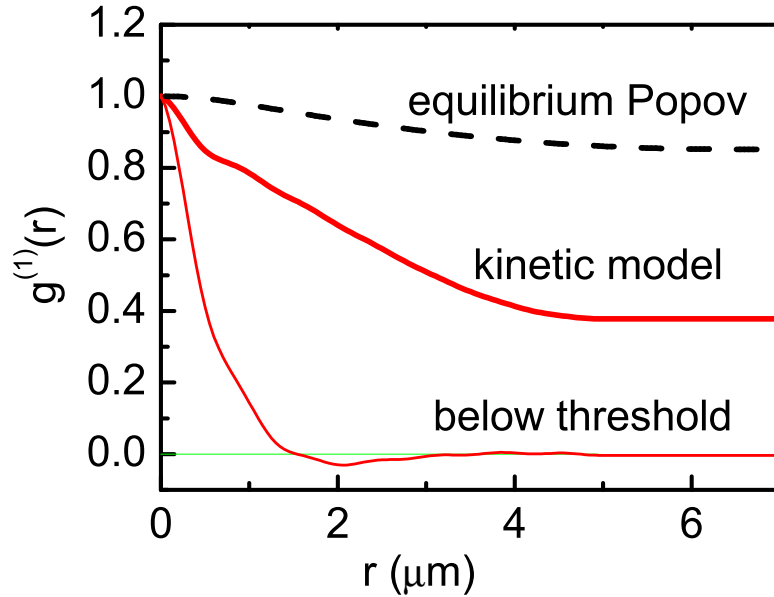
Figure 4.7: First order spatial correlation function below and above threshold, compared to the same quantity resulting from the equilibrium Popov approximation.

equilibrium are present. On the other hand in this case, due to enhanced quantum fluctuations, we predict a correlation (i.e. the amount of contrast for the fringes) well below the equilibrium prediction. In particular, for the typical conditions of the current experiments, we predict correlations below 0.5 even far above the threshold. This estimate turns out to be in very good agreement with the experimental measurement realized by Kasprzak *et al.* [Kasprzak 06], reported in Fig. 4.8. In the experiment, the density distribution is determined by the disorder potential, and thus there is not a regular profile for the spatial correlation. However, it is evident that, while below threshold correlations disappear for distances larger than 2 μm, above threshold correlations extend over distances larger than 12 μm (with a profile that follows the condensate spatial wave function), but never exceed 40%. Another clear evidence of this trend has been recently reported for a GaAs microcavity sample, i.e. a system where the amount of disorder is small, by Balili *et al.* [Balili 07]. In that case the interference pattern is more uniform, correlations extend over the whole area of trapping, i.e. over a distance $r \simeq 20\mu$m, while the amount of correlation at large distance never exceed 25%.

Dependence on system size

As discussed in Chapter 2.2, the occurrence of BEC in a confined 2-D system depends on the size of confinement, because, for large area, the BKT transition is expected to be the relevant transition (on the other hand, for a 3-D system, in principle, the nature of the transition remains the same also in the thermodynamic limit). However, for a system at thermal equilibrium, the dependence on the system size is very weak (as shown for the polariton case in Chapter 3), because the critical density is expected to increase as the logarithm of the area.

For a non-equilibrium system, the dependence on the area of confinement is more dramatic. This is basically due to the fact that, for increasing system size, the density of states just above
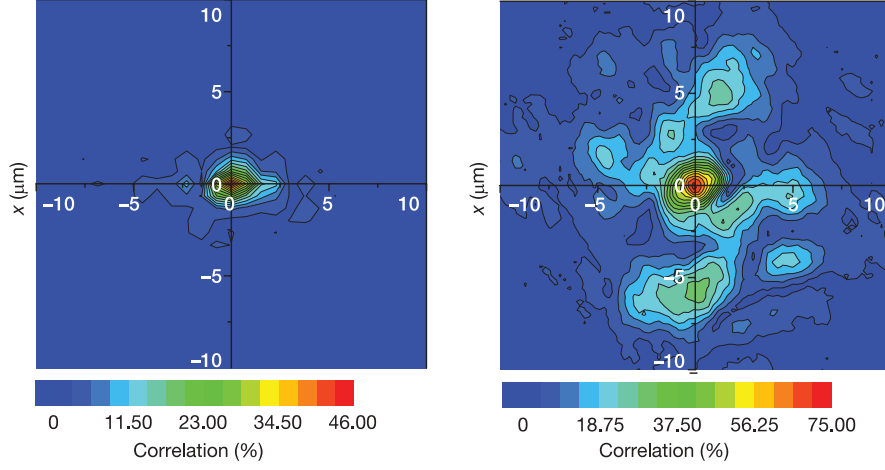
Figure 4.8: Measured one particle spatial correlation function $g^{(1)}(\mathbf{r})$ for an excitation intensity below (c) and above (d) the intensity threshold, from Kasprzak *et al.* [Kasprzak 06]. Notice that in this plot a *mirror* correlation is displayed and the length should be multiplied by 2 in order to relate to the actual correlation length [Kasprzak 06].

the condensate state increases. This results in larger non-equilibrium quantum fluctuations, and consequently in a larger condensate depletion. In Fig. 4.9, we show the condensate fraction in the steady-state regime for increasing system area A, and a fixed excitation intensity. This quantity decreases for increasing area, because coherent scattering is favored by a smaller energy gap Δ. For a system area larger than 1000 μm^2, non-equilibrium quantum fluctuations dominate, eventually resulting in a full condensate depletion (this is required also in the thermodynamic limit, by the Hohenberg-Mermin-Wagner theorem). We can conclude that polariton condensation (and, more generally, non-equilibrium condensation of a 2-D gas) occurs thanks to the locally discrete nature of the energy spectrum, induced either by artificial confinement or by disorder. In a realistic system [Langbein 02, Kasprzak 06, Daif 06, Kaitouni 06, Balili 07, Bajoni 07], localization could therefore affect the polariton BEC, independently of other parameters like Rabi splitting and exciton saturation density.

Role of quantum fluctuations

To better understand the role played by non-equilibrium quantum fluctuations, in Fig. 4.10 we show the values of the coherent scattering rates $v_{\mathbf{k},-\mathbf{k}}^{(\mathbf{k})}\mathrm{Im}\{\tilde{m}_{\mathbf{k}}\}$ as a function of the energy of the corresponding states. As expected, like in the equilibrium limit shown in Fig. 4.3, they decrease dramatically for increasing energy and their contribution to the dynamics vanishes for states outside the coherent region, thus confirming our initial assumption of separation into two energy regions. We see also that, for an increasing excitation intensity the values of the coherent scattering terms increase, resulting in an increased amplitude of quantum fluctuations. This increase counterbalances the fact that the relaxation becomes more efficient due to stimulated scattering. Therefore, increasing the excitation intensity does not imply that the system approach equilibrium.

We will see in the next section that the only possible way to approach thermal equilibrium is in increasing the polariton lifetime.
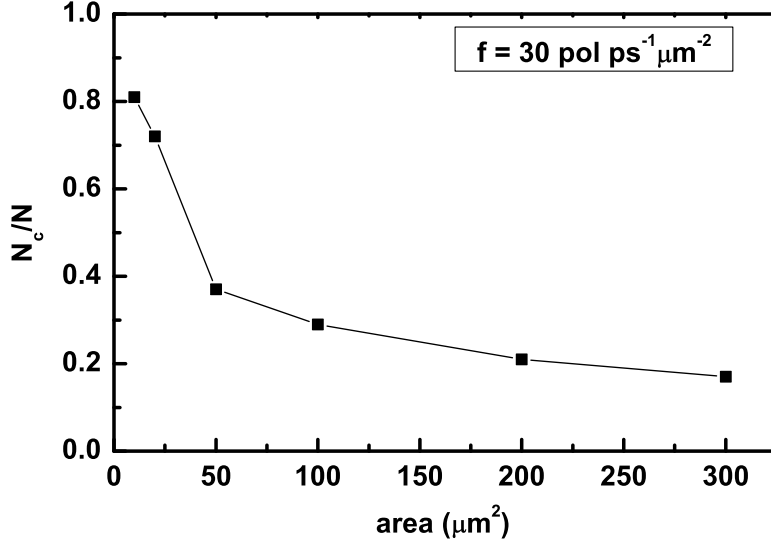
Figure 4.9: Condensate fraction as a function of the system area for $f = 30$ ps^{-1} μm^{-2}.

Dependence on parameters

Before discussing the comparison between equilibrium and non-equilibrium predictions, we point out that we have also applied the kinetic model for system parameters modeling a GaAs microcavity with Rabi splitting $2\hbar\Omega_R = 7$ meV and cavity photon-exciton detuning $\delta = 0$ meV, at the lattice temperature $T = 10$ K and for $A = 100\mu$m^2. In this case $v_{XX} = 6 \times 10^{-5}$ meV, $v_{sat} = -0.15 \times 10^{-5}$ meV and the resulting polariton-polariton interaction matrix element is $v_{0,0}^{(0)} = 1.5\times10^{-5}$ meV. Also for this system we observe the occurrence of polariton condensation and the partial suppression of the ODLRO because of quantum fluctuations. Quantitatively, we notice that in this case the total exciton density at threshold results higher than in the previous case, $n_x \simeq 500\mu$m^{-2}. Nevertheless, considering that in a realistic system the number of quantum wells needed to reach the assumed Rabi splitting is $N_{QW} = 4$, the exciton density per well is one order of magnitude lower than the saturation density for GaAs, $n_{sat} = 2 \times 10^3$ μm^{-2}. Therefore, also in this case, the treatment of the polariton field in terms of a weakly interacting Bose field is well justified.

4.3   Comparison between equilibrium and non-equilibrium results

For several aspects, GaAs microcavities are the most promising system for future studies and applications of the polariton BEC. In this system, due to the small amount of disorder, it would be possible to study the spectral properties of a condensate, in particular the occurrence of the negative energy branch of excitation. For the same reason, the size dependence of the transition could be investigated, possibly observing the BEC-BKT crossover. Furthermore they are the ideal candidate for the fabrication of artificial structures [Daif 06, Kaitouni 06, Bajoni 07] where observing Josephson phenomena and studying correlations and transport properties
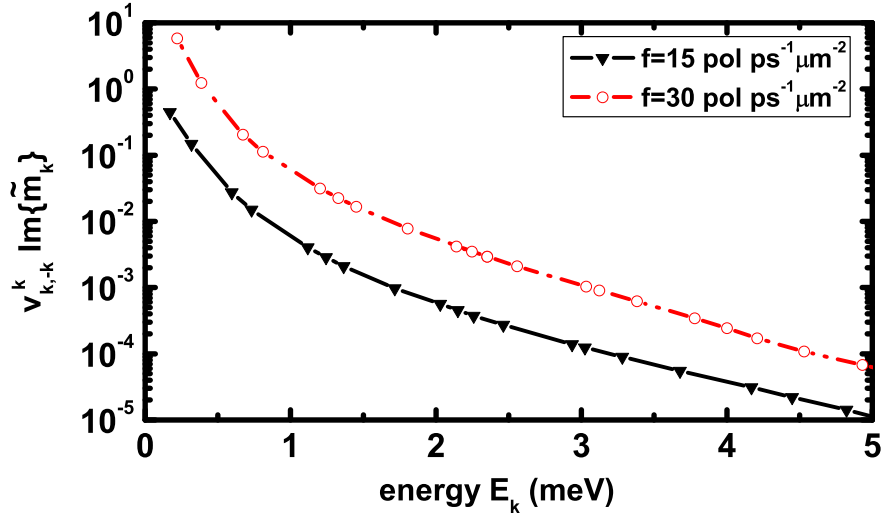
Figure 4.10: Coherent scattering contributions $v_{\mathbf{k},-\mathbf{k}}^{(\mathbf{k})}\mathrm{Im}\{\tilde{m}_{\mathbf{k}}\}$, for two values of the excitation pump f.

[Balili 07]. However, to make these systems appealing for fundamental studies, it is crucial to reach thermal equilibrium.

For this reason, in this section, we focus on the GaAs based microcavity, comparing the equilibrium results with the results of the kinetic model, obtained assuming different polariton lifetimes. We will show the dependence of the effective temperature and of the critical density as a function of the polariton lifetime. In particular we will see that equilibrium is expected for large but realistic values of the polariton lifetime, as also suggested by a recent experimental evidence reported by Deng *et al.* [Deng 06].

The main predictions of the equilibrium theory have been presented in Chapter 3. In particular, the HFP theory allows computing a phase diagram for polariton BEC and corresponding density-dependent energy shifts in quantitative agreement with the results of the recent measurements [Kasprzak 06, Balili 07]. The kinetic model, applied on the same systems, shows the importance of quantum fluctuations in partially suppressing the off-diagonal long-range order, a trend which is in good agreement with the measured one-body spatial correlation function.

For the numerical calculations, we use GaAs parameters for the exciton and photon effective mass [Doan 05], for the deformation potential coupling to acoustic phonons [Tassone 97], and for the Coulomb and Pauli exclusion terms [Rochat 00]. We assume zero detuning and a typical quantization area $A = 800 \ \mu\mathrm{m}^2$ [Balili 07]. Where not specified, the vacuum field Rabi splitting is $2\hbar\Omega_R = 7$ meV and the lattice temperature is $T = 10$ K. This parameter represents the temperature of the phonon bath in the kinetic model, whereas it fixes the polariton temperature in the HFP theory. For the kinetics, we assume a stationary pump intensity f, whereas the total polariton density n is used as an input for the HFP theory. We denote by f_c and n_c the threshold intensity for the kinetic model and the critical density in the HFP theory respectively. Fig. 4.11 shows the polariton distribution $\tilde{N}(E)$ simulated from the kinetic model at two different values of the polariton lifetime $\tau_{pol} = \hbar/\gamma_0$, and $f = 1.5 \ f_c$. For comparison, the distribution obtained from the HFP theory at the same temperature and $n = 1.5 \ n_c$ is plotted. The kinetic result for $\tau_{pol} = 3$ ps has a high-energy exponential tail displaying a significantly larger effective temperature than the temperature of the phonon bath. At still shorter lifetime, the kinetic result displays a considerable deviation from a single exponential, corresponding
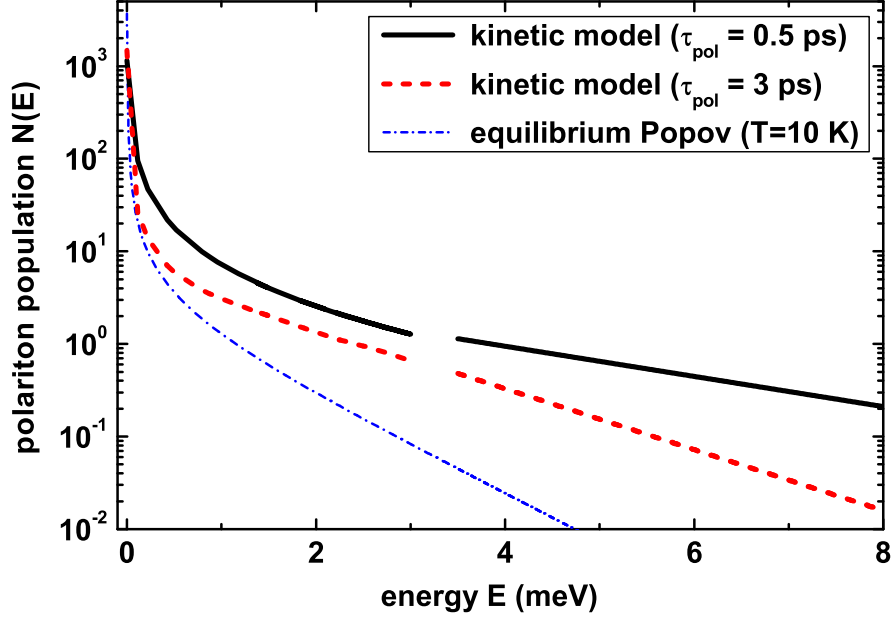
Figure 4.11: Population distribution of polaritons, as obtained from the kinetic model at $f = 1.5f_c$, for two different values of the polariton lifetime. For comparison, the distribution predicted by the HFP theory at $T = 10K$ and polariton density $n = 1.5n_c$, is shown. The gap in the two topmost curves indicates the separation between the polariton and the exciton-like regions of the dispersion.

to a strong departure from full thermalization. We point out that the estimated polariton lifetime was $\tau_{pol} \simeq 1.5$ ps for the sample of Kasprzak *et al.* [Kasprzak 06], and $\tau_{pol} \simeq 4$ ps for the sample of Deng *et al.* [Deng 03, Deng 06] and of Balili et al. *et al.* [Balili 07]. To explore in detail how the polariton lifetime affects the predictions of the kinetic model, we display in Fig. 4.12 the effective temperature T_{eff} at the BEC threshold (Fig. 4.12(a)), and the corresponding exciton density per quantum well n_{QW} (Fig. 4.12(b)), as a function of the polariton lifetime τ_{pol}. The density per QW is given by $n_{QW} = n/N_{QW}$, where N_{QW} is the number of QWs in the sample and n is the total density in the model, accounting for both the polariton population and the exciton reservoir. This is indeed the density produced in each QW and is the relevant quantity to be compared to the exciton saturation density [Deng 03]. For short polariton lifetimes, the main contribution to the relaxation is given by the scattering processes originating from the exciton reservoir. Relaxation within the strong-coupling is slow, compared to the lifetime, and thus not very effective. As a consequence, thermalization at the temperature of the phonon bath cannot be reached. In this regime, condensation is achieved only when the average exchanged energy in a scattering processes is sufficiently large. Consequently, at the condensation threshold, the effective temperature is significantly higher than the lattice temperature [Balili 07] and a polariton density at threshold $n_{QW} \sim 10^2 \mu m^2$ results, which is one order of magnitude larger than the critical density n_c predicted by the equilibrium theory. When the polariton lifetime is increased, phonon relaxation becomes more effective, favoring thermalization and a lower threshold density. Quantitatively, the effective temperature approaches the lattice temperature for lifetimes larger than 10 ps. The total density per QW at threshold then approaches the equilibrium value $n_{QW} \sim 10 \ \mu m^2$. We notice that this result is qualitatively confirmed, although under different experimental conditions, by the experiment by Deng *et al.* [Deng 06], where the energy distribution of polaritons,
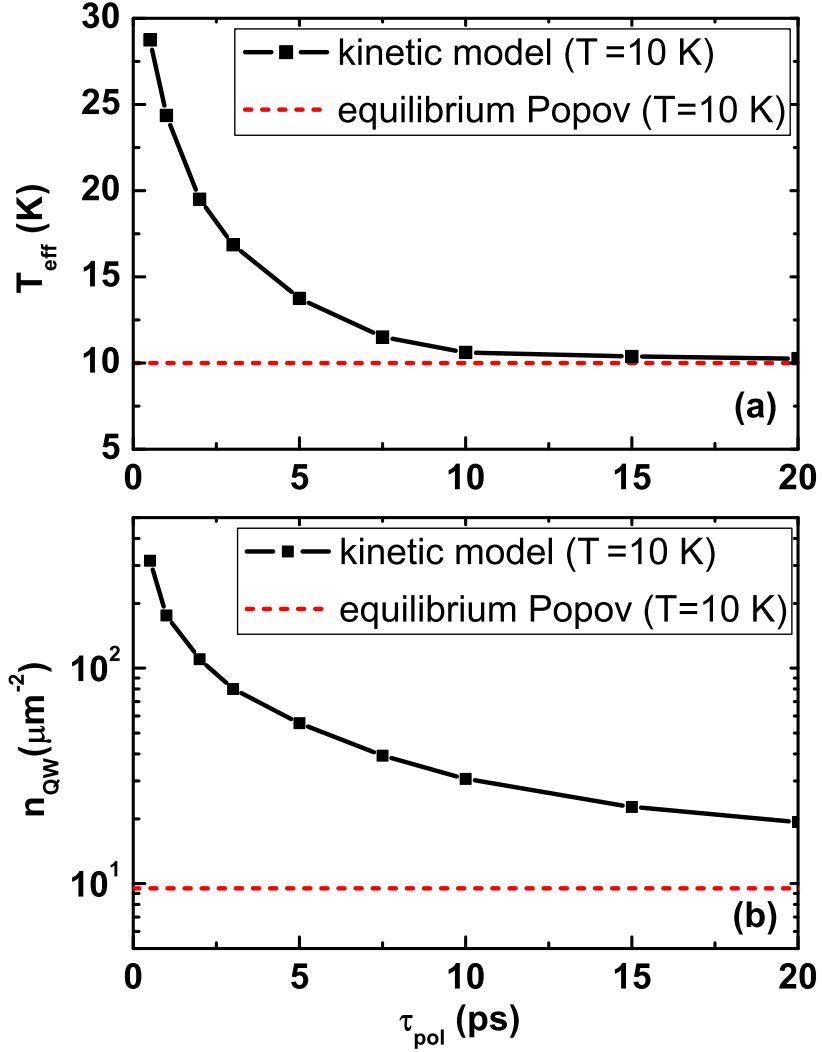
Figure 4.12: Predictions of the kinetic model for the effective temperature in the exciton-like reservoir (a) and exciton density per quantum well (b), computed at the BEC threshold as a function of the polariton lifetime. For comparison, the equilibrium temperature and the corresponding critical density as obtained within the equilibrium HFP theory are also shown.

measured 50 ps after that a pulsed laser pump has excited the system quasi-resonantly, turns out to be very close to the Bose distribution at the lattice temperature. In Fig. 4.13 we report the predictions of the kinetic model for the effective temperature T_{eff} (Fig. 4.13(a)), and the corresponding exciton density per quantum well n_{QW} (Fig. 4.13(b)), computed at the BEC threshold as a function of the Rabi splitting $2\hbar\Omega_R$. For these calculations we have assumed a polariton lifetime $\tau_{pol} = 3$ ps. In Fig. 4.13(b) the corresponding quantity obtained from the equilibrium HFP theory, for temperature $T = 10$ K and $T = 20$ K is also plotted. Increasing the Rabi splitting actually suppresses phonon relaxation along the strong coupling region of the polariton branch. Hence, a higher effective temperature is required for condensation. On the other hand, the density per quantum well decreases, simply due to the increase of the number of quantum wells, as vacuum field Rabi splitting scales as $\sqrt{N_{QW}}$ [Savona 95]. By assuming that $2\hbar\Omega_R = 4$ meV holds for a single QW in the cavity, then a Rabi splitting of 16 meV requires $N_{QW} = 16$, in agreement e.g. with the sample in Ref. [Deng 03]. At large Rabi splitting, the simulated value of n_{QW} at threshold strongly deviates from the corresponding
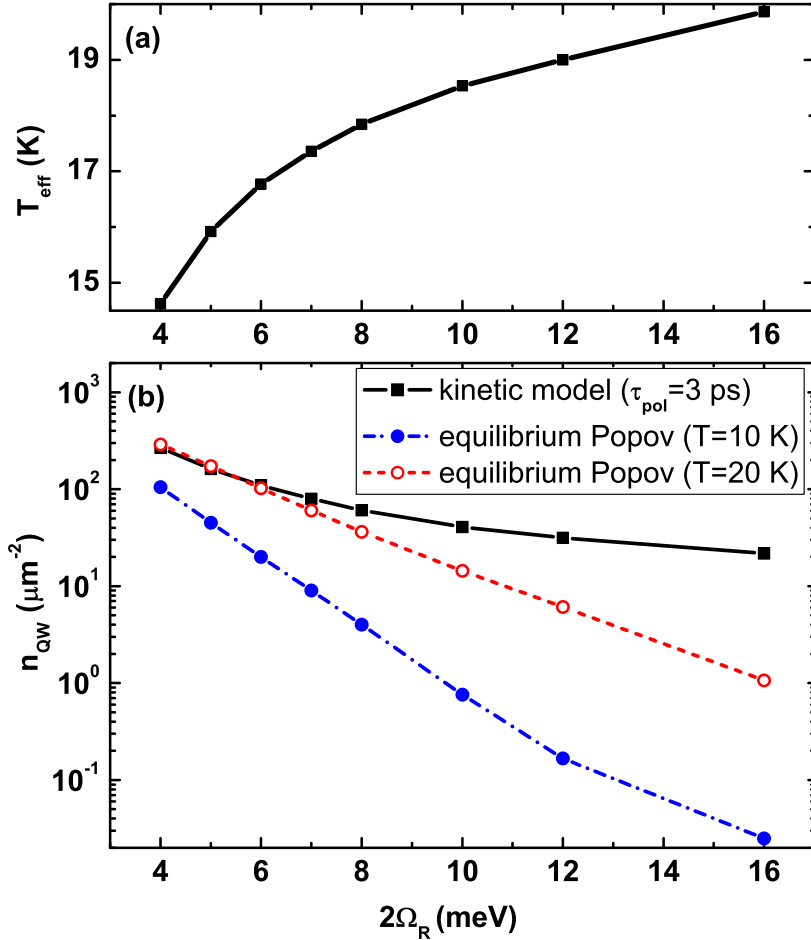
Figure 4.13: Effective temperature T_{eff} (a) and exciton density per QW n_{QW} (b) as a function of the Rabi splitting, as obtained from the kinetic model at the BEC threshold. In (b), the corresponding values obtained from the equilibrium HFP theory, for temperature $T = 10$ K and $T = 20$ K, are plotted for comparison.

value obtained at thermal equilibrium. The two results, at $T = 20\,K$ and $2\Omega_R = 16$ meV differ by a factor 200. The kinetic value of n_{QW} is in this case equal to that obtained at $2\Omega_R = 7$ meV and $\tau_{pol} = 10$ ps, as seen in Fig. 4.12.

It is important to point out that the amplitudes of the scattering processes $\tilde{m}_{\mathbf{k}}$, responsible for increased quantum fluctuations and suppression of off-diagonal long-range order, turn out to be strongly suppressed for increasing lifetimes. Hence, samples with increased polariton lifetime should also be characterized by a larger two-point spatial correlation function at long distance, as compared to the value measured for samples with large Rabi splitting and short lifetime [Kasprzak 06].

Is it really possible to achieve a polariton lifetime close to 20 ps? A common feature of MBE-grown microcavity samples is that the measured cavity-mode *linewidth* does not improve further, as the number of pairs in the distributed Bragg reflectors (DBRs) is increased above 20-22 pairs. This has led to the common belief that the polariton *lifetime* cannot be improved by growing more pairs. This is however a misconception. In reality, the measured cavity mode is mostly inhomogeneously broadened, as a consequence of long-range disorder present both at the cavity interfaces and in the mirrors. This fact was pointed out by several groups

[Stanley 94, Gurioli 01, Langbein 04, Savona 07]. Indeed, if the photon mode is probed on a small enough sample area, quite different results are obtained. As an example, microcavity pillars of 4 μm diameter [Loffler 05] display linewidths as small as 60 μeV, and the linewidth constantly decreases when bringing the number of pairs in the DBR to 27. The reason is that a narrow pillar samples a small homogeneous area of the sample and only the homogeneous linewidth – the one directly related to the photon lifetime – emerges. A similar conclusion can be drawn by recent measurements of polariton photoluminescence spectrum in patterned mesa structures [Kaitouni 06]. There, the measured cavity-mode linewidth in wide regions is 200 μeV, whereas the polariton linewidth measured in a 3.6 μm wide mesa is 70 μeV (with a cavity-exciton detuning of approximately -3 meV). For the parameters of this sample, we have performed a transfer matrix calculation that resulted in a cavity mode linewidth of 80 μeV, significantly smaller than the value measured on the extended structure and in good agreement with the value in the mesa, obtained by accounting for the Hopfield factor in the ground polariton state. This strongly supports the idea that the polariton lifetime is locally determined by the nominal reflectivity of the DBRs. A simple transfer matrix calculation predicts a polariton lifetime $\tau_{pol} > 20$ ps already for a cavity similar to the one in Ref. [Kaitouni 06], with 26 (substrate) and 24 (top) pairs in the DBRs. Several experimental studies lead to similar conclusions [Stanley 94, Richard 05b, Sanvitto 05, Oesterle 05, Bajoni 07].

4.4 Conclusions and outlook

In conclusion, we have developed a kinetic model for the condensation of polaritons under a non-resonant stationary optical excitation. This model accounts for both the field dynamics induced by two-body interaction and the relaxation mechanisms. In particular, since we describe the coherent dynamics of quantum fluctuations within a time-dependent Hartree-Fock-Bogoliubov approach, we expect that the present kinetic model is valid also when condensation occurs.

The present theory reduces to the equilibrium Popov approximation, for infinite lifetimes. On the other hand, when the system is far from equilibrium, the result shows that the dynamics of quantum fluctuations significantly affects polariton BEC and the formation of ODLRO in a polariton condensate. In a typical case, quantum fluctuations partially deplete the condensate, already slightly above threshold. Quantitatively, the effect depends on the locally discrete energy spectrum, due to trapping or to disorder. We predict that the observation of BEC and ODLRO should be favored by smaller polariton size, as in recently studied polariton artificial structures [Daif 06, Kaitouni 06, Bajoni 07], or in local minima of the disorder potential. This suggests that, for a given sample, a study of the polariton localization length in the lowest energy states [Langbein 02] could give deeper insight into the BEC mechanism.

We have compared the predictions of the kinetic model for the BEC of microcavity polaritons with the results obtained within the equilibrium HFP theory developed in Chapter 3. The results prove that the system can reach thermal equilibrium when the polariton lifetime is sufficiently large, i.e. $\tau_{pol} > 10$ ps, even in samples with a reasonably small Rabi splitting (7 meV, that is obtained by embedding 3 or 4 QWs in a microcavity). The critical density, in this case, is expected to be well below the exciton saturation density. GaAs-based microcavities should display this value of τ_{pol} for realistic microcavity geometries, in particular if the number of Bragg reflectors is sufficiently large ($N \geq 24$).

Some aspects of the non-equilibrium regime remain unclear, basically related to the general problem of the condensate formation and stability. In particular, we cannot describe satisfactorily the evolution of the spectral function during the condensate growth. Consequently, it is not clear if a system in a steady-state regime would manifest the phonon-like collective

excitation spectrum, predicted at thermal equilibrium and resulting in the superfluid behavior [Bogoliubov 47]. To solve this problem satisfactorily, a non-equilibrium many-body field theory would be required, accounting microscopically for the coupling with the external electromagnetic field, for two-body interactions and for the non-radiative dephasing mechanisms. Although such a treatment would be prohibitive for describing the polariton condensate formation under non-resonant excitation, it could be perhaps applied to the description of the steady-state limit in the case of resonant excitation.

Chapter 5

Conclusions and perspectives

In this thesis, we have presented a theoretical description of the BEC of microcavity polaritons. The recent experimental observations of high quantum degeneracy with formation of off-diagonal long-range coherence seem to confirm that microcavity polaritons are the first example of BEC in a solid state device [Kasprzak 06, Balili 07]. However, we have seen that the description and the interpretation of this phase transition is made difficult basically for two reasons. First, polaritons have a peculiar composite nature, because they are mixed light-matter quasiparticles originated by the coupling between the exciton (matter) and the photon (light) fields. Second, because of the short polariton lifetime and the inefficient relaxation mechanisms, the deviations from thermal equilibrium are much more important than in other Bose gases. Due to these features, the existing theoretical frameworks rather interpret the phenomenon in strict analogy either with the laser physics or with the BCS transition of Fermi particles. These theoretical descriptions however leave two basic questions still unanswered. Are the experimental findings correctly interpreted in terms of a quantum field theory of interacting bosons? Could the achievement of polariton BEC give new insights into the fundamental physics of interacting Bose systems?

In this work we have answered these two questions in three steps. First, we have shown that polaritons can be modeled borrowing from the theory of interacting Bose particles. This is the main result of the bosonic theory developed in Chapter 3. In particular, we have generalized the Dyson-Beliaev formalism to the case of two coupled Bose fields, thus describing self-consistently the linear exciton-photon coupling and the exciton $\chi^{(3)}$-nonlinearities. We have treated the problem at thermal equilibrium, within the Hartree-Fock-Popov limit. In this way, we have computed the density-dependent energy shifts and the phase diagram, obtaining a very good agreement with the recent experimental findings [Kasprzak 06]. We point out that our theory has four important properties:

- the resulting polariton modes are density dependent and thus we can predict the modification of the spectral functions as a function of density;

- as the poles of the exciton and the photon propagators correspond to the positive and the negative lower- and upper-polariton branches, the thermodynamics is properly determined by the actual polariton dispersion;

- the polariton, the photon and the exciton fields are simultaneously described, thus allowing to make a clear connection between the coherence properties of the polariton field and the typical optical measurements (which can measure only quantities directly related to the photon field).

- the non-condensed population in the excited states is accounted for in the Popov limit, and thus the theory can be applied at finite temperature.

Second, we have investigated how the intrinsic deviations from the equilibrium regime could affect the formation of off-diagonal long-range order. To this purpose, in Chapter 4 we have developed a kinetic theory of the polariton condensation, where the time evolution of populations and the dynamics of the excitation field are solved self-consistently. This model accounts for both the relaxation mechanisms and the coherent dynamics of quantum fluctuations, which is solved within a time-dependent Hartree-Fock-Bogoliubov approach. Within this framework, we have studied the typical experimental conditions where polaritons condense under a non-resonant stationary optical excitation. We have shown that the role of quantum fluctuations is amplified in this non-equilibrium regime, resulting in a significant condensate depletion, confirmed by experiments [Kasprzak 06, Balili 07]. In particular, we have seen that this effect quantitatively depends on the locally discrete energy spectrum, due to trapping or to disorder. Therefore, we expect that the observation of BEC and ODLRO should be favored by smaller polariton size, as in recently fabricated polariton artificial structures [Daif 06, Kaitouni 06, Bajoni 07], or in local minima of the disorder potential.

Third, by comparing the predictions of the kinetic model with the results obtained within the equilibrium HFP theory, we have studied how the deviations from thermal equilibrium can be reduced by increasing the polariton lifetime. In particular, our results suggest that the system can reach thermal equilibrium when the polariton lifetime is sufficiently large, i.e. $\tau_{pol} > 10$ ps, a condition which is expected to hold for high-quality GaAs-based microcavity structures [Stanley 94, Sek 07].

Our analysis thus supports the interpretation of the recent experimental findings in terms of polariton BEC, showing that all the observed features are described by means of a bosonic theory of the polariton gas. In fact, the observed deviations from the behavior expected for a weakly interacting Bose gas at thermal equilibrium are explained as the result of the intrinsic non-equilibrium regime of the present experimental conditions. Furthermore, we predict that the artificial trapping of the polariton gas and the increase of the polariton lifetime would lead to thermal-equilibrium polariton BEC in realistic samples. This would make the polariton system an ideal tool for studying many fundamental aspects of the BEC physics, thanks to the ease of optical measurements. In particular, it would be possible to investigate

- the effect of dimensionality and fluctuations and the possible crossover between BEC of a trapped gas, and BKT transitions;

- the evolution of the excitation spectrum from the single-particle to the collective one;

- the coherence properties in space and time and the connection to the BEC laser;

- the condensate formation and stability.

The formalism developed in Chapter 3 represents the starting point for a future theoretical investigation of these issues. To this purpose, it would be particularly interesting to work in three directions. First, to generalize the formalism to nonuniform system and to apply it to the study of condensation in new artificial polariton traps, like polariton mesas [Daif 06, Kaitouni 06] or pillars [Bajoni 07]. Second, to extend the theory beyond the HF limit, in order to study higher order correlation functions. Third, to include non-equilibrium features, by adopting the Kadanoff-Baym (or Keldysh) treatment, in order to investigate the interplay between the relaxation mechanisms and the field dynamics driven by nonlinearities, in the spirit of the simplified analysis performed in Chapter 4.

Acknowledgments

I owe a big debt of gratitude to my director of thesis Vincenzo Savona, who gave me the opportunity of reaching his newly born group and working on this very stimulating topic. During these four years of strongly synergetic work, I have enormously appreciated his scientific and human support. I am also grateful to him for giving me all kind of opportunity to improve my knowledge and experience.

I am deeply grateful to my PhD colleague Gaetano Parascandolo, for the scientific and non scientific discussions and for helping me feel at home already from the first day and during all these four years, and to the other members of the group Stefano Portolan and Guillaume Tarel, who contributed to make even more pleasant, and scientifically stimulating, the period of the editing of this thesis.

I want to express my gratitude to Prof. Antonio Quattropani and to Dr. Paolo Schwendimann for the instructive discussions on the polariton and laser physics, the precious suggestions and the continuous support and encouragement.

I am gratefully indebted to Prof. Philippe-André Martin for the many discussions on the fundamental problems related to BEC and the very competent advice (in particular for bringing to my attention the studies performed by Prof. Zagrebnov) and for having accepted to be internal Referee of this thesis.

I also wish to thank our Director Prof. Alfonso Baldereschi, Prof. Dmitri Ivanov, Prof. Hervé Kunz and Prof. Christian Gruber.

The direct collaboration with the experimental group of Benoit Deveaud at EPFL has been particularly important and allowed me to follow from a privileged point of view the evolution of the experiments on the polariton condensation. I special thank Prof. Benoit Deveaud and the present and former members of the group, in particular Maxime Richard, Stefan Kundermann, Ounsi El Daif, Augustin Baas, Tao Paraiso and Konstantinos Lagoudakis.

I am deeply indebted to Prof. Roland Zimmermann, for the enlightening discussions, for the invaluable suggestions which have greatly improved the quality of my work and for having accepted to be external Referee of this thesis.

I am particularly grateful to Iacopo Carusotto, who gave me, during each conference, a huge quantity of precious suggestions and comments and offered me the great opportunity of working in synergy with him, for two weeks, in Trento. For the very good time spent there, I thank all the members of the INFM-BEC group at Trento. In particular, I want to express my gratitude to Prof. Sandro Stringari for having accepted to be external Referee of this thesis, and for having contributed with his huge experience in pointing out similarities and differences between polariton and atomic condensation, and suggesting possible new lines of research.

Special thanks to Salvatore Savasta, for the very interesting and enthusiastic discussions and for representing for me a wonderful example of "360°" physicist.

I further acknowledge instructive discussions with Michiel Wouters, Francesca Marchetti, Ivan Shelykh.

I thank Andrea Testa for the continuous support and help with every problem concerning hardware and software, Mme Claudet for the help with all the administrative issues and all the friends and colleagues at EPFL for their support and encouragement. I special thank Severine Pache and Benoit Crouzy, with whom it has been extremely pleasant sharing the office and the work time during these years, Emanuele Pelucchi, Diana Pakrevan, Andrea Fiore, Ludovica Cotta Ramusino, Andrea Dunbar, Pierre Lugan, Pascal Bunzli, Aric Gliesche, Sascha Dalessi, Nicolas Moret, Claude Plocek, Rico Rueedi, Sam Bieri, George Jackeli, Sylvain Tollis, Sanna

Palmgren, Fredrik Karlsson, Kirill Atlasov and every person unintentionally forgotten.

I wish also to thank my friends in Milan, Riccardo, Fabio and Alberto and my friend in USA Marco, for the delightful (and too short) time spent together.

There is not a way to manifest all my gratitude to my parents Anna and Claudio and to my family. They have been a continuous source of force and serenity for me during these four years, across any adversity, and this thesis is ideally dedicated to them, as any good job I could make in my life.

Motivations and happiness are crucial for realizing a project. Every day, Valentina gave me all the motivations and happiness I needed, and I will be eternally grateful to her for having made important and unforgettable any moment of this period.

Appendix A

Polariton T-matrix

We discuss here in detail to the problem of the 2-D T-matrix for polaritons, mentioned in Chapter 3.

We point out that a self-consistent evaluation of the polariton T-matrices would require the inclusion of diagrams mixing the exciton-exciton interaction and the exciton-saturation term. However, since we are only interested in a qualitative evaluation of the correction with respect to the bare potentials, we consider independently the two contributions. Within this simplification, the equation for the exciton-exciton many-body T-matrix has the usual form [Shi 98]

$$
T_x(\mathbf{k}, \mathbf{k}', \mathbf{q}, i\omega_{n_k} + i\omega_{n_{k'}}) = v_x(\mathbf{k}, \mathbf{k}', \mathbf{q}) - \frac{1}{\beta A} \sum_{\mathbf{q}' i\omega_n} v_x(\mathbf{k}, \mathbf{k}', \mathbf{q}') g_{11}^{xx}(\mathbf{k} + \mathbf{q}', i\omega_{n_k} + i\omega_n) \quad \text{(A.1)}
$$
$$
\times g_{11}^{xx}(\mathbf{k}' - \mathbf{q}', i\omega_{n_{k'}} - i\omega_n) T_x(\mathbf{k} + \mathbf{q}', \mathbf{k}' - \mathbf{q}', \mathbf{q} - \mathbf{q}', i\omega_{n_k} + i\omega_{n_{k'}}),
$$

where g_{11}^{xx} is the normal exciton propagator. On the other hand, the exciton-photon two-body interaction defines the corresponding many-body T-matrix

$$
T_s(\mathbf{k}, \mathbf{k}', \mathbf{q}, i\omega_{n_k} + i\omega_{n_{k'}}) = v_s(\mathbf{k}, \mathbf{k}', \mathbf{q}) - \frac{1}{\beta A} \sum_{\mathbf{q}', i\omega_n} v_s(\mathbf{k}, \mathbf{k}', \mathbf{q}') g_{11}^{xc}(\mathbf{k} + \mathbf{q}', i\omega_{n_k} + i\omega_n) \quad \text{(A.2)}
$$
$$
\times \ g_{11}^{xx}(\mathbf{k}' - \mathbf{q}', i\omega_{n_{k'}} - i\omega_n) T_s(\mathbf{k} + \mathbf{q}', \mathbf{k}' - \mathbf{q}', \mathbf{q} - \mathbf{q}', i\omega_{n_k} + i\omega_{n_{k'}})
$$
$$
+ \ \frac{1}{(\beta A)^2} \sum_{\mathbf{q}', i\omega_n} v_s(\mathbf{k}, \mathbf{k}', \mathbf{q}')
$$
$$
\times \ g_{11}^{xx}(\mathbf{k} + \mathbf{q}', i\omega_{n_k} + i\omega_n) g_{11}^{cc}(\mathbf{k}' - \mathbf{q}', i\omega_{n_{k'}} - i\omega_n)
$$
$$
\times \ \sum_{\mathbf{q}'', i\omega_l} v_s(\mathbf{k} + \mathbf{q}', \mathbf{k}' - \mathbf{q}', \mathbf{q}'' - \mathbf{q}')
$$
$$
\times \ g_{11}^{xx}(\mathbf{k} + \mathbf{q}'', i\omega_{n_k} + i\omega_n + i\omega_l) g_{11}^{xx}(\mathbf{k}' - \mathbf{q}'', i\omega_{n_{k'}} - i\omega_n - i\omega_l)
$$
$$
\times \ T_s(\mathbf{k} + \mathbf{q}'', \mathbf{k}' - \mathbf{q}'', \mathbf{q} - \mathbf{q}'', i\omega_{n_k} + i\omega_{n_{k'}})
$$
$$
. \quad \text{(A.3)}
$$

We see that the normal photon propagator and the exciton-photon propagator contribute to T_s. Although the second term can be apparently considered as an higher order term, the two contributions to T_s turn out to be quantitatively equivalent. We have solved numerically these two equations up to convergence, by using the one-particle propagators g^{xx}, g^{cc} and g^{xc}, as obtained by solving the Popov equations with the k-dependent interaction matrix elements v_x and v_s. Therefore we do not solve self-consistently the T-matrix equations. We only aim at
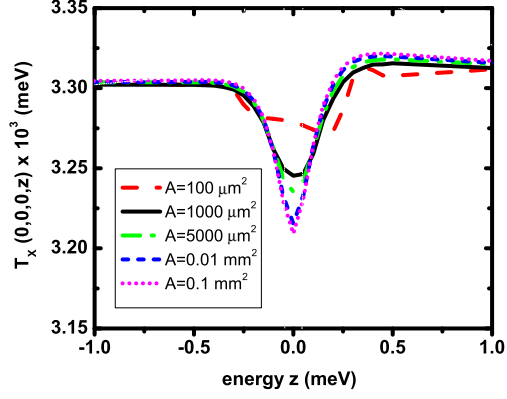
Figure A.1: Evolution of the exciton-exciton T-matrix T_x for increasing system size.
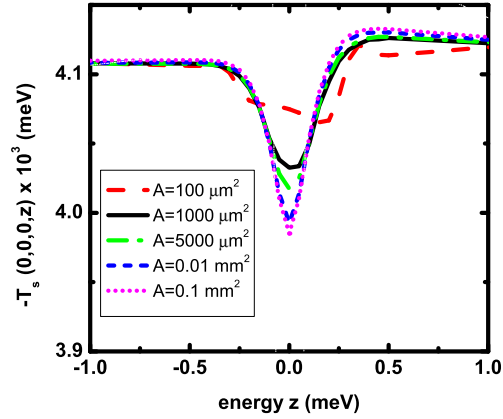
Figure A.2: Evolution of the saturation T-matrix T_s for increasing system size.

comparing the value of the T-matrix at the collision energy with the value of the corresponding bare potential. The resulting T-matrices, in the limit of zero wave vector, are shown in Fig. A.1 (T_x) and Fig. A.2 (T_s), for several values of the system area A. As expected, the T-matrix has a minimum at the collision energy (in this case at $z = 0$), and it would vanish in the thermodynamic limit [Shi 98]. However, up to system size much larger than the typical polariton confinement, the difference between the many-body T-matrix and the corresponding bare potential matrix element is lower than 5%. This result quantitatively justifies the use of v_x and v_s.

Appendix B

Equations of the HFP theory with the full k-dependence

In Chapter 3, Eqs. (3.27-3.30) are synthetically written omitting the k-dependence of the interaction potentials. For completeness, we now write the same equations in the k-dependent form. We stress that all the results shown in Chapter 3 are obtained starting from the k-dependent equations written in this Appendix, i.e. by accounting for the full momentum dependence of the interaction potentials.

For the condensate amplitudes, the two coupled Gross-Pitaevskii equations are

$$
\begin{aligned}
(\epsilon_0^x - \mu)\,\Phi_x &= [-2\mathrm{Re}\left\{v_s(0,0)n_0^{xc} + 2\Sigma'_\mathbf{k} v_s(\mathbf{k},0)\tilde{n}_\mathbf{k}^{xc}\right\} \\
&\quad + (v_x(0,0)n_0^{xx} + 2\Sigma'_\mathbf{k} v_x(\mathbf{k},0)\tilde{n}_\mathbf{k}^{xx})]\,\Phi_x \\
&\quad + (\hbar\Omega_R - \Sigma_\mathbf{k} v_s(\mathbf{k},0)n_\mathbf{k}^{xx})\,\Phi_C \\
(\epsilon_0^c - \mu)\,\Phi_c &= (\hbar\Omega_R - v_s(0,0)n_0^{xx} - 2\Sigma'_\mathbf{k} v_s(\mathbf{k},0)\tilde{n}_\mathbf{k}^{xx})\,\Phi_x,
\end{aligned}
$$

$$(\text{B.1})$$

where $\Sigma'_\mathbf{k} = \Sigma_{\mathbf{k}\neq 0}$ and $v_{x,s}(\mathbf{k},\mathbf{q}) = (1/2)(v_{x,s}(\mathbf{k},\mathbf{q},0) + v_{x,s}(\mathbf{k},\mathbf{q},\mathbf{k}-\mathbf{q}))$. Here $n_\mathbf{k}^{\chi\xi} = \langle \hat{O}_\chi^2(\mathbf{k})\hat{O}_\xi^1(\mathbf{k})\rangle/A$, where $\xi, \chi = x, c$. In our notation $\hat{O}_\xi^1(\mathbf{k}) = \hat{O}_\xi(\mathbf{k})$ while $\hat{O}_\xi^2(\mathbf{k}) = \hat{O}_\xi^\dagger(\mathbf{k})$.

We remind that we have introduced the 4×4 matrix propagator $G(\mathbf{k}, i\omega_n) \equiv \{g_{jl}^{\chi\xi}(\mathbf{k}, i\omega_n)\}_{j,l=1,2}^{\chi,\xi=x,c}$, whose elements are the thermal propagators of the excited particles, [Shi 98] written in terms of the Matsubara frequencies for bosons ω_n, and that the propagator matrix $G(\mathbf{k}, i\omega_n)$ obeys the Dyson-Beliaev equation

$$G(\mathbf{k}, i\omega_n) = G^0(\mathbf{k}, i\omega_n)\left[\mathbf{1} + \Sigma(\mathbf{k}, i\omega_n)\,G(\mathbf{k}, i\omega_n)\right], \qquad (\text{B.2})$$

where we have introduced the matrix of the non-interacting propagators $G^0 \equiv \{g_{jl}^0(\mathbf{k}, i\omega_n)\}_{jl}^{\chi\xi} = \delta_{\chi\xi}\delta_{jl}[(-)^j i\omega_n - \epsilon_\mathbf{k}^{(\xi)} + \mu]^{-1}$ and the 4×4 self-energy matrix

$$\Sigma(\mathbf{k}, i\omega_n) = \begin{pmatrix} \Sigma^{xx}(\mathbf{k}, i\omega_n) & \Sigma^{xc}(\mathbf{k}, i\omega_n) \\ \Sigma^{cx}(\mathbf{k}, i\omega_n) & \Sigma^{cc}(\mathbf{k}, i\omega_n) \end{pmatrix}. \qquad (\text{B.3})$$

Within the HFP theory, the self-energy elements are independent of frequency and read

$$
\begin{aligned}
\Sigma_{jj}^{xx}(\mathbf{k}) &= 2\sum_\mathbf{q}\left[v_x(\mathbf{k},\mathbf{q})n_\mathbf{q}^{xx} - v_s(\mathbf{k},\mathbf{q})\left(n_\mathbf{q}^{cx} + n_\mathbf{q}^{xc}\right)\right], \\
\Sigma_{12}^{xx}(\mathbf{k}) &= (\Sigma_{21}^{xx})^* = v_x(\mathbf{k},0)\Phi_x^2 - 2v_s(\mathbf{k},0)\Phi_x\Phi_c, \\
\Sigma_{11}^{xc}(\mathbf{k}) &= \Sigma_{22}^{xc}(\mathbf{k}) = \hbar\Omega_R\left(1 - 2\frac{\sum_\mathbf{q} v_s(\mathbf{k},\mathbf{q})n_\mathbf{q}^{xx}}{\hbar\Omega_R}\right), \\
\Sigma_{12}^{xc}(\mathbf{k}) &= (\Sigma_{21}^{xc}(\mathbf{k}))^* = -v_s\Phi_x^2,
\end{aligned}
$$

$$(\text{B.4})$$

while $\Sigma_{jl}^{cx} = \Sigma_{jl}^{xc}$ and $\Sigma_{jl}^{cc} = 0$.

Appendix C

Low-energy density of states

We discuss here our choice of modeling artificial confinement and structural disorder by adopting single-particle states in a box with periodic boundary conditions. We point out that the polariton localization length is only determined by disorder at the interfaces, resulting in a confinement for the photon field [Langbein 02]. A realistic disorder potential for the polariton field is displayed in Fig. C.1. We compare the eigenstates obtained for this disorder potential
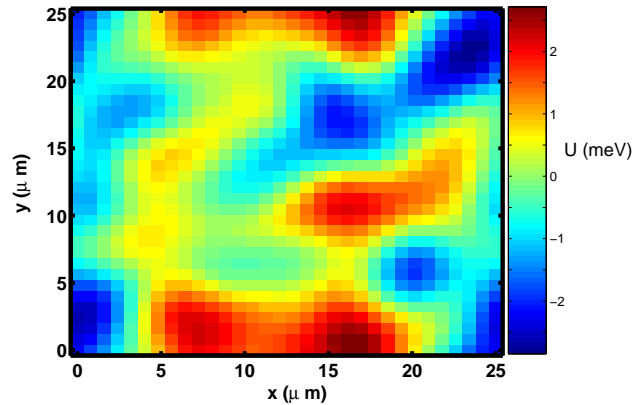
Figure C.1: Typical disorder potential for the polariton field.

with the eigenstates obtained for a square box of area $A = 100$ μm^2 in Fig. C.2. Although at high energy the density of states is obviously larger for the disorder potential, we see that the density of state at low energy, i.e. for $E < 1$ meV, is very similar in the two cases. Since the main effect of confinement in 2-D is in preventing the divergence of long wavelength fluctuations, the choice of adopting a box is sufficient to model the presence of a weak structural disorder.
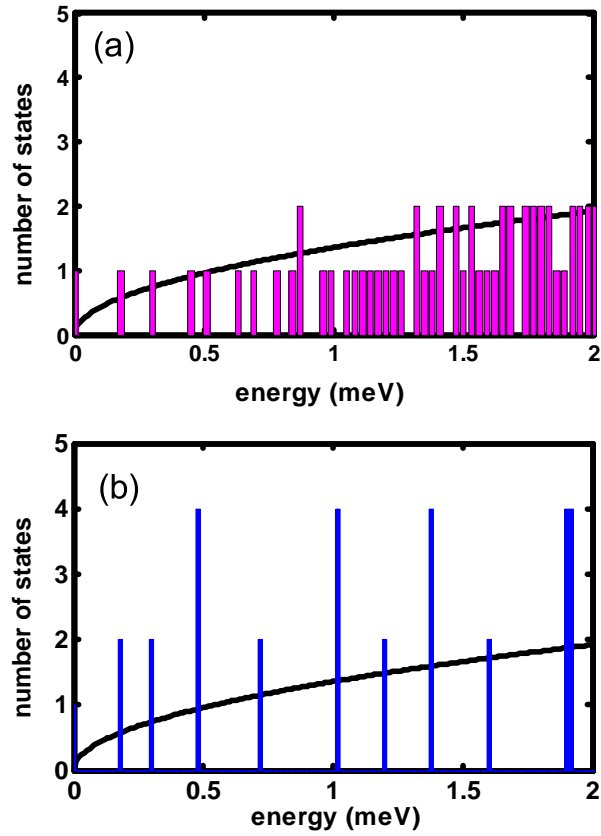
Figure C.2: Number of states at a given energy for a disorder potential (a) and for a box $A = 100 \ \mu\text{m}^2$ (b).

Appendix D

Simple picture of the non-equilibrium regime

We have shown in Chapter 3 that the Hartree-Fock-Popov theory developed for the polariton gas satisfies the Hugenholtz-Pines theorem, i.e. it predicts a gapless one-particle spectrum. This property is due to the fact that the condensate chemical potential, determined by the Gross-Pitaevskii equations, also represents the chemical potential of the excited particles, i.e. it defines the unperturbed Green's functions G_0. This condition is automatically guaranteed at thermal equilibrium. On the other hand, it has been suggested that deviations from equilibrium could manifest themselves via the presence of a new quasiparticle chemical potential differing from the local chemical potential of the condensate [Imamović-Tomasović 99]. Basically, this feature would originate from the different rate of relaxation into the condensate and into the thermal cloud.

Starting from this idea, we naively introduce non-equilibrium effects by assuming the existence of two different chemical potentials for the condensate, μ_{cond}, and the excited particles, μ_{exc}:

$$\mu_{exc} - \mu_{cond} = \delta \neq 0 \,. \tag{D.1}$$

We point out that, while the condensate chemical potential μ_{cond} is fixed by the interaction energy, the quantity μ_{exc} determines the statistical weight of the excitations and thus, within this simple picture, it is a free parameter. In particular, by restricting to the Bogoliubov limit our model (i.e. by neglecting the non-condensed population in the self-energy terms), we study how the excitation spectrum depends on the energy difference δ.[1] The real part of the excitation spectra are shown in Fig. D.1, while the imaginary part for $\delta = 0.2, 0.3$ are shown in Fig. D.2. The spectrum is gapless and phonon-like only if $\delta = 0$, corresponding to the Hugenholtz-Pines condition. On the other hand, if $\delta > 0$, the spectrum is diffusive at small momentum, as predicted in a more rigorous way by Boyanovski *et al.* [Boyanovsky 02], Szymanska *et al.* [Szymanska 06] and Wouters and Carusotto [Wouters 07b]. We point out that the condition $\delta > 0$ means that the creation of an excitation is favored with respect to the creation of a condensed particle, and thus it corresponds to the typical case where the relaxation into the condensate is slower than the relaxation into the thermal cloud [Wouters 07b].[2] On

---

[1]Notice that, for the present analysis, we are obliged to restrict to the Bogoliubov limit, because the population in the excited states cannot be fixed by the thermodynamics but a kinetic evaluation would be required [Boyanovsky 02].

[2]In a symmetry-breaking approach, this fact is due to the absence of a spontaneous scattering term into the coherent state, which is represented by a classical field. It is not clear if this feature remains valid also when the condensate is treated as a quantum field.
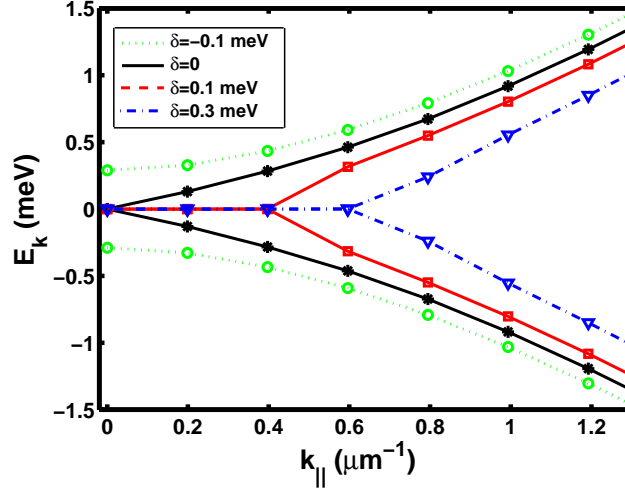
Figure D.1: Excitation spectra for the Bogoliubov approach, as a function of the difference between the condensate and the excitations chemical potentials $\delta = \mu_{exc} - \mu_{cond}$. At equilibrium $\delta = 0$.
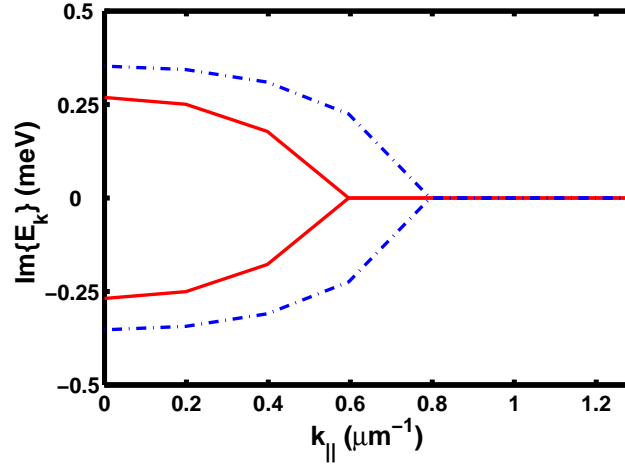
Figure D.2: Imaginary part of the excitation energies for $\delta = 0.2, 0.3$, showing a diffusive behavior at small momentum.

the other hand, for $\delta < 0$, the spectrum has an energy gap at zero momentum, corresponding to the fact that creating an excitation is energetically more difficult. This condition occurs when the relaxation into the coherent state is artificially forced, as in the case of polariton parametric process, where the appearance of an energy gap has been predicted by Carusotto and Ciuti [Carusotto 05].

Appendix E

Landau criterion for polariton superfluidity

In analogy with the Landau criterion for a single Bose gas, we can define the normal density of excitons and photons (having defined an effective mass $m_{x(c)}$ for the two species) by means of

$$\rho_n^{x(c)} = -\frac{1}{3} \sum_{\mathbf{k}} \hbar^2 k^2 \left. \frac{d\bar{N}_{x(c)}(E)}{dE} \right|_{E_{\mathbf{k}}}, \tag{E.1}$$

where

$$\bar{N}_x(E_{\mathbf{k}}) \equiv \langle \hat{\beta}_{\mathbf{k}}^\dagger \hat{\beta}_{\mathbf{k}} \rangle = \left(|X_u^{lp}(\mathbf{k})|^2 - |X_v^{lp}(\mathbf{k})|^2 \right) \bar{N}_{\mathbf{k}}^{lp} = \left(|X_u^{lp}(\mathbf{k})|^2 - |X_v^{lp}(\mathbf{k})|^2 \right) n_B(E_{\mathbf{k}}^{lp}), \tag{E.2}$$

defines the occupation of the exciton quasiparticles

$$\hat{\beta}_{\mathbf{k}} \equiv u_{\mathbf{k}}^x \hat{b}_{\mathbf{k}} + v_{-\mathbf{k}}^x \hat{b}_{-\mathbf{k}}^\dagger, \tag{E.3}$$

with

$$
\begin{aligned}
u_{\mathbf{k}}^x &= \frac{X_u^{lp}(\mathbf{k})}{\left(|X_u^{lp}(\mathbf{k})|^2 - |X_v^{lp}(\mathbf{k})|^2 \right)^{1/2}} \\
v_{\mathbf{k}}^x &= \frac{X_v^{lp}(\mathbf{k})}{\left(|X_u^{lp}(\mathbf{k})|^2 - |X_v^{lp}(\mathbf{k})|^2 \right)^{1/2}},
\end{aligned}
\tag{E.4}
$$

while $\bar{N}_c(E_{\mathbf{k}})$ is the photon quasiparticle population and is defined via

$$\bar{N}_c(E_{\mathbf{k}}) \equiv \langle \hat{\alpha}_{\mathbf{k}}^\dagger \hat{\alpha}_{\mathbf{k}} \rangle = \left(|C_u^{lp}(\mathbf{k})|^2 - |C_v^{lp}(\mathbf{k})|^2 \right) \bar{N}_{\mathbf{k}}^{lp} = \left(|C_u^{lp}(\mathbf{k})|^2 - |C_v^{lp}(\mathbf{k})|^2 \right) n_B(E_{\mathbf{k}}^{lp}), \tag{E.5}$$

defines the occupation of the exciton quasiparticles

$$\hat{\alpha}_{\mathbf{k}} \equiv u_{\mathbf{k}}^c \hat{c}_{\mathbf{k}} + v_{-\mathbf{k}}^c \hat{c}_{-\mathbf{k}}^\dagger, \tag{E.6}$$

with

$$
\begin{aligned}
u_{\mathbf{k}}^c &= \frac{C_u^{lp}(\mathbf{k})}{\left(|C_u^{lp}(\mathbf{k})|^2 - |C_v^{lp}(\mathbf{k})|^2 \right)^{1/2}} \\
v_{\mathbf{k}}^c &= \frac{C_v^{lp}(\mathbf{k})}{\left(|C_u^{lp}(\mathbf{k})|^2 - |C_v^{lp}(\mathbf{k})|^2 \right)^{1/2}}.
\end{aligned}
\tag{E.7}
$$

We point out that in our model the total densities of excitons and photons are directly obtained from the normal exciton and photon propagators, respectively. We can thus extract the superfluid exciton and photon density simply by subtracting the expression (E.1) from the total density

$$\rho_s^{x(c)} = m_{x(c)} n^{xx(cc)} - \rho_n^{x(c)} \,. \tag{E.8}$$

Notice that the superfluid densities of excitons and photons depend on the actual polariton spectrum and in particular are affected by the features of the lower polariton dispersion. To evaluate the quasi-condensate phase diagram, we define the polariton system as superfluid if both the exciton and the photon superfluid densities are finite. Indeed, only in this case we expect a superfluid response to either an optical or a mechanical perturbation.

Appendix F

Factorizations in the kinetic model

The equations (4.61) are derived factoring higher order correlation terms in single-particle or Bogoliubov quasi-particle population terms. In this appendix we give the details of the derivation of the dynamical equations of the scattering amplitudes $\tilde{m}_k$. From the Heisenberg equation and neglecting either the phonon coupling and the contribution of the states lying in the incoherent region, we obtain the expression

$$
\begin{aligned}
i\hbar\dot{\tilde{m}}_{\mathbf{k}} &= 2(\hbar\omega_{\mathbf{k}} - v_{\mathbf{k},0}^{(0)})\tilde{m}_{\mathbf{k}} + v_{\mathbf{k},0}^{(0)}\langle \hat{a}^\dagger\hat{a}^\dagger(\hat{a}^\dagger\hat{a} + \hat{a}\hat{a}^\dagger)\tilde{p}_{\mathbf{k}}\tilde{p}_{-\mathbf{k}}\rangle \\
&\quad - 4\sum_{\mathbf{q}} v_{\mathbf{k},0}^{(0)}\langle \hat{a}^\dagger\hat{a}^\dagger\tilde{p}_{\mathbf{q}}^\dagger\tilde{p}_{\mathbf{q}}\tilde{p}_{\mathbf{k}}\tilde{p}_{-\mathbf{k}}\rangle \\
&\quad + v_{\mathbf{k},-\mathbf{k}}^{(\mathbf{k})}\langle \hat{a}^\dagger\hat{a}^\dagger\hat{a}\hat{a}(\tilde{p}_{-\mathbf{k}}^\dagger\tilde{p}_{-\mathbf{k}} + \tilde{p}_{\mathbf{k}}\tilde{p}_{\mathbf{k}}^\dagger)\rangle \\
&\quad + \sum_{\mathbf{q}\mathbf{q}'} v_{\mathbf{q},\mathbf{q}'}^{(\mathbf{k}-\mathbf{q})}\langle \hat{a}^\dagger\hat{a}^\dagger(\tilde{p}_{\mathbf{q}+\mathbf{q}'-\mathbf{k}}^\dagger\tilde{p}_{-\mathbf{k}} + \tilde{p}_{\mathbf{k}}\tilde{p}_{\mathbf{q}+\mathbf{q}'+\mathbf{k}}^\dagger)\tilde{p}_{\mathbf{q}}\tilde{p}_{\mathbf{q}'}\rangle \\
&\quad - \sum_{\mathbf{q}} v_{\mathbf{q},-\mathbf{q}}^{(\mathbf{q})}\langle (\hat{a}\hat{a}^\dagger + \hat{a}^\dagger\hat{a})\tilde{p}_{\mathbf{q}}^\dagger\tilde{p}_{-\mathbf{q}}^\dagger\tilde{p}_{\mathbf{k}}\tilde{p}_{-\mathbf{k}}\rangle.
\end{aligned}
\tag{F.1}
$$

To rewrite this relation in terms of the populations of the condensate and of the excitations, we use the following factorizations (notice that the condensate wave function corresponds to a single particle eigenstate at $\mathbf{k} = 0$):

$$
\langle \hat{a}^\dagger\hat{a}^\dagger\hat{a}^\dagger\hat{a}\tilde{p}_{\mathbf{k}}\tilde{p}_{-\mathbf{k}}\rangle \simeq (N_c - 2)\tilde{m}_{\mathbf{k}};
\tag{F.2}
$$

$$
\begin{aligned}
\langle \hat{a}^\dagger\hat{a}^\dagger\tilde{p}_{\mathbf{q}}^\dagger\tilde{p}_{\mathbf{q}}\tilde{p}_{\mathbf{k}}\tilde{p}_{-\mathbf{k}}\rangle &\simeq (\tilde{N}_{\mathbf{q}} - \delta_{\mathbf{q},\mathbf{k}}\tilde{N}_{\mathbf{k}} - \delta_{\mathbf{q},-\mathbf{k}}\tilde{N}_{-\mathbf{k}})\tilde{m}_{\mathbf{k}} \\
&\quad + \tilde{N}_{\mathbf{q},\mathbf{k}}\tilde{m}_{\mathbf{q},-\mathbf{k}} + \tilde{N}_{\mathbf{q},-\mathbf{k}}\tilde{m}_{\mathbf{q},\mathbf{k}};
\end{aligned}
\tag{F.3}
$$

$$
\langle \hat{a}^\dagger\hat{a}\tilde{p}_{\mathbf{q}}^\dagger\tilde{p}_{-\mathbf{q}}^\dagger\tilde{p}_{\mathbf{k}}\tilde{p}_{-\mathbf{k}}\rangle \simeq N_c\langle \tilde{p}_{\mathbf{q}}^\dagger\tilde{p}_{-\mathbf{q}}^\dagger\tilde{p}_{\mathbf{k}}\tilde{p}_{-\mathbf{k}}\rangle;
\tag{F.4}
$$

$$
\langle \hat{a}^\dagger\hat{a}^\dagger\hat{a}\hat{a}\tilde{p}_{\mathbf{k}}^\dagger\tilde{p}_{\mathbf{k}}\rangle \simeq N_c(N_c - 1)\tilde{N}_{\mathbf{k}};
\tag{F.5}
$$

$$
\begin{aligned}
\langle \hat{a}^\dagger\hat{a}^\dagger\tilde{p}_{\mathbf{q}+\mathbf{q}'-\mathbf{k}}^\dagger\tilde{p}_{-\mathbf{k}}\tilde{p}_{\mathbf{q}}\tilde{p}_{\mathbf{q}'}\rangle &\simeq 2\tilde{N}_{\mathbf{q}+\mathbf{q}'-\mathbf{k},\mathbf{q}'}\tilde{m}_{\mathbf{q},-\mathbf{k}} \\
&\quad + \tilde{N}_{\mathbf{q}+\mathbf{q}'-\mathbf{k},-\mathbf{k}}\tilde{m}_{\mathbf{q},\mathbf{q}'} \\
&\quad - \delta_{\mathbf{q},\mathbf{k}}\delta_{\mathbf{q}',\mathbf{k}}\tilde{N}_{\mathbf{k}}\tilde{m}_{\mathbf{k}}).
\end{aligned}
\tag{F.6}
$$

From here, within the assumption of a spatially homogeneous system, we recover the relation of Eq. (4.61).

As explained in the text, the two-body correlation $\langle \tilde{p}_{\mathbf{q}}^\dagger\tilde{p}_{-\mathbf{q}}^\dagger\tilde{p}_{\mathbf{k}}\tilde{p}_{-\mathbf{k}}\rangle$ between excitations is evaluated in a quasi-stationary limit, by using the actual solution of the Bogoliubov problem. Using again the fact that the condensate wave-function corresponds to a single state, we rewrite

this quantity in terms of the excitation field $\hat{\Lambda}_{\mathbf{k}}$, defined in Eq. (4.19), as:

$$
\begin{aligned}
\langle \tilde{p}_{\mathbf{q}}^\dagger \tilde{p}_{\mathbf{q}}^\dagger \tilde{p}_{\mathbf{k}} \tilde{p}_{-\mathbf{k}} \rangle &= \frac{\langle \hat{a}\hat{a}\hat{a}^\dagger \hat{a}^\dagger \tilde{p}_{\mathbf{q}}^\dagger \tilde{p}_{-\mathbf{q}}^\dagger \tilde{p}_{\mathbf{k}} \tilde{p}_{-\mathbf{k}} \rangle}{(N_c + 1)(N_c + 2)} \\
&= \frac{N^2}{(N_c + 1)(N_c + 2)} \langle \hat{\Lambda}_{\mathbf{q}}^\dagger \hat{\Lambda}_{-\mathbf{q}}^\dagger \hat{\Lambda}_{\mathbf{k}} \hat{\Lambda}_{-\mathbf{k}} \rangle.
\end{aligned}
\tag{F.7}
$$

The correlation amplitude for the fluctuation field is written by means of the Bogoliubov transformation $\hat{\Lambda}_{\mathbf{k}} = U_{\mathbf{k}} \hat{\alpha}_{\mathbf{k}} + V_{-\mathbf{k}}^* \hat{\alpha}_{-\mathbf{k}}^\dagger$. All the resulting terms are factored as product of the Bogoliubov quasi-particle populations $\bar{N}_{\mathbf{k}} = \langle \hat{\alpha}_{\mathbf{k}}^\dagger \hat{\alpha}_{\mathbf{k}} \rangle$, as:

$$
\langle \hat{\alpha}_{\mathbf{k}}^\dagger \hat{\alpha}_{\mathbf{q}}^\dagger \hat{\alpha}_{\mathbf{k}} \hat{\alpha}_{\mathbf{q}} \rangle \simeq \bar{N}_{\mathbf{k}} \left(\bar{N}_{\mathbf{q}} - \delta_{\mathbf{k},\mathbf{q}} \right).
\tag{F.8}
$$

Collecting all the terms in a compact way, we finally recover Eq. (4.46). The final expression can be written in terms of the single-particle population using the expression

$$
\langle \tilde{p}_{\mathbf{k}}^\dagger \tilde{p}_{\mathbf{k}} \rangle \simeq \frac{N}{N_c + 1} [(|U_{\mathbf{k}}|^2 + |V_{\mathbf{k}}|^2) \bar{N}_{\mathbf{k}} + |V_{\mathbf{k}}|^2].
\tag{F.9}
$$

Appendix G

Semiclassical Boltzmann equations

In deriving the equations of the kinetic model developed in Chapter 4, we have only retained the collision processes describing two exciton-like polaritons scattering into another exciton-like polariton and into one low-energy polariton. This choice was justified by the fact that these processes give the dominant contribution to the relaxation kinetics (see Fig. 4.1). In addition, we have assumed that, in the exciton-like energy region of the lower-polariton dispersion, the population distribution follows a Boltzmann distribution characterized by an effective temperature T_x. In this Appendix, we show the validity of these approximations, by comparing the results of our simplified kinetic equations with the results obtained by solving the full set of semiclassical Boltzmann equations. To derive these latter we follow the derivation made by Tassone and Yamamoto [Tassone 99], i.e. we adopt the cylindrical symmetry and we choose a grid uniformly spaced in energy with an energy step Δ_E. Within this choice, the semiclassical Boltzmann equations for the populations in the lower polariton states read [Tassone 99]

$$
\begin{aligned}
\dot{N}_k &= F_{\mathbf{k}} - \gamma_{\mathbf{k}} N_{\mathbf{k}} \\
&+ \sum_{\mathbf{k'},\mathbf{q},\mathbf{q'}} \left[W^{pp}_{\mathbf{qq'}\to\mathbf{kk'}} N_{\mathbf{q}} N_{\mathbf{q'}}(1+N_{\mathbf{k}})(1+N_{\mathbf{k'}}) - W^{pp}_{\mathbf{kk'}\to\mathbf{qq'}} N_{\mathbf{k}} N_{\mathbf{k'}}(1+N_{\mathbf{q}})(1+N_{\mathbf{q'}}) \right] \\
&+ \sum_{\mathbf{k'}} \left[W^{ph}_{\mathbf{k'}\to\mathbf{k}} N_{\mathbf{k'}}(1+N_{\mathbf{k}}) - W^{ph}_{\mathbf{k}\to\mathbf{k'}} N_{\mathbf{k}}(1+N_{\mathbf{k'}}) \right] .
\end{aligned}
\tag{G.1}
$$

The rates of the phonon-mediated scattering processes are given by (see Eq. (4.9,4.59))

$$
W^{ph}_{\mathbf{k}\to\mathbf{k'}} = \frac{2\pi}{\hbar} \frac{A}{(2\pi)^2} \frac{\Delta_E}{2 \frac{\partial E}{\partial k^2}\big|_{\mathbf{k'}}} \frac{\hbar\Delta_k}{2\rho A u} X_{\mathbf{k}}^2 X_{\mathbf{k'}}^2 R^{ph}_{\mathbf{k},\mathbf{k'}} N_{ph}(E_{\mathbf{k'}} - E_{\mathbf{k}}) ,
\tag{G.2}
$$

where $N_{ph}(E) = n_B(E) + \theta(E)$,

$$
R^{ph}_{\mathbf{k},\mathbf{k'}} = 2 \int_0^{\theta_{max}} d\theta \frac{2\Delta_k}{\hbar u q_z} \left[a_e I_e^{\perp}(q_z) I_e^{\parallel}(\Delta_{k_{\parallel}}) - a_h I_h^{\perp}(q_z) I_h^{\parallel}(\Delta_{k_{\parallel}}) \right]^2 ,
\tag{G.3}
$$

$q_z = \sqrt{\Delta_k^2 - \Delta_{k_{\parallel}}^2}$, $\Delta_{k_{\parallel}}^2 = k^2 + k'^2 - 2kk'\cos\theta$, $\Delta_k = |E_{\mathbf{k'}} - E_{\mathbf{k}}|/\hbar u$ and

$$
\cos\theta_{max} = \frac{k^2 + k'^2 - \Delta_k^2}{2kk'} = c ,
\tag{G.4}
$$

if $|c| \leq 1$ while $\cos\theta_{max} = \text{Sgn}(c)$ if $|c| > 1$.

On the other hand, the rates of the polariton-polariton collision processes are

$$
W^{pp}_{\mathbf{kk'}\to\mathbf{qq'}} = \frac{\pi}{\hbar} \frac{A^2}{(2\pi)^4} |v^{(q-k)}_{\mathbf{kk'}}|^2 \frac{\Delta_E^2}{\frac{\partial E}{\partial k^2}\big|_{\mathbf{k'}} \frac{\partial E}{\partial k^2}\big|_{\mathbf{q}} \frac{\partial E}{\partial k^2}\big|_{\mathbf{q'}}} R_{\mathbf{k},\mathbf{k'},\mathbf{q},\mathbf{q'}} ,
\tag{G.5}
$$

where

$$R_{\mathbf{k},\mathbf{k}',\mathbf{q},\mathbf{q}'} = \frac{1}{2} \int_I \frac{dx}{\sqrt{[(k+q)^2 - x][x - (k-q)^2][(k'+q')^2 - x][x - (k'-q')^2]}} \,, \qquad \text{(G.6)}$$

and the integral is performed over the interval

$$I = \left[(k-q)^2, (k+q)^2 \right] \cap \left[(k'-q')^2, (k'+q')^2 \right] \,. \qquad \text{(G.7)}$$

Notice that the density of states along the energy dispersion enters into these expressions via the derivative $\frac{\partial E}{\partial k^2}$. We mention that, since the thermalization in the exciton-like region is fast, the steady-state solution of Eqs. (G.1) weakly depends on the peculiar k-dependence of the pump terms

$$F_{\mathbf{k}} = f\, C_{\mathbf{k}}, \ \ \sum_{\mathbf{k}} C_k = 1 \qquad \text{(G.8)}$$

(f corresponds to the analogous quantity in Eq. (4.61)) provided that the pump populates only high energy states, i.e. states in the exciton-like energy region.

As an example, in Fig. G.1, we compare the steady-state energy distribution predicted by the kinetic model (already displayed in Fig. 4.11) and by Eqs. (G.1), for $\tau_{pol} = 3$ ps and pump intensity $f = 1.5 f_c$.[1] The two energy distributions are very similar and they differ from
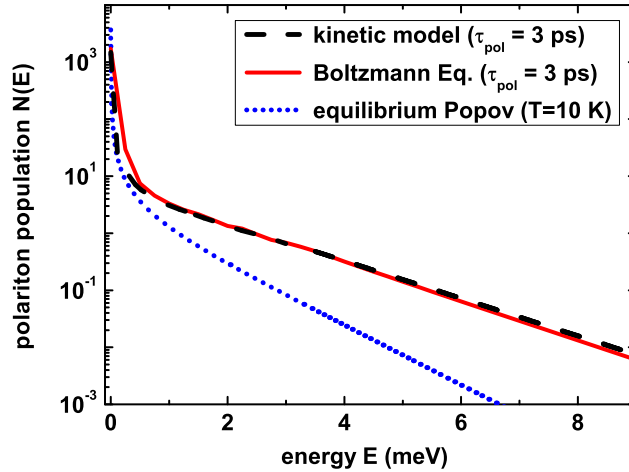
Figure G.1: Energy distribution of populations in the condensed regime. We compare the result of the kinetic model developed in Chapter 4, with the result of the semiclassical Boltzmann equations (G.1), for $\tau_{pol} = 3$ ps and $T_L = 10$ K. We also show the prediction valid at thermal equilibrium.

the distribution expected at thermal equilibrium. This result confirms, also quantitatively, the non-equilibrium features discussed in section 4.3, in particular the heating of the exciton reservoir with respect to the lattice temperature.

---

[1]In fact, we expect that the contributions arising from the scattering processes inside the low-energy region (neglected in the kinetic model) could possibly be relevant only when the occupation of the lower energy states is sufficiently large. On the other hand, we notice that, far above the condensation density threshold, the incoherent collisions within the lower-energy part of the dispersion cannot be treated by means of the semiclassical Boltzmann equations because the single-particle spectrum is modified by the presence of the condensate, and a field theory formalism beyond the HFB approximation would be required.

Bibliography

[Agranovich 66]   V. M. Agranovich & A. O. Dubowskii. *Effect of retarded interaction of exciton spectrum in 1-dimensional and 2-dimensional systems.* JETP LETTERS, vol. 3, page 223, 1966.

[Andersen 04]   J. O. Andersen. *Theory of the weakly interacting Bose gas.* Reviews of Modern Physics, vol. 76, no. 2, page 599, 2004.

[Anderson 95]   M. H. Anderson, J. R. Ensher, M. R. Matthews, C. E. Wieman & E. A. Cornell. *Observation of Bose-Einstein Condensation in a Dilute Atomic Vapor.* Science, vol. 269, no. 5221, pages 198–201, 1995.

[Andreani 88]   L. C. Andreani, F. Bassani & A. Quattropani. *Longitudinal-Transverse Splitting in Wannier Excitons and Polariton States.* Il Nuovo Cimento, vol. 10D, page 1473, 1988.

[Andreani 94]   L. C. Andreani. Confined electrons and photons: new physics and devices: *Optical transitions, excitons, and polaritons in bulk and low-dimensional semiconductor structures.* Edited by E. Burstein and C. Weisbuch (Plenum 1994), 1994.

[Bagnato 91]   Vanderlei Bagnato & Daniel Kleppner. *Bose-Einstein condensation in low-dimensional traps.* Physical Review A (Atomic, Molecular, and Optical Physics), vol. 44, no. 11, pages 7439–7441, 1991.

[Bajoni 07]   D. Bajoni, E. Peter, P. Senellart, J. L. Smirr, I. Sagnes, A. Lemaitre & J. Bloch. *Polariton parametric luminescence in a single micropillar.* Applied Physics Letters, vol. 90, no. 5, page 051107, 2007.

[Balili 07]   R. Balili, V. Hartwell, D. Snoke, L. Pfeiffer & K. West. *Bose-Einstein Condensation of Microcavity Polaritons in a Trap.* Science, vol. 316, no. 5827, pages 1007–1010, 2007.

[Bassani 75]   Pastori Parravicini G. Bassani F. Electronic states and optical transitions in solids. Pergamon Press, Oxford, 1975.

[Bastard 89]   G. Bastard. Wave mechanics applied to semiconductor heterostructures. Les Editions de Physique, Paris, 1989.

[Beloussov 96]   Igor V. Beloussov & Vladimir V. Frolov. *Nonmonotonic decay of nonequilibrium polariton condensate in direct-gap semiconductors.* Phys. Rev. B, vol. 54, no. 4, pages 2523–2531, Jul 1996.

[Ben-Tabou de Leon 01]   S. Ben-Tabou de Leon & B. Laikhtman. *Exciton-exciton interactions in quantum wells: Optical properties and energy and spin relaxation.* Phys. Rev. B, vol. 63, no. 12, page 125306, Mar 2001.

[Blatt 62]   John M. Blatt, K. W. Böer & Werner Brandt. *Bose-Einstein Condensation of Excitons.* Phys. Rev., vol. 126, no. 5, pages 1691–1692, Jun 1962.

[Bleuse 98]   J. Bleuse, F. Kany, A. P. de Boer, P. C. M. Christianen, R. André & H. Ulmer-Tuffigo. *Laser emission on a cavity-polariton line in a II-VI microcavity.* J. Crystal Growth, vol. 184, page 750, 1998.

[Boeuf 00]   F. Boeuf, R. André, R. Romestain, Le Si Dang, E. Péronne, J. F. Lampin, D. Hulin & A. Alexandrou. *Evidence of polariton stimulation in semiconductor microcavities.* Phys. Rev. B, vol. 62, no. 4, pages R2279–R2282, Jul 2000.

[Bogoliubov 47]   N. N. Bogoliubov. *On the Theory of Superfluidity.* J. Phys. (USSR), vol. 11, pages 23–32, 1947.

[Bogoliubov 48]   N. N. Bogoliubov. *Kinetic equations in the theory of superfluidity.* JETP, vol. 18, pages 622–630, 1948.

[Bose 24]   S. N. Bose. *Thermal equilibrium of the radiation field in the presence of matter.* Z. Phys., vol. 26, page 178, 1924.

[Bouwmeester 00]   D. Bouwmeester, A. K. Ekert & A. Zeilinger. The physics of quantum information. Springer, 2000.

[Boyanovsky 02]   D. Boyanovsky, S. Y. Wang, D. S. Lee, H. L. Yu & S. M. Alamoudi. *Nonequilibrium Relaxation of BoseEinstein Condensates: Real-Time Equations of Motion and Ward Identities.* Annals of Physics, vol. 300, page 1, 2002.

[Bradley 95]   C. C. Bradley, C. A. Sackett, J. J. Tollett & R. G. Hulet. *Evidence of Bose-Einstein Condensation in an Atomic Gas with Attractive Interactions.* Phys. Rev. Lett., vol. 75, no. 9, pages 1687–1690, Aug 1995.

[Butov 02]   L. V. Butov, A. C. Gossard & D. S. Chemla. *Macroscopically ordered state in an exciton system.* Nature, vol. 418, no. 6899, pages 751–754, 2002.

[Cao 04]   Huy Thien Cao, T. D. Doan, D. B. Tran Thoai & H. Haug. *Condensation kinetics of cavity polaritons interacting with a thermal phonon bath.* Physical Review B (Condensed Matter and Materials Physics), vol. 69, no. 24, page 245325, 2004.

[Carusotto 04]   I. Carusotto & C. Ciuti. *Probing Microcavity Polariton Superfluidity through Resonant Rayleigh Scattering.* Phys. Rev. Lett., vol. 93, page 166401, 2004.

126

[Carusotto 05]   Iacopo Carusotto & Cristiano Ciuti. *Spontaneous microcavity-polariton coherence across the parametric threshold: Quantum Monte Carlo studies.* Physical Review B (Condensed Matter and Materials Physics), vol. 72, no. 12, page 125335, 2005.

[Castin 97]   Y. Castin & R. Dum. *Instability and Depletion of an Excited Bose-Einstein Condensate in a Trap.* Phys. Rev. Lett., vol. 79, no. 19, pages 3553–3556, Nov 1997.

[Castin 98]   Y. Castin & R. Dum. *Low-temperature Bose-Einstein condensates in time-dependent traps: Beyond the $U(1)$ symmetry-breaking approach.* Phys. Rev. A, vol. 57, no. 4, pages 3008–3021, Apr 1998.

[Chen 95]   Y. Chen, A. Tredicucci & F. Bassani. *Bulk exciton polaritons in GaAs microcavities.* Phys. Rev. B, vol. 52, no. 3, pages 1800–1805, Jul 1995.

[Ciuti 98]   C. Ciuti, V. Savona, C. Piermarocchi, A. Quattropani & P. Schwendimann. *Role of the exchange of carriers in elastic exciton-exciton scattering in quantum wells.* Phys. Rev. B, vol. 58, no. 12, page 7926, Sep 1998.

[Ciuti 01]   C. Ciuti, P. Schwendimann & A. Quattropani. Phys. Rev. B, vol. 63, page 041303R, 2001.

[Ciuti 04]   C. Ciuti. *Branch-entangled polariton pairs in planar microcavities and photonic wires.* Physical Review B (Condensed Matter and Materials Physics), vol. 69, no. 24, page 245304, 2004.

[Combescot 02]   M. Combescot & Betbeder-Matibet O. *The Effective Bosonic Hamiltonian for Excitons Reconsidered.* Europhysics Letters, vol. 58, page 87, 2002.

[Comte 82]   C. Comte & P. Nozières. *Exciton Bose Condensation - The Gound-State of an Electron-Hole Gas.* J. Physique, vol. 43, pages 1069–1098, 1982.

[Daif 06]   O. El Daif, A. Baas, T. Guillet, J.-P. Brantut, R. Idrissi Kaitouni, J. L. Staehli, F. Morier-Genoud & B. Deveaud. *Polariton quantum boxes in semiconductor microcavities.* Applied Physics Letters, vol. 88, no. 6, page 061105, 2006.

[Dalfovo 99]   Franco Dalfovo, Stefano Giorgini, Lev P. Pitaevskii & Sandro Stringari. *Theory of Bose-Einstein condensation in trapped gases.* Rev. Mod. Phys., vol. 71, no. 3, pages 463–512, Apr 1999.

[Dang 98]   Le Si Dang, D. Heger, R. André, F. Bœuf & R. Romestain. *Stimulation of Polariton Photoluminescence in Semiconductor Microcavity.* Phys. Rev. Lett., vol. 81, no. 18, pages 3920–3923, Nov 1998.

[Davis 95]   K. B. Davis, M. O. Mewes, M. R. Andrews, N. J. van Druten, D. S. Durfee, D. M. Kurn & W. Ketterle. *Bose-Einstein Condensation in a Gas of Sodium Atoms*. Phys. Rev. Lett., vol. 75, no. 22, pages 3969–3973, Nov 1995.

[DeGiorgio 70]   V. DeGiorgio & Marlan O. Scully. *Analogy between the Laser Threshold Region and a Second-Order Phase Transition*. Phys. Rev. A, vol. 2, no. 4, pages 1170–1177, Oct 1970.

[Deng 02]   Hui Deng, Gregor Weihs, Charles Santori, Jacqueline Bloch & Yoshihisa Yamamoto. *Condensation of Semiconductor Microcavity Exciton Polaritons*. Science, vol. 298, no. 5591, pages 199–202, 2002.

[Deng 03]   H. Deng, G. Weihs, D. Snoke, J. Bloch & Y. Yamamoto. PNAS, vol. 100, page 15318, 2003.

[Deng 06]   Hui Deng, David Press, Stephan Gotzinger, Glenn S. Solomon, Rudolf Hey, Klaus H. Ploog & Yoshihisa Yamamoto. *Quantum Degenerate Exciton-Polaritons in Thermal Equilibrium*. Physical Review Letters, vol. 97, no. 14, page 146402, 2006.

[Doan 05]   T. D. Doan, Huy Thien Cao, D. B. Tran Thoai & H. Haug. *Condensation kinetics of microcavity polaritons with scattering by phonons and polaritons*. Physical Review B (Condensed Matter and Materials Physics), vol. 72, no. 8, page 085301, 2005.

[Doan 06]   T. D. Doan, Huy Thien Cao, D. B. Tran Thoai & H. Haug. *Microcavity polariton kinetics for bosonic condensation and lasing in II-VI compound materials*. Physical Review B (Condensed Matter and Materials Physics), vol. 74, no. 11, page 115316, 2006.

[Dodd 98]   R. J. Dodd, Mark Edwards, Charles W. Clark & K. Burnett. *Collective excitations of Bose-Einstein-condensed gases at finite temperatures*. Phys. Rev. A, vol. 57, no. 1, pages R32–R35, Jan 1998.

[Eastham 01]   P. R. Eastham & P. B. Littlewood. *Bose condensation of cavity polaritons beyond the linear regime: The thermal equilibrium of a model microcavity*. Phys. Rev. B, vol. 64, no. 23, page 235101, Nov 2001.

[Einstein 24]   A. Einstein. *Quantum theory of monatomic ideal gases*. Sitzber. Kgl. Preuss. Akad. Wiss., page 261, 1924.

[Einstein 25]   A. Einstein. *Quantum Theory of Monatomic Ideal Gases. Second Paper*. Sitzber. Kgl. Preuss. Akad. Wiss., page 3, 1925.

[Eisenstein 04]   J. P. Eisenstein & A. H. MacDonald. *Bose–Einstein condensation of excitons in bilayer electron systems*. Nature, vol. 432, no. 7018, pages 691–694, 2004.

[Erland 01]   J. Erland, V. Mizeikis, W. Langbein, J. R. Jensen & J. M. Hvam. *Stimulated Secondary Emission from Semiconductor Microcavities*. Phys. Rev. Lett., vol. 86, no. 25, pages 5791–5794, Jun 2001.

[Fano 61]   U. Fano. *Effects of Configuration Interaction on Intensities and Phase Shifts.* Phys. Rev., vol. 124, no. 6, pages 1866–1878, Dec 1961.

[Fetter 71]   A. L. Fetter & J. D. Walecka. Quantum theory of many-particle systems. McGraw-Hill, 1971.

[Fortin 93]   E. Fortin, S. Fafard & André Mysyrowicz. *Exciton transport in Cu_2O: Evidence for excitonic superfluidity?* Phys. Rev. Lett., vol. 70, no. 25, pages 3951–3954, Jun 1993.

[Gardiner 97a]   C. W. Gardiner. *Particle-number-conserving Bogoliubov method which demonstrates the validity of the time-dependent Gross-Pitaevskii equation for a highly condensed Bose gas.* Phys. Rev. A, vol. 56, no. 2, pages 1414–1423, Aug 1997.

[Gardiner 97b]   C. W. Gardiner, P. Zoller, R. J. Ballagh & M. J. Davis. *Kinetics of Bose-Einstein Condensation in a Trap.* Phys. Rev. Lett., vol. 79, no. 10, pages 1793–1796, Sep 1997.

[Gardiner 98]   C. W. Gardiner, M. D. Lee, R. J. Ballagh, M. J. Davis & P. Zoller. *Quantum Kinetic Theory of Condensate Growth: Comparison of Experiment and Theory.* Phys. Rev. Lett., vol. 81, no. 24, pages 5266–5269, Dec 1998.

[Gardiner 07]   S. A. Gardiner & S. A. Morgan. *Number-conserving approach to a minimal self-consistent treatment of condensate and noncondensate dynamics in a degenerate Bose gas.* Physical Review A (Atomic, Molecular, and Optical Physics), vol. 75, no. 4, page 043621, 2007.

[Graham 98]   Robert Graham. *Decoherence of Bose-Einstein Condensates in Traps at Finite Temperature.* Phys. Rev. Lett., vol. 81, no. 24, pages 5262–5265, Dec 1998.

[Greiner 02]   M. Greiner, O. Mandel, T. W. Hansch & I. Bloch. *Collapse and revival of the matter wave field of a Bose–Einstein condensate.* Nature, vol. 419, no. 6902, pages 51–54, 2002.

[Griffin 95]   A. Griffin, D. W. Snoke & S. Stringari. Bose-einstein condensation. Cambridge Univ. Press, 1995.

[Griffin 96]   A. Griffin. *Conserving and gapless approximations for an inhomogeneous Bose gas at finite temperatures.* Phys. Rev., vol. B 53, no. 14, pages 9341–9347, 1996.

[Gurioli 01]   M. Gurioli, F. Bogani, D. S. Wiersma, Ph. Roussignol, G. Cassabois, G. Khitrova & H. Gibbs. *Experimental study of disorder in a semiconductor microcavity.* Phys. Rev. B, vol. 64, no. 16, page 165309, Oct 2001.

[Hadzibabic 06]   Z. Hadzibabic, P. Krüger, M. Cheneau, B. Battelier & J. Dalibard. *BerezinskiiKosterlitzThouless Crossover in a Trapped Atomic Gas.* Nature, vol. 441, pages 1118–1121, 2006.

[Hall 98]   D. S. Hall, M. R. Matthews, C. E. Wieman & E. A. Cornell. *Measurements of Relative Phase in Two-Component Bose-Einstein Condensates.* Phys. Rev. Lett., vol. 81, no. 8, pages 1543–1546, Aug 1998.

[Hanamura 77]   E. Hanamura & H. Haug. *Condensation effects of excitons.* Phys. Rev. B, vol. 33, no. 4, page 209, 1977.

[Hasuo 93]   M. Hasuo, N. Nagasawa, T. Itoh & A. Mysyrowicz. *Progress in the Bose-Einstein condensation of biexcitons in CuCl.* Phys. Rev. Lett., vol. 70, no. 9, pages 1303–1306, Mar 1993.

[Haug 90]   H. Haug & S. W. Koch. Quantum theory of the optical and electronic properties of semiconductors. World Scientific Publishing, Singapore, 1990.

[Hohenberg 65]   P. C. Hohenberg & P. C. Martin. *Microscopic Theory of Superfluid Helium.* Annals of Physics, vol. 34, page 291, 1965.

[Hohenberg 67]   P. C. Hohenberg. *Existence of Long-Range Order in One and Two Dimensions.* Phys. Rev., vol. 158, no. 2, pages 383–386, Jun 1967.

[Honerlage 85]   B. Honerlage, R. Levy, J. B. Grun, Klingshirn C. & Bohnert K. *The dispersion of excitons, polaritons and biexcitons in direct-gap semiconductors.* Physics Reports, vol. 124, pages 161–253, 1985.

[Hopfield 58]   J. J. Hopfield. *Theory of the Contribution of Excitons to the Complex Dielectric Constant of Crystals.* Phys. Rev., vol. 112, no. 5, pages 1555–1567, Dec 1958.

[Houdré 00]   R. Houdré, C. Weisbuch, R. P. Stanley, U. Oesterle & M. Ilegems. Phys. Rev. Lett., vol. 85, page 2793, 2000.

[Huang 00]   R. Huang, F. Tassone & Y. Yamamoto. *Experimental evidence of stimulated scattering of excitons into microcavity polaritons.* Phys. Rev. B, vol. 61, no. 12, pages R7854–R7857, Mar 2000.

[Hugenholtz 59]   N. M. Hugenholtz & D. Pines. *Ground-State Energy and Excitation Spectrum of a System of Interacting Bosons.* Physical Review, vol. 116, no. 3, pages 489–506, 1959.

[Imamoglu 96]   A. Imamoglu, R. J. Ram, S. Pau & Y. Yamamoto. *Nonequilibrium condensates and lasers without inversion: Exciton-polariton lasers.* Phys. Rev. A, vol. 53, no. 6, pages 4250–4253, Jun 1996.

[Imamović-Tomasović 99] Milena Imamović-Tomasović & Allan Griffin. *Coupled Hartree-Fock-Bogoliubov kinetic equations for a trapped Bose gas.* Phys. Rev. A, vol. 60, no. 1, pages 494–503, Jul 1999.

[Ivanov 98]   A. L. Ivanov, H. Haug & L. V. Keldysh. *Optics of excitonic molecules in semiconductors and semiconductor microstructures.* Physics Reports, vol. 296, page 237, 1998.

[Jaksch 97]	D. Jaksch, C. W. Gardiner & P. Zoller. *Quantum kinetic theory. II. Simulation of the quantum Boltzmann master equation.* Phys. Rev. A, vol. 56, no. 1, pages 575–586, Jul 1997.
[Kagan 92]	Yu. M. Kagan, B. V. Svistunov & G. V. Shlyapnikov. *Kinetics of Bose condensation in an interacting Bose gas.* Soviet Physics - JETP, vol. 74, no. 2, pages 279–285, 1992.
[Kagan 97]	Yu. Kagan & B. V. Svistunov. *Evolution of Correlation Properties and Appearance of Broken Symmetry in the Process of Bose-Einstein Condensation.* Phys. Rev. Lett., vol. 79, no. 18, pages 3331–3334, Nov 1997.
[Kaitouni 06]	R. Idrissi Kaitouni, O. El Daif, A. Baas, M. Richard, T. Paraiso, P. Lugan, T. Guillet, F. Morier-Genoud, J. D. Ganiere, J. L. Staehli, V. Savona & B. Deveaud. *Engineering the spatial confinement of exciton polaritons in semiconductors.* Physical Review B (Condensed Matter and Materials Physics), vol. 74, no. 15, page 155311, 2006.
[Kasprzak 06]	J. Kasprzak, M. Richard, S. Kundermann, A. Baas, P. Jeambrun, J. M. J. Keeling, F. M. Marchetti, M. H. Szymaska, R. André, J. L. Staehli, V. Savona, P. B. Littlewood, B. Deveaud & Le Si Dang. *BoseEinstein condensation of exciton polaritons.* Nature, vol. 443, page 409, 2006.
[Keeling 04]	Jonathan Keeling, P. R. Eastham, M. H. Szymanska & P. B. Littlewood. *Polariton Condensation with Localized Excitons and Propagating Photons.* Physical Review Letters, vol. 93, no. 22, page 226403, 2004.
[Keldysh 68]	L. V. Keldysh & A. N. Kozlov. *Collective Properties of Excitons in Semiconductors.* Sov. Phys. JETP, vol. 27, page 521, 1968.
[Ketterle 96]	Wolfgang Ketterle & N. J. van Druten. *Bose-Einstein condensation of a finite number of particles trapped in one or three dimensions.* Phys. Rev. A, vol. 54, no. 1, pages 656–660, Jul 1996.
[Khitrova 99]	G. Khitrova, H. M. Gibbs, F. Jahnke, M. Kira & S. W. Koch. *Nonlinear optics of normal-mode-coupling semiconductor microcavities.* Rev. Mod. Phys., vol. 71, no. 5, pages 1591–1639, Oct 1999.
[Kita 06]	T. Kita. *Conserving Gapless Mean-Field Theory for Weakly Interacting Bose Gases.* J. Phys. Soc. Jap., vol. 75, page 044603, 2006.
[Kocharovsky 00]	V. V. Kocharovsky, Marlan O. Scully, Shi-Yao Zhu & M. Suhail Zubairy. *Condensation of N bosons. II. Nonequilibrium analysis of an ideal Bose gas and the laser phase-transition analogy.* Phys. Rev. A, vol. 61, no. 2, page 023609, Jan 2000.
[Kosterlitz 73]	J. M. Kosterlitz & D. J. Thouless. *Ordering, Metastability and Phase Transitions in Two-Dimensional Systems.* J. Phys. C, vol. 6, page 1181, 1973.

[Landau 41]   L. D. Landau. *The Theory of Superfluidity of Helium II*. J. Physique (Moscow), vol. 5, page 71, 1941.

[Langbein 02]   Wolfgang Langbein & Jorn M. Hvam. *Elastic Scattering Dynamics of Cavity Polaritons: Evidence for Time-Energy Uncertainty and Polariton Localization*. Physical Review Letters, vol. 88, no. 4, page 047401, 2002.

[Langbein 04]   Wolfgang Langbein. *Energy and momentum broadening of planar microcavity polaritons measured by resonant light scattering*. Journal of Physics: Condensed Matter, vol. 16, no. 35, pages S3645–S3652, 2004.

[Laussy 04]   Fabrice P. Laussy, G. Malpuech, A. Kavokin & P. Bigenwald. *Spontaneous Coherence Buildup in a Polariton Laser*. Physical Review Letters, vol. 93, no. 1, page 016402, 2004.

[Lauwers 03]   A. Lauwers J. Verbeure & V. A. Zagrebnov. *Proof of BoseEinstein Condensation for Interacting Gases with a One-Particle Spectral Gap*. J. Phys. A, vol. 36, page L169, 2003.

[Lee 02]   M. D. Lee, S. A. Morgan, M. J. Davis & K. Burnett. *Energy-dependent scattering and the Gross-Pitaevskii equation in two-dimensional Bose-Einstein condensates*. Phys. Rev. A, vol. 65, no. 4, page 043617, Apr 2002.

[Leggett 01]   Anthony J. Leggett. *Bose-Einstein condensation in the alkali gases: Some fundamental concepts*. Rev. Mod. Phys., vol. 73, no. 2, pages 307–356, Apr 2001.

[Lenoble 04]   O. Lenoble, L. A. Pastur & V. A. Zagrebnov. *Bose-Einstein Condensation in Random Potentials*. C. R. de Physique, vol. 5, page 129, 2004.

[Lewenstein 96]   M. Lewenstein & L. You. *Quantum Phase Diffusion of a Bose-Einstein Condensate*. Phys. Rev. Lett., vol. 77, no. 17, pages 3489–3493, Oct 1996.

[Liu 04]   Xia-Ji Liu, Hui Hu, A. Minguzzi & M. P. Tosi. *Collective oscillations of a confined Bose gas at finite temperature in the random-phase approximation*. Physical Review A (Atomic, Molecular, and Optical Physics), vol. 69, no. 4, page 043605, 2004.

[Loffler 05]   A. Loffler, J. P. Reithmaier, G. Sek, C. Hofmann, S. Reitzenstein, M. Kamp & A. Forchel. *Semiconductor quantum dot microcavity pillars with high-quality factors and enlarged dot dimensions*. Applied Physics Letters, vol. 86, no. 11, page 111105, 2005.

[Lozovik 76]   Yu. E. Lozovik & V. I. Yudson. *A new mechanism for superconductivity: pairing between spatially separated electrons and holes*. Soviet Physics - JETP, vol. 44, no. 2, pages 389–397, 1976.

[Mahan 81]   G. D. Mahan. Many particle physics. Plenum Press, New York, 1981.

[Mandel 95]   L. Mandel & E. Wolf. Optical coherence and quantum optics. Cambridge University Press, 1995.

[Marchetti 04]   F. M. Marchetti, B. D. Simons & P. B. Littlewood. *Condensation of cavity polaritons in a disordered environment.* Physical Review B (Condensed Matter and Materials Physics), vol. 70, no. 15, page 155327, 2004.

[Marchetti 06]   F. M. Marchetti, J. Keeling, M. H. Szymanska & P. B. Littlewood. *Thermodynamics and Excitations of Condensed Polaritons in Disordered Microcavities.* Phys. Rev. Lett., vol. 96, no. 6, page 066405, 2006.

[Mieck 02]   B. Mieck & H. Haug. *Quantum-kinetic Langevin fluctuations for exciton Bose-Einstein condensation.* Phys. Rev. B, vol. 66, no. 7, page 075111, Aug 2002.

[Morgan 02]   S. A. Morgan, M. D. Lee & K. Burnett. *Off-shell T matrices in one, two, and three dimensions.* Phys. Rev. A, vol. 65, page 022706, 2002.

[Moskalenko 62]   S. A. Moskalenko. *Reversible Optico-Hydrodynamic Phenomena a Nonideal Exciton Gas.* Soviet Physics-Solid State, vol. 4, page 199, 1962.

[Moskalenko 00]   S. A. Moskalenko & D. W. Snoke. Boseeinstein condensation of excitons and biexcitons and coherent nonlinear optics with excitons. Cambridge University Press, 2000.

[Nikuni 99]   T. Nikuni, E. Zaremba & A. Griffin. *Two-Fluid Dynamics for a Bose-Einstein Condensate out of Local Equilibrium with the Noncondensate.* Phys. Rev. Lett., vol. 83, no. 1, pages 10–13, Jul 1999.

[Nozières 89]   P. Nozières & D. Pines. The theory of quantum liquids ii. superfluid bose liquids. Addison-Wesley Publishing Company, 1989.

[Oesterle 05]   U. Oesterle, R. P. Stanley & R. Houdré. *MBE growth of high finesse microcavities.* physica status solidi (b), vol. 242, no. 11, pages 2157–2166, 2005.

[Ohashi 02]   Y. Ohashi & A. Griffin. *BCS-BEC Crossover in a Gas of Fermi Atoms with a Feshbach Resonance.* Physical Review Letters, vol. 89, no. 13, page 130402, 2002.

[Okumura 01]   Satoru Okumura & Tetsuo Ogawa. *Boson representation of two-exciton correlations: An exact treatment of composite-particle effects.* Phys. Rev. B, vol. 65, no. 3, page 035105, Dec 2001.

[Penrose 56]   Oliver Penrose & Lars Onsager. *Bose-Einstein Condensation and Liquid Helium.* Physical Review, vol. 104, no. 3, pages 576–584, 1956.

[Peyghambarian 83] N. Peyghambarian, L. L. Chase & A. Mysyrowicz. *Bose-Einstein statistical properties and condensation of excitonic molecules in CuCl.* Phys. Rev. B, vol. 27, no. 4, pages 2325–2345, Feb 1983.

[Pitaevskii 03]   L. Pitaevskii & S. Stringari. Bose-einstein condensation. Oxford University Press, 2003.

[Popov 72]   V. N. Popov. *On the Theory of the Superfluidity of Two- and One-Dimensional Bose Systems.* Teor. Mat. Fiz., vol. 11, page 354, 1972.

[Porras 02]   D. Porras, C. Ciuti, J. J. Baumberg & C. Tejedor. *Polariton dynamics and Bose-Einstein condensation in semiconductor microcavities.* Phys. Rev. B, vol. 66, no. 8, page 085304, Aug 2002.

[Quattropani 86]   A. Quattropani, L. C. Andreani & F. Bassani. *Quantum Theory of Polaritons with Spatial-Dispersion-Exact-Solution.* Il Nuovo Cimento, vol. 7D, page 55, 1986.

[Richard 05a]   M. Richard, J. Kasprzak, R. Andre, R. Romestain, Le Si Dang, G. Malpuech & A. Kavokin. *Experimental evidence for nonequilibrium Bose condensation of exciton polaritons.* Physical Review B (Condensed Matter and Materials Physics), vol. 72, no. 20, page 201301, 2005.

[Richard 05b]   Maxime Richard, Jacek Kasprzak, Robert Romestain, Regis Andre & Le Si Dang. *Spontaneous Coherent Phase Transition of Polaritons in CdTe Microcavities.* Physical Review Letters, vol. 94, no. 18, page 187401, 2005.

[Ritter 07]   S. Ritter, A. Ottl, T. Donner, T. Bourdel, M. Kohl & T. Esslinger. *Observing the Formation of Long-Range Order during Bose-Einstein Condensation.* Physical Review Letters, vol. 98, no. 9, page 090402, 2007.

[Rochat 00]   G. Rochat, C. Ciuti, V. Savona, C. Piermarocchi, A. Quattropani & P. Schwendimann. *Excitonic Bloch equations for a two-dimensional system of interacting excitons.* Phys. Rev. B, vol. 61, no. 20, pages 13856–13862, May 2000.

[Rubo 03]   Yuri G. Rubo, F. P. Laussy, G. Malpuech, A. Kavokin & P. Bigenwald. *Dynamical Theory of Polariton Amplifiers.* Physical Review Letters, vol. 91, no. 15, page 156403, 2003.

[Sanvitto 05]   D. Sanvitto, A. Daraei, A. Tahraoui, M. Hopkinson, P. W. Fry, D. M. Whittaker & M. S. Skolnick. *Observation of ultrahigh quality factor in a semiconductor microcavity.* Applied Physics Letters, vol. 86, no. 19, page 191109, 2005.

[Sarchi 06]   D. Sarchi & V. Savona. *Collective excitation kinetics in the conden-sation of polaritons.* physica status solidi (b), vol. 243, no. 10, pages 2317–2321, 2006.

[Sarchi 07a]   D. Sarchi & V. Savona. *Long-range order in the Bose-Einstein con-densation of polaritons.* Phys. Rev. B, vol. 75, page 115326, 2007.

[Sarchi 07b]   D. Sarchi & V. Savona. *Towards thermal equilibrium in the Bose Einstein condensation of microcavity polaritons.* Solid State Comm., *in press*, doi:10.1016/j.ssc.2007.07.039, 2007.

[Savona 94]   V. Savona, Z. Hradil, A. Quattropani & P. Schwendimann. *Quantum theory of quantum-well polaritons in semiconductor microcavities.* Phys. Rev. B, vol. 49, no. 13, pages 8774–8779, Apr 1994.

[Savona 95]   V. Savona, L. C. Andreani, P. Schwendimann & A. Quattropani. *Quantum well excitons in semiconductor microcavities:Unified treat-ment of weak and strong coupling regimes.* Solid State Communica-tions, vol. 93, no. 9, pages 733–739, Mar 1995.

[Savona 96]   V. Savona, F. Tassone, C. Piermarocchi, A. Quattropani & P. Schwendimann. *Theory of polariton photoluminescence in ar-bitrary semiconductor microcavity structures.* Physical Review B (Condensed Matter), vol. 53, no. 19, pages 13051–13062, 1996.

[Savona 97]   V. Savona. *Optical Properties of Quantum Well Polaritons in Mi-crocavities.* PhD thesis, EPFL, Lausanne, 1997.

[Savona 98]   Vincenzo Savona. *Strong coupling of exciton-polaritons in semicon-ductor microcavities.* Journal of Crystal Growth, vol. 184, page 737, 1998.

[Savona 99a]   V. Savona, C. Piermarocchi, A. Quattropani, P. Schwendimann & F. Tassone. *Optical properties of microcavity polaritons.* Phase Tran-sitions, vol. 68, no. 1, pages 169–279, 1999.

[Savona 99b]   Vincenzo Savona & Roland Zimmermann. *Time-resolved Rayleigh scattering of excitons: Evidence for level repulsion in a disordered system.* Phys. Rev. B, vol. 60, no. 7, pages 4928–4936, Aug 1999.

[Savona 05]   V. Savona, P. Schwendimann & A. Quattropani. *Onset of coherent photoluminescence in semiconductor microcavities.* Phys. Rev. B, vol. 71, page 125315, 2005.

[Savona 07]   Vincenzo Savona. *Effect of interface disorder on quantum well ex-citons and microcavity polaritons.* Journal of Physics: Condensed Matter, vol. 19, no. 29, page 295208 (23pp), 2007.

[Schmitt-Rink 85] S. Schmitt-Rink, D. S. Chemla & D. A. B. Miller. *Theory of tran-sient excitonic optical nonlinearities in semiconductor quantum-well structures.* Phys. Rev. B, vol. 32, no. 10, pages 6601–6609, Nov 1985.

[Schmitt 01]   O. M. Schmitt, D. B. Tran Thoai, L. Bányai, P. Gartner & H. Haug. *Bose-Einstein Condensation Quantum Kinetics for a Gas of Interacting Excitons.* Phys. Rev. Lett., vol. 86, no. 17, pages 3839–3842, Apr 2001.

[Schwendimann 93]   P. Schwendimann, A. Quattropani & Z. Hradil. *Statistical Properties of Polariton States.* Nuovo Cimento D, vol. 15, page 1421, 1993.

[Schwendimann 06]   Paolo Schwendimann & Antonio Quattropani. *Amplification and quantum statistics of microcavity polaritons under nonresonant excitation.* Physical Review B (Condensed Matter and Materials Physics), vol. 74, no. 4, page 045324, 2006.

[Scully 99]   Marlan O. Scully. *Condensation of N Bosons and the Laser Phase Transition Analogy.* Phys. Rev. Lett., vol. 82, no. 20, pages 3927–3931, May 1999.

[Sek 07]   G. Sek, P. Poloczek, P. Podemski, R. Kudrawiec, J. Misiewicz, A. Somers, S. Hein, S. Höfling & A. Forchel. *Experimental evidence on quantum well–quantum dash energy transfer in tunnel injection structures for 1.55 mu m emission.* Applied Physics Letters, vol. 90, no. 8, page 081915, 2007.

[Senellart 99]   P. Senellart & J. Bloch. *Nonlinear Emission of Microcavity Polaritons in the Low Density Regime.* Phys. Rev. Lett., vol. 82, no. 6, pages 1233–1236, Feb 1999.

[Shelykh 04]   I. Shelykh, G. Malpuech, K. V. Kavokin, A. V. Kavokin & P. Bigenwald. *Spin dynamics of interacting exciton polaritons in microcavities.* Physical Review B (Condensed Matter and Materials Physics), vol. 70, no. 11, page 115301, 2004.

[Shelykh 06]   I. A. Shelykh, Yuri G. Rubo, G. Malpuech, D. D. Solnyshkov & A. Kavokin. *Polarization and Propagation of Polariton Condensates.* Physical Review Letters, vol. 97, no. 6, page 066402, 2006.

[Shi 98]   H. Shi & A. Griffin. *Finite-temperature excitations in a dilute Bose-condensed gas.* Phys. Rep., vol. 304, page 1, 1998.

[Shin 04]   Y. Shin, M. Saba, T. A. Pasquini, W. Ketterle, D. E. Pritchard & A. E. Leanhardt. *Atom Interferometry with Bose-Einstein Condensates in a Double-Well Potential.* Physical Review Letters, vol. 92, no. 5, page 050405, 2004.

[Sinatra 07]   A. Sinatra, Y. Castin & E. Witkowska. *Nondiffusive phase spreading of a Bose-Einstein condensate at finite temperature.* Physical Review A (Atomic, Molecular, and Optical Physics), vol. 75, no. 3, page 033616, 2007.

[Snoke 90]   D. W. Snoke, J. P. Wolfe & A. Mysyrowicz. *Evidence for Bose-Einstein condensation of a two-component exciton gas.* Phys. Rev. Lett., vol. 64, no. 21, pages 2543–2546, May 1990.

[Snoke 91]   D. W. Snoke, Jia Ling Lin & J. P. Wolfe. *Coexistence of Bose-Einstein paraexcitons with Maxwell-Boltzmann orthoexcitons in Cu_2O*. Phys. Rev. B, vol. 43, no. 1, pages 1226–1228, Jan 1991.

[Snoke 02a]   D. Snoke, S. Denev, Y. Liu, L. Pfeiffer & K. West. *Long-range transport in excitonic dark states in coupled quantum wells*. Nature, vol. 418, no. 6899, pages 754–757, 2002.

[Snoke 02b]   David Snoke. *Spontaneous Bose Coherence of Excitons and Polaritons*. Science, vol. 298, no. 5597, pages 1368–1372, 2002.

[Stanley 94]   R. P. Stanley, Houdre R., Oesterle U., Gailhanou M. & Ilegems M. *Ultrahigh Finesse Microcavity with Distributed Bragg Reflectors*. Applied Physics Letters, vol. 65, no. 15, pages 1883–1885, 1994.

[Steinhauer 02]   J. Steinhauer, R. Ozeri, N. Katz & N. Davidson. *Excitation Spectrum of a Bose-Einstein Condensate*. Phys. Rev. Lett., vol. 88, no. 12, page 120407, Mar 2002.

[Stevenson 00]   R. M. Stevenson, V. N. Astratov, M. S. Skolnick, D. M. Whittaker, M. Emam-Ismail, A. I. Tartakovskii, P. G. Savvidis, J. J. Baumberg & Roberts J. S. Phys. Rev. Lett., vol. 85, page 3680, 2000.

[Stolz 81]   H. Stolz, R. Zimmermann & G. Röpke. *Correlated Hartree-Fock Theory of the Electron-Hole Plasma Containing Exciton Bound States*. physica status solidi (b), vol. 105, no. 2, page 585, 1981.

[Stoof 92]   H. T. C. Stoof. *Nucleation of Bose-Einstein condensation*. Phys. Rev. A, vol. 45, no. 12, pages 8398–8406, Jun 1992.

[Svidzinsky 06]   A. A. Svidzinsky & Scully M. O. *Condensation of N Interacting Bosons: A Hybrid Approach to Condensate Fluctuations*. Physical Review Letters, vol. 97, no. 19, page 190402, 2006.

[Szymanska 06]   M. H. Szymanska, J. Keeling & P. B. Littlewood. *Nonequilibrium Quantum Condensation in an Incoherently Pumped Dissipative System*. Physical Review Letters, vol. 96, no. 23, page 230602, 2006.

[Tassone 97]   F. Tassone, C. Piermarocchi, V. Savona, A. Quattropani & P. Schwendimann. *Bottleneck effects in the relaxation and photoluminescence of microcavity polaritons*. Phys. Rev. B, vol. 56, no. 12, pages 7554–7563, Sep 1997.

[Tassone 99]   F. Tassone & Y. Yamamoto. *Exciton-exciton scattering dynamics in a semiconductor microcavity and stimulated scattering into polaritons*. Phys. Rev. B, vol. 59, no. 16, pages 10830–10842, Apr 1999.

[Walser 00]   R. Walser, J. Cooper & M. Holland. *Reversible and irreversible evolution of a condensed bosonic gas*. Phys. Rev. A, vol. 63, no. 1, page 013607, Dec 2000.

[Weisbuch 92]   C. Weisbuch, M. Nishioka, A. Ishikawa & Y. Arakawa. *Observation of the Coupled Exciton-Photon Mode Splitting in a Semiconductor Quantum Microcavity.* Phys. Rev. Lett., vol. 69, no. 23, pages 3314–3317, Dec 1992.

[Wouters 07a]   M. Wouters & I. Carusotto. *Parametric oscillation threshold of semiconductor microcavities in the strong coupling regime.* Phys. Rev. B, vol. 75, page 075332, 2007.

[Wouters 07b]   Michiel Wouters & Iacopo Carusotto. *Excitations in a non-equilibrium Bose-Einstein condensate of exciton-polaritons.* ArXiv:cond-mat/0702431, 2007.

[Yukalov 06]   V. I. Yukalov & H. Kleinert. *Gapless Hartree-Fock-Bogoliubov approximation for Bose gases.* Physical Review A (Atomic, Molecular, and Optical Physics), vol. 73, no. 6, page 063612, 2006.

[Zagrebnov 01]   V. A. Zagrebnov & J. B. Bru. *The Bogoliubov Model of Weakly Imperfect Bose Gas.* Physics Reports, vol. 350, pages 291–434, 2001.

[Zhu 95]   X. Zhu, P. B. Littlewood, Mark S. Hybertsen & T. M. Rice. *Exciton Condensate in Semiconductor Quantum Well Structures.* Phys. Rev. Lett., vol. 74, no. 9, pages 1633–1636, Feb 1995.

[Zimmermann 88]   R. Zimmermann. Many-particle theory of highly excited semiconductors. Teubner-Texte zur Physik. BGB Teubner-Verlag, Leipzig, 1988.

[Zimmermann 95]   R. Zimmermann. *Theory of resonant Rayleigh scattering of excitons in semiconductor quantum wells.* Il Nuovo Cimento D, vol. 17, page 1801, 1995.

[Zimmermann 03]   R. Zimmermann, E. Runge & V. Savona. *Level repulsion of exciton states in disordered semiconductor nanostructures.* physica status solidi (b), vol. 238, page 478, 2003.

[Zimmermann 07]   R. Zimmermann & Schindler C. *Exciton-Exciton Interaction in Coupled Quantum Wells.* Submitted to Solid State Comm., 2007.

Curriculum Vitae of Davide Sarchi

Born on January 5th, 1979 in Milan, Italy

Professional address:

Institute of Theoretical Physics
Ecole Polytechnique Fédérale de Lausanne
SB/ITP/GR-SA (Batiment PH)
Station 3
CH-1015 Lausanne, Switzerland
Tel. (prof.): (+41) 021 693 5418
Fax (prof.): (+41) 021 693 5419
e-mail: davide.sarchi@epfl.ch

Private address:

Place de la Gare 12
CH-1020 Renens, Switzerland
Tel.: (+41) 021 634 1304
Mob.: (+41) 076 232 1946

Nationality: Italian

Marital status: unmarried

Studies:

- High school diploma ("Maturità Scientifica") at the Liceo Scientifico "Vittorio Veneto" in Milan, Italy, with mark 60/60 (1997).

- Master Degree in Physics at the University of Milan (2002). The title of the degree thesis, written under the supervision of Prof. Pier Francesco Bortignon and Dott. Gianluca Colo', is "Calcolo autoconsistente di stati vibrazionali dei nuclei atomici (Self-consistent calculation of the vibrational states of the atomic nuclei).".

- Courses of the Doctoral program in Photonics at EPFL, Lausanne, Switzerland (2003-2007).

Language skills:

- Italian: maternal tongue.

- French: good knowledge.

- English: good knowledge.

Present position:

From October 1st 2003, Scientific Assistant / PhD student at EPFL (Lausanne) in the

Institute of Theoretical Physics, under the direction of Prof. Vincenzo Savona.
The research topic is the theoretical modeling of the Bose-Einstein condensation of microcavity polaritons.

List of recent publications and reports

- V. Savona and D. Sarchi, "Bose-Einstein condensation of microcavity polaritons", *Phys. Status Solidi b* **242**, 2290-2301 (2005).

- D. Sarchi and V. Savona, "Collective excitation kinetics in the condensation of polaritons", *Phys. Status Solidi b*, **243**, 2317 (2006).

- P. Lugan, D. Sarchi and V. Savona, "Theory of trapped polaritons in patterned microcavities", *Phys. Status Solidi c*, **3**, 2428 (2006).

- D. Sarchi and V. Savona, "Kinetics of quantum fluctuations in polariton Bose Einstein condensation", in the Proceedings of the "28th International Conference on the Physics of Semiconductors (ICPS)".

- D. Sarchi and V. Savona, " Long-range order in the Bose-Einstein condensation of polaritons", *Phys. Rev.* B **75**, 115326 (2007).

- D. Sarchi and V. Savona, "Towards thermal equilibrium in the BoseEinstein condensation of microcavity polaritons", *Solid State Comm.*, *in press*, doi:10.1016/j.ssc.2007.07.039 (2007).

- D. Sarchi and V. Savona, "Spectrum and thermal fluctuations of a microcavity polariton Bose-Einstein condensate", submitted to *Phys. Rev.* B, 2007.

List of recent presentations

- "1st International Conference on Spontaneous Coherence in Excitonic Systems (ICSCE-1)", Champion PA, USA, May 25-28, 2004. Contributed poster.

- "2nd International Conference on Spontaneous Coherence in Excitonic Systems (ICSCE-2)", Southampton, United Kingdom, September 5-10, 2005. Contributed talk.

- "EPFL Photonics day 2005", Lausanne, Switzerland, September 28, 2005. Contributed poster.

- "EPFL Research Day", Lausanne, Switzerland, November 11, 2005. Contributed poster.

- "8th International Conference on Nonlinear Optics and Excitations Kinetics in Semiconductors (NOEKS-8)", Muenster, Germany, February 20-24, 2006. Contributed talk.

- "International School of Physics Enrico Fermi, course: Ultra-cold Fermi gases", Varenna, Italy, June 20-30, 2006. Contributed poster.

- "28th International Conference on the Physics of Semiconductors (ICPS)", Vienna, Austria, July 23-29, 2006. Contributed talk.

- "EPFL Photonics day 2006", Lausanne, Switzerland. Contributed poster.

- "EPFL Research Day 2006", Lausanne, Switzerland. Contributed poster.

- "3nd International Conference on Spontaneous Coherence in Excitonic Systems (ICSCE-3)", Les Houches, France, January 15-18, 2007. Contributed talk.

- Invited to the "10th International Meeting on the Optics of Excitons in Confined Systems (OECS-10)", Messina-Patti, Italy, September 10-13, 2007.

Teaching at EPFL

- 2003-2004 (summer semester): assistant of the course "Statistiques de Lévy et applications physiques" by Prof. F. Bardou, ($3^{\text{ème}}$ Cycle de la Physique en Suisse Romande);

- 2004-2005 (winter semester): exercises of the course "Physique mathématique I : groupes et symétries discrets" by Prof. V. Savona;

- 2004-2005 (summer semester): exercises of the course "Physique statistique IV" by Prof. V. Savona;

- 2005-2006 (winter semester): exercises of the course "Physique mathématique I : groupes et symétries discrets" by Prof. V. Savona;

- 2005-2006 (summer semester): exercises of the course "Physique Statistique avancée II" by Prof. V. Savona;

- 2006-2007 (winter semester): exercises of the course "Groupes et symétries discrets en physique" by Prof. V. Savona;

- 2006-2007 (summer semester): exercises of the course "Physique Statistique avancée II" by Prof. V. Savona.

Lausanne, August 1st, 2007.